UNIVERSITÀ DEGLI STUDI DI MILANO
FACOLTÀ DI SCIENZE MATEMATICHE,
FISICHE E NATURALI

DIPARTIMENTO DI MATEMATICA
"FEDERIGO ENRIQUES"

DOTTORATO DI RICERCA IN
MATEMATICA E STATISTICA PER LE SCIENZE
COMPUTAZIONALI (XXII CICLO)

PH.D. THESIS

A Petri Net Model of Liver Response to Visceral Leishmaniasis:

self-regulation and complex interplay in the vertebrate immune system

INF/01

Supervisor
Prof. Jon TIMMIS

Author
Luca ALBERGANTE

Co-Supervisor
Prof. Giovanni NALDI

Ph.D. Program Director
Prof. Vincenzo CAPASSO

A.A. 2008/2009

[This page intentionally left blank]

Contents

Acknowledgments

I am heartily thankful to my supervisor Jon Timmis, whose encouragement, guidance and support, from the initial to the final stage, made this thesis possible. I'm also very thankful to Paul Kaye, whose biological expertise was essential for my understanding of the biology of visceral leishmaniasis.

Additionally, I would like to thank the many people that provided me with useful suggestions, feedbacks and data at various stages of the work: Giovanni Naldi, Anastasia Pagnoni, Monika Hiener, Linette Beattie, Paul Andrews, Mark Read, and the referees of my thesis.

Finally, I would like to thank my family and friends for their support and patience.

Luca Albergante

Introduction

Immunological Modeling

Mathematical models of immunological phenomena have been around for some time. For example, in 1925 McKendrick proposed a model for the dynamics of a population with some individuals affected by a contagious disease (M'Kendrick 1925). Albeit rather simple, the model proved to be quite effective in explaining some characteristics of cholera epidemics.

Early modelers where limited by the available mathematical techniques and limited computing power. Nevertheless, they were able to develop very powerful models of many macroscopic phenomena. Nowadays, the advances in various scientific fields allow modelers to study much more complex models (e.g., Marino & Kirschner 2004).

Ordinary differential equations are probably one of most used formalism in the context of biological models (see for example Murray 2002). However, the availability of powerful computers and the advances in mathematics have allowed the building of models using more powerful techniques such as partial differential equations (see Murray 2002 and Murray 2003) or stochastic differential equations (see Vincenzo Capasso 2005).

Differential equation models (and difference equation models which are their discrete counterpart) are very powerful at predicting the behavior of populations of similar individuals, when we have a good knowledge of the underlying processes. However, they are generally less effective when the behavior of the individuals change greatly among the populations, or the knowledge of the underlying processes is limited. When this is the case, agent based models can be more effective.

Agent based models simulate the behavior of individuals rather than of *populations of* individuals. Each individual is characterized by a, possibly unique, set of rules and the evolution of the model is studied simulating the evolution of a system composed of many individuals in a possibly changing environment. They are generally built using dedicated modeling tools (e.g. Mason (Luke et al. 2005)) or coded using general purpose programming languages (e.g., Java, C++). While the idea of agent based models can be dated back to the 1940s, their usage in the context of immunology is quite recent as a large computing power is generally required to simulate a

meaningful number of entities.

Remarkably, differential equation and agent based modeling techniques can coexist in the same model (see for example Gammack et al. 2005).

In addition to differential equation and agent based models, many formalisms have been used for immunological modeling over the years. Petri nets are probably one of the most relevant examples (see for example Will & Heiner 2002). The main advantages of Petri nets are the possibility of building the model *visually* and the ability to formally verify some properties.

While classical immunological models have been generally developed to test the consequences of quite well-known processes, a more recent trend in immunological modeling is to test the impact of different hypotheses (or feature) of cells on the outcome of a disease (see for example Ray et al. 2009).

Model Validation

A number of key immunological processes are quite well-understood. However, many immunological problems remain open. This limited immunological knowledge generally results in models whose validity heavily reside on the assumptions used during their development.

While many modeling communities share similar concerns, the large number of assumptions used and the complexity of many immunological models call for a precise description of the building process and of a formal validation of the model.

In the context of agent based models, the Unified Modeling Language (UML) has been shown to be helpful in describing the structure a model (see for example Flugge et al. 2009), however, in its current state, it seems to be unable to capture some biological aspects (see for example Read et al. 2009). Note that visual formalisms, such as Petri Nets, generally share with UML similar descriptive features (see for example Heiner et al. 2004).

While different validation techniques have been proposed for immunological models, the two principal means of validation are: comparison with published data (or domain expert opinions) and sensitivity analysis. The former is, obviously, largely used, and allows to understand to which extent the model is able to reproduce reality, the latter is less widespread and allows to assess the robustness of the model.

UML and Petri nets can be very useful in explaining the model to biological experts and thus provide a qualitative validation of the model. If a more quantitative validation is required, sensitivity analysis can be used.

While sensitivity analysis techniques have been generally developed in non-biological contexts, many of them have been shown to be quite successful in dealing with both differential equation and agent based immunological models (Marino et al. 2008).

Visceral Leishmaniasis

Visceral leishmaniasis (also called "Kala-azar") is a widespread disease, which is usually fatal in the absence of treatment. Desjeux 2004 reports that 500,000 new cases per year are discovered and that 350 million people in 88 countries are at risk of infection. Characteristic of the liver immune response to leishmaniasis is a type of inflammation (granulomatous inflammation) that leads to the formation of "granulomas". Granulomas provide a very interesting micro-environment, which is maintained by the coordination of many cells of the immune system (Phagocytes, NK cells, NKT cells, and T cells). Some of these cells promote the infection, others control the infections, and some others do both.

Only a limited amount of modeling works exists in the context of granulomatous infection. Tuberculosis leads to the formation of granuloma in the lungs, and is probably the most studied disease (see Ray et al. 2009 and references within). In the context of leishmaniasis the only notable work up to date is Flugge et al. 2009. However, all the models presented so far focus on the formation of the granuloma, but disregard the full dynamics of the *granuloma process*. Therefore, we aimed at building a model that could describe the full course of visceral leishmaniasis, from infection to resolution.

While a number of data on leishmaniasis have been published, at the current stage of biological technology it is possible to track the evolution of a single granuloma in a living organism only for a short period of time (Beattie at al. 2010 (PLoS Pathog)). Moreover, it is currently impossible to reproduce the formation of a granuloma in a controlled environment such as a Petri dish.

The primary goal of this thesis is to gain insights into the process of formation and development of a granuloma. To this end we built a model of the granuloma formation and resolution in the liver, and validated the model both qualitatively and quantitatively using both data and sensitivity analysis.

Following some preliminary considerations, we opted for a stochastic Petri net model. Stochastic Petri nets have a precise formalization (Marsan et al. 1995) and fast simulation algorithm (Heiner, Richter, Schwarick & Rohr 2008). Moreover, their *visual structure* greatly facilitates the interaction with immunological experts.

Given the complicate nature of granuloma formation, we aimed at describing carefully the building process of our model. Specifically, for all the cells involved, we provided a precise, albeit minimal, description. Moreover, most of the information provided will be referenced by up to date articles on the subject, to provide the reader with an overview of the current immunological open problems.

Some key mechanisms underlying the behavior of the cells of the immune system contributing to the evolution of a granuloma are open research prob-

lems (e.g., Trinchieri 2007 or Godfrey et al. 2010). Therefore, we will clearly document all the biological assumptions that will be used in the model, and will discuss to which extent these assumptions affect our results. Additionally, whenever possible, we will analyze the effect of different contrasting assumptions on the outcome of the model. Moreover, all the important simplifications introduced by the model will be described along with their implications.

Since biological experiments can lead to different quantitative results (e.g. Amprey et al. 2004 and Stanley et al. 2008), we listed all the data source used, and, whenever possible, we described alternatives outcomes present in the literature. Biological data have been used both to parametrize the model and to validate its results.

The behavior of the model has been qualitatively validated both in wild type and gene knockout conditions (e.g., Murray et al. 2006 and Amprey et al. 2004), and the results for the most relevant cells have been discussed.

Finally, we performed sensitivity analysis following the indication of Marino et al. 2008 to assess the importance of the cells involved and of the effect of our limited knowledge of certain biological parameters.

Secondary Goals

Besides the primary goal described above, we tried to achieve some important secondary goals.

A second goal of this thesis is to help biologists in designing more focused experiments and ultimately better, and cheaper, therapies to fight visceral leishmaniasis. To this end, we compared different therapeutic options, with the purpose of determining which mechanisms should be targeted by drugs.

As described above, the vertebrate immune system is far from being completely understood, and many hypotheses on its behavior are currently difficult to test by biological experiments. Therefore, we used our model of a granuloma as an *advanced Petri dish* to test hypotheses on immune cells and their interactions. Hence, *a third goal of this thesis is to build an environment that can be used to test biological hypotheses.*

In building our model we had to decide in favor of certain biological assumptions and to introduce a number of simplifications. *A fourth goal of this thesis is to clearly document the modeling process*, with the purpose of documenting the building of a complex model from a complicated process by explaining how we managed the available — and the unavailable — information on the biology of leishmaniasis. To this end, we carefully described all the fundamental modeling steps and the implications of our choices, with the purpose of providing a template that can be used when facing similar problems.

Organization of the Thesis

The first part of the thesis ("Preliminaries") briefly introduces all the fundamental concepts used to build the model. Most notions are presented only briefly. However, the bibliography provides the references to more detailed books or articles. Chapter 1 introduces some basics of biology and immunology, Chapter 2 describes the biology of visceral leishmaniasis, Chapter 3 discusses some aspects of immunological modeling with a focus on granuloma formation, and Chapter 4 presents some basics of Petri nets and sensitivity analysis.

The second part of the thesis ("Model") focuses on the actual model. Chapter 5 describes the main assumptions used and simplifications introduced, Chapter 6 presents the details of the Petri net model, Chapter 7 compares the outcomes of the model with biological experiments, Chapter 8 presents the main results of the experiments performed on our model, Chapter 9 discusses the sensitivity analysis of the parameters used by the model, and Chapter 10 presents some concluding remarks on the thesis.

The appendices presents few mathematical proofs and additional data.

Part I

Preliminaries

Chapter 1

Biological Preliminaries

This chapter presents a concise description of the basics of the vertebrate immune system. The material presented is based on Alberts et al. 2008 and Murphy & Kenneth 2007, which we refer to for a more systematic discussion.

1.1 The Cell and Its Interactions: An Informal Introduction

1.1.1 Inside the Cell: DNA, RNA, and Proteins

The cellular biology of multicellular organisms is very complex. This complexity arises from the many functions that the cells perform, and the multitude of stimuli that the cells are expected to respond to.

The behavior of the cell is controlled, more or less directly, by its deoxyribonucleic acid (DNA). The DNA is a very large protein that resides in the nucleus of the cell and encodes most of the information used by the cell to survive. While it is not completely understood which percentage of the DNA encodes actual information, it is well-known that some parts of it contain the instructions to build specific proteins. These parts, are called genes.

When the information contained in a gene is actively used, and therefore when the cell is producing the protein encoded by the gene, the gene is said to be active, or expressed. Otherwise, the gene is said to be inactive, or not expressed.

When a gene is expressed, it is transcripted into a specific type of Ribonucleic acid (RNA), called messenger RNA (mRNA). As suggested by the term "transcription", the gene and mRNA contain the same information. The mRNA travels to a ribosome, where it is used to build proteins. Genes can be expressed at different levels, that is, different quantities of mRNA — and therefore proteins — per unit of time can be produced from the same gene.

Albeit similar from an informational point of view, RNA and DNA are functionally different. The DNA is fundamental to the life of the cell, and many error-correction mechanisms exist to ensure that the information is preserved unaltered. The RNA, on the other hand, is only a temporary vector, and less safe, but faster, mechanisms are used during its manipulation.

Measuring the quantity of mRNA encoding a protein inside the cell is a common way to estimate how much of such protein is being produced by that cell (See for example Melby et al. 1998). However, the time required for a specific concentration of mRNA to produce an effect outside the cell — for example expelling the protein — can be quite long (e.g., Maroof et al. 2008 reports a high concentration of mRNA encoding the protein IL10 days before the protein is actually detectable outside the cell).

The expression of a gene is controlled by specific proteins called "activators" and "repressors". As suggested by their names, activators up-regulate, while repressors down-regulate, gene expression. The DNA encodes different activators and repressors. Therefore the expression of a gene can result into the activation or deactivation of other genes, leading to very complex networks of interdependencies among genes (usually called "gene regulatory networks"). Finally, "transcription factors" are proteins characterized by their ability to regulate the expression of different genes.

1.1.2 Beyond the Cell: Intracellular Communication

The interior of a cell (the "cytoplasm") is separated from the environment by a semi-permeable membrane (the "plasma or cell membrane"). A variable number of proteins is attached to this membrane. Some of these proteins allow the cell to interact with the environment: they are used the cell to ingest the substances it needs to survive and to send (or receive) different signals.

Of particular interest for signaling are certain types of "transmembrane proteins". These proteins cross the membrane, and the binding of the external part of the protein (the "external domain") generally leads to a modification of the structure of the internal part (the "internal domain"). This structural modification generally results in the release proteins that will travel to the nucleus, and ultimately to the activation of genes that *manage* the binding. The external domain of these transmembrane proteins is usually called "receptor".

Two main strategies can be used by a cell to send a signal: producing proteins that will be sent into the environment or displaying proteins on the external surface of the membrane. Sending proteins allows the signal to travel far away from the cell; however, the cell cannot directly determine if the signal has been received. On the other hand, displaying proteins on the surface of the membrane requires the direct contact with the cell that receives the signal, but allows the cell to determine directly when the signal

has been received. Similarly, a cell can receive a signal either by internalizing signaling proteins, or by detecting the binding of surface receptors.

The transmission of a signal by direct contact is called "juxtacrine signaling", while the transmission of a signal by signaling proteins is called "paracrine signaling" (if the signal reaches only the neighbor cells) or "enodcrine signaling" (if the signal reaches distant cells).

Most signals do not have a direct effect on the nucleus of the cell, but trigger a chain of reactions that will eventually act on the DNA (e.g., by the synthesis of an activator). This sequence is called a pathway. Pathways allow the cell to control, or even block, a signal if antagonist signals are received.

1.2 Experiments

Different types of experimental models exist in biology. The most common are *in vivo*, *in vitro*, and *in silico*.

In vivo experiments are performed on living organisms. Mice are commonly used nowadays in immunology, but many other animals have been used in the past. These experiments are very important, as they allow the study of a biological phenomenon in a systemic way. However, they usually permit only a limited control on the experimental conditions.

In vitro experiments are performed on controlled environments, such as Petri dishes. These experiments permit a tight control on the experimental conditions. However, due to the difficulties of recreating the multitude of stimuli of a living organism, they may lead to hard to interpret, or inconclusive, results.

In silico experiments are relatively new in the field of biology. These experiments are performed on a computer using a mathematical model of the biological entities. Complex *in silico* experiments require a lot of computational resources, but they are generally easier to perform than their *in vivo* counterpart. The validity of *in silico* experiments is limited by the ability of the mathematical model to represent reality; however they allow a direct control on all the experimental conditions.

1.3 The Vertebrate Immune System

This Section provides an introduction to the immune system. Unless specified, the material presented is based on Murphy & Kenneth 2007, which we refer to for a more extensive discussion.

Most multicellular organisms on Earth have a way to fight infections. However, the jawed vertebrate immune system is by far the most evolved[1].

[1] The jaw-less vertebrate immune system is believed to be very similar to the jawed vertebrate immune system (see for example Litman & Cannon 2009 or Boehm 2009). However it is not completely clear if it shares the same complexity and power.

Moreover, since humans are jawed vertebrates, it is by far the most studied. Unless specified, the following description pertains to the jawed vertebrate immune system, therefore, to easy the reading, we will use the expression *immune system* instead of *jawed vertebrate immune system*, when no ambiguity arises.

The cells of the immune system are called "white blood cells" or "leukocytes". All these cells develop from "pluripotent hematopoietic stem cells" that are found in the bone marrow.

The four main tasks of the immune system are:

1) detecting pathogens (immunological recognition)

2) containing and possibly overcoming the infection caused by pathogens (immune effector function)

3) controlling the immune response to prevent damage to the organism (immune regulation)

4) remembering the characteristics of pathogens so that they can be fought more efficiently if they are reencountered (immune memory).

The means used by the immune system to recognize a pathogen are a debatable subject. Some immunologists believe that the leukocytes are able to distinguish the substances and cells belonging to the organism (the "self") from the other substances and cells (the "non-self"); the former are ignored while the latter are attacked (this is referred as the "self / non-self" model). While other immunologists believe that leukocytes react to the substances and cells that display a behavior dangerous to the organism (this is referred as the "danger response" model).

No clear evidence in favor (or against) the above models exists, and it is well-possible that both models coexist. However, the fact that some commensal bacteria do not trigger an immune response when they are in the intestine, but do when they enter the bloodstream, suggests that the danger response model may be a better representation of the working of the immune system.

The immune system is usually divided into two subsystems: the "innate" and "adaptive" immune systems.

The innate immune system is non specific and responds very fast (between 0 to 4 hours) to conserved features common to many pathogens. The adaptive immune system, on the other hand, is much slower to respond to an infection (more than 96 hours); however, it is able to identify a larger class of pathogens and to overcome infections that the innate immune system is not able to control. As we will see later, the two systems are not independent, and collaborate to overcome an infection.

Leukocytes make use of a large repertoire of signaling proteins. These proteins are called "cytokines". The cytokines most commonly produced

by leukocytes are TNF (Tumor Necrosis Factor), IL (Interleukin) and INF (Interferon). Section 1.4 presents a brief description of the main functions of the cytokines that we will encounter in our discussion.

In the following, we will discuss the essential characteristics of the most important cells of the immune system. We will preserve the standard division of leukocytes between the innate and adaptive immune systems. That is, macrophages, granulocytes, dendritic cells, natural killer cells, and natural killer T cells belong to the innate immune system while T cells and B cells belong to the adaptive immune system.

1.3.1 Innate Immune System

Dendritic Cells

Dendritic cells (DCs) are a first type of phagocytes. Two main subpopulation of DCs exist: conventional or myeloid dendritic cells (cDCs, mDCs or simply DCs) and plasmacytoid dendritic cells (pDCs). In the following, unless specified, we will refer to conventional dendritic cells.

The main role of DCs is to break up the proteins of the parasites they ingest into fragments that are then displayed on the surface of the DC complexed with "Major Histocompatibility Complex" (MHC) class I or II molecules. This allows the activation of naïve T cells in the lymph nodes. Therefore, DCs are a fundamental link between the innate and the adaptive immune systems. Given their function, DCs are often called "professional antigen presenting cells".

After ingesting a pathogen, DCs generally migrate to the nearest lymph node where they mature. During this maturation, different genes are activated (Huang et al. 2001) and the morphology of the DCs visibly changes. This allows the DCs to be very efficient in priming T cells (the process of priming will be briefly described in Section 1.3.2).

No clear evidence on the lifespan of a mature dendritic cell exists; however, it is believed to be in the order of few days.

Macrophages

Macrophages (MΦs) are a second type of phagocytes. The main role of MΦs is to phagocytose and possibly destroy both parasites and substances recognized as dangerous by the organism. However, from their original role of *professional eaters* discovered by Elie Metchnikoff, macrophages have been showed to perform different functions ranging from protection of the organism to tissue healing. A partial review of macrophage functions can be found in Pollard 2009.

Different macrophage subpopulations are present in different organs. These macrophages share common functions, but specialize to better respond to the environment where they reside and can display different responses to

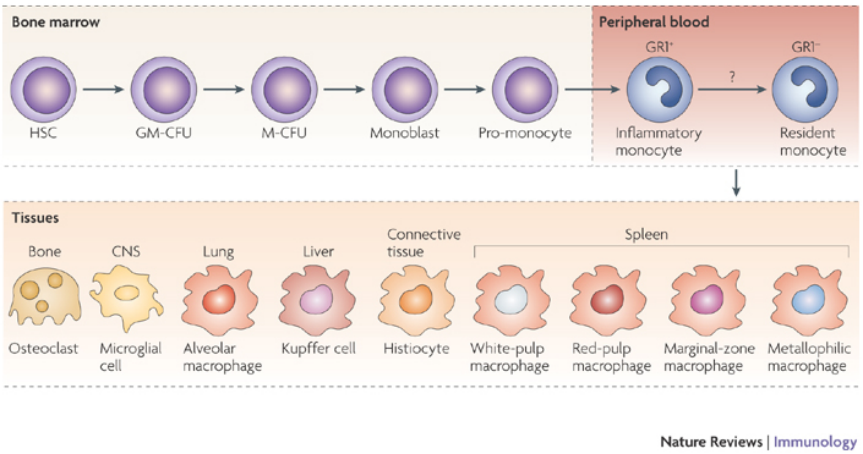

Figure 1.1: Monocyte heterogeneity (from Mosser & Edwards 2008)

pathogens and signals of other leukocytes. The mechanisms behind the differentiation of macrophages is not completely understood, and, for example, it is unclear if the specialization occurs before a resident macrophage reaches its target organ, or after. Resident macrophages have different names in relation to the organ where they reside (see Figure 1.1). For reviews on the differentiation and specialization of macrophages see Mosser & Edwards 2008 and Pollard 2009.

From the perspective of the immune response to parasites, one of the most important feature of macrophages is their ability to change their behavior according to the signals received from other leukocytes. Of particular interest is the process of "activation".

In the following we provide only a schematic description of macrophages activation, a more detailed characterization can be found in Mantovani et al. 2004 and Mosser & Edwards 2008. Additionally, a, possibly incomplete, diagram of the biological pathways involved in the activation of macrophages can be found on GeneNET (Ananko et al. 2002).

"Classical activation" is triggered by the exposure of a macrophage to INFγ and TNF. Note that TNF can be produced by the macrophage and act in an autocrine way after the binding of its Toll Like Receptors (TLRs), or by other cells such as Antigen Presenting Cells (APCs). These macrophages are characterized by:

- an increased production of nitric oxides (NO) and reactive intermediates (ROI), which leads to an increased parasiticidal activity
- the production of pro-inflammatory cytokines such as IL1, IL6, IL12, IL23, and TNF
- an increased ability to present MHC class II peptides

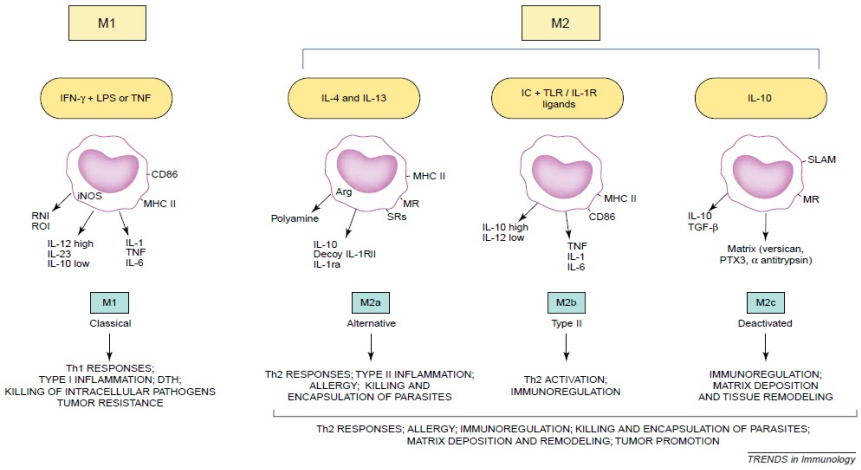

Figure 1.2: Different macrophage activations (from Mantovani et al. 2004)

Classically activated macrophages are very effective in killing parasites. However, they can also damage the organism. These macrophages are sometimes indicated by caMΦs or M1s to stress their relation with type I immune response.

"Alternative activation" is triggered by the exposure to IL4 and IL13. These macrophages are characterized by:

- the production of polyamines
- the production of low quantities of pro-inflammatory cytokines, and moderate quantities of the immunosuppressive cytokine IL10
- an increased ability to present MHC class II peptides

Alternatively activated macrophages contribute to the production of the extracellular matrix, hence they are called "wound-healing macrophages" by Mosser & Edwards 2008. These macrophages are sometimes indicated by aaMΦs, M2s or M2as to stress their relation with type II T cells.

A different type of activation is triggered by exposure to IL10. These macrophages are characterized by the production of high quantities of IL10 and TNF-β, low quantities of IL12, and are associated with an immunoregulatory activity. These macrophages are generally called *deactivated* (Mantovani et al. 2004) or *regulatory* (Mosser & Edwards 2008). They are sometimes indicated by M2cs to stress their relation with type II immune response.

Additionally, the binding of the SIRP-α transmembrane protein on the surface of macropahges with the ligand CD47 has been associated with deactivation (Matozaki et al. 2009).

Activation is not an irreversible process: macrophages can change activation type or return to their inactivated state. Moreover, Mosser & Edwards

2008 suggests that in each macrophage the different activation types can coexist, with the role of a macrophage being determined by the predominance of one activation type over the others. A schematic representation of the activities of a macrophage in response to different activations is depicted in Figure 1.2.

Macrophages can join the forces and fuse, creating a so called "multinucleated giant cell" (MGC). MGCs are generally found in granulomas. The advantages and disadvantages of these cells are not completely clear, and very large MGCs in a model of human tuberculosis appear to be "unable to mediate any bacterial uptake Lay et al. 2007". IL4 has been found to promote the fusion of macrophages (Helminga & Gordon 2008).

To prevent two macrophage from phagocytosing each other during fusion, their activities need to be down regulated (for example by deactivation). For a review of macrophages fusion see Helminga & Gordon 2008.

Granulocytes

Lastly, Granulocytes or polymorphonuclear leukocytes, are phagocytes characterized by the presence of granules in their cytoplasm. There are three types of granulocytes: neutrophils, eosinofils, and basofils. Their lifespan is quite short and they live only few days. Granulocytes are recruited in large numbers to the site of infection during an immune response.

The main function of neutrophils is to phagocyte and destroy pathogens. However, they have been reported to perform immunoregulatory functions (Bordon 2010). In contrast to macrophages, neutrophils usually do not survive the phagocytosis of a pathogen, and dying or dead neutrophils make up a large part of the pus that forms in acutely infected wounds. The diversity of macrophage population is not observed in neutrophils.

While neutrophils are generally believed to be part of the innate immune system, it has been found out that some neutrophils display a T cell receptor (a characteristic that is generally associated with the adaptive immune system). This discovery suggests the possibility that neutrophils may be also using pathogen recognition mechanisms typical of adaptive immunity (Leavy 2006). For a partial review of neutrophil functions see Nathan 2006.

The functions of eosinophils and basophils are less well understood. However, they are believed to be important in the defense against large parasites.

Natural Killer T cells

Natural Killer T (NKT) cells are a relatively new discovery, and have been shown to both promote and suppress immune responses (see Bendelac et al. 2007 for a review of their functions and Godfrey et al. 2010 for a review of their diversity). NKT cells express both the T cells receptor (TCR) and the marker NK1.1. Some NKT cells express nor CD4 or CD8, while others

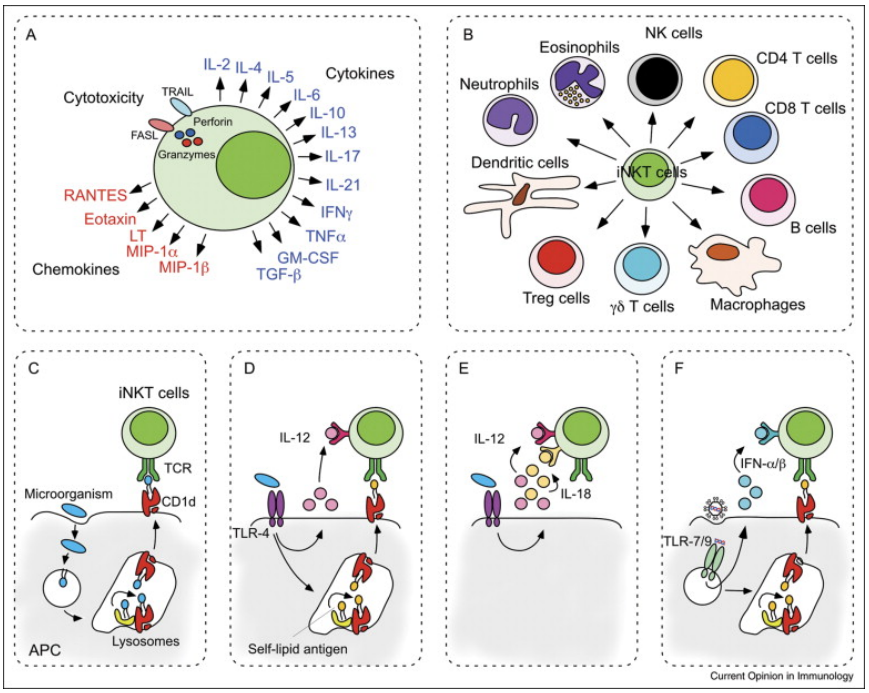

Figure 1.3: iNKT cells cytokine production (A), interaction (B), and activation mechanism (C-F) (from Matsuda et al. 2008)

express CD4 or CD8 (Godfrey et al. 2010). Two major groups of natural killer T cells exist: invariant natural killer T cells (also called iNKT cells or NKT cells type I) and variant natural killer T cells (also called NKT cells type II). In this section we will focus on iNKT cells, as they are more numerous than variant NKT cells and they have been studied more extensively.

Different mechanism of iNKT cell activation have been discovered (Matsuda et al. 2008 and Figure 1.3C-F). Once activated, iNKT cells interact with many leukocytes (see Matsuda et al. 2008 and Figure 1.3B).

One of the main characteristic of iNKT cells is the sustained production of IL4 and INFγ within minutes after activation. However, iNKT cells have been shown to produce many other cytokines: IL2, IL5, IL6, IL10, IL13, IL17, IL21, TNF-α, TNF-β, GM-CSF, and TGFβ. They also produce chemokines: CCL-3, CCL4, CCL5, CCL11. Figure 1.3A provides a schematic representation of the cytokines produced by iNKT cells.

iNKT cells can bind their surface protein CD47 to the transmembrane proteins SIRP-α displayed by macrophages (Matozaki et al. 2009). As noted before, the ligation of SIRP-α to CD47 leads to the deactivation of macrophages.

Activation of iNKT cells is reported to temporary down-regulate their surface receptor (Parekh et al. 2004), making these cells harder to identify

for some time after activation. As a consequence of that, it was thought that these cells underwent activation-induced apoptosis (Eberl & MacDonald 2000).

Natural Killer Cells

The main role of Natural Killer (NK) cells seems to be the induction of apoptosis in infected cells (see Yokoyama et al. 2004*a* for a review of NK cells life). The mechanism used by NK cells to identify infected cells is not completely characterized yet. However, the activation is inhibited by some MHC class I peptides displayed by uninfected cells. Intracellular parasites usually interfere with the production of these MHC I peptides, and therefore infected cells do not inhibit NK cells activation. It is, however, to be noted that some parasites have evolved the ability to produce MHC class I peptides that NK cells are not able to distinguish from the ones produced by uninfected cells (Yang & Bjorkman 2008). The cytotoxic activity of NK cells is increased by the exposure to INF-α and INF-β or IL12.

Besides their role of professional killer, NK cells produce a large number of cytokine (Biron et al. 1999). This production is enhanced by IL12 (see Maroof et al. 2008 and Mehrotra et al. 1998).

The activation of NK cells is sometimes amplified by NKT cells, this process is called by some authors "trans-activation". Trans-activation is not completely characterized yet. However, the results of Amprey et al. 2004 and Sullivan et al. 2010 suggest the importance of DCs in the process. More precisely Fujii et al. 2004 and Sullivan et al. 2010 indicate the ligation of CD40 on the surface of DCs as one of the mechanisms used by NKT cells to activate NK cells. Moreover, Sullivan et al. 2010 reports that activations of NKT cells performed by different proteins lead to different degrees of trans-activations. Example of trans-activation of NK cells are reported by Carnaud et al. 1999 and Paget et al. 2009.

1.3.2 Adaptive Immune System

T cells

T cells develop in the thymus (hence the "T" of their name) and are responsible for the so called "cell-mediated immune response". Instead of targeting a specific pathogen, they target cells that are infected by that pathogen. Each T cell possesses a possibly unique TCR, that binds to a class of peptides complexed with a MHC class I or II molecule. T cells that have not encountered their specific peptides are called "naïve T cells", they have no effector functions and circulate in the peripheral lymphoid tissues. Once the TCR of a T cell binds to a peptide, the cell differentiates into an "effector T cells" and undergoes clonal expansion. The process that gives effector functions to T cells is called *priming*, and is generally coadjuvated by dendritic cells.

Once it binds to a cell displaying the correct peptide, an effector T cell activates and initiates the production of cytokines and chemokines that influence the local environment.

Naïve T cells mainly develop into two lineage, those expressing surface protein CD4 — called $CD4^+$ T cells — and those expressing surface protein CD8 — called $CD8^+$ T cells. $CD8^+$ T cells develop into cytotoxic T cells, whose main role is to kill infected cells. $CD4^+$ T cells develop into helper or regulatory T cells, whose role is to stimulate and control the immune response.

While different subpopulations of $CD4^+$ T cells have been discovered, helper T cells are probably the better characterized. After the acquisition of effector functions, helper T cells are generally called T_H0 cells. T_H0 cells move to the bloodstream in search of the source of the infection and can differentiate into various types of mature helper T cells. Among the latter T_H1, T_H2, and T_H17 cells are the better characterized. This differentiation is controlled by the signals that T_H0 cells receive:

- T_H0 cells exposed to INFγ or IL12 differentiate into T_H1 cells
- T_H0 cells exposed to IL4 and IL10 differentiate into T_H2 cells
- T_H0 cells exposed to IL6 (or IL21) and TGFβ differentiate into T_H17 cells

Once activated, T_H1 cells are characterized by the production of high level of INFγ, IL2, and TNF-β. T_H1 cells express CD40 and FAS. Additionally, they can produce GM-CFS, TNF-α, IL3, and CXCL2. Experiments indicate that IL18 enhances their production of INFγ. Their proliferation is promoted by IL2 and INFγ, and antagonized by IL4. The main transcription factor responsible for the differentiation of T_H1 cells is believed to be "T-bet".

Due to the nature of cytokines they produce, the main role of T_H1 cells is to enhance the immune response by increasing the capability of macrophages to kill parasites. Experiments (e.g., Cooper 2009 in the context of tuberculosis) indicate that various populations of T_H1 cells with different phenotypes exist. These populations range from early activated cells producing mainly IL2, to cells producing mainly INFγ, to multifunctional cells producing sustained level of both IL2 and INFγ. The latter are very important since they are regarded as precursors of T_H1 memory cells, that is, long lived cells that allow to rapidly mount a response to a subsequent infection of the same type.

While both INFγ and IL12 promote the expression of T-bet, their effect is remarkably different. INFγ is an early promoter: it stimulates the expression of T-bet 2-4 days after differentiation. IL12 is a late promoter: it promotes the expression of T-bet 4-5 days after differentiation (Schulz et al. 2009). This "two-step activation (Leavy 2009)" limits the activity of T_H1 cells as IL12 is not produced directly by them.

Beside the one mentioned above, an additional mechanism that limits the pro-inflammatory activity of T_H1 cells exists. Some of these cells produce IL10 (Trinchieri 2007, and Rutz et al. 2008 for a possible explanation of the causes). T_H1 cells seem to initiate the production of IL10 after a prolonged exposure to INFγ. However, the biological bases of this change in their phenotype are still being studied.

Once activated, T_H2 cells are characterized by the production of high level of IL4 and IL5, and the expression of CD40. They also produce IL3, IL6, IL9, IL10, IL13, TGFβ, GM-CFS, CCL11, and CCL17. Their proliferation is promoted by IL2 and IL4 and antagonized by INFγ. The main transcription factor responsible for the differentiation of T_H2 cells is believed to be GATA-4.

The role of T_H2 cells is somewhat opposed to that of T_H1 cells. T_H2 cells are fundamental to the formation of certain types of granulomas (e.g. Schistosome granulomas). The IL10 they produce deactivates macrophages, decreasing their ability to kill parasite while allowing them to heal the extracellular matrix. Since classical activation can lead to the damage of local tissues, some authors believe that T_H2 cells alternatively activate macrophages to help the healing of the damage caused by classical activation.

T_H17 cells are a relatively new discovery. Once activated, they are characterized by the production of high level of IL17 and IL6. They also produce IL21, IL22, TNF, and CXCL1. It has been also shown that they can produce INFγ. IL23 supposedly supports their clonal expansion.

The role of T_H17 cells is not fully understood, however "the primary functions of T_H17 appears to be the clearance of pathogens that are not adequately handled by T_H1 or T_H2 cells (Korn et al. 2009)".

Yang et al. 2008 suggests that T_H17 cells and T_{REG} cells antagonize each other development, similarly to T_H1 and T_H2 cells. Moreover, T_H17 cells are generally the first type of $CD4^+$ cells to get to the site of infection. The main transcription factor responsible for the differentiation of T_H17s is believed to be RORγt.

The area of regulatory T cells is an active field of research (for a review see Feuerer et al. 2009). In the following we will only outline $CD4^+CD25^+$ regulatory T or T_{REG} cells. T_{REG} cells develop from naïve T cells exposed to TGFβ. Once activated, they produce IL10, TGFβ and GM-CSF. The main transcription factor responsible for their differentiation is an active research subject.

The role of T_{REG} cells is to control the immune response. For example, they reduce the inflammation by dampening the proliferation of T_H1 cells and reducing the growth of T_H2 cells. When T_{REG} cells do not work properly the organism is subject to autoimmune diseases.

$CD8^+$ T cells are called cytotoxic T cells. Once activated, these T cells have two main ways of killing a cell: either by releasing perforin, which *dig holes* into the membrane of the target cell, or by binding to FAS transmem-

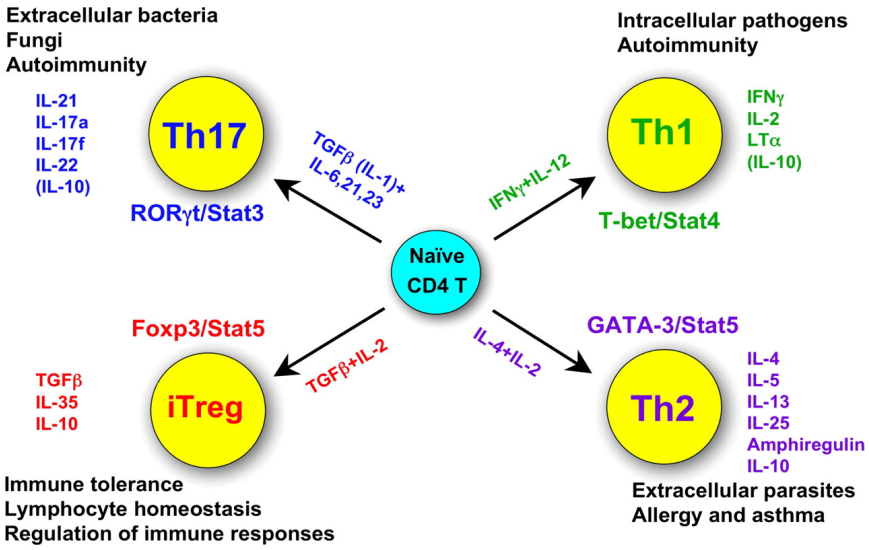

Figure 1.4: Different types of $CD4^+$ T cells (from Zhu & Paul 2008)

brane proteins. This binding activates the "extrinsic apoptosis pathway" resulting in the infected cells to undergo apoptosis.

Similarly to $CD4^+$ cells, $CD8^+$ cells have different subpopulations. T_C0, T_C1 and T_C2 cells have almost the same dynamics of T_H0, T_H1 and T_H2 cells, with the important difference that no IL10 production has been detected in T_C1 cells. The signals that promote the differentiation of T_C0 cells are the same as T_H0 cells.

If T_H1 and T_C1 cells are predominant, the immune response is said to be of type I, and if T_H2 and T_C2 are predominant, the immune response is said to be of type II.

B cells

While very important for many diseases, B cells do not seem to have a fundamental role in the immune response to leishmaniasis. Therefore, this section only provide a brief description of their working.

B cells develop in the bone marrow (hence the "B" of their name) and are responsible for the so called "antibody-mediated immunity". Each B cell possesses a possibly unique B cell receptor (BCR). When the BCR of a mature B cell binds to an antigen, the B cell proliferates and differentiates to a plasma cell. Plasma cells produce antibodies molecules, which are a free form of the BCR and have the same specificity. Antibodies molecules as a class are known as "Immunoglobulins".

Antibodies have three main functions:

- preventing pathogens from infecting cells by binding to them

- *marking* the pathogens, so that they can be easily recognized by phagocytes
- triggering nonspecific immune responses, such as the "complement pathway"

1.4 Cytokines and Chemokines

In the previous sections we mentioned a number of cytokines and chemokines. These proteins have different effects on cells. Moreover, some of them have different effects on the same cells depending to their concentration. Since the number of cytokines and chemokines used by the immune system is rather large, this section describes those that are more relevant to leishmaniasis. Unless specified, information is taken from Murphy & Kenneth 2007 and *COPE: Horst Ibelgaufts' Cytokines & Cells Online Pathfinder Encyclopaedia* 2010. Note that some of these proteins have many alternative names. These names are not indicated here unless used in articles cited in the bibliography, but can be found in *COPE: Horst Ibelgaufts' Cytokines & Cells Online Pathfinder Encyclopaedia* 2010.

- **Interleukin 1 (IL1)** is produced by classically activated macrophages. IL1 stimulates the proliferation and activation of NK cells, and promotes the adhesion of leukocytes, by stimulating the expression of adhesion proteins like CAM-1.
- **Interleukin 2 (IL2)** is produced by T_H0, T_H1, T_C0, and T_C1 cells. IL2 is a growth factor for all T cell subpopulations. IL2 also stimulates the growth of activated B and NK cells.
- **Interleukin 3 (IL3)** is produced by T_H1 cells, T_H2 cells, and some cytotoxic T cells. IL3 is a growth factor for hematopoietic cells, a type of stem cells that are progenitors of all blood cells.
- **Interleukin 4 (IL4)** is produced by T_H2 and T_C2 cells. IL4 induces the differentiation of T_H0 cells to T_H2 cells, and T_C0 cells to T_C2 cells. Additionally, IL4 promotes the proliferation of activated T cells, and up-regulates the expression of MHC class II molecules.
- **Interleukin 5 (IL5)** is produced by T_H2, T_C2 and activated NKT cells. IL5 is a hematopoietic growth factor responsible for the growth and differentiation of eosinophils and B cells. Moreover, IL5 promotes the generation of cytotoxic T cells from thymocytes.
- **Interleukin 6 (IL6)** is produced by classically activated macrophages, T_C2, T_H2, T_H17, and activated NKT cells. In the presence of TGFβ, IL6 induces the differentiation of T_H0 cells to T_H17 cells.

Cytokine	T-cell source	Effects on					Effect of gene knockout
		B cells	T cells	Macrophages	Hemato-poietic cells	Other somatic cells	
Interleukin-2 (IL-2)	Naive, T_H1, some CD8	Stimulates growth and J-chain synthesis	Growth	–	Stimulates NK cell growth	–	↓ T-cell responses IBD
Interferon-γ (IFN-γ)	T_H1, CTL	Differentiation IgG2a synthesis (mouse)	Inhibits T_H2 cell growth	Activation, ↑ MHC class I and class II	Activates NK cells	Antiviral ↑ MHC class I and class II	Susceptible to mycobacteria, some viruses
Lymphotoxin (LT, TNF-β)	T_H1, some CTL	Inhibits	Kills	Activates, induces NO production	Activates neutrophils	Kills fibroblasts and tumor cells	Absence of lymph nodes Disorganized spleen
Interleukin-4 (IL-4)	T_H2	Activation, growth IgG1, IgE ↑ MHC class II induction	Growth, survival	Inhibits macrophage activation	↑ Growth of mast cells	–	No T_H2
Interleukin-5 (IL-5)	T_H2	Mouse: Differentiation IgA synthesis	–	–	↑ Eosinophil growth and differentiation	–	Reduced eosinophilia
Interleukin-10 (IL-10)	T_H2 (human: some T_H1), T_{reg}	↑ MHC class II	Inhibits T_H1	Inhibits cytokine release	Co-stimulates mast cell growth	–	IBD
Interleukin-3 (IL-3)	T_H1, T_H2 some CTL	–	–	–	Growth factor for progenitor hematopoietic cells (multi-CSF)	–	–
Tumor necrosis factor-α (TNF-α)	T_H1, some T_H2 some CTL	–	–	Activates, induces NO production	–	Activates microvascular endothelium	Susceptibility to Gram –ve sepsis
Granulocyte-macrophage colony-stimulating factor (GM-CSF)	T_H1, some T_H2 some CTL	Differentiation	Inhibits growth?	Activation Differentiation to dendritic cells	↑ Production of granulocytes and macrophages (myelopoiesis) and dendritic cells	–	–
Transforming growth factor-β (TGF-β)	CD4 T cells (T_{reg})	Inhibits growth IgA switch factor	Inhibits growth, promotes survival	Inhibits activation	Activates neutrophils	Inhibits/ stimulates cell growth	Death at ~10 weeks
Interleukin-17 (IL-17)	CD4 T cells (T_H17) macrophages	–	–	–	Stimulates neutrophil recruitment	Stimulates fibroblasts and epithelial cells to secrete chemokines	–

Figure 8-34 Immunobiology, 7ed. (© Garland Science 2008)

Figure 1.5: The main T cells derived cytokines (from Murphy & Kenneth 2007)

- **Interleukin 9 (IL9)** is produced by T_H2 and T_C2 cells. IL9 stimulates the proliferation of a number of helper T cell clones in the absence of antigens or antigen-presenting cells.

- **Interleukin 10 (IL10)** is produced by T_H2, T_C2, T_{REG} and activated NKT cells. T_H1 cells also produce IL10 as a mean of self-regulation (Trinchieri 2007). IL10 inhibits the differentiation of T_H1 cells and deactivate macrophages.

- **Interleukin 12 (IL12)** is produced by classically activated macrophages, and, in low quantities, by alternatively activated macrophages. IL12 promotes the differentiation of T_H0 into T_H1 and the cytotoxic activity of NK cells.

- **Interleukin 13 (IL13)** is produced by T_H2, T_C2 and NKT cells. In conjunction with IL4, IL13 promotes alternative activation of macrophages.

- **Interleukin 17 (IL17)** is produced by T_H17 and NKT cells. IL17 promotes angiogenesis.

- **Interleukin 18 (IL18)** is produced by T_H1 and T_C1 cells. IL18 is a growth and differentiation factor for T_H1 and T_C1 cells. In presence of IL12, IL18 increases the production of INFγ by T_H1 and NK cells.

- **Interleukin 21 (IL21)** is produced by T_H17 and NKT cells. In conjunction with INFγ, IL21 promotes the differentiation of T_H0 to T_H1 cells.

- **Interleukin 23 (IL23)** is produced by classically activated macrophages. IL23 supports the clonal expansion of T_H17 cells.

- **Interferon γ (INFγ)** is produced by T_H1, T_C1, NKT, and some T_H17 and NK cells. INFγ induces the differentiation of T_H0 and T_C0 to T_H1 and T_C1 cells. In conjunction with TNF, INFγ classically activates macrophages. INFγ promotes the clonal expansion of T_H1 and T_C1 cells while inhibiting T_H2 and T_C2 cells growth.

- **Tumor necrosis factor α (TNFα)**, or simply Tumor Necrosis Factor (TNF) is produced by macrophages, T_H1, T_C1, T_H17, and NKT cells. TNFα increases the phagocytic activity of macrophages and, in conjunction with INFγ, leads to their classical activation.

- **Tumor necrosis factor β (TNFβ)** — sometimes also called Lymphotoxin α (LTα) or simply Lymphotoxin (LT) — is produced by regulatory macrophages, T_H1 cells, and T_C1 cells. TNFβ usually has the same effector functions of TNF-α but is less effective.

- **Transforming growth factor β (TGFβ)** is produced by T_H2, T_C2, T_{REG}, and NKT cells. TGFβ is fundamental in the differentiation of T_{REG} cells. TGFβ inhibits classical activation of macrophages.
- **Granulocyte-macrophages colony-stimulating factor (GM-CSF)** is produced by T_H1, some T_H2, T_{REG} and NKT cells. GM-CSF stimulates the differentiation of hematopoietic cells into macrophages and dendritic cells.
- **Chemokine (C-X-C motif) ligand 1 (CXCL1)** is produced by T_H17 cells and **Chemokine (C-X-C motif) ligand 2 (CXCL2)** is produced by T_H1 and T_C1 cells. Both chemokines have an angiogenetic fucntion and are chemoattractants for neutrophils.
- **Chemokine (C-C motif) ligand 3 (CCL3)** — also called MIP-1α — is produced by macrophages and NKT cells. CCL3 attracts monocytes, T, NK, and dendritic cells. Moreover, it stimulates dendritic cells to produce IL12 and promotes type I immunity.
- **Chemokine (C-C motif) ligand 4 (CCL4)** — also called MIP-1β — is produced by macrophages and iNKT cells. CCL4 attracts monocytes, T, NK, and dendritic cells.
- **Chemokine (C-C motif) ligand 5 (CCL5)** — also called RANTES — is produced by NKT cells and promotes the infiltration into tissues of a range of leukocytes, including effector T cells.
- **Chemokine (C-C motif) ligand 11 (CCL11)** — also called Eotaxin 1 — is produced by T_H2, T_C2 and NKT cells. CCL11 is a chemoattractant and activator for eosinophils.
- **Chemokine (C-C motif) ligand 17 (CCL17)** is produced by T_H2 and T_C2 cells and is believed to induce the adhesion of lymphocytes to the surface of blood vessels.

Chapter 2

The Biology of Experimental Visceral Leishmaniasis

This chapter presents the details of experimental visceral leishmaniasis, focusing the parasites activity and the immune response in the liver.

2.1 *Leishmania Donovani*

Leishmania donovani is an obligate intracellular protozoan of the genus Leishmania that causes the human systemic disease visceral leishmaniasis. The protozoan has two morphological stages: a flagellate stage called *promastigote*, and a flagellum-free stage called *amastigote*. When in promastigote form, it can move freely inside the bloodstream. Both forms of the protozoan are recognized and internalized by phagocytes; however, the amastigote form is more resistant to killing. Specifically, macrophages are able to efficiently kill the protozoan in promastigote form without the intervention of other leukocytes. However, they need to be classically activated to be able to kill the protozoan in amastigote form (see Section 1.3.1 for the description of classical activation of macrophages).

When in amastigote form, *leishmania donovani* is able to replicate inside macrophages, however "while their presence in dendritic cells, neutrophils, and even fibroblasts has been described, there is no evidence that amastigotes can actively replicate in a cell other than a macrophage (Peters & Sacks 2006)".

The mutation to the amastigote form is triggered by phagocytosis and takes about 24 hours.

2.2 Visceral Leishmaniasis

Leishmania donovani uses sand flies as vectors for the infection. When an infected sand fly bites a vertebrate, the parasite is transferred to the vertebrate skin, and subsequently moves to a number of internal organs — mainly spleen, liver and bone marrow —, hence the name visceral. The mechanism that allows the protozoan in promastigote form to move from the skin to the internal organs is still unclear. However, some time after the infection, some resident macrophages of internal organs are infected by the protozoa in amastigote form.

Experiments on murine models suggest the importance of neutrophils for the migration of the parasites inside the body. Leishmania major has been shown to use neutrophils to move from the skin to the internal organs and Peters et al. 2008 indicates that depleting the neutrophils reduces the ability of the parasite to establish an infection. Moreover, van Zandbergen et al. 2004 suggests that macrophages are not able to promptly responds to infection because, instead of consuming the parasite, they are consuming infected apoptotic neutrophils. However, *leishmania donovani* seems to act differently, and McFarlane et al. 2008 reports that depleting neutrophils increases the number of parasite in the spleen and bone marrow, thus suggesting that the course of infection differs in *leishmania donovani* and major.

Figure 2.1 gives a schematic representation of the mechanism used by leishmania to spread leishmaniasis.

Once the parasite has infected the internal organs, three outcomes are possible:

- **healing**: if the host is able to mount and adequate immune response all the protozoa are killed and the infection is cleared
- **death of the host**: if the immune response is too weak (or too strong) the parasite (or the infection) kills the host
- **chronic infection**: if the immune response is not strong enough to completely clear the infection, but is able to control and stabilize the number of parasite, leishmaniasis develops into a chronic disease.

In the following we will focus on the immune response in the liver. In this organ, the outcome of the disease largely depends on the characteristics of a localized immune response called "granuloma". The granulomas are complex multicellular structures that allow the immune system to build a controlled environment to better respond to an infection. Besides being characteristic of leishmaniasis, granulomas are important for the outcome of other diseases such as tuberculosis.

Schematically, a granuloma is an agglomerate of resident and non-resident macrophages, surrounded by different types of cells — mainly T cells. The

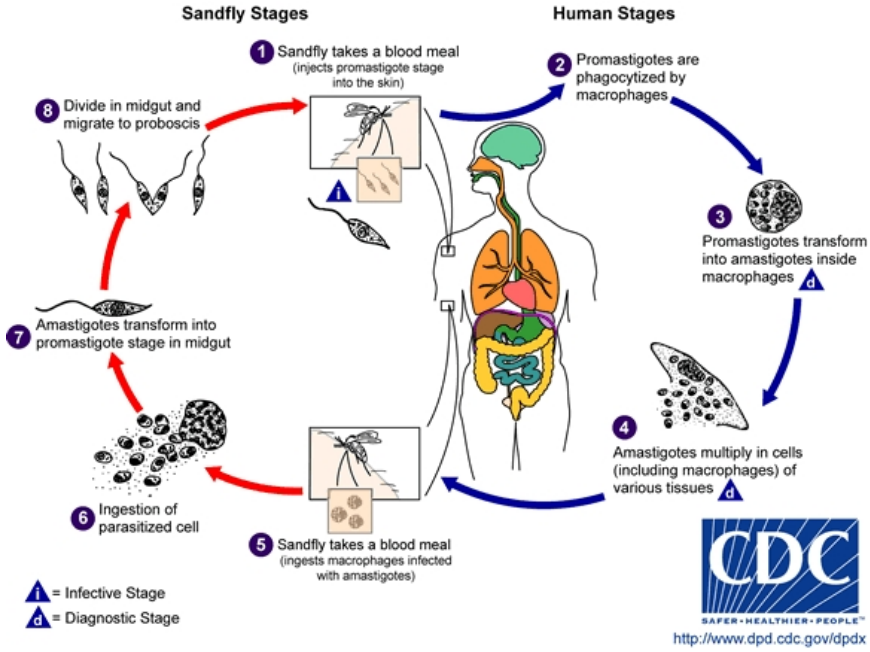

Figure 2.1: Life cycle of Leishmania (from http://www.dpd.cdc.gov/dpdx/hTML/ImageLibrary/Leishmaniasis_il.htm)

roles of T cells are to control and regulate the activity of macrophages. T_H1 and T_C1 cells classically activate macrophages, allowing resident macrophages to kill phagocytosed parasites more efficiently. When classically activated, macrophages can be dangerous for the organism, as they can harm the cells of the blood vessels. Therefore, this activation needs to be controlled. A healing infection is characteristic by a *just right* level of activation achieved by a regulation of the inflammatory response response possibly by T_H2 and T_{REG} cells (see Choi & Kropf 2009 for some data on leishmania major infection).

Due to the incomplete understanding of the initial stage of the infection, many experiments consider "experimental visceral leishmaniasis". Experimental visceral leishmaniasis is a wet lab approximation of visceral leishmaniasis: the infection is initiated by injecting leishmania protozoa in amastigote form directly in the body of specific strains of mice (generally in the tail).

2.3 Functions of the Immune Cells

The systemic activity associated with the formation, and maintenance, of a granuloma in the liver is complex, and yet to be completely understood. In this section we describe the leukocytes that are reported to play major roles

in the process. We also present the details of the interactions between these leukocytes and *leishmania donovani* when data are available.

Macrophages

Two types of macrophages form the main structure of a granuloma: resident and non-resident macrophages. The former are called "Kupffer cells" (see Figure 1.1). While both types of macrophages contribute to the outcome of the disease, only Kupffer cells internalize the protozoa. Kupffer cells need to be classically activated to be able to kill *leishmania donovani*, and experiments suggest that the protozoa interfere with the biological pathway for classical activation (see Ghosh et al. 2005, Ghosh et al. 2002 and Nandana & Reiner 2005). Moreover, *leishmania donovani* has been reported to increase the production of IL10 by macrophages (Bhattacharyya et al. 2001) and induce a reduced secondary MCH I expression in macrophages (Reiner et al. 1987). These facts suggest that leishmania may deactivate Kupffer cells.

Note that, deactivated and alternatively activated macrophages are an ideal environment for the amastigotes, as they both have a low parasiticidal activity. Additionally, alternatively activated macrophages provide the protozoan with additional nutriments (polyamines).

T cells

Together with macrophages, type I T cells (both $CD4^+$ and $CD8^+$) are the most important leukocytes for the formation and maintenance of granulomas, as they are the main source of INFγ that drive macrophages towards a sustained classical activation. Note that the cytotoxic activity of $CD8^+$ T cells seems to be not relevant for the immune response to leishmaniasis.

Dentritic Cells

DCs have an indirect role in granuloma formation in the liver, as they ingest the parasite and migrate to the spleen to prime T cells. They have been shown to have a direct role in granuloma formation in the spleen as infection from *leishmania donovani* amastigotes stimulate DCs to produce IL12 (Gorak et al. 1998), which may be responsible for the activation of NK cells and the drift of T cells towards a type I phenotype.

Natural Killer Cells

Beige mice are reported to have defective NK cells. However, their NKT cells activate correctly in response to α-galactosylceramide (Nakagawa et al. 2001). Since Kirkpatrick & Farrell 1982*a* reports that beige mice are unable to control the growth of the parasites in the liver, NK cells seem to play a

very important in the immune response to *leishmania donovani*. However, their role is still being investigated.

NK cells react to leishmaniasis by the production of INFγ within the first days after infection (Schleicher et al. 2007), and later initiate the production of IL10 (Maroof et al. 2008). However, it must be pointed out that NK-derived INFγ seems to be ineffective in activating macrophages (Svensson et al. 2005). IL12 has a role in NK activation (Amprey et al. 2004), and dendritic cells may be an early source of IL12, while classically activated macrophages are the main contributors at a later stage.

Natural Killer T cells

There is not a general consensus on the populations of NKT cells reacting to leishmania -nfected macrophages. However, it is clear that iNKT cells play a major role, since they contribute to the formation of granulomas as an early source of INFγ (Amprey et al. 2004). Experiments indicate that the immune system is able to mount an adequate response which ultimately lead to healing even without iNKT (see Stanley et al. 2008 for C57BL/6 and Amprey et al. 2004 for BALB/c mice).

Additionally, the data of Stanley et al. 2008 indicate that activation of iNKTs by α-galactosylceramide 7 days after infection enhances parasite growth. There is, however, a caveat in interpreting these data: iNKTs produce large quantities of both INFγ and IL4 after the stimulation with α-galactosylceramide (Kawano et al. 1997). IL4 production peaks at around 2 hours after activation and then rapidly decreases, while INFγ production is very low 2 hours after activation, but is sustained 4 hours later (Parekh et al. 2004). However, in experimental visceral leishmaniasis, iNKTs are reported to produce sustained levels of INFγ but non detectable levels of IL4 2 hours after infection (Amprey et al. 2004).

Therefore, while Stanley et al. 2008 indicates that α-galactosylceramide is not an effective way of treating leishmania, it does not rule out the possibility that activating iNKTs by other means can be beneficial. Moreover, some authors believe that different populations of iNKT cells exists, each reacting to different stimuli (Godfrey et al. 2010).

2.4 The Time Line of a Granuloma

Schematically, the development of an effective granuloma in the liver during experimental visceral leishmaniasis is characterized by the following time line. Note that these values are derived from to the scientific literature presented above, and large variabilities are to be expected when considering different experimental conditions.

hour 0 The parasites reach the liver.

from hour 0 to hour 5 Kupffer cells phagocytose the parasite, produce TNF, and initiate the display of leishmania-related MHC class I and II peptides on their surface. Dendritic cells ingest the parasite and migrate to the spleen to mature. The parasites initiate to replicate and to stimulate the production of IL10 from Kupffer cells (Bhattacharyya et al. 2001).

from hour 5 to hour 96 (day 4) NKT cells activate and produce INFγ (Amprey et al. 2004). The binding of SIRPα on the surface of Kupffer cells deactivates them (Matozaki et al. 2009). NK cells activate and produce INFγ (Schleicher et al. 2007). Chemokines produced by NKT cells, stimulate the arrival of non-resident macrophages. The parasite burden increases (Murray et al. 2006).

from hour 96 (day 4) to hour 336 (day 14) Effector T cells get to the liver and initiate to differentiate. The differentiation is driven toward a type I immune response (Miralles et al. 1994). The cytokines produced by the T cells classically activate macrophages. The chemokines produced by type I T cells stimulate the arrival of non-resident macrophages. The parasite burden increases (Murray et al. 2006).

from hour 336 (day 14) to hour 504 (day 21) The parasite burden increases (Murray et al. 2006).

from hour 504 (day 21) to hour 672 (day 28) There is a detectable presence of IL10-producing NK cells (Maroof et al. 2008). The parasite burden reaches a maximum, and initiates to decrease (Murray et al. 2006).

from hour 672 (day 28) to hour 1344 (day 56) The parasite burden decreases (Murray et al. 2006).

from hour 1344 (day 56) to hour 2016 (day 84) The parasite burden is low, and reaches a non-detectable level by day 84 (Murray et al. 2006).

Chapter 3

Modeling preliminaries

This chapter discusses some aspects of immunological modeling, with a focus on previous works in the context of granuloma modeling.

3.1 General Remarks on Biological Modeling

3.1.1 Problems and Challenges in Immunological Modeling

While a lot of progress has been made in understanding the working of the vertebrate immune system, many details of its development and behavior are still active areas of research. For example, the factors leading to the *lineage decision* of many leukocytes are unknown, and even the roles of some leukocytes are not well-understood.

Additionally, different mice models can lead to different behaviors, which can be a problem because "in April 2006 [...] scientists at the US National Institutes of Health found that nearly 4,000 unique mice strains had been created (*The sharing principle* 2009)".

Finally, performing experiments *in vivo* or *in vitro* can lead to results very different both quantitatively and qualitatively. This is a consequence of the many interactions that take place *in vivo* which are not reproducible *in vitro*.

In the context of leishmaniasis, iNKT cells are a good example of these problems. Their activation mechanisms are not completely understood and their lifespan is unknown; they seem to behave differently in C57BL/6 (Stanley et al. 2008) and BALB/c (Amprey et al. 2004) mice; moreover, data suggest the presence of different numbers of liver iNKT cells in the two strain of mice (Matsuda et al. 2000). Finally, liver iNKT cells react to leishmania infected macrophages by producing INFγ (Amprey et al. 2004); however, activation of iNKT cells by α-galactosylceramide, which is commonly used in experiments, leads to a sustained production of both INFγ and IL4 (Kawano et al. 1997 or Bendelac et al. 2007)

Since these problems will likely be solved by the advances in technology, why not just wait for the immunological research instead of building numerical models to address them? To begin with, we do not know when the required technology will be available, and how expensive it will be. Additionally, numerical models help immunologists in designing experiments that can be used to increase their understanding with the current technology.

However, to achieve this goal, we must carefully describe the building of the model. We need to explicitly document the assumptions and data sources used, with the ultimate goal of understating how the outcomes of the model are influenced by them. Moreover, when different hypotheses exist, the model should be able to test their consequences, trying to determine which one fits better the experiments.

3.1.2 Modeling Techniques: Population Dynamics VS Agent Based

While many different modeling techniques have been used over the years, most of them can be categorized into two approaches: "population dynamics" and "agent based".

In population dynamics approaches, the behavior of the system is studied at the population level. This means that all the individuals are equal, and therefore assumed to behave in the same way. Many mathematical models fall in this category.

Classical techniques to study population dynamics of systems are: real valued differential equations (where the value of the functions indicates the number of individual of a population), difference equations, or Petri nets (where different places indicate different populations and the number of tokens in a place indicates the number of individual of the population represented by that place).

A detailed discussion of many differential equation models in biology can be found in the two volume book by J. D. Murray "Mathematical Biology" (Murray 2002 and Murray 2003). While many examples of the uses of different types of Petri nets in modeling biology can be found in Will & Heiner 2002. Classical examples of population dynamics models include Susceptible-Infectious-Recovered (SIR) models for epidemics — originally proposed by McKendrick in 1925 (M'Kendrick 1925) — and Lotka-Volterra models — proposed independently by Lotka in 1925 (Lotka 1925) and Volterra in 1926 (Volterra 1927).

Population dynamics approaches are able to deal efficiently with very large populations, but assume homogeneous populations.

Agent based models describe the behavior of the system at the individual level. This means that each individual of the population is dealt with independently. Many computer science or engineering models belong to this category. Each agent is associated with a behavior (usually prob-

abilistic), which specifies how it interacts with the environment and other agents. Given the large number of cells involved in most biological process, agent based models have been applied to biology only in recent years.

From a descriptive point of view, agent based system can be specified by UML diagrams such as activity and state machine diagrams. While actual simulations are generally performed using specific programming toolkits such as MASON (Luke et al. 2005). Historically, the game of life by John Conway is probably one of the first agent based models (Gardner 1970). Important contributions to the theory of agent based models (specifically on "cellular automata") have been provided by Stephen Wolfram (see for example Wolfram 1994, which collects some of his most important papers on the subject).

Agent based models are relatively slow, as the simulation of realistic models requires a lot of computing power. They rarely allow the precise analysis that can be performed on mathematical population dynamics models, and validation of agent-based models is a particularly active field of research (see for example Klügl 2008).

3.2 Granuloma modeling so far

Modeling the formation and evolution of the granuloma, considered as general immunological phenomenon is far from straightforward. This is due to a number of reasons:

- **Complexity**. The process of formation and maintenance of a granuloma is achieved by the interaction of many types of cells.

- **Diversity**. While granuloma formation is quite ubiquitous in the body, different diseases have remarkably different dynamics. Moreover, even in the context of the same disease, the differences in the microenvironments of the different organs lead again to different dynamics. Finally, even for the same disease and organ, granulomas usually vary, both in size and time of formation.

- **Limited biological knowledge**. Many important biological processes behind the formation of granulomas are still incompletely characterized.

- **Experiments**. It is difficult to design experiments focusing on the formation (and dissolution) of a single granuloma.

Therefore, even if some modeling attempts have been published, many of them have severe limitations.

3.2.1 Tuberculosis

In the context of tuberculosis (which causes the formation of granulomas in the lungs), an important modeling effort is being carried out by the group directed by Denise Kirschner. In the following we will describe how the model evolved over the years. These models focus on the formation of the granuloma, rather than on the full process, and do not attempt to model healing infections.

In Wigginton & Kirschner 2001, the authors develop a deterministic population based model using ordinary differential equations. The model studies the populations of entities that contribute locally to the formation of granulomas: macrophages (resting, activated and chronically infected), cytokines (INFγ, IL12, and IL10), helper T cells (T_H0, T_H1, and T_H2), and bacteria (intracellular and extracellular). The several parameter used by the model are estimated using values obtained from experiments whenever possible.

In Marino & Kirschner 2004, the authors extend the previous model by introducing the dynamics of dendritic cells and naïve T cells. Adding these new populations has a deep impact on the model, as granuloma formation can be studied from a systemic point of view. This allows, for example, to study the impact of systemic processes (such as the decrease of T cells diversity, which is believed to be a consequence of aging Naylor et al. 2005) on granuloma formation.

In Gammack et al. 2004, the authors extend the model of Wigginton & Kirschner 2001 by considering the space distribution of the cells. Granuloma is studied locally (the dynamics of dendritic cells is not included) as a three-dimensional process. This allows for a more direct control of cell-to-cell interactions which are very important as T cells require direct contact to activate. The space is introduced by the use of partial differential equations. While partial differential equations give a clear representation of granuloma formation, dealing with them is usually quite difficult and to study the model from a numerical point of view, the authors introduced many simplifications.

In Ganguli et al. 2005 the authors present a two-dimensional model using multiple compartments ordinary differential equations (that is, a model in which the space is divided into multiple zones and to each zone is associated with a system of differential equations). This formalism does not require the simplification used in Wigginton & Kirschner 2001, and can be used to study a broader parameter space.

In Gammack et al. 2005, the authors introduce a local agent based approach. While the details of the model are not presented, the authors discuss the advantages and disadvantages of the developed model. This discussion allows the reader to understand how some problems of granuloma formation are better dealt with by different simpler models, rather than by a single complicated model, which would be hard both to understand and solve or simulate.

In Ray et al. 2009, the authors used an agent based model, based on Gammack et al. 2005, to understand the role of TNF in the conformation of granulomas. Besides the importance of the results from a biological point of view — the shape of granuloma affects its effectiveness —, this article is useful in understanding the evolution of the models and of their goals over the years.

The agent based model described by Ray et al. 2009 is used just like a murine model. The article even contains a "Materials and Methods" section. This section is common in biological articles, and describes the fundamental biological information used to replicate the experiments (e.g., the mice strain). This implies an important change in the role of the model. While in Wigginton & Kirschner 2001 the mathematical model is used to describe the *results of biological experiments*, in Ray et al. 2009 the computational model is used to study the *consequences of the biological assumptions* used to build the model.

The model has become a tool to *test*, and possibly increase, the biological knowledge rather than a way to use the current biological knowledge to predict the behavior of a phenomenon. This trend is not limited to leishmaniasis, and the number of papers presenting qualitative mathematical and computer science models are increasing in popular immunological journals such as "The Journal of Immunology[1]" or "Nature Immunology[2]".

The above modeling effort is also useful in understanding how the different modeling techniques provide different insights into the biology of a disease. A population dynamics model can provide important insights into the global behavior of the disease. However, an agent based model can provide important insights into the local behavior of the model. More importantly, the two modeling techniques complement each other, and provide important information that can be used both by modelers and biologists.

3.2.2 Leishmaniasis

In the context of leishmaniasis, an agent based model of the formation of the granuloma is being developed by the group of Jon Timmis. Flugge et al. 2009 presents a qualitative model of the granuloma formation, and stresses the importance of a precise characterization of the assumptions used. While the model is quite limited from a global point of view, its focus on the local interactions gives a good understanding of some mechanisms underlying granuloma formation.

[1] http://www.jimmunol.org/
[2] http://www.nature.com/ni/

Chapter 4

Some Fundamentals of Petri Nets and Sensitivity Analysis

This chapter presents the rationale for our modeling decisions. Additionally, the basics of stochastic Petri nets and some aspects of sensitivity analysis are introduced. The material presented is based on Marsan et al. 1995 (for stochastic Petri nets) and Saltelli et al. 2000 (for sensitivity analysis), which we refer to for more systematic discussions.

4.1 Modeling Decisions

4.1.1 Why Stochastic Petri Nets?

As discussed in Section 3.2.1, different formalisms can be used for immunological modeling. However, the characteristics of liver granuloma and the type of study that we wanted to perform, provided a number of indications that suggested the use of stochastic Petri nets.

The number of certain cells contributing to the liver immune response to leishmaniasis is very low. For example, direct observations of liver granulomas indicate that the number of NK cells is usually between 0 and 2. Therefore, a formalism characterized by discrete entities (e.g., Petri nets, difference equations) seemed preferable to a formalism characterized by continuous entities (e.g., continuous Petri nets, differential equations).

The population of liver granulomas is characterized by a large variability in the size of the single granuloma. The source of this variability is not evident, but is likely connected to different initial conditions of the microenvironment. Moreover, our preliminary tests indicated that using stochasticity led to a parasite burden qualitatively very similar to the one observed in experiments, suggesting that a stochastic model should be preferred.

Given the complexity of the phenomenon, and the relatively simple mod-

els of liver granulomas developed so far, we decided to focus on the role of whole population of cells. This approach allowed us to determine the role of the different leukocytes and to understand how a therapy should be designed. Therefore, we preferred a population dynamics modeling which allows a faster simulation and a focus on population-to-population rather than cell-to-cell interaction.

The above observations, in conjunction with the advantages of a visual modeling provided by Petri nets, persuaded us to use stochastic Petri nets.

4.1.2 Additional Remarks on Space

Our model disregarded two aspects of the immune response to leishmaniasis:

1. the spacial interaction of the cells in the local environment of a granuloma
2. the interaction among the various granulomas (and thus the structure of the *network* of granulomas)

Given their importance, we will provide a rationale for our choice.

Space plays a very important role in immunology: cells live in a complex environment that restricts some of their movements while promoting others. Moreover, leukocytes change in size during their life, and some immune responses heavily rely on these changes (e.g., the priming of T cells). However, determining which aspects of spatial interactions are fundamental can be difficult in a complex environment such as a granuloma, and modeling all the aspects of spatial interactions can lead to a model too complicated to understand. Additionally, only few data exist on the dynamics of the spatial interactions of cells at the level of a single granuloma (some data can be found in Beattie at al. 2010 (EJI)), making the validation of a *spatial-aware* model tricky.

The network of granulomas is another important aspect to be considered for the immune response, as some cells migrate from one granuloma to another. However, the topology of the liver is complex, and additional angiogenic processes may change it during the infection. Therefore, determining the topology to be used in the model, and its possible variation is not an easy task.

A possible solution to the above problems is to build a *space-less local* model. Such a model will likely be able to provide us with some important insights of the fundamental characteristics of the immune response to leishmaniasis, and can subsequently be used as touchstone to determine the role of local, and global, spacial interactions.

Therefore, while we comprehend the importance of space in biological modeling, we believe that such an aspect should be considered only after a good understanding has been gained either by biological experiments, or by space-less modeling.

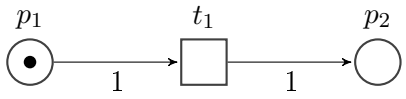

Figure 4.1: A very simple Petri Net

While our Petri net model can be extended to consider a fixed network of granulomas, space-aware models are easier build using agent based models (as in Flugge et al. 2009) or partial differential equations (as in Gammack et al. 2004). However, the stochasticity of the process suggests that an agent based model may be the preferable choice if spatial interactions are to be analyzed.

4.2 Petri Nets

Petri nets are a formalism widely-used by many modeling communities. This section presents only some fundamental definitions, focusing on stochastic Petri nets, as that is the formalism that we used for our model. Some important concepts (e.g., p-invariants and t-invariants) are not presented because not relevant to our model.

4.2.1 General Definitions

Figure 4.1 depicts a simple Petri net, which contains its three main parts: places, transitions and arcs. Place are represented by circles, while transitions are represented by squares. Places contain a variable number of tokens, which are generally indicated by black dots or Arabic numbers. Tokens moves from, or to, a place by means of transitions. The marking of the net is defined by the number of tokens in each place. Three fundamental types of arc are possible:

- input arcs, represented by arrows-headed arcs connecting places to transitions
- output arcs, represented by arrows-headed arcs connecting transitions to places
- inhibitor arcs, represented by circle-headed arcs connecting places to transitions

Each arc is associated with a multiplicity, which indicates the number of tokens it acts on. A Petri net describes a system from a structural point of view, and is formalized by Definition 1.

Definition 1 (Petri Net (Marsan et al. 1995, p. 33))**.** *A Petri net is a 5-tuple* $N = \{P, T, I, O, H\}$ *where*

- P *is the set of places*
- T *is the set of transitions,* $T \cap P = \varnothing$
- $I, O, H : T \to Bag(P)$*, are the input, output and inhibition functions, respectively, where* $Bag(P)$ *is the multiset on* P*.*

Over a Petri net, we can build a Petri net model by adding information on the marking. Definition 2 provides a formal characterization of a Petri net model.

Definition 2 (Petri Net Model (Marsan et al. 1995, p. 30))**.** *A Petri net model is an 8-tuple* $M = \{P, T, I, O, H, PAR, PRED, MP\}$ *where*

- P *is the set of places*
- T *is the set of transitions,* $T \cap P = \varnothing$
- $I, O, H : T \to Bag(P)$*, are the input, output and inhibition functions, respectively, where* $Bag(P)$ *is the multiset on* P
- PAR *is a set of parameters*
- $PRED$ *is a set of predicates restricting parameter ranges*
- $MP : P \to \mathbb{N} \cup PAR$ *is the function that associates with each place either a natural number or a parameter ranging on the set of natural, and is the parametric initial marking.*

Additionally, for a transition $t \in T$, we define

- ${}^\bullet t = \{p \in P : I(t,p) > 0\}$, which represents the input sets of transition t
- $t^\bullet = \{p \in P : O(t,p) > 0\}$, which represents the output sets of transition t
- ${}^\circ t = \{p \in P : H(t,p) > 0\}$, which represents the inhibition set of transition t

where $I(t,p)$, $O(t,p)$, and $H(t,p)$ denote the multiplicity of element p in the multisets $I(t)$, $O(t)$, and $H(t)$.

A Petri net model describes a family of real systems. If we want to model a specific system, we need to assign a value to each parameter used by MP. A Petri net system is a Petri net model with an initial marking completely specified, and is formally described by Definition 3.

Definition 3 (Petri Net System (Marsan et al. 1995, p. 32))**.** *A Petri net system is the 6-tuple* $S = \{P, T, I, O, H, M_0\}$ *where*

- P *is the set of places*

- T *is the set of transitions,* $T \cup P = \varnothing$
- $I, O, H : T \to Bag(P)$*, are the input, output and inhibition functions, respectively, where* $Bag(P)$ *is set of all possible multisets on* P
- $M_0 : P \to \mathbb{N}$ *is the initial marking, that is, a function that associates with each place a natural number.*

So far, we described the *statics* of Petri net systems, now we will move to the *dynamics*. To this end, we need to discuss how transitions change the marking. When an enabled transition fires, it removes tokens from its input place(s) and add tokens to its output place(s). Formal definitions of these concepts are introduced by Definitions 4 and 5

Definition 4 (Enabling (Marsan et al. 1995, p. 34))**.** *Transition* t *is enabled in marking* M *if and only if*

- $\forall p \in {}^\bullet t, M(p) \geq O(t,p)$ *and*
- $\forall p \in {}^\circ t, M(p) < H(t,p)$

Definition 5 (Firing (Marsan et al. 1995, p. 34))**.** *The firing of transition* t*, enabled in marking* M*, produces marking* M' *such that*

$$M' = M + O(t) - I(t)$$

The rules describing the actual firing of transitions vary among different Petri nets formalisms. Section 4.2.2 describes the firing rules of stochastic Petri nets. However other rules exist in the literature.

4.2.2 Stochastic Petri Nets

The original Petri net model does not include the notion of time. However, most real systems require a specific amount of time to change their configuration. To account for this fact, stochastic Petri nets associate each transition with parameter that characterize the time elapsed between the enabling and the actual firing. The waiting time of a transition is exponentially distributed, this choice has several advantages that will be described later.

The definition and properties of exponentially distributed variables presented below can be found on any introductory book on statistic (e.g., Mood et al. 1974).

Definition 6 (Exponential distribution)**.** *A random variable* X *is said to be (negative) exponentially distributed, if its probability density function is*

$$f_X(x, \lambda) = \begin{cases} \lambda e^{-\lambda x} & \text{if } x \geq 0 \\ 0 & \text{if } x < 0 \end{cases}$$

The cumulative density function of an exponentially distributed variable X is

$$F_X(x,\lambda) = \begin{cases} 1 - \lambda e^{-\lambda x} & \text{if } x \geq 0 \\ 0 & \text{if } x < 0 \end{cases}$$

its expected value is

$$E[X] = \frac{1}{\lambda}$$

while its variance is

$$\mathrm{Var}[X] = \frac{1}{\lambda^2}$$

An exponentially distributed variable X is memoryless, that is

$$P[X > x + k | X > x] = P[X > k]$$

for all $x, k \geq 0$ (see Section A.2 for the proof). As we will discuss later, this property is very important for stochastic Petri nets.

Finally, given n independent exponentially distributed random variables $X_1, \ldots X_n$ with parameters $\lambda_1, \ldots, \lambda_n$, then

$$X_{\min} = \min(X_1, \ldots X_n)$$

is exponentially distributed with parameter

$$\lambda_{\min} = \lambda_1 + \cdots + \lambda_n$$

(see Section A.1 for the proof).

Assume now that we have a stochastic Petri net with marking M_j, the generic transition t_i is associated with a possibly marking-dependent parameter $\lambda_i(M_j)$ which should be interpreted as the parameter of a negative exponentially distributed random variable. Therefore, the expected waiting time of t_i is $1/\lambda_i$.

Using the properties of exponentially distributed variables, we can easily determine the expected "sojourn time" of the system in a marking M_j. Let $E(M_j)$ be the set of all enabled transitions in M_j, the sojourn time in marking M_j is the minimum of the random variables associated with the enabled transitions (Marsan 1990), and therefore a negative exponentially distributed random variable $\tau(M_j)$ with mean

$$\left(\sum_{i:t_i \in E(M_j)} \lambda_i(M_j) \right)^{-1} \tag{4.1}$$

Additionally, the probability that a given transition, say t_k, samples the minimum delay instance, and hence determines the change of marking by firing is (Marsan 1990):

$$P\{t_k | M_j\} = \frac{\lambda_k(M_j)}{\sum_{i:t_i \in E(M_j)} \lambda_i(M_j)} \tag{4.2}$$

Given a stochastic Petri net system with marking M_j, to simulate its evolution we will sample from $\tau(M_j)$ to determine how long the system will stay in that marking, and then we will use the probabilities of Formula 4.2 to determine the transition to be fired. This simplicity is largely due to the memoryless property of negative exponentially distributed random variables.

Note that, since the probability that two negative exponentially distributed random variables samples a specific value x equals zero, the probability of two transitions firing at the same time is zero.

A stochastic Petri net system with initial marking m_0 and a simulation interval $[t_0, t_{max}]$, can be simulated by Algorithm 4.1. The algorithm is an adaptation of "Gillespie's algorithm" (Gillespie 1977) to stochastic Petri net systems and is mainly from Heiner, Richter, Schwarick & Rohr 2008.

Algorithm 4.1 Simulation for SPNS

$t \leftarrow t_0$
$m \leftarrow m_0$
print (t, m)
while $t < t_{max}$ **do**
  determine duration τ until next firing
  $t \leftarrow t + \tau$
  determine transition i firing at time t
  $m \leftarrow \text{fire}(m, i)$
  print (t, m)
end while

Notably, stochastic Petri net systems can be converted to other formalisms. More precisely, stochastic Petri net systems can be converted to discrete Markov chains (see chapter 6 of Marsan et al. 1995), with different marking of the nets corresponding to different states of the chain. However, the state space can be very large (or even infinite), making this conversion meaningful only for certain net types. Additionally, stochastic Petri net systems can be approximated by continuous Petri net systems, which can then be converted into systems of ordinary differential equations (see for example Heiner, Gilbert & Donaldson 2008*a*).

4.2.3 Snoopy and Additional Remarks

The tool used during the designing and the simulation of our model is Snoopy version 2 (build 0.9) (Heiner, Richter, Schwarick & Rohr 2008) on Windows® 7 Professional. The hardware used is a personal computer with an Intel® Core™ 2 Quad Processor Q9550 and 4 Gb of RAM.

The implementation of stochastic Petri net system of Snoopy include some features which are not included in the classical model. Specifically, our model used read and modifier arcs, immediate transitions, and deterministic-

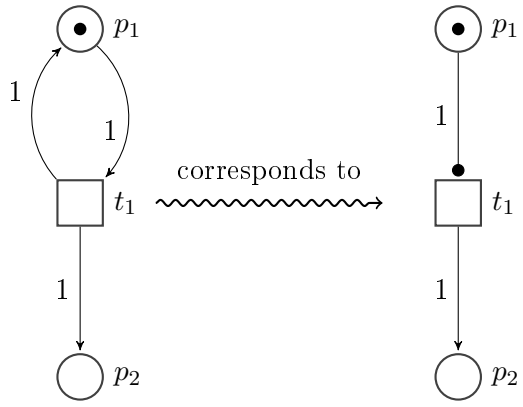

Figure 4.2: Test Arcs

timed transitions.

Read (or test) arcs connect places to transitions. They check the number of tokens in a place, but do not remove the tokens when the transition is fired. A read arc r with cardinality c from place p to transition t corresponds to an output arc o of cardinality c from p to t plus an input arc i of cardinality c from t to p (See figure 4.2). Modifier arcs connect places to transitions, but do not change the number of tokens of the places when they fire. They are used to indicate that the number of tokens of one of more places is uses to define the parameter of that transition. Enforcing the use of modifier arcs leads to a more understandable net.

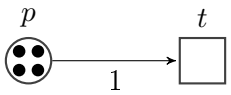

Figure 4.3: A Petri net system modeling a decay process

Since they have been extensively used in our model, we will describe how to parametrize a transition to model an entity with a specific half-life. The half-life of a quantity is the expected time for that quantity to decrease by half. Consider the Petri net system of Figure 4.3, if the parameter of transition t is:

$$\lambda = \frac{n_p}{t_{1/2}} \cdot \log_e(2)$$

where n_p indicates the number of tokens of place p, then the number of tokens of place p decreases with half-life $t_{1/2}$ (see Section A.3 for the proof).

Figure 4.4 shows the evolution of the number of tokens in p averaged over 100 simulations, when $t_{1/2} = 10$.

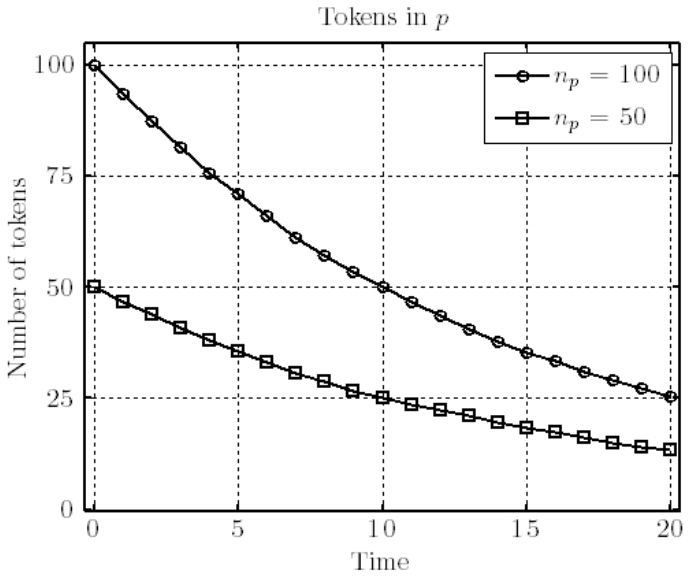

Figure 4.4: Number of tokens in p (See Figure 4.3). n_p indicates the number of tokens at time 0.

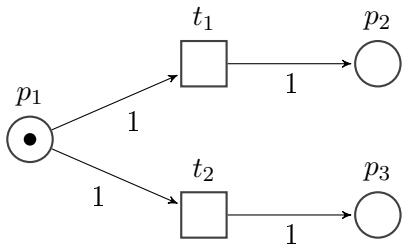

Figure 4.5: Conflicting transitions

The above result can be generalized to consider parameters of the form

$$\lambda = \frac{n_p}{t_{1/2}} \cdot \log_e(k)$$

which indicates that after $t_{1/2}$ the experted number of times the transition t has fired is

$$\left(1 - \frac{1}{k}\right) n_p$$

This generalization will not be proven.

Immediate transitions are a feature of the so called "generalized stochastic Petri net models". These transitions fire as soon as they are enabled and do not consume any time. Note that immediate transitions introduce the problem of "conflicts".

The formal definition of conflicting transition is not straightforward, and will not be presented here (we refer the interested reader to Section 2.3.4 of Marsan et al. 1995), we will, however, outline the problem. Transitions t_1 and t_2 of Figure 4.5 illustrate a simple example of conflict: if t_1 fires, t_2 will be disabled, and if t_2 fires, t_1 will be disabled. This is not a problem for stochastic Petri nets system, as the transition to fire is chosen by the so called "race-policy", which uses the probabilities defined in Formula 4.2. For immediate transitions different policies exist (e.g., choose at random, or enforce the user to associate a priority with each transition), but they depend on the specific situation.

The algorithm to simulate generalized stochastic Petri net systems differs only slightly from Algorithm 4.1: all enabled immediate transition must be fired using the chosen conflict-resolution policy (without increasing the time) before timed transitions are considered.

Deterministic-timed transitions fire after a deterministic, rather that probabilistic, time after being enabled. It is easily guessed that they have the same issues of immediate transitions when it comes to conflicts (Imagine t_1 and t_2 both firing one second after being enabled). Again, it is quite easy to think of modifications to 4.1 to account for deterministic-timed transitions.

While our model used both immediate and deterministic-timed transitions, they are never conflicting. Immediate transitions have been used to determine when a granuloma change its status from infected to healed and to remove cytokines. Deterministic-timed transitions have been used to enable, or disable, other transitions (e.g., to account for the delayed T cells response).

Petri net models have been extensively used in biology. Some notable examples can be found in Heiner, Gilbert & Donaldson 2008*b*

4.3 Sensitivity Analysis

This section presents a brief introduction to sensitivity analysis. Unless specified, the material presented is based on Chapter 6 of Saltelli et al. 2000 ("Sampled-Based Methods" by J. Helton and F. Davis). Sensitivity analysis can be applied to both physical and numerical experiments; however, we will focus on the latter. Moreover, given the vastity of the field, only some fundamentals, important for the understanding of the following chapters, will be presented.

4.3.1 Why Sensitivity Analysis?

Saltelli defines sensitivity analysis (SA) as "the study of how the variation in the output of a model [...] can be apportioned [...] to different sources of variation, and how the given model depends upon the information fed into it (Saltelli et al. 2000, p. 3)".

In the context of complicated mathematical, or software, models, SA is a way to determine the most influential parameters, and therefore to validate the model when we know, at least roughly, which parameters are expected to be the most influential.

This is especially important when we deal with models characterized by strong simplifications, or uncertainty in the input parameters; and immunological models often display both characteristics.

As described in Section 1.3, the immune system is complicated, and many important mechanisms are still being investigated. Moreover, even when a mechanism is well-understood, it is usually quite complex and depends on many stimuli often hard to measure. Therefore, especially when dealing with leukocytes instead of proteins, many immunological models introduce working assumptions and simplifications. Using SA we can determine the impact of these simplifications. For example, simplifications pertaining cells that are not fundamental for the outcome of the model, are probably not worthy an extensive investigation.

Many biological quantities are difficult to determine due to technical problems (e.g., the concentration of cytokines in a specific point in space), structural problems (e.g., the number of NKT cells is reported to largely vary among individuals Godfrey et al. 2010), or different results (e.g., the large difference of LDU in infected C57BL/6 mice reported by Stanley et al. 2008 and Murray et al. 2006). Using SA, we can determine how much effect the variability observed in experiments influences the model.

Recent examples of the use of SA in immunological modeling can be found in Linderman et al. 2010 and Fallahi-Sichani et al. 2010. Finally, a discussion on the advantages and disadvantages of some SA methodologies when applied to immunological modeling can be found in Marino et al. 2008.

4.3.2 A Brief Introduction Sensitivity Analysis

The process of SA can be summarized by the following steps:

1. Determine a set of input configurations
2. Run the model on the chosen input configurations
3. Evaluate the impact of the variations of the input parameters on the output of the model

The methodologies used for the first step are called "sampling procedures", while the metrics used in the last step are called "importance measures". Some importance measures require a specific sampling procedure, while others are more flexible. For example, extended Fourier amplitude sensitivity test (eFAST) requires Fourier amplitude sensitivity test sampling (Saltelli et al. 1999), while partial rank correlation coefficients (PRCC) (Iman & Conover 1979) works with any procedure that provides a good sample of

the parameter space, such as random sampling, importance sampling, or Latin hypercube sampling (LHS).

The number of experiments required to provide a valid importance measure varies with the number of parameters that are being studied: the number of experiments increases with the number of parameters. Additionally, for a fixed number of parameters, the number of experiments varies among various importance measures. For example, eFAST requires many more experiments than PRCC on the same model. The increased computational effort required by eFAST is compensated by its ability to better deal with non-monotonic models.

As suggested by the above discussion, each SA technique has strengths and weaknesses that must be carefully considered when deciding the technique(s) to be used on a particular model. In the context of biological modeling, a comparative analysis of different SA techniques is available in Marino et al. 2008.

SA on our model was performed using two widely-used techniques: LHS and PRCC. Since the motivations for our choice depends on the nature of the model, they are presented later (see Section 9.1).

Before being able to introduce PRCC, we need to describe some methodologies: Regression Analysis, LHS, and Partial Correlation Coefficient (PCC). Note that, in the following, we will use the term "parameter" to designate both the parameters and the inputs of a model.

4.3.3 A Few Notations

To present a precise and consistent description of SA, the following notations will be used throughout this chapter:

- k is the number of parameter under consideration
- n is the number of experiments
- $x_{i,j}$ is the value of the parameter j for the i-th experiment
- $x_{i,-}$ is a row vector with the values of the parameters for the i-th experiment
- $x_{-,j}$ is a column vector with the values of the j-th parameter for the experiments. We will also use $x_{-,j}$ to name the j-th parameter.
- y_i is the output of the model for the i-th experiment

Note that, for simplicity, we assume the $x_{i,j}$ and the y_i to be real numbers.

4.3.4 Latin Hypercube Sampling

Among the various sampling procedures, LHS is one of the most used when the number of possible experiments is limited. LHS has been introduced by McKay et al. 1979 for independent input parameters, and has subsequently been extended to consider correlated parameters by Iman & Conover 1982.

LHS proceeds as follows: the range of each parameter $x_{-,1}, \ldots x_{-,k}$ is divided into n intervals. For each interval a random value is selected with uniform probability. Then, n k-uples are generated by assigning at random one of these values to the i-th component $(1 \leq i \leq k)$, in such a way that, for each variable, each value is used only once. Note that the intervals can be of different size to account for possibly different *importance ranges* for the parameter.

4.3.5 Regression Analysis and Standardized Regression Coefficients

Given a collection of n pairs

$$\{y_i \ , \ x_{i,-}\}_{i=1..n} \tag{4.3}$$

a linear regression model $\hat{y}$ of the model y is defined as

$$\hat{y} = b_0 + \sum_{j=i}^{k} b_j x_{-,j} \tag{4.4}$$

where the b_j are coefficients to be determined. Let $\hat{y}_i = \hat{y}(x_{i,-})$, then for each pair of the Formula 4.3, the error introduced by this regression is defined as

$$\varepsilon_i = y_i - \hat{y}_i$$

More compactly, we can write:

$$\mathbf{y} = \mathbf{xb} + \boldsymbol{\varepsilon}$$

where

$$\mathbf{y} = \begin{bmatrix} y_1 \\ \vdots \\ y_n \end{bmatrix}, \qquad \mathbf{x} = \begin{bmatrix} 1 & x_{1,1} & \cdots & x_{1,k} \\ \vdots & \vdots & & \vdots \\ 1 & x_{n,1} & \cdots & x_{n,k} \end{bmatrix}, \qquad \mathbf{b} = \begin{bmatrix} b_0 \\ \vdots \\ b_k \end{bmatrix}, \qquad \boldsymbol{\varepsilon} = \begin{bmatrix} \varepsilon_1 \\ \vdots \\ \varepsilon_n \end{bmatrix}$$

The b_j are then calculated by minimizing the sum of the squared errors:

$$\sum_{i=1}^{n} \varepsilon_i^2$$

which corresponds to minimizing:

$$(\mathbf{y} - \mathbf{xb})^{\mathrm{T}} (\mathbf{y} - \mathbf{xb}) = \sum_{i=i}^{n} \left(y_i - b_0 - \sum_{j=1}^{k} b_j x_{i,j} \right)^2$$

which leads to the following matrix equation

$$\mathbf{x}^{\mathrm{T}}\mathbf{x}\mathbf{b} = \mathbf{x}^{\mathrm{T}}\mathbf{y}$$

If $\mathbf{x}^{\mathrm{T}}\mathbf{x}$ is invertible, $\mathbf{b}$ has a unique solution that can be calculated by

$$\mathbf{b} = (\mathbf{x}^{\mathrm{T}}\mathbf{x})^{-1}\mathbf{x}^{\mathrm{T}}\mathbf{y}$$

Since the invertibility of $\mathbf{x}^{\mathrm{T}}\mathbf{x}$ depends on n, this value should be carefully chosen. When $\mathbf{x}^{\mathrm{T}}\mathbf{x}$ is diagonal, the previous equation becomes:

$$b_j = \sum_{i=1}^{n} x_{i,j}y_i \Big/ \sum_{i=1}^{n} x_{i,j}^2$$

The model of Formula 4.4, can be reformulated as

$$\frac{\hat{y} - \overline{y}}{\hat{s}} = \sum_{i=1}^{k} \frac{b_i \hat{s}_i}{\hat{s}} \frac{x_i - \overline{x}_i}{\hat{s}_i} \tag{4.5}$$

where

$$\overline{y} = \sum_{i=1}^{k} \frac{y(x_{i,-})}{m}, \qquad \hat{s} = \left(\sum_{i=1}^{k} \frac{(y_i - \overline{y})^2}{m-1} \right)^{1/2}$$

$$\overline{x}_j = \sum_{i=1}^{k} \frac{x_{i,j}}{m}, \qquad \hat{s}_j = \left(\sum_{i=1}^{k} \frac{(x_{i,j} - \overline{x}_j)^2}{m-1} \right)^{1/2}$$

The coefficients $b_i\hat{s}_i/\hat{s}$ of Formula 4.5 are called standardized regression coefficients (SRCs), and provide an importance measure when the x_i are independent.

4.3.6 Correlation and Partial Correlation Coefficients

If only one parameter is under consideration, and therefore if $k = 1$, the sample or Pearson correlation between $x_{-,1}$ and y, indicated by $r_{yx_{-,1}}$, is defined as

$$r_{yx_{-,1}} = \frac{\sum_{i=1}^{n} (x_{i,1} - \overline{x})(y_i - \overline{y})}{\left(\sum_{i=1}^{n} (x_{i,1} - \overline{x})^2 \right)^{1/2} \left(\sum_{i=1}^{n} (y_i - \overline{y})^2 \right)^{1/2}}$$

where $\overline{x}$ and $\overline{y}$ are defined as in Formula 4.5. The correlation coefficient (CC) $r_{yx_{-,1}}$ provides a way to measure the linear relationship between $x_{-,1}$ and y. A large positive $r_{yx_{-,1}}$ indicates that a small increase of $x_{-,1}$ leads to a large increase of y.

When two or more parameters are being analyzed (that is, $k > 1$), PCC can be used. To compute the PCC between $x_{\sim,j}$ and y, we calculate the following regression models:

$$\hat{x}_{\sim,j} = c_0 + \sum_{\substack{m=1 \\ m \neq j}}^{k} c_m x_{\sim,m}, \qquad \hat{y} = b_0 + \sum_{\substack{m=1 \\ m \neq j}}^{k} b_m x_{\sim,m}$$

and use them to define the variables

$$\widetilde{x}_{\sim,j} = x_{\sim,j} - \hat{x}_{\sim,j}$$
$$\widetilde{y} = y - \hat{y}$$

The PCC $r_{yx_{\sim,j}}$ between y and $x_{\sim,j}$ is $r_{\widetilde{y}\widetilde{x}_{\sim,j}}$. PCC provides a way to measure the linear relationship between a parameter and the output, with the linear effects of the other parameters removed.

4.3.7 P-Value

CC and PCC give an indication of the correlations between the input parameters and the output, but give no indication of the statistical significance of the results. Therefore, additional statistical test have been developed. Under certain statistical assumptions, we can calculate "the probability of observing a stronger correlation due to chance (Saltelli et al. 2000, p. 132)". This probability is called p-value. Therefore a small p-value — usually lower than 0.01 — is an indication of the validity of the CC or PCC.

We will not present the details of the definition of p-value, as it would require the introduction of many statistical concepts, and we refer the interested reader to the references of chapter 6 of Saltelli et al. 2000. We want however, to stress that the "the distributional assumptions that lead to the p-values [...] are not satisfied in sampling-based sensitivity studies. However, these p-values still provide a useful criterion for assessing variable importance, because they provide an indication of how viable the relationship between input and output variables would appear to be in a study in which the underlying distributional assumptions were satisfied (Saltelli et al. 2000, p. 128)."

4.3.8 Ranking

SRC, CC and PCC generally perform poorly when the relation between the parameters and the output is nonlinear. This problem can be mitigated by using this importance measures on rank-transformed data. The concept of rank transformation is quite simple: the values of the parameters and the output are replaced by their "rank". Therefore, the values of a parameter

are replaced by the values $1, \ldots, n$, which indicate the rank (1 replacing the smaller values, 2 the second smaller value, and so on). Consequently, "the use of rank-transformed data results in an analysis based on the strength of monotonic relationship rather than on the strength of linear relationships (Saltelli et al. 2000, p. 139)." Rank-transformed SRC, CC and PCC are referred as standardized rank regression coefficient (SRRC), rank correlation coefficient (RCC), and partial rank correlation coefficient (PRCC).

Part II

Model

Chapter 5

Working Assumptions

Modeling a physical phenomenon requires the introduction of a number of assumptions and simplifications. This is especially true when dealing with complex biological processes such as a granuloma. This chapter explicitly documents the most important assumptions pertinent to the biology of the granuloma that have been used. Moreover, the most significant simplifications introduced by our model are discussed.

5.1 Biology: Qualitative Assumptions

The biological knowledge of the immune system is steadily growing. Sometimes this knowledge *converges*, and all the data point to a specific explanation of a phenomenon. For example, we have a good understanding of the processes underlying the activation of T cells. However, as already pointed out in Section 3.1.1, sometimes data are inconclusive, or even contradictory, and more than one hypothesis is able to explain a specific phenomenon. The possibility of testing the validity of different hypotheses is however, one of the advantages of *in silico* models.

The following assumptions are mostly widely accepted, and described on books such as Murphy & Kenneth 2007. When this is not the case, and no specific references or justifications are provided, the source of information are to be considered biological experts.

5.1.1 Cytokines

Assumption 1. *All the cytokines of the same type are identical.*

This means that, for example, all IL10 cytokines behave identically. While this may seem obvious, some biological evidence suggests otherwise. For instance, Svensson et al. 2005 reports that in the early stages of gran-

uloma formation, macrophages react to INFγ produced by NKT cells, but not to INFγ produced by other liver cells.

5.1.2 *Leishmania Donovani*

Assumption 2. *The rate of reproduction of leishmania donovani amastigotes is the same in both (de)activated and normal macrophages.*

While, theoretically, the rate of reproduction could increase in alternatively activated macrophages due to the increase in nutrient supply (polyamines), no data are available.

Assumption 3. *All leishmania donovani amastigotes are equal.*

This assumption implies that all amastigotes have the same reproduction rate and resistance to killing by macrophages. While no specific experiments exist for *leishmania donovani*, it is worth noticing that leishmania major has been reported to have sexual reproduction, and therefore a possible evolution (Akopyants et al. 2009).

Assumption 4. *Leishmania donovani amastigotes interact with the Kupffer cell in the same way at different stages of reproduction.*

This assumption implies that the effect of an amastigote on the Kupffer cell that ingested it is independent on the stage of reproduction of the amastigote.

Assumption 5. *Leishmania donovani amastigotes promote the deactivation of the Kupffer cell that ingested them.*

This assumption is very difficult to test *in vivo* or *in vitro*. However, macrophages infected with *leishmania donovani* produce IL10 (Bhattacharyya et al. 2001) and display a reduced secondary MHC expression (Reiner et al. 1987), and both activities are associated with deactivated macrophages.

Assumption 6. *The alteration of Kupffer cell activities by leishmania donovani is proportional to the number of parasites ingested by the Kupffer cell.*

Given the complex feedback mechanisms usually displayed by cells, it is possible that the ability of the parasites to interfere with the Kupffer cell by promoting deactivation reaches a maximum, which may be independent of the number of parasites. However, currently no data exist on the possible existence of this maximum.

5.1.3 Macrophages

Assumption 7. *Proliferation of Kupffer cells is mostly negligible during leishmaniasis.*

Biological experts indicate that the proliferation of Kupffer cells during leishmaniasis, if any, is very limited.

Assumption 8. *Classically activated macrophages mainly produce TNF and IL12.*

While classically activated macrophages have been reported to produce a number of different types of cytokines (Mantovani et al. 2004), IL12 and TNF are the cytokines produced in larger quantities.

Assumption 9. *Alternatively activated macrophages mainly produce IL10.*

While alternatively activated macrophages have been reported to produce a number of different types of cytokines (Mantovani et al. 2004), IL10 is the cytokine produced in larger quantities.

Assumption 10. *Deactivated macrophages mainly produce IL10.*

While deactivated macrophages have been reported to produce a number of different types of cytokines (Mantovani et al. 2004), IL10 is the cytokine produced in larger quantities.

Assumption 11. *Classical activation, alternative activations, and deactivation coexist, but down-regulate each other.*

Some biologists suggest that, in a macrophage, the different types of activations can coexist (see for example Mosser & Edwards 2008). The down-regulation is a consequence of the possible internal reactions and of the antagonizing effect of the cytokine produced.

Assumption 12. *Classical activation of macrophages is triggered by TNF and INFγ.*

It is generally recognized that classical activation of macrophages is triggered by TNF and INFγ (Mantovani et al. 2004).

Assumption 13. *Alternative activation of macrophages is triggered by IL4 and IL13.*

It is generally recognized that alternative activation of macrophages is triggered by IL4 and IL13 (Mantovani et al. 2004).

Assumption 14. *Deactivation of macrophages is triggered by IL10.*

It is generally recognized that deactivation of macrophages is triggered by IL10 (Mantovani et al. 2004).

Assumption 15. *When infected, macrophages produce TNF.*

Infected macrophages produce TNF. The production of TNF subsequently increases the activity of macrophages in an autocrine way.

Assumption 16. *Gigantic Multinucleated cells do not affect the behavior of liver granulomas.*

We assume that a gigantic multinucleated cells with n nuclei is functionally equivalent to a group of n macrophages. This rather strong assumption is due to the limited knowledge on the effect of macrophage fusion in the context of leishmania-induced granulomas. Moreover, even considering granuloma formed in response to tuberculosis, there is no clear evidence indicating whether the role of gigantic multinucleated cells is positive or negative. Finally, liver granuloma are quite small, and the number of gigantic multinucleated cells is generally low.

Assumption 17. *Kupffer cells need to be classically activated to kill leishmania donovani amastigotes.*

Experiments indicate that classical activation is fundamental to kill leishmania amastigotes. Moreover, the efficiency in killing the parasites depends on the level of classical activation, and thus on the level of external stimuli promoting classical activation.

Assumption 18. *The ligation of iNKT cells on the surface of macrophages deactivate them.*

According to the current biological opinion, the ligation of CD47, which is displayed by iNKT cells, on the surface of a macrophage promotes its deactivation. This is believed, for example, to be one of the mechanisms that allows macrophage fusion (the deactivation allows the macrophages not to phagocytose each other).

5.1.4 T Cells

Assumption 19. *The only subsets of T cells that impact on the formation and maintenance of a granuloma are T_H0, T_H1, T_H2, T_C0, T_C1, and T_C2 cells.*

While a number of other subsets of T cells exist — such as T_H17 cells —, the cell populations mentioned above appear to be the most numerous.

Assumption 20. *Spleen is the main source of T cells, but the priming of T cells is also possible in the liver.*

The role of the spleen as *incubator* of mature T cells is well established. However, a growing body of evidence indicates that T cells can mature in other places. Notably, Greter et al. 2009 suggests the maturation directly in the liver.

Assumption 21. *T_H0, T_H1, T_H2, T_C0, T_C1, and T_C2 cell populations exist and are stable.*

It is common to classify the populations of helper and cytotoxic T cells by the cytokines they produce. However, some authors are beginning to question this classification, or at least to point out that it is not *strict*. This is due to the large variability that seems to exist within the same population, and to the plasticity of T cells (see for example Bluestone et al. 2009).

Assumption 22. *T_H0 cells differentiate to T_H1 cells when exposed to INFγ (and later IL12).*

The process of differentiation of T_H0 cells into T_H1 cells is usually believed to be triggered by INFγ and IL12. However, recent articles describe how the activity of T-Bet is promoted by INFγ and IL12 independently (see Schulz et al. 2009).

Assumption 23. *T_C0 cells differentiate to T_C1 cells when exposed to INFγ.*

INFγ is believed to be the main cytokine responsible for the differentiation of T_C0 cells to T_C1 cells.

Assumption 24. *T_H0 and T_C0 cells differentiate to T_H2 and T_C2 cells when exposed to IL4.*

IL4 is believed to be the main cytokine responsible for the differentiation of T_H0 and T_C0 cells to T_H2 and T_C2 cells.

Assumption 25. *Newly differentiated T_H1 and T_C1 cells produce mainly INFγ and IL2.*

T_H1 and T_C1 cells produce different types of cytokines. However, newly differentiated T_H1 and T_C1 cells produce mainly INFγ (responsible for the initial expansion of the cell population) and IL2 (responsible for the expansion of all T cells subtypes).

Assumption 26. *T_H1 cells initiate the production of IL10 after the second wave of T-bet expression caused by IL12.*

As described in Trinchieri 2007, T_H1 cells display *self-control* by producing IL10. This phenomenon is clearly visible in an established liver granuloma where $2 - 5$ % of T cells produce INFγ and IL10. Different factors have been proposed to be responsible for this phenotypic change, and no evidence clearly indicate when this change happens. However, it is reasonable to divide the response of T_H1 cells into three phases. In the first phase, their activity is auto-promoted by INFγ. In the second phase, their activity is promoted by IL12. Since IL12 is not produced by T_H1 cells, they need to be sustained *externally*. In the third phase, besides requiring IL12, T_H1 cells initiate the production of IL10 to self-control their activity.

Assumption 27. *T_H2 and T_C2 cells mainly produce IL4 and IL10.*

T_H2 cells produce different types of cytokines. However, they mainly produce IL4 and IL10.

Assumption 28. *INFγ promotes the proliferation of T_H1 and T_C1 cells.*

INFγ is commonly considered to be a promoter of the proliferation of T_H1 and T_C1 cells.

Assumption 29. *IL4 promotes the proliferation of T_H2 and T_C2 cells.*

IL4 is commonly considered to be a promoter of the proliferation of T_H2 and T_C2 cells.

5.1.5 Natural Killer T Cells

Assumption 30. *NKT cells are very important for the formation of granulomas (specifically before the arrival of effector T cells).*

The role of NKT cells in the early stages of granuloma formation has been extensively confirmed (e.g., Amprey et al. 2004 and Stanley et al. 2008).

Assumption 31. *NKT cells mainly produce high quantities of INFγ and low quantities of IL4 in response to leishmania donovani infection.*

As described for example in Matsuda et al. 2008, NKT cells can produce a broad range of cytokines. However, IL4 and INFγ appear to be the cytokines produced in larger quantities. Experiments indicate that IL4 production by NKT cells is low during the response to liver infection by *leishmania donovani.*

Assumption 32. *NKT cells detect an infected macrophage and activate.*

NKT cells can be activated by a number of mechanisms (see Matsuda et al. 2008). However, peptides displayed by CD1d seems to have a fundamental role in leishmaniasis (Amprey et al. 2004).

Assumption 33. *NKT cells remain active for some time and then deactivate.*

It is currently unclear if the deactivation of NKT cells is *time-controlled.* But their lineage connection with T cells, makes this assumption plausible.

Assumption 34. *At homeostasis, the liver population of NKT cells is stable, but they have a high turnover rate.*

The exact mechanism behind the stability of the number of homeostatic NKT cells in the liver is not well-understood, however: "The number of NK1.1+ T cells found in the liver of adult mice did not steadily increase. These results suggest that liver NK1.1+ T cells have a high death rate, migrate from the liver, or undergo a phenotypic change. The BrdU data suggest either that NK1.1+ T cells begin proliferating after emigration from the thymus to the liver, or that the liver is populated by a special set of thymic NK1.1+ T cells, which are proliferating or were recently generated from proliferating precursors (Coles & Raulet 2000)".

Assumption 35. *The population of homeostatic NKT cells is stable, even when an infection is present.*

It is not possible to test this assumption with the current technology. However, during leishmaniasis, the number of NKT cells increases (Stanley et al. 2008). One possible explanation is that the population of homeostatic NKT cells remains relatively stable while NKT cells get activated.

Assumption 36. *Peripheral blood reproduction of NKT cells is negligible.*

No clear evidence exists for peripheral blood reproduction of NKT cells. Therefore, we will disregard the phenomenon.

5.1.6 Natural Killer Cells

Assumption 37. *NK cells produce INFγ in response to leishmania donovani infection.*

The exact mechanism used by NK cells to recognize infected cells is not completely understood. However, they have been shown to be a source of INFγ during leishmaniasis. Possible sources of activation are IL12 (Amprey et al. 2004) or direct recognition of infected macrophages.

Assumption 38. *NK cells produce high level of IL10 in the later stages of granuloma development.*

Maroof et al. 2008 reports that, while NK cells produce mainly INFγ in the early stages of granuloma, later on they initiate the production of IL10. A sustained production of IL10 is reported 21 days after infection.

Assumption 39. *Peripheral blood reproduction of NK cells is negligible.*

No clear evidence exists for peripheral blood reproduction of NK cells. Therefore, we will disregard the phenomenon.

Assumption 40. *Death of activated NK cells can be ignored.*

No clear evidence exists on the expected life of an activated NK. However, the data of Maroof et al. 2008 reports that NK cells synthesize IL10 mRNA for about 21 days before initiating the production of IL10. A possible explanation is that activated NK cells synthesize IL10 mRNA long before initiating the production of IL10. This suggests that activated NK cells survive for a long time (at least 21 day).

Assumption 41. *NK cells deactivate after a fixed probabilistic time.*

The mechanism behind the (de)activation of NK cells are not completely understood. Given the limited role that NK cells seem to play in leishmaniasis we opted for a simple model of deactivation (similar to T and NKT cells).

5.2 Biology: Quantitative Assumptions

So far we described the qualitative behaviors of the cells. Designing experiments to determine the quantitative behavior of these cells is usually much more complex. This section aims at presenting available quantitative data that can be used to construct and validate our model.

5.2.1 *Leishmania Donovani*

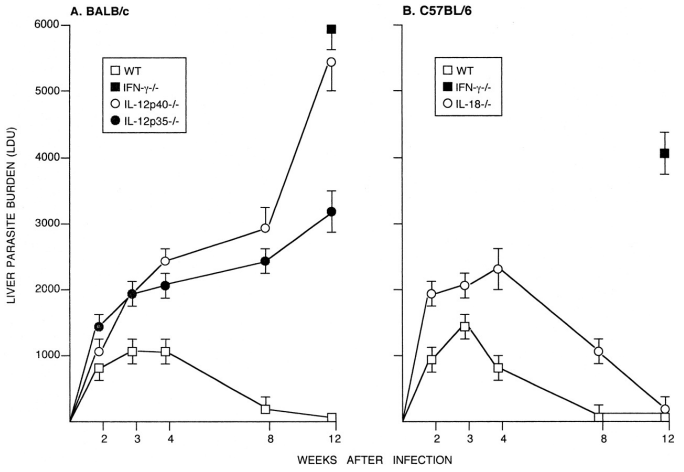

Figure 5.1: Liver parasite burden of wild type C57BL/6 mice. (LDU = *Leishmania Donovani* Units) (from Murray et al. 2006)

Assumption 42. *The liver parasite burden of a granuloma follows the data marked WT of Figure 5.1B.*

The liver parasite burden during the course of *leishmania donovani*-induced leishmaniasis can be found in many article. Figure 5.1 is taken from Murray et al. 2006, and has been used as reference.

Assumption 43. *Leishmania donovani amastigotes take about 1 day to reproduce.*

In vitro experiments indicate that the reproduction cycle of *leishmania donovani* amastigotes is about 24 hours long.

5.2.2 Macrophages

Assumption 44. *The number of Kupffer cells constituting the core of a granuloma is generally between 5 and 10.*

These numbers derive from direct observations under *in vivo* conditions.

Assumption 45. *The half-life of MHC I - peptide complexes is 3 hours.*

The half-life of MHC I peptides is generally reported to be either 3 or 6 hours (Henrickson et al. 2008). We used the value 3, but characterized the effect of increasing it to 6 by sensitivity analysis.

Assumption 46. *The half-life of MHC II - peptide complexes is 60 hours.*

The literature indicates a large variability in the half-life of MHC II - peptide complexes (see for example Lazarski et al. 2005), and it difficult to characterize the full spectrum of peptides displayed by antigen-presenting cells in response to *leishmania donovani* infection (see Afrin et al. 2002 for some data). However, MHC II - peptide complexes are generally believed to be quite stable and their half-life is believed to be in the order of days. The chosen value (60 hours), was also used by Linderman et al. 2010 (albeit in a different context) and should be a reasonable trade off.

Assumption 47. *The half-life of CD1d - peptides complexes is 20 hours.*

CD1d - α-galactosylceramide complexes are probably the most well-known CD1d-peptide complexes. However, the reported half-life varies between few minutes and few days (Benlagha et al. 2000). We used a baseline value of 20 hours to account for the fact that the complexes are believed to be quite stable.

Assumption 48. *Kupffer cells can sustain about 100 amastigotes.*

Direct observations of granulomas indicate the presence of macrophages with more than 100 amastigotes *in vivo*. This number is likely affected by many external conditions, as during *in vitro* experiments the number of amastigotes that a macrophage can sustain before being killed is about 50. 100 should be a reasonable mean value.

Assumption 49. *Activated Kupffer cells kill the amastigotes in about 1 day.*

In vitro experiments indicate that a strongly activated macrophage is able to kill 10 parasites in 24-48 hours. However, this activity is likely to be strongly parallel.

5.2.3 Dendritic Cells

Assumption 50. *The time required by a dendritic cell to ingest leishmania, migrate to the lymph node, and mature is 16 hours.*

This value is obtained from Huang et al. 2001, which is the source of Figure 5.2. A more recent article confirming this value is McIlroy et al. 2005. The time line of Figure 5.2 should be compatible with dendritic cells migrating to the spleen too.

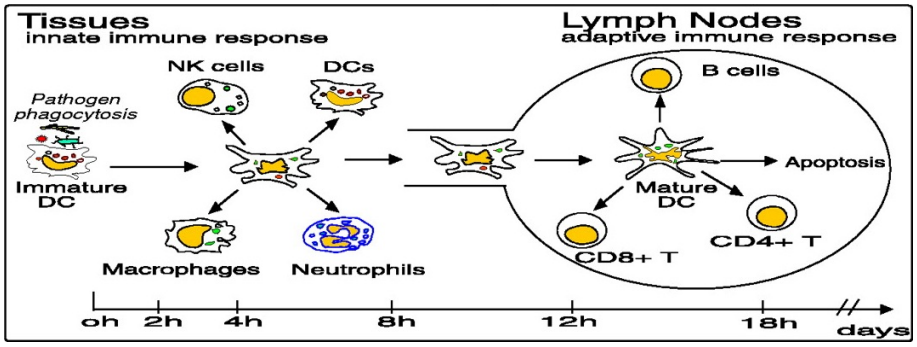

Figure 5.2: The life of a Dendritic Cell (Huang et al. 2001)

5.2.4 T Cells

Assumption 51. *The time needed by a naïve T cell to reproduce is 10.6 hours.*

The source of this value is Gudmundsdottir et al. 1999. While the value had been determined for naïve T cells, we assume that all T cells have the same reproduction rate.

Assumption 52. *T cells get to the liver 4 days after infection.*

This value has been confirmed experimentally and is compatible with the T cell dynamics described in Murphy & Kenneth 2007 (see Figure 5.3). During these 4 days various events happen:

1. Infected dendritic cells migrate to the lymph nodes, or spleen, and mature (about 16 hours)

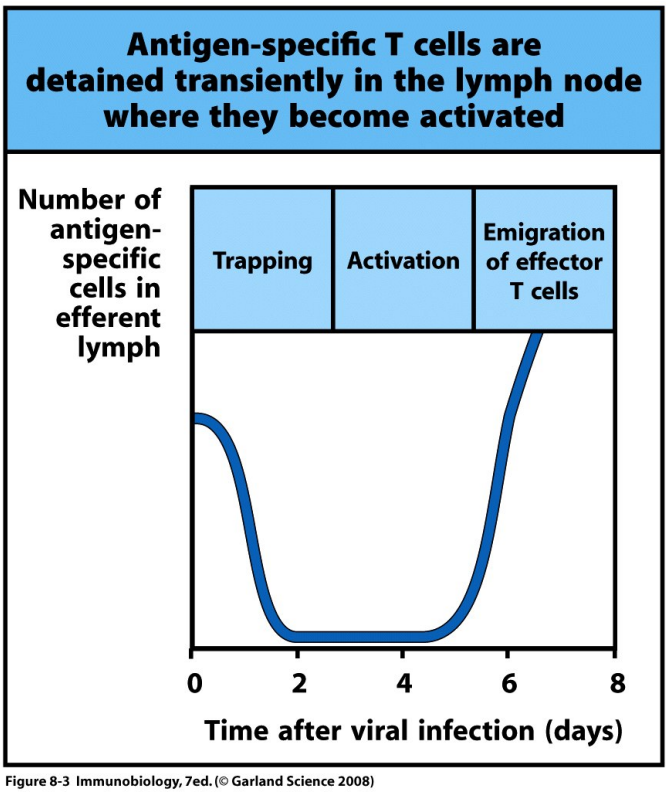

Figure 5.3: Priming and activation of T-Cells (Murphy & Kenneth 2007)

2. Naïve T cells with a matching TCR get in contact with the mature dendritic cell (about 1 day)

3. The naïve T cells mature and replicate (probably at least 53 hours, as this is the time needed by a naïve T Cell to reach the fifth generation and therefore its full cytokine production profile Gudmundsdottir et al. 1999)

4. The T cells migrate to the liver (few hours)

Assumption 53. *Spleen-derived T cells stop getting to the liver 5 days after infection.*

The half-life of mature dendritic cells is not fully characterized yet. However, a too long half-live would lead to an excessive immune response. A 1-day influx of cells from the spleen seemed a reasonable value. Note that, given the peripheral blood reproduction of T cells, and the influx of mature T cells from other granulomas, this value appeared not to be worth an extensive investigation.

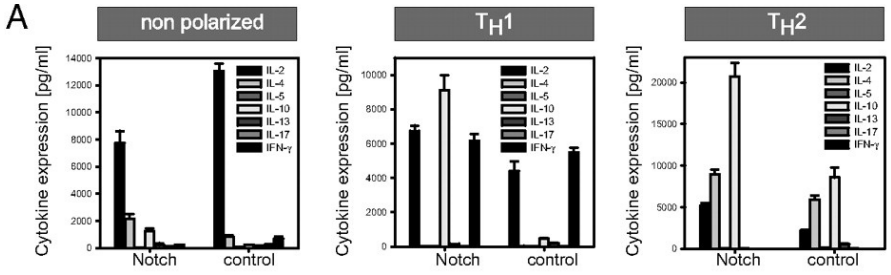

Figure 5.4: Cytokines production helper T-Cells (Rutz et al. 2008)

Assumption 54. *Activated T_H1 cells require INFγ to sustain the production of cytokines in the first 5 days, and IL12 subsequently.*

Schulz et al. 2009 indicates that INFγ and IL12 sustain two distinct waves of T-bet expression. The two waves peak one and five days after activation respectively.

Assumption 55. *When the TCR of a T cell senses a matching peptides on a macrophage, the cell interacts with the macrophage for about 30 minutes.*

This result is from Beattie at al. 2010 (PLoS Pathog) and is relative to $CD8^+$ cells.

Assumption 56. *The ratios of cytokines produced by T cells are as follow:*

T_H1- *INFγ : IL2 = 6 : 5*

T_H1- *IL2 : IL10 = 7 : 9 (When IL10 production is active and assume notch is responsible)*

T_H2- *IL10 : IL4 : IL2 = 9 : 6 : 2*

T_H*- *(T_H0 derived IL2) : (T_H1 derived IL2) = 13 : 5*

T_H*- *(T_H0 derived IL2) : (T_H2 derived IL2) = 13 : 3*

Helper T cells produce different types of cytokines. While the production profile are not necessarily stable, it is easy to obtain data for highly polarized subpopulation. It is theoretically possible to determine the exact quantity of cytokines produced by a single T cell in vitro. However, in the liver, cytokines are subject to diffusion, and moreover it is hard to track the population of T cells. Nevertheless, we can use the data on cytokine production to determine the ratio of production of the different types of cytokines produced by the cells. The ratios are extracted from figure 5.4, which is taken from Rutz et al. 2008.

Assumption 57. *The percentage of cytokine producing helper T cells follows Table 5.1.*

Day	% of $CD4^+INF\gamma^+IL10^-$	% of $CD4^+INF\gamma^+IL10^+$
0	3 ± 0.75	0.12 ± 0.01
21	12.14 ± 0.71	1.03 ± 0.23
38	9.75 ± 1.87	0.38 ± 0.07

Table 5.1: Percentage of helper T cells

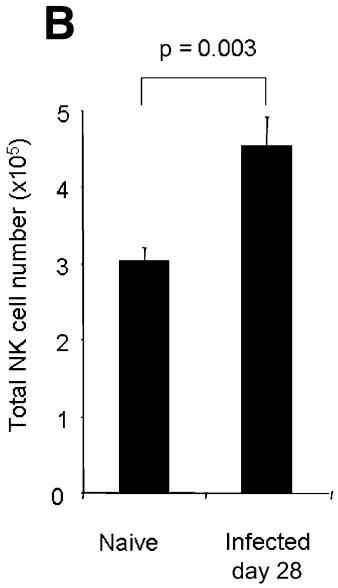

Figure 5.5: Number of NK cells in the liver of control and infected wild type C57BL/6 mice (from Maroof et al. 2008)

These data are courtesy of the laboratory of Paul Kaye of the University of York, and are currently unpublished. Table 5.1 indicates the mean value and the standard deviation. The value at day 0 and the percentage of NKT cells from Amprey et al. 2004 were used to calculate a fixed number of *leishmania donovani* non-specific activated helper T cells (assuming the same number of $CD4^+$ and $CD8^+$ T cells).

5.2.5 Natural Killer Cells

Assumption 58. *The number of NK cells follows Figure 5.5.*

The number of NK cells at day 0 and 28 was obtained from Maroof et al. 2008. The value for naïve mice was used for day 0.

Assumption 59. *NK cells detect an infected target and activate in about 4 hours.*

The exact time required for a NK cell to detect its target and activate

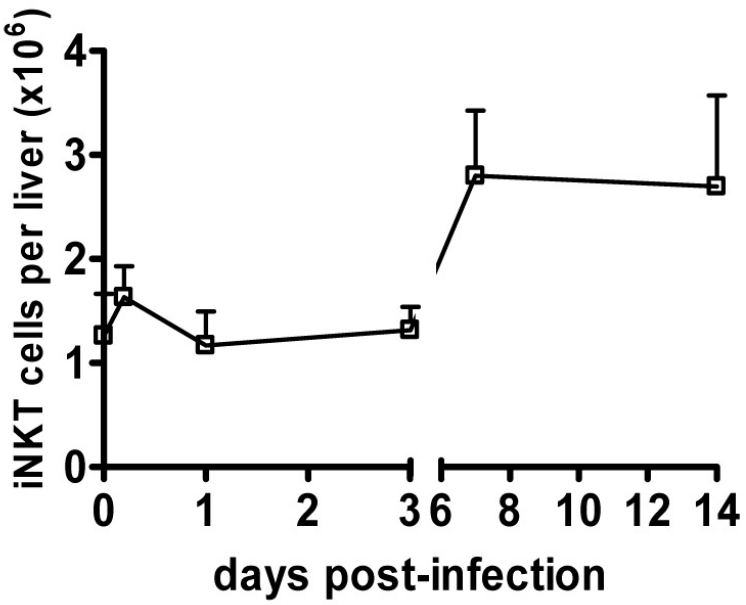

Figure 5.6: Number of NKT cell in the liver during infection of wild type C57BL/6 mice (from Stanley et al. 2008)

is hard to determine. However, Yokoyama et al. 2004*b* reports that, in the lungs, 4 hours after infection NK cells are clearly detectable and activated.

Assumption 60. *The half-life of mature NK cells in the liver is about 400 hours (about 17 days).*

Yokoyama et al. 2004*b* reports that "the half-life of mature NK cells in the periphery appears to be about seven to ten days based on the survival of adoptively transferred NK cells". However, the half-life of splenic NK cells is reported to be 17 days (Jamieson et al. 2004). Since we were not able to find any data for hepatic NK cells, we used the value for spleen.

Assumption 61. *NK cells initiate the production of IL10 after 21 days of activation.*

The experiments reported by Maroof et al. 2008 indicate that NK cells are sources of IL10 21 days after infection.

5.2.6 Natural Killer T Cells

Assumption 62. *The number of NKT cells in the liver during leishmaniasis follows Figure 5.6.*

Assumption 63. *The percentage of activated NKT cells is* 1.4 *two hours after infection and* 10.9 ± 1.2 *sixteen hours after infection.*

The sources of these data are Amprey et al. 2004 (which used BALB/c mice) and Beattie at al. 2010 (EJI) (which used C57BL/6 mice)

Assumption 64. *The half-life of mature NKT cells in the liver is about 400 hours (about 17 days).*

Since we were not able to find any data on the half-life of liver NKT cells, given the connection between NK and NKT cells, we used the same value of NK cells (see Assumption 60)

5.2.7 Granulomas

Assumption 65. *The number of granulomas in the liver is about* $5 \cdot 10^5$.

This estimate is courtesy of Lynette Beattie of the Centre for Immunology and Infection of the Hull York Medical School (Beattie 2010).

5.3 Modeling: Simplifications

Constructing a *good* model of a *complicate* system is challenging. Too many simplifications lead to an easily manageable model, that, however, is not able to replicate the reality of the phenomenon. On the other hand, a model that tries to use all the information available on the phenomenon without introducing simplifications that remove non essential features is very hard to build and validate.

This section describes the simplifications introduced by our model. We tried to keep the number of simplifications to a minimum, to preserve the fundamental characteristics of granuloma.

5.3.1 Global

Simplification 1. *The functions and characteristics of cells that are not present in the modeled are negligible for the development of granuloma.*

We should consider this simplification the *master simplification.* As described before, many cells perform a wide range of functions, with new functions being discovered as research proceeds. When building a model, it is assumed, usually implicitly, that what is not in the model is not fundamental for the outcome of the model itself.

Simplification 2. *Fully (de)activated macrophages, activated NK cells, NKT cells, and T cells produce the same amount of cytokines.*

As described by Assumption 56, it is quite hard to determine the cytokine production of the various types of cells. Therefore, we set the value to be the same. Note that, as pointed out by 56, the level of production of the modeled cytokines produced by T cells is quite similar.

Simplification 3. *All the cells that produce cytokines reach a stable level of production.*

The quantity of cytokines produced by a leukocyte is not constant, and may depend on many factors, such as on co-stimulatory signals. Moreover, the cytokine production of T cells is likely to be affected by the affinity of their TCR with the specific peptide displayed by MHC molecules. For instance, T_H1 cells reach a stable level of cytokines production after 5 cycles of reproduction (Gudmundsdottir et al. 1999) and to maintain that level they need a favorable environment (Schulz et al. 2009).

Simplification 4. *The level of cytokine production of the cells is fixed.*

Many factors influence the cytokine production of T cells. However, given our modeling formalism, we used a fixed values.

5.3.2 Cytokines

Simplification 5. *Only one type of chemokines exists and its role is purely chemoattractive.*

While different types of chemokines exist, their effects are usually similar. We assume that only one type of chemokines exists, and that chemokines affect only the arrival of non-resident macrophages. Additionally, the role of CCL3 in promoting T_H1 cells - based immunity will be ignored. This is justifiable by the fact that, in our model, iNKT cells, which are the only sources of CCL3, produce INFγ, which is by itself a strong promoter of the proliferation of T_H1 cells. We will not use any specific name for chemokines, and refer generically to "chemokines". Moreover, we will model only the effect of chemokines on non-resident mononuclear phagocytes.

Simplification 6. *The chemoattractive effect of chemokines is proportional to the number of chemokine-producing cells.*

Cytokines have two fundamental roles: they facilitate the passage of leukocytes through the wall of the blood vessels and stimulate the leukocytes to move towards a place with a higher density of chemokines. We will simply assume that the level of chemokines influences the arrival rate of affected leukocytes.

Simplification 7. *TNF can be ignored in the model.*

TNF has three main roles for the cells in our model:

1) Inducing the expression of adhesion molecules on the surface of endothelial cells

2) Increasing the killing activity of a macrophage

3) Classically activating a macrophage in conjunction with INFγ

We will not model the actual binding of a macrophage to the surface of endothelial cells and therefore 1) can be ignored. TNF is not sufficient by itself to classically activate a macrophage, and a non classically activated macrophage is ineffective in killing leishmania, therefore 2) can be ignored. Function 3) is very important for the model, and modifying the mechanism of classical activation leads to many consequences that need to be discussed carefully. In our model the only sources of TNF are macrophages (unless deactivated), and some type I T cells.

Designing experiments with no type I T cells is useless, as they are the main sources of INFγ, and their role in controlling the infection is well-established. Unfortunately, removing TNF from the model strongly limits our ability in experimenting with the deactivation of macrophages in the early stages of infection. A strong deactivation of macrophages in the initial phases of the infection could lead to a scenario in which TNF is very low and the macrophages activate too late to control the infection. However, designing such an experiment is hard for another reason: no clear data link the quantities of INFγ and TNF to the level of classical activation. The main reason is that the level of classical activation is not straightforward to measure, as it is a more of a *qualitative* than *quantitative* behavior.

Simplification 8. *All the cytokines are subject to the same diffusion and drift, due to bloodstream.*

Cytokines have different, albeit comparable, sizes and shapes. Therefore, it is possible that different cytokines diffuse differently. We will ignore this variation, as difficult to measure *in vivo*.

Simplification 9. *Cytokine tokens represent more than one molecule.*

Determining the number of cytokine molecules produced by cells is technically very difficult. Moreover, cytokine production varies over time in accordance with the stimuli received by the cell. Cytokine tokens, which are used by our model, should be considered as a group of molecules.

5.3.3 Macrophages

Simplification 10. *A macrophage can undergo classical activation, alternative activation, or deactivation.*

The current biological opinion is that a macrophage is able to undergo a number of different types of activations. However, liver granulomas are not so disruptive to require a healing macrophage to repair the extracellular matrix. Moreover, classical activation, alternative activation, and deactivation are by far the most studied activation types.

Simplification 11. *Classically activated macrophages only produce IL12.*

While classically activated macrophages have been reported to produce a number of different types of cytokines, IL12 is the cytokine produced in larger quantities.

Simplification 12. *Alternatively activated and deactivated macrophages only produce IL10.*

While alternatively activated and deactivated macrophages have been reported to produce a number of different types of cytokines, IL10 is the cytokine produced in larger quantities.

Simplification 13. *Alternative activation of macrophages is triggered by IL4 alone.*

It is generally recognized that alternative activation is triggered by IL4 and IL13. However, in our model, the only recognized sources of IL13 — iNKT and T_H2 cells — produce also IL4. Therefore, we assign to IL4 the role of both IL4 and IL13.

Simplification 14. *The ligation of iNKT cells on the surface of macrophages promotes their deactivation.*

According to the current biological opinion, the ligation of CD47 on the surface of a macrophage down-regulate its activity. This is believed, for example, to be one of the mechanisms allowing macrophage fusion (the down-regulation allows the macrophages not to phagocytose each other). Since we imposed that classical activation is required for killing of leishmania amastigotes (Simplification 17), we are not interested in the normal killing activity of macrophages. Therefore, increasing the deactivation of a macrophage implies a down-regulation of its killing activity.

5.3.4 T Cells

Simplification 15. *T_H1 cells produces IL2 and INFγ or IL2, INFγ and IL10 only.*

T_H1 cells produce a number of cytokines. However, IL2, INFγ and IL10 are the cytokine produced in larger quantities (see for example Figure 5.4). Note that the production of TNF is ignored due to Simplification 7.

Simplification 16. *T_C1 cells produces IL2, and INFγ only.*

T_C1 cells produce a number of cytokines. However, IL2, and INFγ are the cytokines produced in larger quantities. Note that the production of TNF is ignored due to Simplification 7.

Simplification 17. *T_H2 and T_C2 cells produces IL4 and IL10 only.*

T_H2 and T_C2 cells produce a number of cytokines. However, IL4, and IL10 are the cytokines produced in larger quantities (see for example Figure 5.4). Note that the production of IL13 is ignored due to Simplification 13.

Simplification 18. *T cells deactivates after a fixed probabilistic time.*

T cells activation is a complex and a not yet fully understood process (see Smith-Garvin et al. 2009). It seems, however, possible that a T cell internalizes a peptide before deactivating, thus continuing to be in active state for some time. Modeling this mechanism would have required a much more complex model of T cells (and additional parameters).

Simplification 19. *Apoptosis of T cells can be ignored.*

Many mechanisms regulate the activities of activated T cells, and apoptosis is one of the most important. While the network of signals that leads to apoptosis is not yet fully characterized, we know that many competing signals (see for example Holtzman et al. 2000) regulate it. Most of these signals require many cell phenotypes that are not described by our models. Therefore, activated T cells will simply not die on our model.

Simplification 20. *Cytokines have no effect on the deactivation of T cells.*

Many cytokines regulate the behavior of T cells, while some of them promote the emergence of a phenotype, other antagonize it. For example, INFγ promotes the differentiation of T_H0 cells to T_H1 cells while blocking the differentiation to T_H2 cells. We will consider the effect of cytokines only on reproduction, but ignore the effect on deactivation.

Simplification 21. *T Cells consume their flag cytokine to keep their phenotype active.*

Each T cell subpopulation produce a *flag cytokines*, that is, a cytokine which is characteristic of that subpopulation (INFγ for type I, IL4 for type II, and IL2 for T_H0 and T_C0). The flag cytokine has a positive feedback effect on the phenotype by which it is produced and a negative feedback effect on the others. For example, INFγ promotes the expansion of T_H1 cells and down-regulates the expansion of T_H2 cells. Moreover, from the data of Schulz et al. 2009 we know that T_H1 cells need a constant exposure to INFγ and IL12 to preserve their ability to produce INFγ. Therefore, part of the flag cytokines produced needs to be used by the producing cell itself.

Simplification 22. *The cytokine production of a T_H1 cell requires INFγ up to 120 hours after activation, and IL12 subsequentially.*

As described by Schulz et al. 2009, INFγ and IL12 stimulate the expression of T-bet rather independently. Given the modeling technique used, we simplified this behavior using two distinct populations. Note that, in our model, T_H0 cells differentiate only to INFγ-consuming T_H1 cells, and only at this point IL12 is considered as a factor for the promotion of the population of T_H1 cells. This is due to the fundamental role of INFγ in our model, which leads to a limited interest in a model without INFγ.

Simplification 23. *The inflow of T cells in the granuloma is constituted only by T_H0 cells.*

Different populations of T cells enter the granuloma micro-environment. Notably, different types of T_H1 cells migrate from other granulomas, and contribute to a stronger inflammatory response. Given the local nature of our model, this aspect was not modeled.

5.3.5 Natural Killer T Cells

Simplification 24. *There is a constant influx of homeostatic NKT cells, but no reproduction.*

As described by Assumption 34, the mechanism employed by the immune system to keep the population of liver homeostatic NKT cells stable is not well characterized. Since the model we used is local, we are not able to test hypotheses on the behavior of NKT cells in the whole liver. Therefore, we are not able to test whether NKT cells reproduce in the liver or not. We will just assume that there is a constant influx of NKT cells (as documented by Coles & Raulet 2000), ignoring the source of this influx.

5.3.6 Natural Killer Cells

Simplification 25. *There is a constant influx of homeostatic NK cells, but no reproduction.*

Considerations similar to those described by Simplification 24, led to this simplification.

Chapter 6

Model Description

This chapter describes the details of our model. Section 6.1 presents a brief description of the working of the model, while the subsequent sections describe the details of the parameters (Section 6.3), places (Section 6.4), and transition (Section 6.5) of the Petri net model.

6.1 A Brief Description of the Model

6.1.1 Entities Modeled

This section briefly describes the entities considered by the model. Besides the parasite, various leukocytes are modeled: Kupffer cells, Non-resident macrophages, NKT cells, NK cells, and T cells (T_C0, T_C1, T_C2, T_H0, T_H1, T_H2). These leukocytes communicate via surface proteins (MHC I/II - peptides complexes, CD1d - peptides complexes, and CD47-SIRPα ligations) and cytokines (IL2, IL4, IL10, IL12, and INFγ). Additionally, the level of the different types of (de)activation of Kupffer cells and non-resided macrophages are modeled.

6.1.2 General Considerations on Cytokines and Active Cells

Many leukocytes produce cytokines upon activation. Cytokines are a mean of paracrine signaling, this means that the source cell — the cell producing the cytokines — must be near the target cell — the cell reacting to the cytokines — for the communication to be effective. If the source and target cells are far apart, the concentration of the cytokines near the target cells is generally too low to produce an effect. This fact poses a problem in interpreting the data on serum cytokines and cytokine-producing leukocytes: not all the active cells are producing and effect, as some of them can be too far from the target cells.

A possible approach to this problem would be to consider two populations of active leukocytes: those producing effects and those not producing effects. However, determining how a leukocyte moves between them is not easy and would require the introduction of space in the model, and parameters which are very hard to estimate. Therefore, we decided to model all the active cells as affecting the target cells. This implies that each active cell produces cytokines and the cytokines affect all the cells.

6.1.3 Leishmania Donovani

Leishmania donovani parasites (LDs from now on) reproduce, get killed by classically activated Kupffer cells, and deactivate Kupffer cells. Note that we are modeling only internalized parasites.

6.1.4 Kupffer Cells

The state of Kupffer cells (KCs from now on) is characterized by their levels of classical activation, alternative activation, and deactivation.

Classical activation is increased by exposure to INFγ. Alternative activation is increased by exposure to IL4. Deactivation is increased by

- exposure to IL10
- active NKT
- parasites

Classical activation, alternative activation, and deactivation down-regulate each other. Moreover, their levels decrease as a consequence of time.

KCs produce a quantity of IL10 proportional to their level of deactivation and alternative activation, and a quantity of IL12 proportional to their level of classical activation.

The number of MHC/CD1d peptides produced to be displayed on the surface is proportional to the number of parasites.

The ability of KCs to kill LDs is proportional to the level of classical activation.

6.1.5 Non-Resident Macrophages

Just like KCs, the state of non-resident macrophages (NRMPs from now on) is characterized by their levels of classical activation, alternative activation, and deactivation. However, the increase in their levels is controlled only by cytokines (as NRMPs are not infected by leishmania). NRMPs produce cytokines in the same way as KCs.

6.1.6 Natural Killer T Cells

We considered two mechanisms of NKT cells (NKTCs from now on) activation: by direct contact via a CD1d-TCR mechanism and by stress detection. In both cases NKTCs are activated only by infected KCs. The level of stress of KCs is proportional to the number of parasites.

Inactive NKTCs have an inflow, an outflow, and a death rate. Active NKTCs do not die. The inflow of NKTCs is limited by *space* constraint, and no inflow is present when more than 3 inactive NKTCs are present. The number of active NKTCs does not influence the inflow.

Both NKTCs activated by direct contact and NKTCs activated by stress deactivate the KC population by CD47-SIRPα ligation. Deactivation of NKTCs is time dependent and is parameterized.

Active NKTCs produce IL4 (at very low amount) and INFγ. Moreover, they attract NRMPs. The model allows additional activation of NKTCs by direct stimulation. NKTCs activated by direct stimulations preserve the aforementioned cytokine production profile (INFγ^{high}IL4$^{\text{low}}$). Additionally, the model allows for the blocking of the activation.

6.1.7 Natural Killer Cells

NK cells (NKCs from now on) can be activated by stress-detection of infected KCs and by exposure to IL12. The deactivation of NKCs is triggered by time or by a low level of IL12. Active NKCs change their phenotype from INFγ^{+}IL10^{-} to INFγ^{+}IL10^{+} as a consequence of time.

Inactive NKCs have an inflow, an outflow, and a death rate. Active NKCs do not die. The inflow of NKCs is limited by *space* constraint to 1 inactive NKC.

Active NKCs produce INFγ or INFγ and IL10 according to their phenotype.

6.1.8 T Cells

Only antigen specific T cells (TCs from now on) have been modeled. Additionally, memory and regulatory TCs have been ignored. Each TC is inactive until it gets activated by internalizing a peptide presented by KCs.

Inactive TCs have an inflow (as T_H0 and T_C0 cells), and outflow, but do not die. Active TCs do not die and do not outflow. Once differentiated, TCs do not display any phenotype decay (e.g., T_H1 cells never change their phenotype back to T_H0 cells).

Once activated, a TC consumes cytokines to keep its phenotype active. When the required cytokine is not present, the active TC moves to an *active but non cytokine-producing* state that we will call *silent*. The deactivation TCs is time dependent: after a fixed probabilistic time TCs deactivate (both

in the producing and non-producing state). Active TCs reproduce into TCs of the same phenotype.

Helper T Cells

Antigen specific helper TCs get to the place of infection as inactive T_H0 cells (T_H0Cs from now on). T_H0Cs differentiate to T_H1 cells (T_H1Cs from now on) when exposed to INFγ and to T_H2 cells (T_H2Cs from now on) when exposed to IL4. T_H0Cs have an $IL2^+$ phenotype (when active, they produce IL2) and consume IL2 to keep their phenotype active.

Newly differentiated T_H1Cs (which will be called $T_H1_{INF\gamma}$Cs) have an $IL2^+INF\gamma^+IL10^-$ phenotype (when active, they produce IL2 and INFγ) and use INFγ to sustain their phenotype. After a fixed probabilistic time, $T_H1_{INF\gamma}$Cs evolve to T_H1_{IL12}Cs. T_H1_{IL12}Cs cells have an $IL2^+INF\gamma^+IL10^-$ phenotype (when active, they produce IL2 and INFγ) but use IL12 to sustain their phenotype.

T_H1_{IL12}Cs subsequently evolve to an $IL2^+INF\gamma^+IL10^+$ phenotype (when active, they produce IL2, INFγ, and IL10) and use IL12 to sustain their phenotype (these cells will be called T_H1_{IL10}Cs). The model will test three possible mechanisms underlying this evolution:

1. Exposure to IL12
2. Exposure to INFγ
3. Prolonged activation

T_H2 cells (T_H2Cs from now on) have an $IL4^+IL10^+$ phenotype (when active, they produce IL4 and IL10) and use IL4 to sustain their phenotype.

There are two sources of T_H0Cs:

1. Liver (from other granulomas)
2. Spleen

Helper TCs activate by internalizing MHC class II peptides. The rate of activation depends on the number of peptides and TCs available. Both inactive and active T_H0Cs cells can differentiate to $T_H1_{INF\gamma}$Cs or T_H2Cs cells. The deactivation is time dependent. The reproduction rate of T_H0Cs is proportional to the concentration of IL2, the reproduction rate of T_H1Cs is proportional to the concentration of INFγ, and the reproduction rate of T_H2Cs is proportional to the concentration of IL4.

Cytotoxic T Cells

Antigen specific cytotoxic TCs get to the place of infection as inactive T_C0 cells (T_C0Cs from now on). T_C0Cs differentiate to T_C1 cells (T_C1Cs from

now on) when exposed to INFγ and T_C2 cells (T_C2Cs from now on) when exposed to IL4. T_C0Cs have an $IL2^+$ phenotype (when active, they produce IL2) and consume IL2 to keep their phenotype active.

T_C1Cs have an $IL2^+INF\gamma^+$ phenotype (when active, they produce IL2 and INFγ) and use INFγ to sustain their phenotype. T_C2Cs have an $IL10^+IL4^+$ phenotype (when active, they produce IL4 and IL10) and use IL4 to sustain their phenotype.

Cytotoxic TCs activate by internalizing MHC class I peptides. The rate of activation depends on the number of peptides and TCs available. Both inactive and active T_C0Cs can differentiate to T_C1Cs or T_C2Cs. The deactivation is time dependent. The reproduction rate of T_C0Cs is proportional to the concentration of IL2, the reproduction rate of T_C1Cs is proportional to the concentration of INFγ, and the reproduction rate of T_C2Cs is proportional to the concentration of IL4.

6.2 Main model: A Few Initial Remarks

The following description of the model is completely *textual*. Since Petri nets are a *visual* formalism, this may seem strange. However, the net used in our model is quite large and highly connected, and, while handling the net on a computer is feasible, displaying it on a sheet of paper would make it quite unreadable. Therefore, besides indicating the parameters used, we provide all the information needed to reconstruct the net.

6.3 Main model: Parameters

This section describes the parameters of the model. Parameter names are typeset using SMALL CAPS characters. Many parameters have been tuned to obtain the expected behavior from the model, when parameters have been taken from direct biological data, references to the specific qualitative assumptions are provided.

6.3.1 Environment

- CytDiff controls cytokines diffusion and drift due to the blood flow. A larger value indicates that cytokines leave the granuloma more rapidly.

- CellDiff controls cell diffusion and drift due to blood flow. A larger value indicates that cells leave the granuloma more rapidly. Cells are bigger and diffuse more slowly that cytokines, this is due to their size and to the effect of other stimuli (e.g., chemokines).

- IL4Effectiveness controls the effectiveness of IL4. A larger value indicates that less IL4 is needed to produce an effect.

- IL10Effectiveness controls the effectiveness of IL10. A larger value indicates that less IL10 is needed to produce an effect.
- IL12Effectiveness controls the effectiveness of IL12. A larger value indicates that less IL12 is needed to produce an effect.
- INFgEffectiveness controls the effectiveness of INFγ. A larger value indicates that less INFγ is needed to produce an effect.
- IL2Effectiveness controls the effectiveness of IL2. A larger value indicates that the cells react to IL2 more rapidly. IL12 has a lower effectiveness with respect to the other cytokines as it is less specific.
- INFgStart indicates when the injection of INFγ starts.
- INFgEnd indicates when the injection of INFγ ends.
- INFgLevel indicates the quantities of INFγ tokens injected per hours

Table 6.1 summarizes the values used for the parameters described above.

Parameter name	value
CytDiff	0.25
CellDiff	0.05
IL2Effectiveness	0.1
IL4Effectiveness	1
IL10Effectiveness	1
IL12Effectiveness	1
INFgEffectiveness	1
INFgStart	varies (default value 10^3)
INFgEnd	varies (default value 10^3)
INFgLevel	10

Table 6.1: Value of environment-related parameters

6.3.2 *Leishmania Donovani*

- LDKill controls the ability of amastigotes to kill macrophages. A larger value indicates that amastigotes need less time to kill the KCs.
- LDRep controls the reproduction rate of parasites. A larger value indicates a faster reproduction. The order of magnitude of the value was obtained from Assumption 43.
- LDDA controls the ability of amastigotes to deactivate KCs. A larger value indicates that amastigotes need less time to deactivate KCs.

Table 6.2 summarizes the values used for the parameters described above.

Parameter name	value
LDKill	0.00001
LDRep	0.009
LDDA	0.0001

Table 6.2: Value of Leishmania-related parameters

6.3.3 Macrophages

- CytAct controls the effect of cytokines on the activation of macrophages. This parameter represents the sensitivity of macrophages to cytokines. A larger value indicates that cytokines activate macrophages more rapidly.
- MKill controls the ability of KCs to kill LDs. A larger value indicates that KCs kill LDs more rapidly. The order of magnitude of the value was obtained from Assumption 49.
- MacArr controls the arrival rate of KCs. A larger value indicates a more rapid influx of KC, and thus leads to a larger core of the granuloma.
- MacCyt controls the cytokine production of macrophages. A larger value indicates a faster production.
- MHCILife represents the half-life of MHC I - peptide complexes. See Assumption 45 for the source of the value.
- MHCIILife represents the half-life of MHC II - peptide complexes. See Assumption 46 for the source of the value.
- CD1dLife represents the half-life of CD1d - peptide complexes. See Assumption 47 for the source of the value.
- MacActivationDecay represents the decay of (de)activation due to time. A larger value indicates a faster decay.
- MHCIIProd controls the production of MHCII peptides by KCs. A larger value indicates a faster production.
- CD1dProd controls the production of CD1d peptides by KCs. A larger value indicates a faster production.
- MHCIProd controls the production of MHCI peptides by KCs. A larger value indicates a faster production.
- MonoLeave controls the speed of the outflow of NRMPs. A larger value indicates a faster outflow.

- KCEscapeRate controls the migration of KCs not belonging to the granuloma in the initial stages of formation. A larger value leads to smaller granulomas.
- KCIncomeRate controls the inflows of new KCs. A larger value indicates a faster inflow.
- ActivationFight control the time needed for the different types of (de)activations to reciprocally down-regulate. A larger value indicates a slower down-regulation.
- KCCC controls the carrying capacity of KCs relative the parasites, that is, the number of parasites that a single cell can sustain. See Assumption 48 for the source of the value.

Table 6.3 summarizes the values used for the parameters described above.

Parameter name	value
CytAct	0.0049
MKill	0.025
MacArr	0.4
MacCyt	2
MHCILife	3
MHCIILife	60
CD1dLife	20
MacActivationDecay	0.001
MHCIProd	0.037
MHCIIProd	0.015
CD1dProd	0.024
MonoLeave	0.05
KCEscapeRate	0.4
KCIncomeRate	0.0001
ActivationFight	0.02
KCCC	100

Table 6.3: Value of phagocytes-related parameters

6.3.4 Natural Killer T Cells

- iNKTDA controls NKTCs-mediated deactivation of KCs. A larger value indicates that NKTCs deactivate macrophages more rapidly.
- iNKTStressAct controls stress-mediated activation of NKTCs. A larger value indicates that NKTCs respond more rapidly to the number of parasites of the infected KCs.

- iNKTCD1dAct controls CD1d-mediated activation of NKTCs. A larger value indicates that NKTCs respond more rapidly to the display of CD1d by macrophages.

- iNKTDeact controls deactivation of NKTCs. A smaller value indicates that NKTCs are more rapidly deactivated.

- iNKTLife represents the half-life of NKTCs. See Assumption 60 for the source of the value.

- iNKTArr controls the arrival of NKTCs. A larger value indicates a more rapid influx.

- iNKTIL4Prod controls the production of IL4 by NKTCs. A larger value indicates that NKTCs require less time to produce IL4.

- iNKTINFgProd controls the production of INFγ by NKTCs. A larger value indicates that NKTCs require less time to produce INFγ.

- iNKTChem indicates the ability of NKTCs to attract NRMPs by chemokines. A larger value indicates that NKTCs attract NRMPs faster.

- iNKTPool indicates the maximum number or homeostatic NKTCs that can be simultaneously present in the granuloma. See Assumptions 62 and 65 for the source of the value.

- iNKTEffPool indicates the maximum number or active NKTCs that can be simultaneously present in the granuloma.

- ExternalActivationRate controls the external activation of NKTCs. A larger value indicates a faster activation.

- NKTActivationStart indicates when the external activation of NKTCs starts.

- NKTActivationEnd indicates when the external activation of NKTCs ends.

- NKTBlockActivationStart indicates when the blocking of NKTCs activation starts.

- NKTBlockActivationEnd indicates when the blocking of NKTCs activation ends.

Table 6.4 summarizes the values used for the parameters described above.

Parameter name	value
NKTDA	0.05
NKTArr	0.3
NKTStressAct	0.0035
NKTCD1dAct	0.13
NKTDeact	0.3
NKTLife	400
NKTIL4Prod	0.2
NKTINFgProd	2
NKTChem	0.01
NKTPool	3
NKTEffPool	10^3
ExternalActivationRate	1
NKTActivationStart	varies (default value 10^3)
NKTActivationEnd	varies (default value 10^3)
NKTBlockActivationStart	varies (default value 10^3)
NKTBlockActivationEnd	varies (default value 10^3)

Table 6.4: Value of NKT cell-related parameters

6.3.5 Natural Killer Cells

- NKMacAct controls the macrophage-mediated activation of NKCs. A larger value indicates that NKCs respond more rapidly to the number of parasites of the infected KCs.

- NKDeact controls the deactivation of NKCs. A larger value indicates that NKCs are more rapidly deactivated.

- NKArr controls the arrival of NKCs. A larger value indicates a more rapid influx of NKCs.

- NKLife represents the half-life of inactive NKCs. See Assumption 60 for the source of the value.

- NKEvol controls the time required by NKCs to initiate the production of IL10. A larger value indicates that NKCs initiate the production of IL10 later. See Assumption 61 for the source of the value.

- IL12NKAct controls the IL12-mediated activation of NKCs. A larger value indicates that less IL12 is required for activation.

- IL12NKDeact controls the IL12-mediated deactivation of NKCs. A larger value indicates that even larger quantities of IL12 can deactivate NKCs.

- NKCytProd controls the production of cytokines by NKCs. A larger value indicates that NKCs need less time to produce cytokines.
- NKPool indicates the maximum number or homeostatic NKCs that can be simultaneously present in the granuloma. See Assumptions 58 and 65 for the source of the value.
- NKEffPool indicates the maximum number or active NKCs that can be simultaneously present in the granuloma

Table 6.5 summarizes the values used for the parameters described above.

Parameter name	value
NKMacAct	0.002
NKDeact	0.3
NKArr	0.08
NKLife	400
NKEvol	500
IL12NKAct	0.0005
IL12NKDeac	0.01
NKCytProd	2
NKPool	1
NKEffPool	10^6

Table 6.5: Value of NK cell-related parameters

6.3.6 T Cells

- Th1IL10Diff controls the emergence of IL10-producing phenotype by T_H1Cs. A larger value indicates a higher probability of mutation. The specific meaning and value depends on the model used (INFγ- , IL12-, or time-dependent evolution)
- TCellDiff controls the differentiation of TCs. A larger value indicates that T_H0Cs and T_C0Cs react more rapidly to cytokines by differentiating.
- TRep controls the reproduction of TCs. A larger value indicates that TCs react more rapidly to cytokines by reproducing.
- SpleenTCellArr controls the arrival of T_H0Cs and T_C0Cs from spleen. A larger value indicates a more rapid influx.
- LiverTCellArr controls the arrival of T_H0Cs and T_C0Cs from other granulomas in the liver. A larger value indicates a more rapid influx.

- TCellAct controls the activation of TCs. A larger value indicates that TCs react more rapidly to the display of MHC I/II peptides by KCs.

- TDeact controls the deactivation of TCs. A larger value indicates that TCs deactivate more rapidly.

- TChem indicates the ability of TCs to attract NRMPs by chemokines. A larger value indicates that the TCs attract NRMPs faster.

- ToZeroProd controls the quantity of cytokine needed to keep TCs active. A larger value indicates that a larger quantity is needed.

- FromZeroProd controls the reprise of cytokine production by silent TCs. A larger value indicates that less cytokines are needed.

- Th1Evol controls the evolution of T_H1Cs from an INFγ- to an IL12-consuming stage. A larger value indicates that the process takes more time. See Simplification 22 for the source of the value.

- TCellKeepProd controls the consumption of cytokines by TCs. A larger value indicates that TCs consume more cytokines to keep their phenotype active.

- TCellCytProd controls the production of cytokines by TCs. A larger value indicates that TCs need less time to produce cytokines.

- Th1IL10RepMod controls the reproduction of IL10-producing T_H1_{IL10}Cs. A smaller value indicates a more reduced reproduction ability.

- TimeTStart indicates the time of arrival of antigens specific TCs to the granuloma. See Assumption 52 for the source of the value.

- TimeTStop indicates the time after which antigens specific TCs stop getting to the granuloma from the spleen. See Assumption 53 for the source of the value.

Table 6.6 summarizes the values used for the parameters described above.

6.3.7 Parameter Simplifications

As described before, we set the values of some parameters to be the same with the aim of building a more meaningful, albeit less precise, model. Table 6.7 recaps the group of parameters that share the same values.

Note that, to assess the importance of the various cell populations, these parameters vary independently for sensitivity analysis.

Parameter name	value
Th1IL10Diff	0.013 for Time-Model 0.0004 for IL12-Model 0.00025 for INFγ-Model
TCellDiff	0.004
TRep	0.004
SpleenTCellArr	0.05
LiverTCellArr	0.05
TCellAct	0.0069
TDeact	0.3
TChem	0.01
ToZeroProd	0.001
FromZeroProd	0.001
Th1Evol	120
TCellKeepProd	0.4
TCellCytProd	2
TimeTStart	96
TimeTStop	125
Th1IL10RepMod	0.75

Table 6.6: Value of T cell-related parameters

Parameters meaning	Parameters
Cytokine production	MacCyt, iNKTINFgProd, NKCytProd, TCellCytProd
Deactivation	TDeact, iNKTDeact, NKDeact
Effectiveness	INFgEffectiveness, IL4Effectiveness, IL10Effectiveness, IL12Effectiveness
Chemokine production	TChem, iNKTChem
Inflow of T cells	SpleenTCellArr, LiverTCellArr

Table 6.7: Group of equal parameters

6.4 Main model: Places

This section describes the places of the model. Place names are typeset using **bold** characters.

6.4.1 Environment

The places **IL2**, **IL4**, **IL10**, **IL12**, and **INFg** model the number of IL2, IL4, IL10, IL12, and INFγ tokens.

Additionally, a number of control places have been introduced to control the behavior of the model.

- if **Remove – INFg** is marked INFγ is excluded from the model.
- if **Remove – IL10** is marked IL10 is excluded from the model.
- if **Remove – IL12** is marked IL12 is excluded from the model.

Finally, **EnvTime** counts the hours passed from the beginning of the infection.

6.4.2 Non-Resident Macrophages

Phagocytes models the number of NRMPs, while **PhagocytesAlternativeActivation**, **PhagocytesCalssicalActivation**, and **PhagocytesDeactivation** model their level of alternative activation, classical activation and deactivation.

6.4.3 Kupffer Cells

KC models the number of KCs, while **KCAlternativeActivation**, **KCCalssicalActivation**, and **KCDeactivation** model their level of alternative activation, classical activation and deactivation. Additionally, **AvailableKC** models the number of KCs available to form the granuloma.

Finally, **MHCI**, **MHCII**, and **CD1d** model the number of antigen specific MHC - peptide complexes displayed by KCs.

6.4.4 *Leishmania Donovani*

LD models the number of leishmania donovani amastigotes phagocytosed by the KCs.

6.4.5 Natural Killer Cells

NK and **NKEff** model inactive and active INFγ^+IL10$^-$ NKCs, while **NKIL10** and **NKIL10Eff** model inactive and active INFγ^+IL10$^+$ NKCs. Additionally, **NKNumber** models the total number of NKCs (both inactive and active). Finally, if **Remove – NK** is marked NKCs are excluded from the model.

6.4.6 Natural Killer T Cells

iNKT, **iNKTEffCd1d**, and **iNKTEffStress** model inactive, CD1d-activated and stress-activated NKTCs. Additionally, **CD47Binded** models the number of CD47-SIRPα ligations and **NKTNumber** models the total number of NKTCs (both inactive and active).

Moreover, a number of control places have been introduced to control the behavior of the model.

- if **Remove – iNKT** is marked NKTCs are excluded from the model.
- it **iNKT – CD1d** is marked NKTCs can be activated by a CD1d-mediated mechanism.
- it **iNKT – stress** is marked NKTCs can be activated by a stress-mediated mechanism.
- **PreventActivationToken** is marked and used to prevent activation of NKTCs if necessary.
- when **PreventActivation** is marked NKTCs cannot activate

Finally, **iNKTTime** counts the hours passed from the beginning of the infection.

6.4.7 T Cells

Three states are possible for T cells:

- Inactive: **Th0**, **Th1I**, **Th1II**, **Th1IL10**, **Th2**, **Tc0**, **Tc1**, and **Tc2**, model inactive T_H0Cs, $T_H1_{INF\gamma}Cs$, $T_H1_{IL12}Cs$, $T_H1_{IL10}Cs$, T_C0Cs, T_C1Cs, and T_C2Cs, respectively.
- Active: **Th0Eff**, **Th1IEff**, **Th1IIEff**, **Th1IL10Eff**, **Th2Eff**, **Tc0Eff**, **Tc1Eff**, and **Tc2Eff**, model active T_H0Cs, $T_H1_{INF\gamma}Cs$, $T_H1_{IL12}Cs$, $T_H1_{IL10}Cs$, T_C0Cs, T_C1Cs, and T_C2Cs, respectively.
- Silent: **Th0ZeroProd**, **Th1IZeroProd**, **Th1IIZeroProd**, **Th1IL10ZeroProd**, **Th2ZeroProd**, **Tc0ZeroProd**, **Tc1ZeroProd**, and **Tc2ZeroProd**, model active T_H0Cs, $T_H1_{INF\gamma}Cs$, $T_H1_{IL12}Cs$, $T_H1_{IL10}Cs$, T_C0Cs, T_C1Cs, and T_C2Cs, respectively.

Moreover, **ThNumber** and **TcNumber** model the total number of helper and cytotoxic TCs (both inactive and active). Additionally, if **Remove – T** is marked, TCs are excluded from the model.

Finally, **TCellTime** counts the hours passed from the beginning of the infection.

6.4.8 Others

The place **Infected** is marked only if the number of LDs is greater than 0.

6.4.9 Initial Marking

The initial number of entities is fixed for all wild type conditions, specifically:

- 4 tokens in **LD**.
- 1 token in **KC**.
- 10 tokens in **AvailableKC**
- 2 tokens in **iNKT**.
- 2 tokens in **iNKTNumber**.
- 1 token in **NK**.
- 1 token in **NKNumber**.
- 1 token in **Infected**.
- 1 token in **PreventActivationToken**.

When cell populations are removed form the model, the corresponding tokens are removed.

Additionally, under "baseline conditions", **iNKT – CD1d** contains 1 token.

6.5 Main model: Transitions

This section describes the transitions of the model. Transition names are typeset using *italics* characters. The pre- and post-places of a transition are followed by an indication of the type and cardinality of the arc connecting that place to/from the transition. Only cardinalities different from 1 are explicitly indicated. The following arc types are possible:

- Standard arc ($\rightarrow$)
- Read arc ($\multimap$)
- Inhibitory arc ($\multimap$)
- Modifier arc ($\dashrightarrow$)

The following Snoopy-specific function have been used:

- ImmediateFiring() indicates an immediate transition.

- TimedFiring(x) indicates a transition that, when enabled, fires every x time units (in our models x hours).
- leq(x, y) is 0 if $x \leq y$, and 1 otherwise.
- geq(x, y) is 0 if $x \geq y$, and 1 otherwise.

6.5.1 Environment

Cytokine tokens are produced and consumed by various cells. The transitions controlling this production are described in the subsections relative to these cells. Additionally, cytokine tokens are affected by a diffusion and drift due to blood flow. We used a simple exponential decay model, and therefore CytDiff and the half-life of the cytokines are inversely proportional.

$IL2 - Diff$ models the diffusion and drift due to blood flow of IL2. The preplace is

- **IL2**$(\rightarrow)$

The coefficient is

$$\text{CytDiff} \cdot \mathbf{IL2}$$

$IL4 - Diff$ models the diffusion and drift due to blood flow of IL4. The preplace is

- **IL4**$(\rightarrow)$

The coefficient is

$$\text{CytDiff} \cdot \mathbf{IL4}$$

$IL10 - Diff$ models the diffusion and drift due to blood flow of IL10. The preplace is

- **IL10**$(\rightarrow)$

The coefficient is

$$\text{CytDiff} \cdot \mathbf{IL10}$$

$IL12 - Diff$ models the diffusion and drift due to blood flow of IL12. The preplace is

- **IL12**$(\rightarrow)$

The coefficient is

$$\text{CytDiff} \cdot \mathbf{IL12}$$

$INFg - Diff$ models the diffusion and drift due to blood flow of INFγ. The preplace is

- **INFg**(→)

The coefficient is

$$\text{CytDiff} \cdot \mathbf{INFg}$$

$Drain - IL10$ models the removal of IL10. The preplaces are

- **RemoveIL10**(⇀)
- **IL10**(→)

The coefficient is

ImmediateFiring()

$Drain - IL12$ models the removal of IL12. The preplaces are

- **RemoveIL12**(⇀)
- **IL12**(→)

The coefficient is

ImmediateFiring()

$Drain - INFg$ models the removal of INFγ. The preplaces are

- **RemoveINFg**(⇀)
- **INFg**(→)

The coefficient is

ImmediateFiring()

$Inject - INFg$ models the injection of INFγ. The preplaces are

- **RemoveINFg**(⇀)
- **INFg**(→)

The coefficient is

$$\text{INFgLevel} \cdot geq(\mathbf{EnvTime}, \text{INFgStart}) \cdot leq(\mathbf{EnvTime}, \text{INFgEnd})$$

When this transition is enabled, that is when INFgStart ≤ **EnvTime** ≤ INFgEnd, an average number INFgLevel of INFγ tokens are injected per hour.

6.5.2 *Leishmania Donovani* (LD)

LD – Reproduce models the reproduction of amastigotes. The reproduction is assumed to be logistic with carrying capacity equal to $\text{KCCC} \cdot \mathbf{KC}$. The preplace is

- $\mathbf{LD}(\multimap)$

The postplace is

- $\mathbf{LD}(\to)$

The coefficient is

$$\text{LDREP} \cdot \mathbf{LD} \cdot \left(1 - \frac{\mathbf{LD}}{\text{KCCC} \cdot \mathbf{KC}}\right)$$

KC – Kill – LD models the killing of amastigotes by KCs. The preplaces are

- $\mathbf{LD}(\to)$
- $\mathbf{KC}(\multimap)$

The coefficient is

$$\text{MKILL} \cdot (0.01 \cdot \mathbf{ClassicalAcivation}) \cdot \mathbf{Macrophage}$$

Since $\mathbf{ClassicalAcivation} \leq 100$, on average, n fully classically activated macrophages kill a parasite every $1/(n \cdot \text{MKILL})$ hours.

LD – Deactivate models the deactivation of KCs by amastigotes. The preplaces are

- $\mathbf{LD}(\multimap)$
- $\mathbf{KC}(\multimap)$
- $\mathbf{KCDeactivation}(100 \multimap)$

The postplaces is

- $\mathbf{KCDeactivation}(\to)$

The coefficient is

$$\text{LDDA} \cdot \mathbf{LD}$$

Therefore, the deactivation activity of the parasites is proportional to the number of LDs.

LD – Kill – KC models the death of KCs due to the amastigotes. The preplaces are

- **KC**(→)
- **LD**(⇀)

The coefficient is

$$\text{LDKILL} \cdot \frac{\mathbf{LD}}{\mathbf{KC}}$$

As we can see from the coefficient, the death rate depends on the ratio of LDs to KCs.

6.5.3 Non-Resident Macrophages (NRMPs)

NRMPs are attracted to the granuloma by the chemokines produced by by NKTCs and Type I TCs. Once they get to the granuloma, they can get (de)activated by various cytokines. (De)activations down-regulate each other and decay over time. NRMPs produce different cytokines according to their (de)activations, and leave the granuloma when the level of infection decreases.

$Mono - Arr$ models the arrival of NRMPs due to the chemokines produced by NKTCs, T_H1 and T_C1 cells. The preplaces are

- **iNKTEffCD1d**(⇀)
- **iNKTEffStress**(⇀)
- **Th1IEff**(⇀)
- **Th1IIEff**(⇀)
- **Th1IL10Eff**(⇀)
- **Tc1Eff**(⇀)

The postplace is

- **Phagocytes**(→)

The coefficient is

$$\begin{aligned}&\text{iNKTCHEM} \cdot (\mathbf{iNKTEffCD1d} + \mathbf{iNKTEffStress}) \\ &+ \text{TCHEM} \cdot (\mathbf{Th1IEff} + \mathbf{Th1IIEff} + \mathbf{Th1IL10Eff}) \\ &+ \text{TCHEM} \cdot \mathbf{Tc1Eff}\end{aligned}$$

More chemokine-producing cells imply a faster arrival rate.

The various (de)activations of NRMPs are proportional to the quantity of specific cytokines and their effectiveness. For example, the classical activation is proportional to the quantity of **INFg** and its effectiveness.

$INFg - Mono - CActivate$ models the classical activation of NRMPs by INFγ. The preplaces are

- **PhagocytesClassicalActivation**(100 $\multimap$)
- **Phagocytes**($\bullet\!\!\rightarrow$)
- **INFg**($\rightarrow$)

The postplace is

- **PhagocytesClassicalActivation**($\rightarrow$)

The coefficient is

$$\text{CytAct} \cdot \text{INFgEffectiveness} \cdot \mathbf{INFg}$$

$IL4-Mono-AActivate$ models the alternative activation of NRMPs by IL4. The preplaces are

- **PhagocytesAlternativeActivation**(100 $\multimap$)
- **Phagocytes**($\bullet\!\!\rightarrow$)
- **IL4**($\rightarrow$)

The postplace is

- **PhagocytesAlternativeActivation**($\rightarrow$)

The coefficient is

$$\text{CytAct} \cdot \text{IL4Effectiveness} \cdot \mathbf{IL4}$$

$IL-10-Mono-DA$ models the deactivation of NRMPs by IL10. The preplaces are

- **PhagocytesDeactivation**(100 $\multimap$)
- **Phagocytes**($\bullet\!\!\rightarrow$)
- **IL10**($\rightarrow$)

The postplace is

- **PhagocytesDeactivation**($\rightarrow$)

The coefficient is

$$\text{CytAct} \cdot \text{IL10Effectiveness} \cdot \mathbf{IL10}$$

The (de)activations down-regulate each-other. This down-regulation is proportional to the sum of the (de)activations considered. For example, the reciprocal down-regulation of deactivation and classical activation is proportional to the sum of **PhagocytesClassicalActivation**+**PhagocytesDeactivation**.

$Mono-DA-vs-CA$ models the reciprocal downregulation of deactivation and classical activation of NRMPs. The preplaces are

- **PhagocytesClassicalActivation**(→)
- **PhagocytesDeactivation**(→)

The coefficient is

$$\text{ActivationFight} \cdot (\mathbf{PhagocytesClassicalActivation} + \mathbf{PhagocytesDeactivation})$$

Mono–DA–vs–AA models the reciprocal downregulation of deactivation and alternative activation of NRMPs. The preplaces are

- **PhagocytesAlternativeActivation**(→)
- **PhagocytesDeactivation**(→)

The coefficient is

$$\text{ActivationFight} \cdot (\mathbf{PhagocytesAlternativeActivation} + \mathbf{PhagocytesDeactivation})$$

Mono – CA – vs – AA models the reciprocal downregulation of classical and alternative activation of NRMPs. The preplaces are

- **PhagocytesClassicalActivation**(→)
- **PhagocytesAlternativeActivation**(→)

The coefficient is

$$\text{ActivationFight} \cdot (\mathbf{PhagocytesAlternativeActivation} + \mathbf{PhagocytesClassicalActivation})$$

The decay of (de)activations is assumed to be exponential, and a larger MacActivationDecay indicates a shorter half-life of (de)activations.

PhagocytesClassicalActivation – Decay models the decay of classical activation of NRMPs as a consequence of time. The preplace is

- **PhagocytesClassicalActivation**(→)

The coefficient is

$$\text{MacActivationDecay} \cdot \mathbf{PhagocytesClassicalActivation}$$

PhagocytesAlternativeActivation – Decay models the decay of alternative activation of NRMPs as a consequence of time. The preplace is

- **PhagocytesAlternativeActivation**(→)

The coefficient is

$$\text{MacActivationDecay} \cdot \mathbf{PhagocytesAlternativeActivation}$$

PhagocytesDeactivation – Decay models the decay of deactivation of NRMPs as a consequence of time. The preplace is

- **PhagocytesDeactivation**$(\rightarrow)$

The coefficient is

$$\text{MacActivationDecay} \cdot \mathbf{PhagocytesDeactivation}$$

The cytokine production of NRMPs is proportional to their number and levels of (de)actiavations.

$Mono{-}DA{-}IL10$ models the production of IL10 by deactivated NRMPs. The preplaces are

- **Phagocytes**$(\multimap)$
- **PhagocytesDeactivation**$(\multimap)$

The postplace is

- **IL10**$(\rightarrow)$

The coefficient is

$$\text{MacCyt} \cdot (0.01 \cdot \mathbf{PhagocytesDeactivation}) \cdot \mathbf{Phagocytes}$$

$Mono - AA - IL10$ models the production of IL10 by alternatively activated NRMPs. The preplaces are

- **Phagocytes**$(\multimap)$
- **PhagocytesAlternativeActivation**$(\multimap)$

The postplace is

- **IL10**$(\rightarrow)$

The coefficient is

$$\text{MacCyt} \cdot (0.01 \cdot \mathbf{PhagocytesAlternativeActivation}) \cdot \mathbf{Phagocytes}$$

$Mono - IL12$ models the production of IL12 by classically activated NRMPs. The preplaces are

- **Phagocytes**$(\multimap)$
- **PhagocytesClassicalActivation**$(\multimap)$

The postplace is

- **IL12**(→)

The coefficient is

$$\text{MacCyt} \cdot (0.01 \cdot \textbf{PhagocytesClassicalActivation}) \cdot \textbf{Phagocytes}$$

The departure of NRMPs is assumed to be inversely proportional to the number of parasites. This transition is partly responsible for the dissolution of the granuloma.

PhagocyteDepart models the departure of NRMPs due to the reduced parasite burden. The preplaces are

- **Phagocytes**(→)
- **LD**(→)

The coefficient is

$$\text{MonoLeave} \cdot \frac{1}{\textbf{LD} + 1}$$

6.5.4 Kupffer Cells (KCs)

The inflow and outflow of available KCs is assume to be constant.

KCINflow models the inflow of available KCs. The postplace is

- **AvailableKC**(→)

The coefficient is

$$\text{KCIncomeRate}$$

MigrateToOtherGranulomas models the outflow of available KCs due to other granulomas. The preplace is

- **AvailableKC**(→)

The coefficient is

$$\text{KCEscapeRate}$$

The aggregation of a KC to a granuloma is proportional to the infection level of the granuloma, and therefore to the ratio of LDs to KCs.

KC−Arrival models the formation of the core of the granuloma by KCs. The preplace is

- **AvailableKC**(→)

The postplace is

- **KC**(→)

The coefficient is

$$\textsc{MacArr} \cdot \frac{\mathbf{LD}}{\mathbf{KC} + 1}$$

The (de)activation activities and cytokine production of KCs is the same as NRMPs.

$IL4 - KC - AActivate$ models the alternative activation of KCs by IL4. The preplaces are

- **KCAlternativeActivation**(100 ⊸)
- **KC**(⊸)
- **IL4**(→)

The postplace is

- **KCAlternativeActivation**(→)

The coefficient is

$$\textsc{CytAct} \cdot \text{IL4}\textsc{Effectiveness} \cdot \mathbf{IL4}$$

$INFg - KC - CActivate$ models the classical activation of KCs by INFγ. The preplaces are

- **KCClassicalActivation**(100 ⊸)
- **KC**(⊸)
- **INFg**(→)

The postplace is

- **KCClassicalActivation**(→)

The coefficient is

$$\textsc{CytAct} \cdot \text{INFg}\textsc{Effectiveness} \cdot \mathbf{INFg}$$

$IL10 - KC - DA$ models the deactivation of KCs by IL10. The preplaces are

- **KCDeactivation**(100 ⊸)
- **KC**(⊸)
- **IL10**(→)

The postplace is

- **KCDeactivation**(→)

The coefficient is

$$\text{CytAct} \cdot \text{IL10Effectiveness} \cdot \mathbf{IL10}$$

$KC-DA-vs-CA$ models the reciprocal down-regulation of deactivation and classical activation of KCs. The preplaces are

- **KCClassicalActivation**(→)
- **KCDeactivation**(→)

The coefficient is

$$\text{ActivationFight} \cdot (\mathbf{KCClassicalActivation} + \mathbf{KCDeactivation})$$

$KC-DA-vs-AA$ models the reciprocal down-regulation of deactivation and alternative activation of KCs. The preplaces are

- **KCAlternativeActivation**(→)
- **KCDeactivation**(→)

The coefficient is

$$\text{ActivationFight} \cdot (\mathbf{KCAlternativeActivation} + \mathbf{KCDeactivation})$$

$KC-CA-vs-AA$ models the reciprocal down-regulation of classical and alternative activations of KCs. The preplaces are

- **KCAlternativeActivation**(→)
- **KCClassicalActivation**(→)

The coefficient is

$$\text{ActivationFight} \cdot (\mathbf{KCAlternativeActivation} + \mathbf{KCClassicalActivation})$$

$KCClassicalActivation-Decay$ models the decay of classical activation of KCs as a consequence of time. The preplace is

- **KCClassicalActivation**(→)

The coefficient is

$$\text{MacActivationDecay} \cdot \mathbf{KCClassicalActivation}$$

KCAlternativeActivation – Decay models the decay of alternative activation of KCs as a consequence of time. The preplace is

- **KCAlternativeActivation**$(\rightarrow)$

The coefficient is

$$\text{MacActivationDecay} \cdot \mathbf{KCAlternativeActivation}$$

KCDeactivation – Decay models the decay of deactivation of KCs as a consequence of time. The preplace is

- **KCDeactivation**$(\rightarrow)$

The coefficient is

$$\text{MacActivationDecay} \cdot \mathbf{KCDeactivation}$$

$KC-DA-IL10$ models the production of IL10 by deactivated KCs. The preplaces are

- **KC**$(\multimap)$
- **KCDeactivation**$(\multimap)$

The postplace is

- **IL10**$(\rightarrow)$

The coefficient is

$$\text{MacCyt} \cdot (0.01 \cdot \mathbf{KCDeactivation}) \cdot \mathbf{KC}$$

$KC-AA-IL10$ models the production of IL10 by alternatively activated KCs. The preplaces are

- **KC**$(\multimap)$
- **KCAlternativeActivation**$(\multimap)$

The postplace is

- **IL10**$(\rightarrow)$

The coefficient is

$$\text{MacCyt} \cdot (0.01 \cdot \mathbf{KCAlternativeActivation}) \cdot \mathbf{KC}$$

$KC-IL12$ models the production of IL12 by classically activated KCs. The preplaces are

- **KC**(⇀•)
- **KCClassicalActivation**(⇀•)

The postplace is

- **IL12**(→)

The coefficient is

$$\text{MacCyt} \cdot (0.01 \cdot \textbf{KCClassicalActivation}) \cdot \textbf{KC}$$

The production of peptides is proportional to the number of LDs. This is due to the fact that the whole population of KCs produces the peptides.

$KC - Produce - MHCI$ models the production of MHC I peptides by KCs. The preplaces are

- **KC**(⇀•)
- **LD**(⇀•)

The postplace is

- **MHCI**(→)

The coefficient is

$$\text{MHCIProd} \cdot \textbf{LD}$$

$KC - Produce - MHCII$ models the production of MHC II peptides by KCs. The preplaces are

- **KC**(⇀•)
- **LD**(⇀•)
- **KCClassicalAcivation**(-⇀)
- **KCAlternativeActivation**(-⇀)
- **KCDeactivation**(-⇀)

The postplace is

- **MHCII**(→)

The coefficient is

$$\text{MHCIIProd} \cdot \textbf{LD} \cdot \frac{1 + \textbf{KCClassicalAcivation}/50 + \textbf{KCAlternativeActivation}/50}{1 + \textbf{KCDeactivation}/50}$$

The coefficient implies that the production of MHC II peptides is promoted by activations and advertised by deactivation.

$KC - Produce - CD1d$ models the production of CD1d peptides by KCs. The preplaces are

- **KC**(⇀)
- **LD**(⇀)

The postplace is

- **CD1d**(→)

The coefficient is

$$\text{CD1dProd} \cdot \mathbf{LD}$$

MHC I/II and CD1d complexes have an exponential decay.

MHCI – Decay models the decay of MHC I peptides displayed KCs. The preplace is

- **MHCI**(→)

The coefficient is

$$\frac{\mathbf{MHCI}}{\text{MHCILife}} \cdot \log(2)$$

MHCII – Decay models the decay of MHC II peptides displayed KCs. The preplace is

- **MHCII**(→)

The coefficient is

$$\frac{\mathbf{MHCII}}{\text{MHCIILife}} \cdot \log(2)$$

CD1d – Decay models the decay of CD1d peptides displayed KCs. The preplace is

- **CD1d**(→)

The coefficient is

$$\frac{\mathbf{CD1d}}{\text{CD1dLife}} \cdot \log(2)$$

KC – Kill – LD models the parasiticidal activity of KCs. The ability of KCs to kill the amastigotes is assumed to proportional to their level of classical activation. The preplaces are

- **LD**(→)
- **KC**(⇀)
- **KCClassicalAcivation**(⇀)

The coefficient is

$$\text{MKILL} \cdot (0.01 * \mathbf{KCClassicalAcivation}) \cdot \mathbf{KC} \cdot \mathbf{LD}$$

KC – Depart models the departure of KCs after the clearance of the parasites. The preplaces are

- **LD**($\multimap$)
- **KC**($\rightarrow$)

The coefficient is

$$\text{CELLDIFF} \cdot \mathbf{KC}$$

Note that no KC departs unless all the parasites have been cleared.

6.5.5 Natural Killer Cells (NKCs)

NK – Arrival models the arrival of inactive INFγ^+IL10$^+$ NKCs. This inflow is assumed to be constant and limited by space constraints. The preplaces are

- **NK**($\dashrightarrow$)
- **NKIL10**($\dashrightarrow$)
- **RemoveNK**($\multimap$)

The postplaces are

- **NK**($\dashrightarrow$)
- **NKNumber**($\dashrightarrow$)

The coefficient is

$$\text{NKARR} \cdot \text{leq}(\mathbf{NK} + \mathbf{NKIL10}, \text{NKPOOL} - 1)$$

Note that this transition is enabled only if no more than NKPOOL inactive NKCs are presents and **RemoveNK** is not marked.

NKIL10–Act models the KCs-mediated activation of INFγ^+IL10$^+$ NKCs. This activation is proportional to the number of **LD**. The preplaces are

- **NKIL10**($\rightarrow$)
- **KC**($\rightarrow\bullet$)
- **LD**($\rightarrow\bullet$)
- **NKNumber**($\dashrightarrow$)

The postplaces are

- **NKEff**$(\rightarrow)$

The coefficient is

$$\text{NKMacAct} \cdot \mathbf{NKIL10} \cdot \mathbf{LD} \cdot \text{leq}(\mathbf{NKNumber}, \text{NKEffPool} - 1)$$

Note that this transition is enabled only if no more than NKEffPool active NKCs are presents.

$IL12\text{–}NKIL10\text{–}Act$ models the IL12-mediated activation of INFγ^+IL10$^+$ NKCs. This activation is proportional to the number of **IL12**. The preplaces are

- **NKIL10**$(\rightarrow)$
- **IL12**$(\rightarrow)$
- **NKNumber**$(\cdot\rightarrow)$

The postplaces are

- **NKEff**$(\rightarrow)$

The coefficient is

$$\text{IL12NKAct} \cdot \mathbf{NKIL10} \cdot \mathbf{IL12} \cdot \text{leq}(\mathbf{NKNumber}, \text{NKEffPool} - 1)$$

Similarity to $NKIL10 - Act$, this transition is enabled only if no more than NKEffPool active NKCs are presents.

$NK\text{–}Evol$ models the mutation of the phenotype of NKCs from INFγ^+IL10$^-$ to INFγ^+IL10$^+$. The preplace is

- **NKEff**$(\rightarrow)$

The postplaces is

- **NKIL10Eff**$(\rightarrow)$

The coefficient is

$$\mathbf{NKEff}\text{NKEvol} \cdot \log(9)$$

The coefficient indicates that, if the number of **NKEff** were unaffected by other transitions, after NKEvol hours, 90% of tokens in **NKEff** wuold be expected to have moved to **NKIL10Eff**.

The cytokine production of each NKC is assumed to be constant.

$NK - Cyt$ models the production of INFγ by active INFγ^+IL10$^-$ NKCs. The preplace is

- **NKEff**$(\multimap)$

The postplaces is

- **INFg**$(\rightarrow)$

The coefficient is

$$\mathbf{NKEff} \cdot \text{NKCytProd}$$

$NKIL10\text{–}Cyt$ models the production of INFγ and IL10 by active INFγ^{+}IL10^{+} NKCs. The preplace is

- **NKIL10Eff**$(\multimap)$

The postplaces are

- **INFg**$(\rightarrow)$
- **IL10**$(\rightarrow)$

The coefficient is

$$\mathbf{NKEff} \cdot \text{NKCytProd}$$

Two mechanisms of deactivation of NKCs are present. A timed deactivation, which is exponentially distributed, and an IL12-dependent deactivation, which is inversely proportional to the quantity of **IL12**.

$NK - Deact$ models the deactivation of active INFγ^{+}IL10^{-} NKCs. The preplaces are

- **NKEff**$(\rightarrow)$

The postplaces is

- **NK**$(\rightarrow)$

The coefficient is

$$\text{NKDeact} * \mathbf{NKEff}$$

$NKIL10 - Deact$ models the deactivation of active INFγ^{+}IL10^{+} NKCs. The preplace is

- **NKIL10Eff**$(\rightarrow)$

The postplaces is

- **NKIL10**$(\rightarrow)$

The coefficient is

$$\text{NKDeact} * \mathbf{NKIL10Eff}$$

$IL12 - NK - Deact$ models the deactivation active INFγ^+IL10$^-$ NKCs due to a low concentration of IL12. The preplaces are

- **NKEff**$(\rightarrow)$
- **IL12**$(\cdot\rightarrow)$

The postplaces is

- **NK**$(\rightarrow)$

The coefficient is

$$\frac{\text{IL12NKDeact} \cdot \mathbf{NKEff}}{1 + \mathbf{IL12}}$$

$IL12 - NKIL10 - Deact$ models the deactivation of active INFγ^+IL10$^+$ NKCs due to a low concentration of IL12. The preplaces are

- **NKIL10Eff**$(\rightarrow)$
- **IL12**$(\cdot\rightarrow)$

The postplaces is

- **NKIL10**$(\rightarrow)$

The coefficient is

$$\frac{\text{IL12NKDeact} \cdot \mathbf{NKIL10Eff}}{1 + \mathbf{IL12}}$$

Similarly to cytokines, inactive NKCs are affected by a diffusion and drift due to blood flow.

$NK - Diff$ models the diffusion and drift of inactive INFγ^+IL10$^-$ NKCs due to blood flow. The preplaces are

- **NK**$(\rightarrow)$
- **NKNumber**$(\rightarrow)$

The coefficient is

$$\text{CellDiff} \cdot \mathbf{NK}$$

$NKIL10 - Diff$ models the diffusion and drift of inactive INFγ^+IL10$^+$ NKCs due to blood flow. The preplaces are

- **NKIL10**($\rightarrow$)
- **NKNumber**($\rightarrow$)

The coefficient is

$$\textsc{CellDiff} \cdot \mathbf{NKIL10}$$

$NK - Death$ and $NKIL10 - Death$ models the death of NKCs. These transitions use the half-life obtained by biological data.

$NK - Death$ models the death of inactive INFγ^+IL10$^-$ NKCs. The preplaces are

- **NK**($\rightarrow$)
- **NKNumber**($\rightarrow$)

The coefficient is

$$\frac{\mathbf{NK}}{\textsc{NKLife}} \cdot \log(2)$$

$NKIL10 - Death$ models the death of inactive INFγ^+IL10$^+$ NKCs. The preplaces are

- **NKIL10**($\rightarrow$)
- **NKNumber**($\rightarrow$)

The coefficient is

$$\frac{\mathbf{NKIL10}}{\textsc{NKLife}} \cdot \log(2)$$

6.5.6 Natural Killer T Cells (NKTCs)

The transitions modeling the arrival, diffusion and drift, and death of NKTCs are similar to those of NKCs.

$iNKT - Arrival$ models the arrival of NKTCs. The preplaces are

- **iNKT**($\dashrightarrow$)
- **RemoveNKT**($\multimap$)

The postplaces are

- **iNKT**($\rightarrow$)
- **iNKTNumber**($\rightarrow$)

The coefficient is

$$\text{iNKTArr} \cdot \text{leq}(\mathbf{iNKT}, \text{NKTPool} - 1)$$

Two activation mechanisms are possible for NKTCs: CD1d-mediated, which is proportional to the number of **CD1d**, and stress-mediated, which is proportional to the number of **LD**.

iNKT – CD1d – Act models the CD1d-mediated activation of NKTCs. The preplaces are

- **iNKT**(→)
- **iNKT – CD1d**(⇸)
- **CD1d**(→)
- **iNKTNumber**(⇢)
- **PreventActivation**(⊸)

The postplaces are

- **iNKTEffCD1d**(→)
- **CD47Binded**(→)

The coefficient is

$$\text{iNKTCD1dAct} \cdot \mathbf{iNKT} \cdot \mathbf{CD1d} \cdot \text{leq}(\mathbf{iNKTNumber}, \text{iNKTEffPool} - 1)$$

Note that this transition is enabled only if no more than iNKTEffPool active NKTCs are presents, **iNKT – CD1d** is marked, and **PreventActivation** is not marked.

iNKT – Stress – Act models the stress-mediated activation of NKTCs. The preplaces are

- **iNKT**(→)
- **iNKT – Stress**(⇸)
- **LD**(⇸)
- **iNKTNumber**(⇢)
- **PreventActivation**(⊸)

The postplaces are

- **iNKTEffStress**(→)
- **CD47Binded**(→)

The coefficient is

$$\text{iNKTStressAct} \cdot \mathbf{iNKT} \cdot \mathbf{LD}$$

Note that this transition is enabled only if no more than iNKTEffPool active NKTCs are presents, **iNKT – Stress** is marked, and **PreventActivation** is not marked.

The deactivation activity of NKTCs is proportional to the number of **CD47Binded**.

iNKT – Deactivate models the deactivation of KCs by NKTCs. The preplaces are

- **CD47Binded**$(\multimap\bullet)$
- **KC**$(\multimap\bullet)$
- **KCDeactivation**$(100 \multimap\circ)$

The postplaces is

- **KCDeactivation**$(\to)$

The coefficient is

$$\text{iNKTDA} \cdot \mathbf{CD47Binded}$$

The cytokine production of each NKC is assumed to be constant, but different quantities of **INFg** and **IL4** are produced.

$iNKTCD1d-INFg$ models the production of INFγ by CD1d-activated NKTCs. The preplace is

- **iNKTEffCD1d**$(\multimap\bullet)$

The postplaces is

- **INFg**$(\to)$

The coefficient is

$$\text{iNKTINFgProd} \cdot \mathbf{iNKTEffCD1d}$$

$iNKTCD1d-IL4$ models the production of IL4 by CD1d-activated NKTCs. The preplace is

- **iNKTEffCD1d**$(\multimap\bullet)$

The postplaces is

- **IL4**$(\to)$

The coefficient is

$$\text{iNKTIL4Prod} \cdot \mathbf{iNKTEffCD1d}$$

$iNKTEffStress - INFg$ models the production of INFγ by stress-activated NKTCs. The preplace is

- **iNKTEffStress(⇸)**

The postplaces is

- **INFg(→)**

The coefficient is

$$\text{iNKTINFgProd} \cdot \mathbf{iNKTEffStress}$$

$iNKTEffStress - IL4$ models the production of IL4 by stress-activated NKTCs. The preplace is

- **iNKTEffStress(⇸)**

The postplaces is

- **IL4(→)**

The coefficient is

$$\text{iNKTIL4Prod} \cdot \mathbf{iNKTEffStress}$$

The deactivation of NKTCs is time-dependent.
$iNKT - CD1d - Deact$ models the deactivation of CD1d-activated NKTCs. The preplaces are

- **iNKTEffCD1d(→)**
- **iNKT – CD1d(⇸)**
- **CD47Binded(→)**

The postplaces is

- **iNKT(→)**

The coefficient is

$$\text{iNKTDeact} \cdot \mathbf{iNKTEffCD1d}$$

$iNKT - Stress - Deact$ models the deactivation of stress-activated NKTCs. The preplaces are

- **iNKTEffStress(→)**

- **iNKT – Stress**(⇀•)
- **CD47Binded**(→)

The postplaces is

- **iNKT**(→)

The coefficient is

$$\text{iNKTDeact} \cdot \textbf{iNKTEffStress}$$

iNKT – Diff models the diffusion and drift of NKTCs due to blood flow. The preplaces are

- **iNK**(→)
- **iNKNumber**(→)

The coefficient is

$$\text{CellDiff} \cdot \textbf{iNK}$$

iNKT – Death models the death of NKTCs. The preplaces are

- **iNKT**(→)
- **iNKTNumber**(→)

The coefficient is

$$\frac{\textbf{iNKT}}{\text{iNKTLife}} \cdot \log(2)$$

iNKT – Time – Passes models time flow for NKTCs. The postplaces is

- **iNKTTime**(→)

The coefficient is

$$\text{TimedFiring}(1)$$

ExternalActivation models the external activation of NKTCs. The preplaces are

- **iNKT**(→)
- **iNKTTime**(⇀•)

The postplaces are

- **iNKTEffCD1d**(→)

- **CD47Binded**(→)

The coefficient is

$$\mathbf{iNKT} \cdot \text{ExternalActivationRate} \cdot \text{geq}(\mathbf{iNKTTime}, \text{NKTActivationStart}) \cdot \text{leq}(\mathbf{iNKTTime}, \text{NKTActivationEnd})$$

When this transition is enabled, that is when NKTActivationStart ≤ **iNKTTime** ≤ NKTActivationEnd, an average of ExternalActivationRate NKTCs are activated per hours (if enough $iNKTEffCD1d$ are available).

NKTCs can be prevented from activating for a certain period. Transitions *StartPreventingActivation* and *StopPreventingActivation* are used to model this feature.

StartPreventingActivation models the start of the blocking of activation of NKTCs. The preplaces are

- **PreventActivationToken**(→)
- **iNKTTime**(→)

The postplaces is

- **PreventActivation**(→)

The coefficient is

$$\text{geq}(\mathbf{iNKTTime}, \text{NKTBlockActivationStart})$$

This transition is enabled only when NKTActivationStart ≤ **iNKTTime**.

StopPreventingActivation models the end of the blocking of activation of NKTCs. The preplaces are

- **PreventActivation**(→)
- **iNKTTime**(→)

The coefficient is

$$\text{geq}(\mathbf{iNKTTime}, \text{NKTBlockActivationEnd})$$

This transition is enabled only when NKTBlockActivationEnd ≤ **iNKTTime**.

6.5.7 T Cells (TCs)

The mechanism of cytokine production, diffusion and drift, and deactivation of TCs is the same as NKTCs and will not be further commented.

TCell – Time – Passes models time flow for TCs. The postplaces is

- **TCellTime**(→)

The coefficient is

$$\text{TimedFiring}(1)$$

6.5.8 Type 0 Helper T Cells (T_H0Cs)

A constant inflow of T_H0Cs and T_C0Cs is modeled. This inflow lasts only few hours from the spleen, but is constant from the liver.

CD4 + TCell – Arrival – Spleen models the arrival of inactive T_H0Cs from spleen. The preplaces are

- **Remove – T**($\multimap$)
- **TCellTime**($\dashrightarrow$)

The postplaces are

- **ThNumber**($\rightarrow$)
- **Th0**($\rightarrow$)

The coefficient is

$$\textsc{SpleenTCellArr} \cdot \text{geq}(\textbf{TCellTime}, \textsc{TimeTStart}) \cdot \text{leq}(\textbf{TCellTime}, \textsc{TimeTStop})$$

This transition is enabled only when **Remove – T** is not marked and $\textsc{TimeTStart} \leq$ **TCellTime** $\leq \textsc{TimeTStop}$.

CD4+TCell – Arrival – Liver models the arrival of inactive T_H0Cs from other granulomas. The preplaces are

- **Remove – T**($\multimap$)
- **TCellTime**($\dashrightarrow$)

The postplaces are

- **ThNumber**($\rightarrow$)
- **Th0**($\rightarrow$)

The coefficient is

$$\textsc{LiverTCellArr} \cdot \text{geq}(\textbf{TCellTime}, \textsc{TimeTStart})$$

This transition is enabled only when **Remove – T** is not marked and $\textsc{TimeTStart} \leq$ **TCellTime**.

Th0 – Act models the activation of T_H0Cs by internalization of a MHC II peptide. The preplaces are

- **MHCII**($\rightarrow$)
- **Th0**($\rightarrow$)

The postplace is

- **Th0Eff**(→)

The coefficient is

$$\text{TCellAct} \cdot \mathbf{Th0} \cdot \mathbf{MHCII}$$

$Th0 - IL2$ models the production of IL2 by active T_H0Cs. The preplace is

- **Th0Eff**(⇀)

The postplace is

- **IL2**(→)

The coefficient is

$$\text{TCellCytProd} \cdot \mathbf{Th0Eff}$$

$Th0 - IL2$ models the reproduction of active T_H0Cs. The preplaces are

- **Th0Eff**(⇀)
- **IL2**(⇀)

The postplace is

- **Th0**(→)
- **ThNumber**(→)

The coefficient is

$$\text{TRep} \cdot \mathbf{IL2} \cdot \text{IL2Effectiveness} \cdot \mathbf{Th0Eff}$$

Note that the reproduction rate is proportional to both **IL2** and **Th0Eff**.

$Th0EffKeppProd$ models the consumption of IL2 by active T_H0Cs. The preplaces are

- **Th0Eff**(⇀)
- **IL2**(→)

The coefficient is

$$\text{TCellKeepProd} \cdot \frac{\mathbf{Th0Eff}}{\text{IL2Effectiveness}}$$

$Th0Eff - to - Th0EffZeroProd$ models the silencing of T_H0Cs due to the lack of IL2. The preplaces are

- **Th0Eff**(→)

- **IL2**(⇢)

The postplace is

- **Th0EffZeroProd**(→)

The coefficient is

$$\frac{\text{ToZeroProd}}{1 + \mathbf{IL2} \cdot \text{IL2Effectiveness}}$$

Note that the probability that a T_H0C get silenced is inversely proportional to the number of **IL2**.

$Th0Eff - to - Th0EffZeroProd$ models the reprise of IL2 production by silent T_H0Cs due to the increased concentration of IL2. The preplaces are

- **Th0EffZeroProd**(→)
- **IL2**(⇻)

The postplace is

- **Th0Eff**(→)

The coefficient is

$$\text{FromZeroProd} \cdot \text{IL2Effectiveness} \cdot \mathbf{IL2}$$

Note that the probability that a T_H0C exits silenced state is proportional to the number of **IL2**.

$Th0Eff - Deact$ models the deactivation T_H0Cs. The preplace is

- **Th0Eff**(→)

The postplace is

- **Th0**(→)

The coefficient is

$$\text{TDeact} \cdot \mathbf{Th0Eff}$$

$Th0EffZeroProd - Deact$ models the deactivation of silent T_H0Cs. The preplace is

- **Th0EffZeroProd**(→)

The postplace is

- **Th0**(→)

The coefficient is

$$\text{TDeact} \cdot \mathbf{Th0EffZeroProd}$$

$Th0 - Diff$ models the diffusion and drift due to blood flow of inactive T_H0Cs. The preplace is

- **Th0**($\rightarrow$)

The coefficient is

$$\text{CellDiff} \cdot \mathbf{Th0}$$

The differentiation of T_H0Cs depends on the cytokines that the cells encounter, and is proportional to the number of those cytokines.

$Th0 - to - Th1$ models the differentiation of inactive T_H0Cs to inactive T_H1Cs. The preplaces are

- **Th0**($\rightarrow$)
- **INFg**($\multimap$)

The postplace is

- **Th1**($\rightarrow$)

The coefficient is

$$\text{TCellDiff} \cdot \text{INFgEffectiveness} \cdot \mathbf{INFg}$$

$Th0 - to - Th2$ models the differentiation of inactive T_H0Cs to inactive T_H2Cs. The preplaces are

- **Th0**($\rightarrow$)
- **IL4**($\multimap$)

The postplace is

- **Th2**($\rightarrow$)

The coefficient is

$$\text{TCellDiff} \cdot \text{IL4Effectiveness} \cdot \mathbf{IL4}$$

$Th0Eff - to - Th1Eff$ models the differentiation of active T_H0Cs to active T_H1Cs. The preplaces are

- **Th0Eff**($\rightarrow$)
- **INFg**($\multimap$)

The postplace is

- **Th1Eff**(→)

The coefficient is

$$\text{TCellDiff} \cdot \text{INFgEffectiveness} \cdot \mathbf{INFg}$$

$Th0Eff - to - Th2Eff$ models the differentiation of active T_H0Cs to active T_H2Cs. The preplaces are

- **Th0Eff**(→)
- **IL4**(⇀)

The postplace is

- **Th2Eff**(→)

The coefficient is

$$\text{TCellDiff} \cdot \text{IL4Effectiveness} \cdot \mathbf{IL4}$$

6.5.9 Type I Helper T Cells ($T_H1_{INF\gamma}$Cs)

The transitions of $T_H1_{INF\gamma}$Cs are similar to those of T_H0Cs, and will not be further commented.

$Th1I - Act$ models the activation of $T_H1_{INF\gamma}$Cs by internalization of a MHC II peptide. The preplaces are

- **MHCII**(→)
- **Th1I**(→)

The postplace is

- **Th1IEff**(→)

The coefficient is

$$\text{TCellAct} \cdot \mathbf{Th1I} \cdot \mathbf{MHCII}$$

$Th1I - IL2$ models the production of IL2 by active $T_H1_{INF\gamma}$Cs. The preplace is

- **Th1IEff**(⇀)

The postplace is

- **IL2**(→)

The coefficient is

$$\text{TCellCytProd} \cdot \mathbf{Th1IEff}$$

Th1 – INFg models the production of INFγ by $T_H1_{INF\gamma}Cs$. The preplace is

- **Th1IEff**$(\multimap)$

The postplace is

- **INFg**$(\rightarrow)$

The coefficient is

$$\text{TCellCytProd} \cdot \mathbf{Th1IEff}$$

Th1IEff – Rep models the reproduction of active $T_H1_{INF\gamma}Cs$. The preplaces are

- **Th1IEff**$(\multimap)$
- **INFg**$(\multimap)$

The postplace is

- **Th1I**$(\rightarrow)$
- **ThNumber**$(\rightarrow)$

The coefficient is

$$\text{TRep} \cdot \mathbf{INFg} \cdot \text{INFgEffectiveness} \cdot \mathbf{Th1IEff}$$

Th1IEffKeppProd models the consumption of INFγ by active $T_H1_{INF\gamma}Cs$. The preplaces are

- **Th1IEff**$(\multimap)$
- **INFg**$(\rightarrow)$

The coefficient is

$$\text{TCellKeepProd} \cdot \frac{\mathbf{Th1IEff}}{\text{INFgEffectiveness}}$$

Th1IEff–to–Th1IEffZeroProd models the silencing of active $T_H1_{INF\gamma}Cs$ due to the lack of INFγ. The preplaces are

- **Th1IEff**$(\rightarrow)$
- **INFg**$(\dashrightarrow)$

The postplace is

- **Th1IEffZeroProd**$(\rightarrow)$

The coefficient is

$$\frac{\text{ToZeroProd}}{1 + \mathbf{INFg} \cdot \text{INFgEffectiveness}}$$

$Th1IEff-to-Th1IEffZeroProd$ models the reprise of cytokine production by silent $T_H1_{INF\gamma}Cs$ due to the increased concentration of $INF\gamma$. The preplaces are

- **Th1IEffZeroProd**$(\rightarrow)$
- **INFg**$(\multimap)$

The postplace is

- **Th1IEff**$(\rightarrow)$

The coefficient is

$$\text{FromZeroProd} \cdot \text{INFgEffectiveness} \cdot \mathbf{INFg}$$

$Th1IEff-Deact$ models the deactivation of $T_H1_{INF\gamma}Cs$. The preplace is

- **Th1IEff**$(\rightarrow)$

The postplace is

- **Th1I**$(\rightarrow)$

The coefficient is

$$\text{TDeact} \cdot \mathbf{Th1IEff}$$

$Th1IEffZeroProd-Deact$ models the deactivation of silent $T_H1_{INF\gamma}Cs$. The preplace is

- **Th1IEffZeroProd**$(\rightarrow)$

The postplace is

- **Th1I**$(\rightarrow)$

The coefficient is

$$\text{TDeact} \cdot \mathbf{Th1IEffZeroProd}$$

$Th1I-Diff$ models the diffusion and drift due to blood flow of inactive $T_H1_{INF\gamma}Cs$. The preplace is

- **Th1I**(→)

The coefficient is

$$\text{CellDiff} \cdot \mathbf{Th1I}$$

$Th1IEff-to-ThIIEff$ models the differentiation of active $T_H1_{INF\gamma}Cs$ to active $T_H1_{IL12}Cs$. The preplace is

- **Th1IEff**(→)

The postplace is

- **Th1IIEff**(→)

The coefficient is

$$\frac{\mathbf{Th1IEff}}{\text{Th1Evol}} \cdot \log(9)$$

6.5.10 Type I Helper T Cells ($T_H1_{IL12}Cs$)

The transitions of $T_H1_{IL12}Cs$ are similar to those of T_H0Cs, and will not be further commented.

Th1II – Act models the activation of inactive $T_H1_{IL12}Cs$ by internalization of a MHC II peptide. The preplaces are

- **MHCII**(→)
- **Th1II**(→)

The postplace is

- **Th1IIEff**(→)

The coefficient is

$$\text{TCellAct} \cdot \mathbf{Th1II} \cdot \mathbf{MHCII}$$

$Th1II-IL2$ models the production of IL2 by active $T_H1_{IL12}Cs$. The preplace is

- **Th1IIEff**(⇀)

The postplace is

- **IL2**(→)

The coefficient is

$$\text{TCellCytProd} \cdot \mathbf{Th1IIEff}$$

$Th1II-INFg$ models the production of INFγ by active $T_H1_{IL12}Cs$. The preplace is

- **Th1IIEff**(⇸)

The postplace is

- **INFg**(→)

The coefficient is

$$\text{TCellCytProd} \cdot \mathbf{Th1IIEff}$$

*Th*1*IIEff* – *Rep* models the reproduction of active $T_H1_{IL12}Cs$. The preplaces are

- **Th1IIEff**(⇸)
- **INFg**(⇸)

The postplace is

- **Th1II**(→)
- **ThNumber**(→)

The coefficient is

$$\text{TRep} \cdot \mathbf{INFg} \cdot \text{INFgEffectiveness} \cdot \mathbf{Th1IIEff}$$

*Th*1*IIEffKeppProd* models the consumption of IL12 by active $T_H1_{IL12}Cs$. The preplaces are

- **Th1IIEff**(⇸)
- **INFg**(→)

The coefficient is

$$\text{TCellKeepProd} \cdot \frac{\mathbf{Th1IIEff}}{\text{IL12Effectiveness}}$$

*Th*1*IIEff*–*to*–*Th*1*IIEffZeroProd* models silencing of active $T_H1_{IL12}Cs$ due to the lack of IL12. The preplaces are

- **Th1IIEff**(→)
- **IL12**(⇢)

The postplace is

- **Th1IIEffZeroProd**(→)

The coefficient is

$$\frac{\text{ToZeroProd}}{1 + \mathbf{IL12} \cdot \text{IL12Effectiveness}}$$

$Th1IIEff - to - Th1IIEffZeroProd$ models the reprise of cytokine production by silent $T_H1_{IL12}Cs$ due to the increased concentration of IL12. The preplaces are

- **Th1IIEffZeroProd**$(\rightarrow)$
- **IL12**$(\rightarrow\bullet)$

The postplace is

- **Th1IIEff**$(\rightarrow)$

The coefficient is

$$\text{FromZeroProd} \cdot \text{IL12Effectiveness} \cdot \mathbf{IL12}$$

$Th1IIEff - Deact$ models the deactivation of active $T_H1_{IL12}Cs$. The preplace is

- **Th1IIEff**$(\rightarrow)$

The postplace is

- **Th1II**$(\rightarrow)$

The coefficient is

$$\text{TDeact} \cdot \mathbf{Th1IIEff}$$

$Th1IIEffZeroProd-Deact$ models the deactivation of silent $T_H1_{IL12}Cs$. The preplace is

- **Th1IIEffZeroProd**$(\rightarrow)$

The postplace is

- **Th1II**$(\rightarrow)$

The coefficient is

$$\text{TDeact} \cdot \mathbf{Th1IIEffZeroProd}$$

$Th1II-Diff$ models the diffusion and drift due to blood floow of inactive $T_H1_{IL12}Cs$. The preplace is

- **Th1II**$(\rightarrow)$

The coefficient is

$$\text{CellDiff} \cdot \mathbf{Th1II}$$

$Th1IEff\text{–}to\text{–}Th1IL10Eff$ models the differentiation of active $T_H1_{IL12}Cs$ to $IL10^+$ T_H1Cs. The preplace is

- **Th1IIEff**$(\rightarrow)$

The postplace is

- **Th1IL10Eff**$(\rightarrow)$

The coefficient of the INFγ-dependent model is

$$\text{Th1IL10Diff} \cdot \text{INFgEffectiveness} \cdot \mathbf{INFg}$$

The coefficient of the IL12-dependent model is

$$\text{Th1IL10Diff} \cdot \text{IL12Effectiveness} \cdot \mathbf{IL12}$$

The coefficient of the time-dependent model is

$$\text{Th1IL10Diff} \cdot \mathbf{Th1IIEff}$$

6.5.11 Type I Helper T Cells ($T_H1_{IL10}Cs$)

The transitions of $T_H1_{IL10}Cs$ are similar to those of T_H0Cs, and will not be further commented.

$Th1IL10 - Act$ models the activation of inactive $T_H1_{IL10}Cs$ by internalization of a MHC II peptide. The preplaces are

- **MHCII**$(\rightarrow)$
- **Th1IL10**$(\rightarrow)$

The postplace is

- **Th1IL10Eff**$(\rightarrow)$

The coefficient is

$$\text{TCellAct} \cdot \mathbf{Th1IL10} \cdot \mathbf{MHCII}$$

$Th1IL10 - IL2$ models the production of IL2 by active $T_H1_{IL10}Cs$. The preplace is

- **Th1IL10Eff**$(\rightarrow\!\bullet)$

The postplace is

- **IL2**(→)

The coefficient is

$$\text{TCellCytProd} \cdot \textbf{Th1IL10Eff}$$

$Th1IL10 - INFg$ models the production of INFγ by active T_H1_{IL10}Cs. The preplace is

- **Th1IL10Eff**(⇸)

The postplace is

- **INFg**(→)

The coefficient is

$$\text{TCellCytProd} \cdot \textbf{Th1IL10Eff}$$

Th1IL10 – IL10 models the production of IL10 by active T_H1_{IL10}Cs. The preplace is

- **Th1IL10Eff**(⇸)

The postplace is

- **IL10**(→)

The coefficient is

$$\text{TCellCytProd} \cdot \textbf{Th1IL10Eff}$$

$Th1IL10Eff - Rep$ models the reproduction of active T_H1_{IL10}Cs. The preplaces are

- **Th1IL10Eff**(⇸)
- **INFg**(⇸)

The postplace is

- **Th1IL10**(→)
- **ThNumber**(→)

The coefficient is

$$\text{Th1IL10RepMod} \cdot \text{TRep} \cdot \textbf{INFg} \cdot \text{INFgEffectiveness} \cdot \textbf{Th1IL10Eff}$$

$Th1IL10EffKeppProd$ models the consumption of IL12 by active T_H1_{IL10}Cs. The preplace is

- **Th1IL10Eff**(⇸)
- **IL12**(→)

The coefficient is

$$\text{TCellKeepProd} \cdot \frac{\textbf{Th1IL10Eff}}{\text{IL12Effectiveness}}$$

$Th1IL10Eff\text{–}to\text{–}Th1IL10EffZeroProd$ models the silencing of $\text{T}_\text{H}1_{\text{IL10}}$Cs due to the lack of IL12. The preplaces are

- **Th1IL10Eff**(→)
- **IL12**(↛)

The postplace is

- **Th1IL10EffZeroProd**(→)

The coefficient is

$$\frac{\text{ToZeroProd}}{1 + \textbf{IL12} \cdot \text{IL12Effectiveness}}$$

$Th1IL10Eff\text{–}to\text{–}Th1IL10EffZeroProd$ models the reprise of cytokine production by silent $\text{T}_\text{H}1_{\text{IL10}}$Cs due to the increased concentration of IL12. The preplaces are

- **Th1IL10EffZeroProd**(→)
- **IL12**(⇸)

The postplace is

- **Th1IL10Eff**(→)

The coefficient is

$$\text{FromZeroProd} \cdot \text{IL12Effectiveness} \cdot \textbf{INFg}$$

$Th1IL10Eff - Deact$ models the deactivation of active $\text{T}_\text{H}1_{\text{IL10}}$Cs. The preplace is

- **Th1IL10Eff**(→)

The postplace is

- **Th1IL10**(→)

The coefficient is

$$\text{TDeact} \cdot \textbf{Th1IL10Eff}$$

$Th1IL10EffZeroProd–Deact$ models the deactivation of silent $T_H1_{IL10}Cs$. The preplace is

- **Th1IL10EffZeroProd**(→)

The postplace is

- **Th1IL10**(→)

The coefficient is

$$\text{TDeact} \cdot \textbf{Th1IL10EffZeroProd}$$

$Th1IL10 - Diff$ models the diffusion and drift due to blood flow of inactive $T_H1_{IL10}Cs$. The preplace is

- **Th1IL10**(→)

The coefficient is

$$\text{CellDiff} \cdot \textbf{Th1IL10}$$

6.5.12 Type II Helper T Cells (T_H2Cs)

The transitions of T_H2Cs are similar to those of T_H0Cs, and will not be further commented.

$Th2 - Act$ models the activation of inactive T_H2Cs by internalization of a MHC II peptide. The preplaces are

- **MHCII**(→)
- **Th2**(→)

The postplace is

- **Th2Eff**(→)

The coefficient is

$$\text{TCellAct} \cdot \textbf{Th2} \cdot \textbf{MHCII}$$

$Th2 - IL4$ models the production of IL4 by active T_H2Cs. The preplace is

- **Th2Eff**(⇀)

The postplace is

- **IL4**(→)

The coefficient is

$$\text{TCellCytProd} \cdot \mathbf{Th2Eff}$$

$Th1-IL10$ models the production of IL10 by active T_H2Cs. The preplace is

- **Th2Eff**(⇀)

The postplace is

- **IL10**(→)

The coefficient is

$$\text{TCellCytProd} \cdot \mathbf{Th2Eff}$$

$Th2Eff-Rep$ models the reproduction of active T_H2Cs. The preplaces are

- **Th2Eff**(⇀)
- **IL4**(⇀)

The postplace is

- **Th2**(→)
- **ThNumber**(→)

The coefficient is

$$\text{TRep} \cdot \mathbf{IL4} \cdot \text{IL4Effectiveness} \cdot \mathbf{Th2Eff}$$

$Th2EffKeppProd$ models the consumption of IL4 by active T_H2Cs. The preplace is

- **Th2Eff**(⇀)
- **IL4**(→)

The coefficient is

$$\text{TCellKeepProd} \cdot \frac{\mathbf{Th2Eff}}{\text{IL4Effectiveness}}$$

$Th2Eff-to-Th2EffZeroProd$ models the silencing of active T_H2Cs due to the lack of IL4. The preplaces are

- **Th2Eff**(→)

- **IL4**(⇢)

The postplace is

- **Th2EffZeroProd**(→)

The coefficient is

$$\frac{\text{ToZeroProd}}{1 + \mathbf{IL4} \cdot \text{IL4Effectiveness}}$$

$Th2Eff - to - Th2EffZeroProd$ models the reprise of cytokine production by silent T_H2Cs due to the increased concentration of IL4. The preplaces are

- **Th2EffZeroProd**(→)
- **IL4**(⇢)

The postplace is

- **Th2Eff**(→)

The coefficient is

$$\text{FromZeroProd} \cdot \text{IL4Effectiveness} \cdot \mathbf{IL4}$$

$Th2Eff - Deact$ models the deactivation of active T_H2Cs. The preplace is

- **Th2Eff**(→)

The postplace is

- **Th2**(→)

The coefficient is

$$\text{TDeact} \cdot \mathbf{Th2Eff}$$

$Th2EffZeroProd - Deact$ models the deactivation of silent T_H2Cs. The preplace is

- **Th2EffZeroProd**(→)

The postplace is

- **Th2**(→)

The coefficient is

$$\text{TDeact} \cdot \mathbf{Th2EffZeroProd}$$

$Th2 - Diff$ models the diffusion and drift due to blood flow of T_H2s. The preplace is

- **Th2**(→)

The coefficient is

$$\text{CellDiff} \cdot \mathbf{Th2}$$

6.5.13 Type 0 Cytotoxic T Cells (T_C0Cs)

The transitions of T_C0Cs are basically the same as those of T_H0Cs, and will not be further commented.

CD8 + TCell – Arrival – Spleen models the arrival of inactive T_C0Cs from spleen. The preplaces are

- **Remove – T**$(\multimap)$
- **TCellTime**$(\dashrightarrow)$

The postplaces are

- **TcNumber**$(\rightarrow)$
- **Tc0**$(\rightarrow)$

The coefficient is

$$\textsc{SpleenTCellArr} \cdot \text{geq}(\textbf{TCellTime}, \textsc{TimeTStart}) \cdot \text{leq}(\textbf{TCellTime}, \textsc{TimeTStop})$$

This transition is enabled only when **Remove – T** is not marked and $\textsc{TimeTStart} \leq \textbf{TCellTime} \leq \textsc{TimeTStop}$.

CD8 + TCell – Arrival – Liver models the arrival of T_C0Cs from other granulomas in the liver. The preplaces are

- **Remove – T**$(\multimap)$
- **TCellTime**$(\dashrightarrow)$

The postplaces are

- **TcNumber**$(\rightarrow)$
- **Tc0**$(\rightarrow)$

The coefficient is

$$\textsc{LiverTCellArr} \cdot \text{geq}(\textbf{TCellTime}, \textsc{TimeTStart})$$

This transition is enabled only when **Remove – T** is not marked and $\textsc{TimeTStart} \leq \textbf{TCellTime}$.

Tc0 – Act models the activation of inactive T_C0Cs by internalization of a MHC I peptide. The preplaces are

- **MHCI**$(\rightarrow)$
- **Tc0**$(\rightarrow)$

The postplace is

- **Tc0Eff**(→)

The coefficient is

$$\text{TCellAct} \cdot \mathbf{Tc0} \cdot \mathbf{MHCI}$$

$Tc0 - IL2$ models the production of IL2 by active T_C0Cs. The preplace is

- **Tc0Eff**(⇸)

The postplace is

- **IL2**(→)

The coefficient is

$$\text{TCellCytProd} \cdot \mathbf{Tc0Eff}$$

$Tc0 - Rep$ models the reproduction of active T_C0Cs. The preplaces are

- **Tc0Eff**(⇸)
- **IL2**(⇸)

The postplace is

- **Tc0**(→)
- **TcNumber**(→)

The coefficient is

$$\text{TRep} \cdot \mathbf{IL2} \cdot \text{IL2Effectiveness} \cdot \mathbf{Tc0Eff}$$

$Tc0EffKeppProd$ models the consumption of IL2 by active T_C0Cs. The preplace is

- **Tc0Eff**(⇸)
- **IL2**(→)

The coefficient is

$$\text{TCellKeepProd} \cdot \frac{\mathbf{Tc0Eff}}{\text{IL2Effectiveness}}$$

$Tc0Eff - to - Tc0EffZeroProd$ models the silencing of active T_C0Cs due to the lack of IL2. The preplaces are

- **Tc0Eff**(→)
- **IL2**(↛)

The postplace is

- **Tc0EffZeroProd**$(\rightarrow)$

The coefficient is

$$\frac{\text{ToZeroProd}}{1 + \mathbf{IL2} \cdot \text{IL2Effectiveness}}$$

$Tc0Eff - to - Tc0EffZeroProd$ models the reprise of IL2 production by silent T_C0Cs due to the increased concentration of IL2. The preplaces are

- **Tc0EffZeroProd**$(\rightarrow)$
- **IL2**$(\multimap)$

The postplace is

- **Tc0Eff**$(\rightarrow)$

The coefficient is

$$\text{FromZeroProd} \cdot \text{IL2Effectiveness} \cdot \mathbf{IL2}$$

$Tc0Eff - Deact$ models the deactivation of active T_C0Cs. The preplace is

- **Tc0Eff**$(\rightarrow)$

The postplace is

- **Tc0**$(\rightarrow)$

The coefficient is

$$\text{TDeact} \cdot \mathbf{Tc0Eff}$$

$Tc0EffZeroProd - Deact$ models the deactivation of silent T_C0Cs. The preplace is

- **Tc0EffZeroProd**$(\rightarrow)$

The postplace is

- **Tc0**$(\rightarrow)$

The coefficient is

$$\text{TDeact} \cdot \mathbf{Tc0EffZeroProd}$$

Tc0 – Diff models the diffusion and drift due to blood flow of T_C0Cs. The preplace is

- **Tc0**(→)

The coefficient is

$$\text{CellDiff} \cdot \mathbf{Tc0}$$

$Tc0 - to - Tc1$ models the differentiation of inactive T_C0Cs to inactive T_C1Cs. The preplaces are

- **Tc0**(→)
- **INFg**(⇀)

The postplace is

- **Tc1**(→)

The coefficient is

$$\text{TCellDiff} \cdot \text{INFgEffectiveness} \cdot \mathbf{INFg}$$

$Tc0 - to - Tc2$ models the differentiation of inactive T_C0Cs to inactive T_C2Cs. The preplaces are

- **Tc0**(→)
- **IL4**(⇀)

The postplace is

- **Tc2**(→)

The coefficient is

$$\text{TCellDiff} \cdot \text{IL4Effectiveness} \cdot \mathbf{IL4}$$

$Tc0Eff - to - Tc1Eff$ models the differentiation of active T_C0Cs to active T_C1Cs. The preplaces are

- **Tc0Eff**(→)
- **INFg**(⇀)

The postplace is

- **Tc1Eff**(→)

The coefficient is

$$\text{TCellDiff} \cdot \text{INFgEffectiveness} \cdot \mathbf{INFg}$$

$Tc0Eff - to - Tc2Eff$ models the differentiation of active T_C0Cs to active T_C2Cs. The preplaces are

- **Tc0Eff**($\rightarrow$)
- **IL4**($\multimap$)

The postplace is

- **Tc2Eff**($\rightarrow$)

The coefficient is

$$\text{TCellDiff} \cdot \text{IL4Effectiveness} \cdot \mathbf{IL4}$$

6.5.14 Type I Cytotoxic T Cells (T_C1Cs)

The transitions of T_C1Cs are similar to those of T_C0Cs, and will not be further commented.

$Tc1 - Act$ models the activation of inactive T_C1Cs by internalization of a MHC I peptide. The preplaces are

- **MHCI**($\rightarrow$)
- **Tc1**($\rightarrow$)

The postplace is

- **Tc1Eff**($\rightarrow$)

The coefficient is

$$\text{TCellAct} \cdot \mathbf{Tc1} \cdot \mathbf{MHCI}$$

$Tc1 - IL2$ models the production IL2 by active T_C1Cs. The preplace is

- **Tc1Eff**($\multimap$)

The postplace is

- **IL2**($\rightarrow$)

The coefficient is

$$\text{TCellCytProd} \cdot \mathbf{Tc1Eff}$$

$Th1 - INFg$ models the production of INFγ by active T_C1Cs. The preplace is

- **Tc1Eff**($\multimap$)

The postplace is

- **INFg**($\rightarrow$)

The coefficient is

$$\text{TCellCytProd} \cdot \mathbf{Tc1Eff}$$

$Tc1Eff - Rep$ models the reproduction of active T_C1Cs. The preplaces are

- **Tc1Eff**(⇀)
- **INFg**(⇀)

The postplace is

- **Tc1**(→)
- **ThNumber**(→)

The coefficient is

$$\text{TRep} \cdot \mathbf{INFg} \cdot \text{INFgEffectiveness} \cdot \mathbf{Tc1Eff}$$

$Tc1EffKeppProd$ models the consumption of INFγ by active T_C1Cs. The preplaces are

- **Tc1Eff**(⇀)
- **INFg**(→)

The coefficient is

$$\text{TCellKeepProd} \cdot \frac{\mathbf{Tc1Eff}}{\text{INFgEffectiveness}}$$

$Tc1Eff - to - Tc1EffZeroProd$ models the silencing of active T_C1Cs due to the lack of INFγ. The preplaces are

- **Tc1Eff**(→)
- **INFg**(⇀)

The postplace is

- **Tc1EffZeroProd**(→)

The coefficient is

$$\frac{\text{ToZeroProd}}{1 + \mathbf{INFg} \cdot \text{INFgEffectiveness}}$$

$Tc1Eff - to - Tc1EffZeroProd$ models the reprise of cytokine production by silent T_C1Cs due to the increased concentration of INFγ. The preplaces are

- **Tc1EffZeroProd**($\rightarrow$)
- **INFg**($\rightarrow\bullet$)

The postplace is

- **Tc1Eff**($\rightarrow$)

The coefficient is

$$\text{FROMZEROPROD} \cdot \text{INFGEFFECTIVENESS} \cdot \mathbf{INFg}$$

$Tc1Eff - Deact$ models the deactivation of active T_C1Cs. The preplace is

- **Tc1Eff**($\rightarrow$)

The postplace is

- **Tc1**($\rightarrow$)

The coefficient is

$$\text{TDEACT} \cdot \mathbf{Tc1Eff}$$

$Tc1EffZeroProd - Deact$ models the deactivation of silent T_C1Cs. The preplace is

- **Tc1EffZeroProd**($\rightarrow$)

The postplace is

- **Tc1**($\rightarrow$)

The coefficient is

$$\text{TDEACT} \cdot \mathbf{Tc1EffZeroProd}$$

$Tc1 - Diff$ models the diffusion and drift due to blood flow of T_C1Cs. The preplace is

- **Tc1**($\rightarrow$)

The coefficient is

$$\text{CELLDIFF} \cdot \mathbf{Tc1}$$

6.5.15 Type II Cytotoxic T Cells (T_C2Cs)

The transitions of T_C2Cs are similar to those of T_C0Cs, and will not be further commented.

$Tc2 - Act$ models the activation of inactive T_C2Cs by internalization of a MHC I peptide. The preplaces are

- **MHCI**$(\rightarrow)$
- **Tc2**$(\rightarrow)$

The postplace is

- **Tc2Eff**$(\rightarrow)$

The coefficient is

$$\text{TCellAct} \cdot \mathbf{Tc2} \cdot \mathbf{MHCI}$$

$Tc2 - IL4$ models the production of IL4 by active T_C2Cs. The preplace is

- **Tc2Eff**$(\multimap)$

The postplace is

- **IL4**$(\rightarrow)$

The coefficient is

$$\text{TCellCytProd} \cdot \mathbf{Tc2Eff}$$

$Th1 - Il10$ models the production of IL10 by active T_C2Cs. The preplace is

- **Tc2Eff**$(\multimap)$

The postplace is

- **IL10**$(\rightarrow)$

The coefficient is

$$\text{TCellCytProd} \cdot \mathbf{Tc2Eff}$$

$Tc2Eff - Rep$ models the reproduction of active T_C2Cs. The preplaces are

- **Tc2Eff**$(\multimap)$
- **IL4**$(\multimap)$

The postplace is

- **Tc2**(→)
- **TcNumber**(→)

The coefficient is

$$\text{TREP} \cdot \mathbf{IL4} \cdot \text{IL4EFFECTIVENESS} \cdot \mathbf{Tc2Eff}$$

$Tc2EffKeppProd$ models the consumption of IL4 by active T_C2Cs. The preplace is

- **Tc2Eff**(⇸)
- **IL4**(→)

The coefficient is

$$\text{TCELLKEEPPROD} \cdot \frac{\mathbf{Tc2Eff}}{\text{IL4EFFECTIVENESS}}$$

$Tc2Eff-to-Tc2EffZeroProd$ models the silencing of active T_C2Cs due to the lack of IL4. The preplaces are

- **Tc2Eff**(→)
- **IL4**(⇢)

The postplace is

- **Tc2EffZeroProd**(→)

The coefficient is

$$\frac{\text{TOZEROPROD}}{1 + \mathbf{IL4} \cdot \text{IL4EFFECTIVENESS}}$$

$Tc2Eff-to-Tc2EffZeroProd$ models the reprise of cytokine production by silent T_C2Cs due to the increased concentration of IL4. The preplaces are

- **Tc2EffZeroProd**(→)
- **IL4**(⇸)

The postplace is

- **Tc2Eff**(→)

The coefficient is

$$\text{FromZeroProd} \cdot \text{IL4Effectiveness} \cdot \mathbf{IL4}$$

$Tc2Eff-Deact$ models the deactivation of active T_C2Cs. The preplace is

- **Tc2Eff**($\rightarrow$)

The postplace is

- **Tc2**($\rightarrow$)

The coefficient is

$$\text{TDeact} \cdot \mathbf{Tc2Eff}$$

$Tc2EffZeroProd-Deact$ models the deactivation of silent T_C2Cs. The preplace is

- **Tc2EffZeroProd**($\rightarrow$)

The postplace is

- **Tc2**($\rightarrow$)

The coefficient is

$$\text{TDeact} \cdot \mathbf{Tc2EffZeroProd}$$

$Tc2-Diff$ models the diffusion and drift due to blood flow of inactive T_C2Cs. The preplace is

- **Tc2**($\rightarrow$)

The coefficient is

$$\text{CellDiff} \cdot \mathbf{Tc2}$$

6.5.16 Others

$InfectionClearence$ models the clearance of infection. This transition is not fundamental for the model, but allows for an easier interpretation of the data. The preplaces are

- **Infected**($\rightarrow$)
- **LD**($\multimap$)

The coefficient is

$$\text{ImmediateFiring}()$$

Chapter 7

Model Validation

This chapter validates the results of our model against the results of *in vivo* experiments. The comparisons are displayed by means of graphical representations of the data. Whenever possible, the data where obtained from published articles. In a few cases, the data and feedback were provided by professor Paul M. Kaye of the Center for Immunology and Infection, Hull York Medical School and Department of Biology, University of York. A preliminary discussion of these results has been presented in Albergante et al. 2010.

Most of the data on leishmaniasis describe the cell populations at the organ level (for example Stanley et al. 2008 reports the number of NKT cells per liver). To account for this fact, during each experiment we simulated 50 independent granulomas with the same initial conditions, taking the averages of the values we were interested in, and multiplying these values by $5 \cdot 10^5$.

The only exception to this rule are $CD4^+$ cells. In this case, a fixed number of inactive $CD4^+$, activated $CD4^+INF\gamma^+IL10^-$ and activated $CD4^+INF\gamma^+IL10^+$ T cells were considered in the calculation. These values represent $CD4^+$ T cells present in a mouse under control condition, and, as such, *leishmania donovani* non-specific. Therefore, while considered for the calculation, these cells were not modeled.

In silico data presented in this chapter and in the following indicate the average of 5 experiments performed under the same conditions and the error bars represent the standard deviation. Note that the standard deviation δ_N of the sample $x_1, \ldots, x_N$ was calculated using the formula

$$\delta_N = \sqrt{\frac{1}{N-1} \sum_{i=1}^{N} (x_i - \overline{x})^2}$$

which is sometime referred as "sample standard deviation".

The time required to perform each experiment varies according go the experimental conditions. For example, the model described in Section 7.1

requires about half a minute to be simulated, while the model described in Section 7.2.3 requires several minutes.

7.1 Validation of Baseline Model

This section presents *in silico* results obtained from a *baseline model*. This model is characterized by:

- CD1d-dependent activation of NKT cells
- INFγ-dependent phenotype change of T_H1 cells

Whenever possible, we considered *in vivo* experiment on C57BL/6 mice. In a few cases, however, data were obtained from experiment on BALB/c mice.

7.1.1 Control

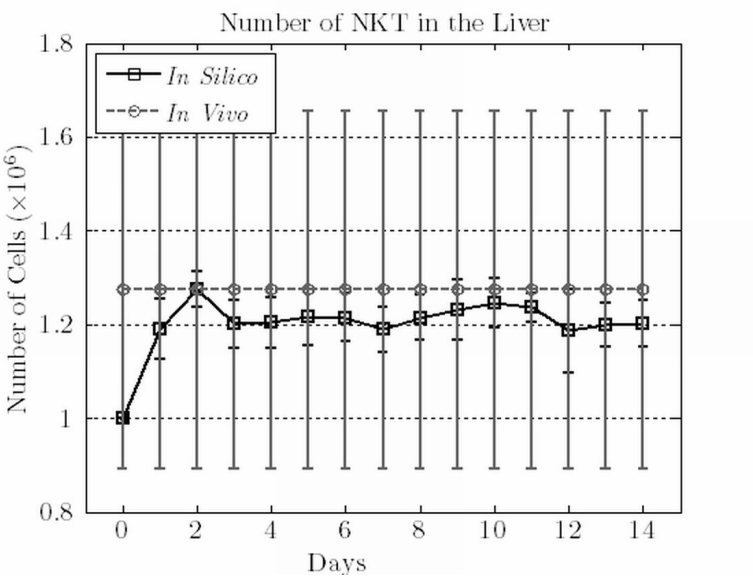

Figure 7.1: Number of NKT cells in the liver. *In silico* data describe baseline model. *In vivo* data are taken from Stanley et al. 2008.

Figures 7.1 and 7.2 display the number of NKT and NK cells when no infection is present. The data compare very well to the values obtained from *in vivo* experiments on mice before infection, or under control conditions (Stanley et al. 2008 and Maroof et al. 2008). Other checks performed on parasites, phagocytes and T cells (not presented) confirmed that the model behaves as expected.

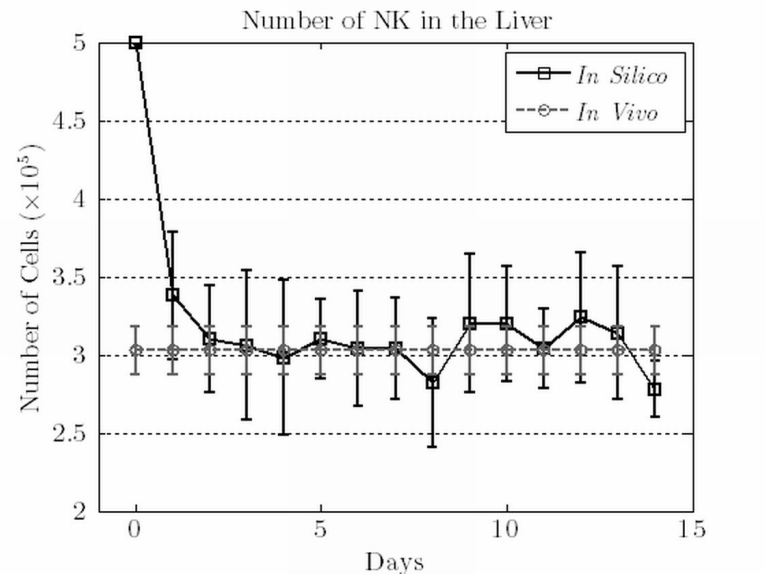

Figure 7.2: Number of NK cells in the liver. *In silico* data describe baseline model. *In vivo* data are taken from Maroof et al. 2008.

7.1.2 Parasite Burden

The standard way of reporting parasite burdens in the context of *leishmania donovani* infection of the liver and spleen is by means of *Leishman-Donovan Units* — also called *Leishmania Donovani Units* — (LDU). LDU is an indirect estimation of the number of the parasites, and is calculated by

$$\text{LDU} = (\#\text{ of parasites per 500 host nuclei}) \times (\text{the organ weight in mg})$$

or

$$\text{LDU} = (\#\text{ of parasites per 1000 host nuclei}) \times (\text{the organ weight in mg})$$

While LDU is a clear indication of the level of infection, using it to estimate the number of parasites in the organ is rather difficult. This difficulty arises from the fact that both the number of host cells and the weight of the organ vary both among individuals and during the course of infection. However, the number of parasites in the organ is estimated to be from about $10^7 \cdot LDU$ (Bradley & Kirkley 1977) to about $10^8 \cdot LDU$ (Gutierrez et al. 1984).

Additionally, the literature reports largely different LDU, even in experiments performed under similar conditions. For example, in the context of wild type C57BL/6 mice, 2 weeks after infection Murray et al. 2006 reports about 1000 LDU, while Stanley et al. 2008 reports more than 2000. However, even if LDU varies quantitatively among articles, the qualitative behavior is generally the same.

Therefore, we decided to estimate the number of parasites in the liver by multiplying the LDU reported by Murray et al. 2006 with a number K such that:

$$\frac{K \cdot (\text{LDU at Week 4})}{\text{Number of Granulomas}} = 60$$

The choice of the number 60 is due to the opinion of biological experts.

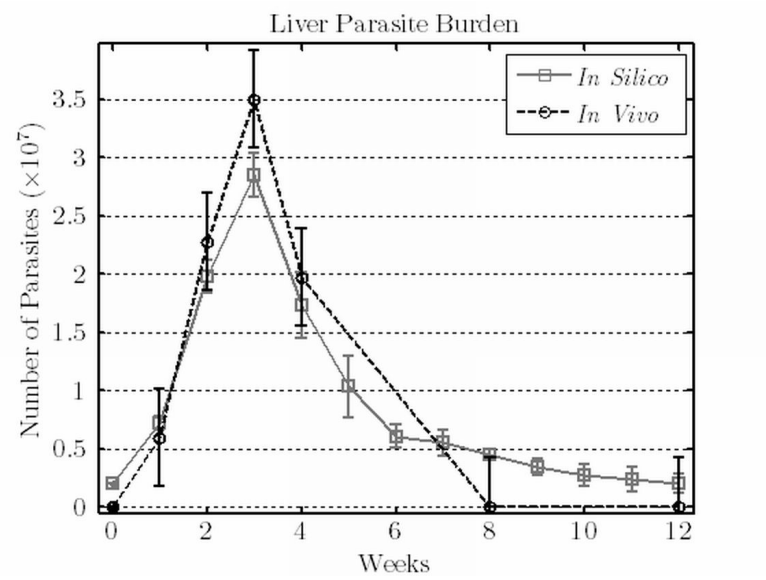

Figure 7.3: Parasite Burden. *In silico* data describe the results of baseline model. *In vivo* data are adapted from Murray et al. 2006.

The number of parasites predicted by the model is very similar to the expected values (see Figure 7.3). However, the infection takes more time to resolve *in silico*. This is likely due to the fact that the number of antigens specific T cells *in silico* is lower than *in vivo* (see Section 7.1.5 for a discussion of this problem).

7.1.3 Natural Killer T Cells

The number of NKT cells in the liver is compatible with the data reported by Stanley et al. 2008 (see Figure 7.4). While, the two curves look different at first sight, the large standard deviation indicate the large uncertainty of *in vivo* data, thus suggesting the validity of the *in silico* results.

The percentage of activated NKT cells is very similar to the *in vivo* data reported by Amprey et al. 2004 — 2 hours after infection using BALB/C mice — and Beattie at al. 2010 (EJI) — 10 hours after infection using C57BL/6 mice — (see Figure 7.5).

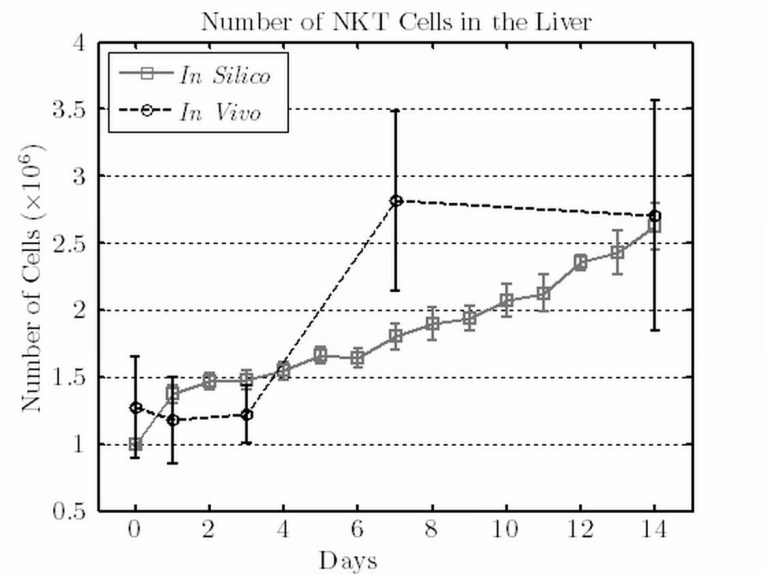

Figure 7.4: Number of NKT cells. *In silico* data describe the results of baseline model. *In vivo* data are taken from Stanley et al. 2008.

7.1.4 Natural Killer Cells

The number of NK cells is very similar to the *in vivo* data reported by Maroof et al. 2008 (see Figure 7.6).

7.1.5 T Cells

Figure 7.7 indicates the number of $CD4^+$ and $CD8^+$ T cells obtained by the *in silico* model. While the author was not able to find any specific published data, professor Paul M. Kaye reported that Figure 7.7 captures correctly the fact that $CD8^+$ T cells response is delayed with a cell population comparable to that of $CD4^+$ T cells. The decrease in cell population, is, however, too rapid when compared to *in vivo* experiments. This discordance is likely due to the larger number of antigen specific T cells available in the later stages of infection as a consequence of the migration from other granulomas. This increased number of T cells is likely to promote a more effective T cell response. Given the *non-connected* nature of the model it was not possible to capture this aspect.

The percentages of different types of T_H1 cells in the liver compare quite well to the data obtained from *in vivo* experiments (See Figure 7.8). Moreover, considering the history of these percentage (see Figure 7.9), we can clearly see that these values are the consequence of a *trend* rather than the result of stochastic fluctuations.

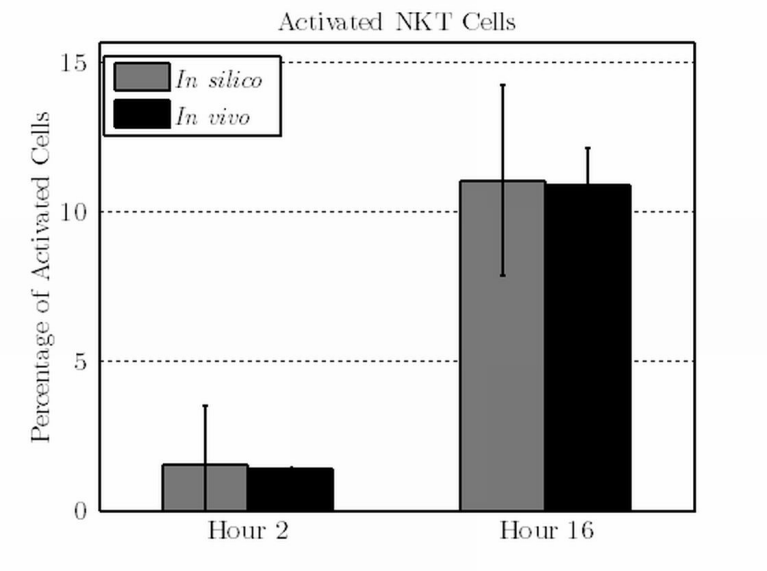

Figure 7.5: Percentage of activated NKT cells. *In silico* data describe the results of baseline model. *In vivo* data are taken from Amprey et al. 2004 and Beattie at al. 2010 (EJI).

7.2 Validation of Gene Knock-Out Models

This section describes the behavior of the model when specific populations of cells or cytokines are removed and compares the results with experiments under gene knock-out conditions. The mechanisms underlying the activation of NKT cells and the phenotype changes of T cells are the same of Section 7.1

7.2.1 Natural Killer T Cells

The immune response in mice with defective NKT cells is characterized by an about twofold amount of parasites and an eventual disease resolution (See for example Figure 1A of Stanley et al. 2008). Removing NKT cells form the model (NKT^- model) leads to comparable results (see Figure 7.10 and Section B.1 for additional data and comments).

Note that, removing NKT cells from our model leads to a faster disease resolution, which is not observed *in vivo*. A possible explanation for this discordance is the fact that the pool of effector T cells is limited *in vivo* by space constraints and possibly other stimuli. This limitation is relative to the liver, and was not considered by the model due to its nature.

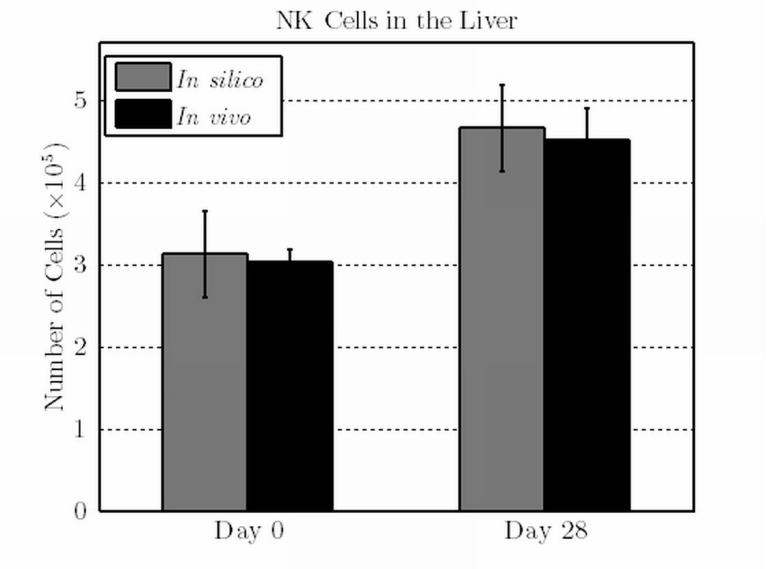

Figure 7.6: Number of NK Cells. *In silico* data describe the results of baseline model. *In vivo* data are taken from Maroof et al. 2008.

7.2.2 T Cells

T cells are considered fundamental for the immune response to leishmaniasis. Removing T cells from the model (T^- model) correctly leads to a high parasite load and a non-resolving disease (see Figure 7.11 and Section B.2 for additional data and comments).

7.2.3 INFγ

INFγ is the main cytokine responsible for the inflammatory response to leishmaniasis (see Murray et al. 2006 for example). Removing INFγ from the model (INFγ^- model) correctly leads to a very high parasite load and to a non-resolving disease (see Figure 7.12 and Section B.3 for additional data and comments).

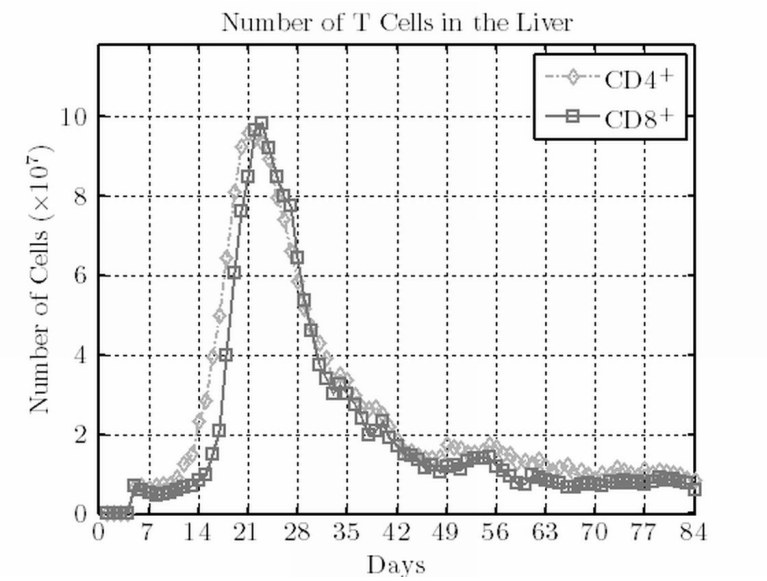

Figure 7.7: Number of $CD4^+$ and $CD8^+$ cells. *In silico* data were obtained from baseline model.

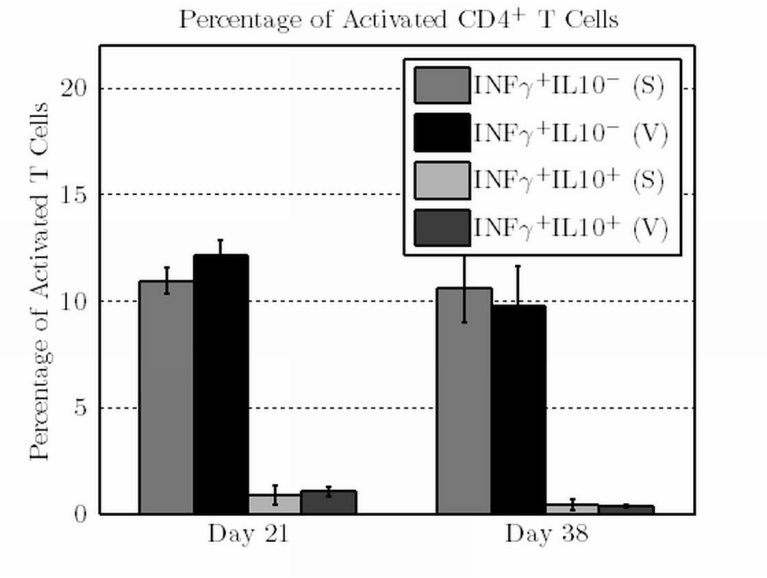

Figure 7.8: Percentage of activated T_H1 cells. *In silico* data describe the results of baseline model. *In vivo* data are taken from unpublished data.

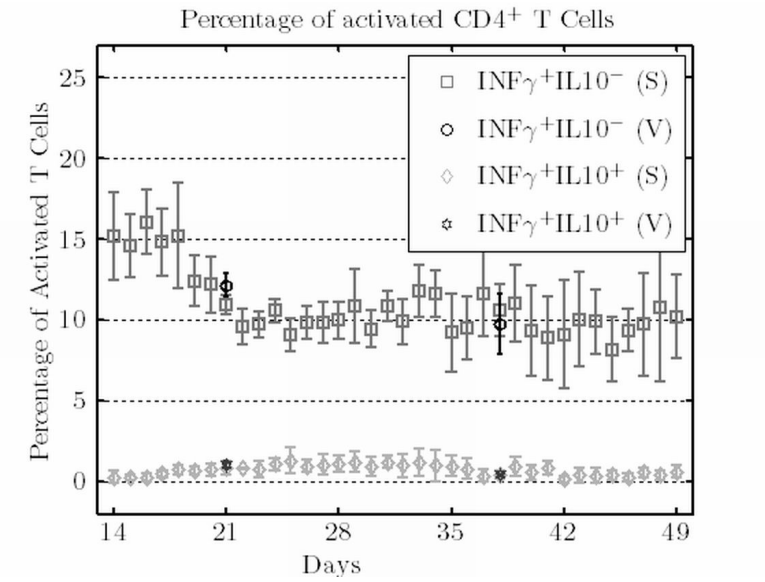

Figure 7.9: Percentage of activated T_H1 cells. *In silico* data describe the results of baseline model. *In vivo* data are taken from unpublished data.

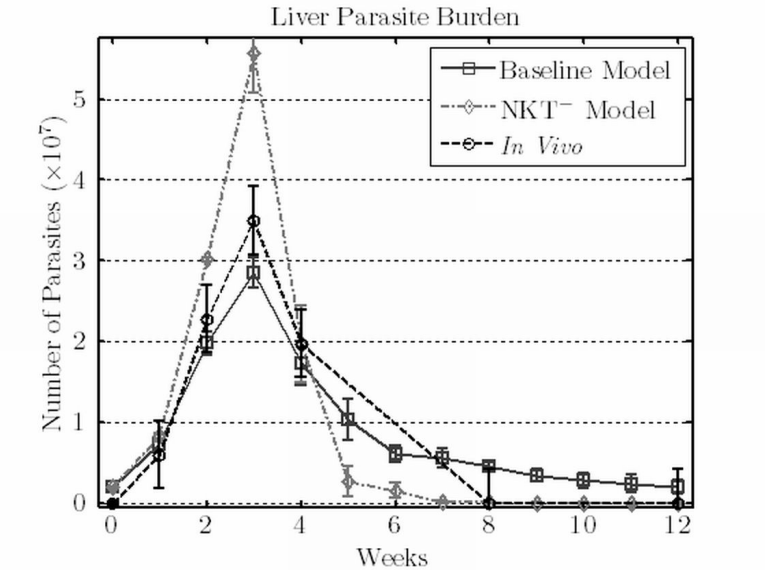

Figure 7.10: Parasite burden. *In silico* data describe the results of baseline and NKT^- model. *In vivo* data are adapted from Murray et al. 2006.

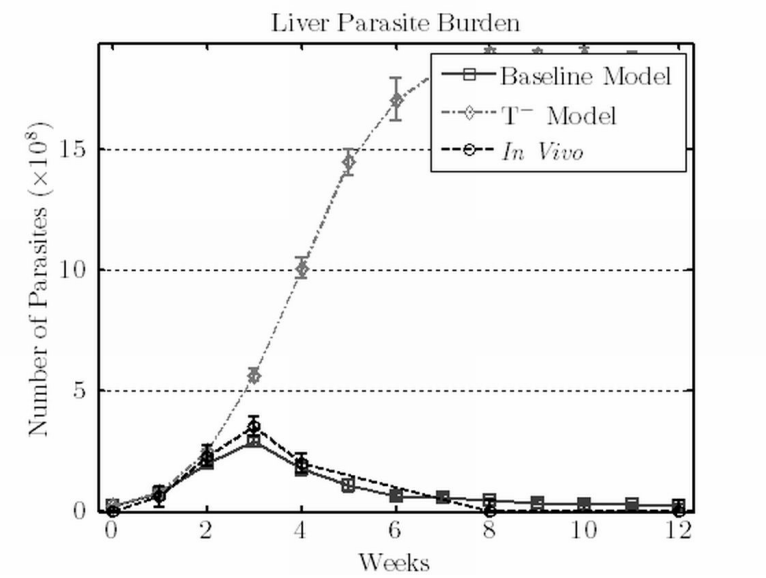

Figure 7.11: Parasite burden. *In silico* data describe the results of baseline and T^- model. *In vivo* data are adapted from Murray et al. 2006.

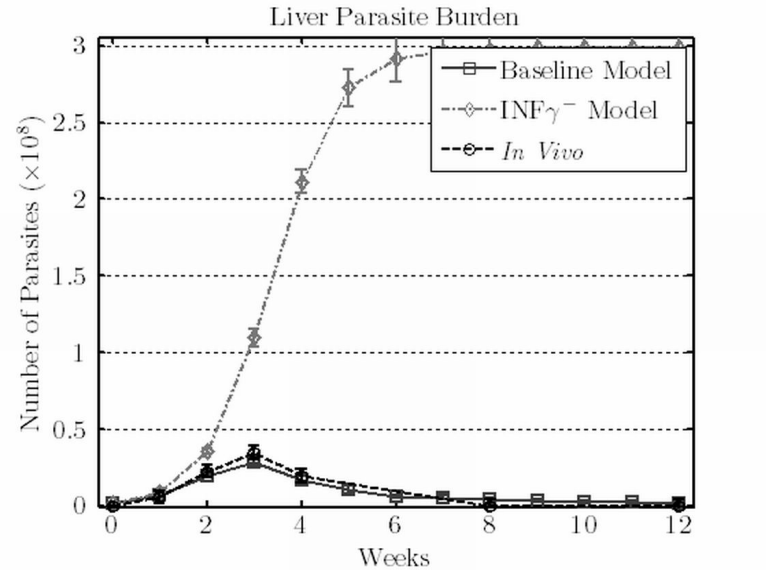

Figure 7.12: Parasite burden. *In silico* data describe the results of baseline and $INF\gamma^-$ model. *In vivo* data are adapted from Murray et al. 2006.

Chapter 8

Model Results

This chapter illustrates the main results of our model. The topics discussed are:

- the various types of granulomas
- the comparison of different causes of the phenotypic mutation of T_H1 cells
- the comparison of different mechanisms of NKT cells activation
- the role of NK cells in leishmaniasis
- the comparison of possible therapeutic options for leishmaniasis

8.1 Different Types of Granulomas

At the current stage of biological technology, it is not possible to track the evolution of a single granuloma during the whole course of leishmaniasis, it is, however, well-known that granulomas develop differently (see Figure 8.1). Therefore, using our *in silico* model, we studied how single granulomas evolve during the whole course of infection.

As expected, different types of granulomas are obtained from the model. The most common granulomas have a *one-peak* type: the number of parasites increases to a maximum (usually between 50 and 100), and then decreases to zero. We will call these granulomas "normal" (see Figure 8.2 for the number of parasites in a sample of them). Normal granulomas account for about 60% of the total population, and are characterised by a very effective immune response.

When the immune response is less effective, the number of parasites oscillates, leading to two, or more, peaks. We will call these granulomas "many-peaked" (see Figure 8.3 for the number of parasites in a sample of them). Many-peaked granulomas account for about 30% of the total population.

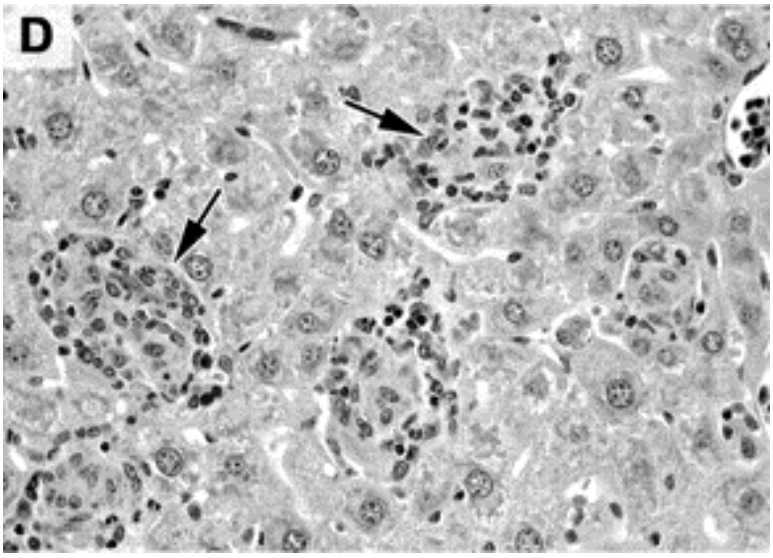

Figure 8.1: Various well-established granulomas 2 weeks after infection in C57BL/6 mice from Figure 4 of Murray et al. 2006.

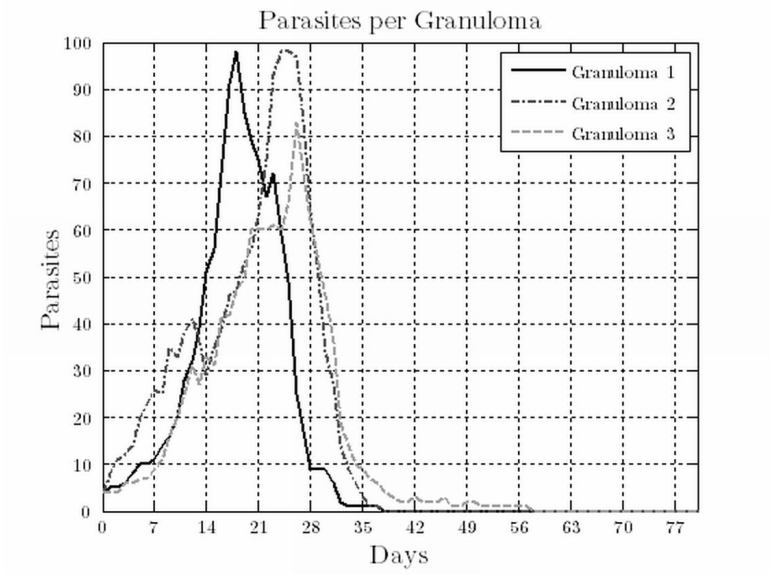

Figure 8.2: Parasites of normal granulomas.

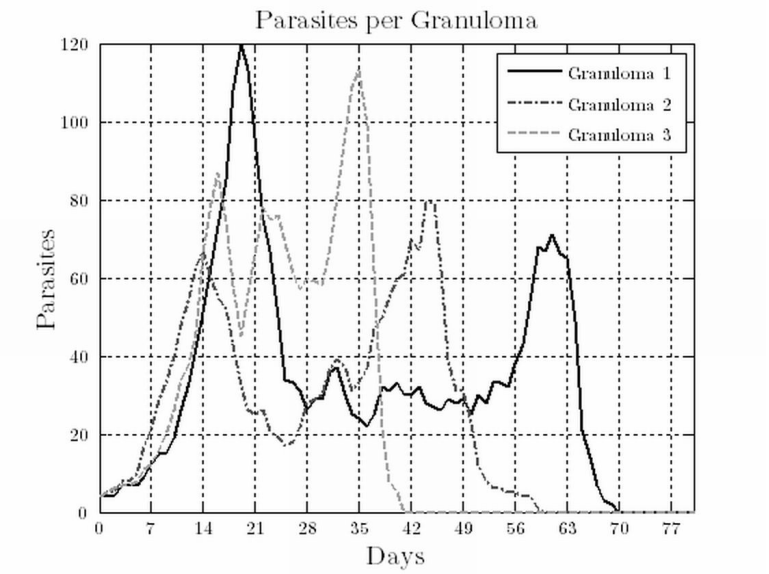

Figure 8.3: Parasites of many-peaked granulomas.

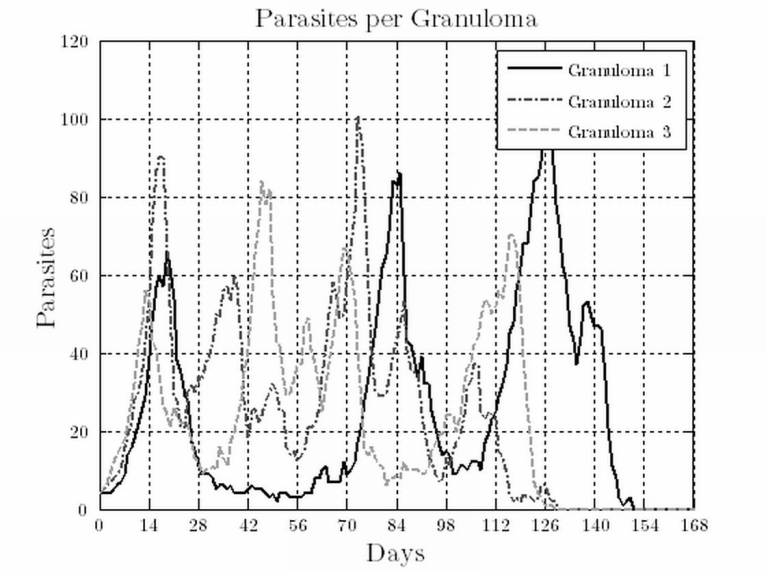

Figure 8.4: Parasites of long-lasting granulomas.

Finally, when the immune response is not effective enough, we observe a long-lasting equilibrium between the parasites and the immune system: the infection is controlled, but is cleared only after a long time. We will call these granulomas "long-lasting" (see Figure 8.4 for the number of parasites in a sample of them). These granulomas account for less that 10% of the total population, and are a likely cause of recrudescence observed in some models of visheral leishmaniasis (e.g., Kirkpatrick & Farrell 1982*b*).

More detailedly, ten weeks after infection, normal and many-peaked granulomas have successfully killed all the parasites. However, long-lasting granulomas are still controlling them. This results in a quiescent infection. If this equilibrium in broken in favor of the parasites, the Kupffer cells are likely to get killed and the parasites will spread in the liver, causing a secondary infection.

Interestingly, recrudescence is observed in other granulomatous infection such as tuberculosis (e.g., De Steenwinkel et al. 2009), suggesting that this result may apply to other diseases as well.

This diversity in the granuloma population gives us important insights on the way a therapy should deal with visceral leishmaniasis. Specifically, while improving the immune response in normal and many-peaked granuloma is useful in decreasing the parasite burden, targeting long-lasting granulomas should help in preventing recrudescence.

Ideally, a therapy should stimulate each granuloma to be of the normal type. Unfortunately, as we will see later, this goal is not easily achieved. This difficulty arises from the fact that the micro-environments of long-lasting and normal granulomas are substantially very similar, and the formation of the former seems to be promoted by the interactions with some cells rather than others.

Finally, it is worth noticing how the parasite burden in the liver emerges from remarkably different populations of granulomas.

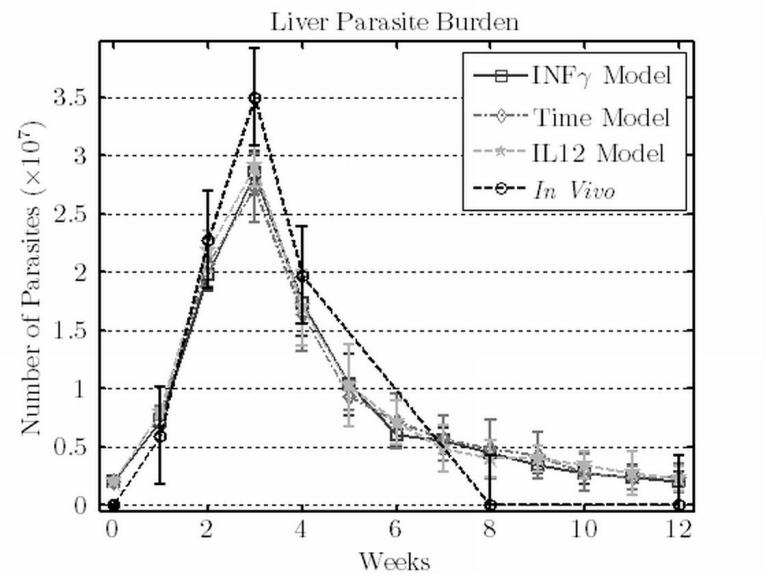

Figure 8.5: Parasite Burden. *In silico* data describe the results of INFγ, IL12, and Time models. *In vivo* data are adapted from Murray et al. 2006.

8.2 Self-Control of T_H1 Cells

8.2.1 Different Models of Phenotypic Changes in T_H1 cells

The development of an immunoregulatory phenotype by T_H1 cells is an important topic of the immunological research, as understanding the mechanisms underlying this development is helpful in designing better therapies.

We tested three possible causes of this phenotypical change:

- Exposure to INFγ (INFγ model)
- Exposure to IL12 (IL12 model)
- Prolonged activation (Time model)

More precisely, the probability that T_H1 cells change their phenotype is proportional to INFγ concentration in the INFγ model and to IL12 concentration in the IL12 model; while it is constant in the Time model.

According to our model, all the above mechanisms lead to comparable results for parasite burden, response of NKT cells, and response of NK cells (see Figure 8.5 for parasite burden and Section B.4 for additional data). However, Figures 8.6 and 8.7 indicate that the percentages of activated T_H1 cells of INFγ and Time models fit better *in vivo* data. This suggests that INFγ and time are more likely to be causes of the phenotypical change.

Additionally, Figures 8.8 and 8.9 show that the percentage of the different populations of T cells diverges around the fifth week, thus indicating that our

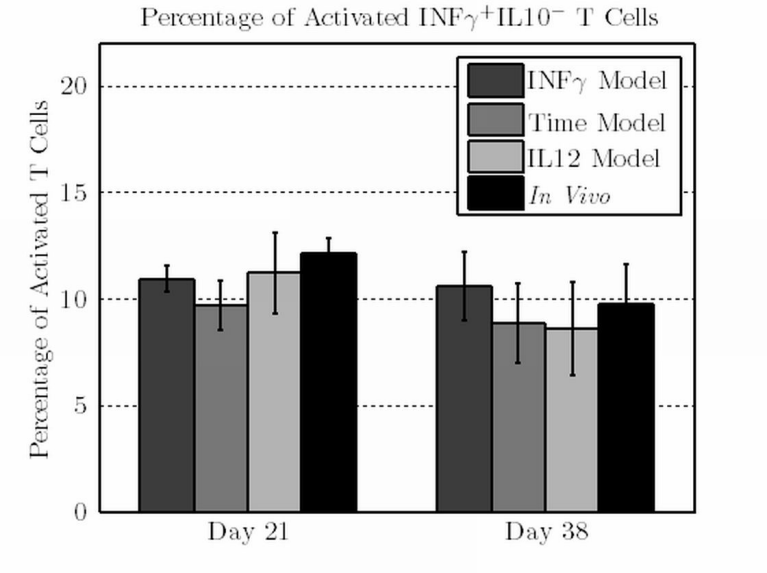

Figure 8.6: Percentage of INFγ^+IL10$^-$ T Cells. *In silico* data describe the results of INFγ, IL12, and Time models. *In vivo* data are taken from unpublished data.

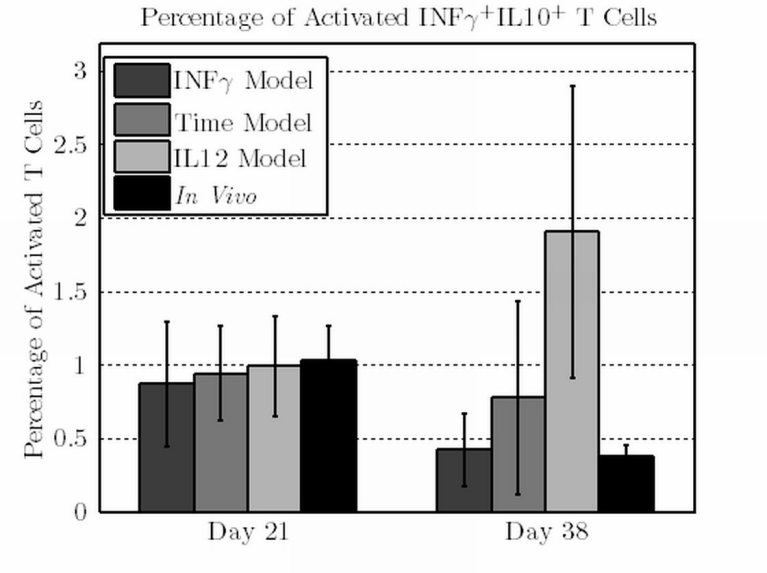

Figure 8.7: Percentage of INFγ^+IL10$^+$ T Cells. *In silico* data describe the results of INFγ, IL12, and Time models. *In vivo* data are taken from unpublished data.

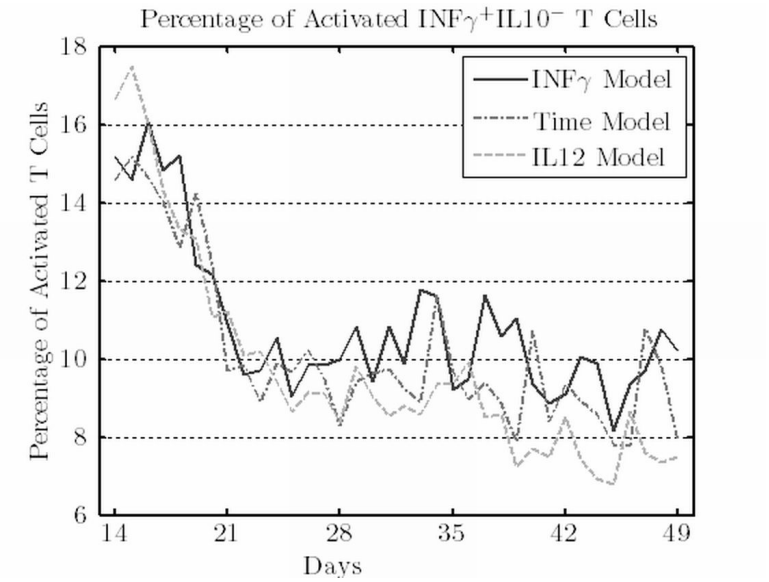

Figure 8.8: Percentage of INFγ^+IL10$^-$ T Cells. Data describe INFγ, IL12, and Time model.

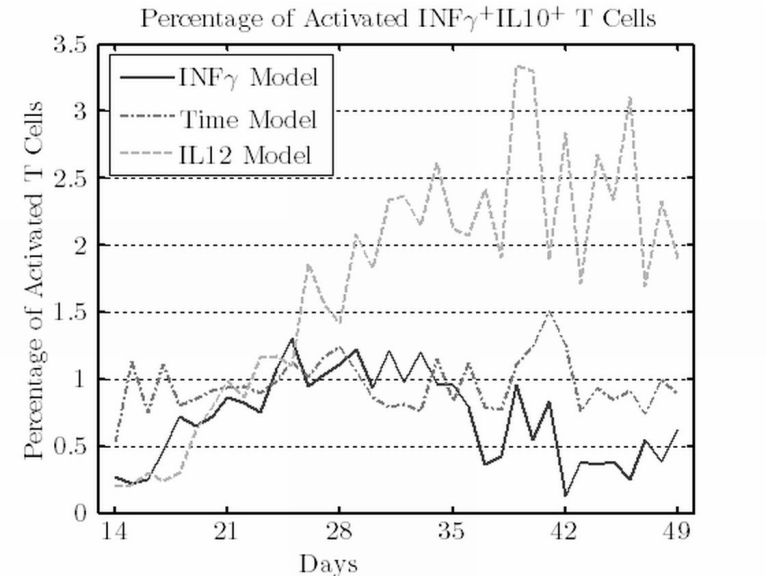

Figure 8.9: Percentage of INFγ^+IL10$^+$ T Cells. Data describe INFγ, IL12, and Time model.

results are due to the differences in the three models rather that to stochastic effects.

Note that our conclusions strongly depend on the assumption that classically activated phagocytes are the main source of IL12, and thus, that the production of IL12 is delayed with respect to INFγ.

8.2.2 Considerations on the IL12-Dependent Model

Effector T cells that do not develop a memory phenotype are assumed to be able to replicate only a limited number of times, and since $CD4^+INF\gamma^+IL10^+$ T cells are probably quite old, it is likely that their reproduction capability, if any, is limited. To assess the relevance of this consideration, we investigated to which extent the outcome of the IL12 model depends on the aforementioned reproduction ability.

The percentages of activated $CD4^+INF\gamma^+IL10^+$ cells decrease when their reproduction ability is reduced (see Figures 8.11 and 8.10), while the overall model remains compatible with *in vivo* data (see Figure 8.10 for parasite burden and Section B.5 for additional data), making IL12 a viable candidate for the phenotypic change of T_H1 cells under the assumption that the reproduction ability of $CD4^+INF\gamma^+IL10^+$ T cells is much lower that the reproduction ability of $CD4^+INF\gamma^+IL10^-$ T cells.

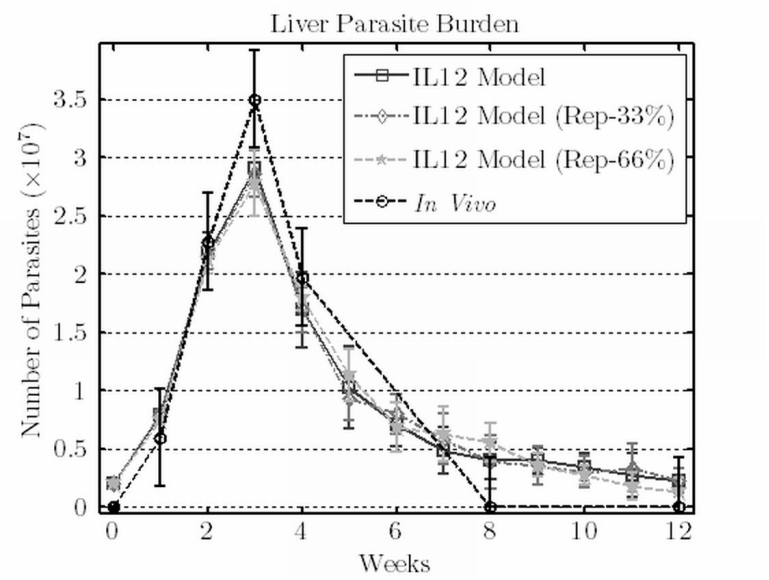

Figure 8.10: Parasite Burden. *In silico* data describe IL12 model, IL12 model with reproduction ability of INFγ^+IL10$^+$ T Cells reduced by 33%, and IL12 model with reproduction ability of INFγ^+IL10$^+$ T Cells reduced by 66%. *In vivo* data are adapted from Murray et al. 2006.

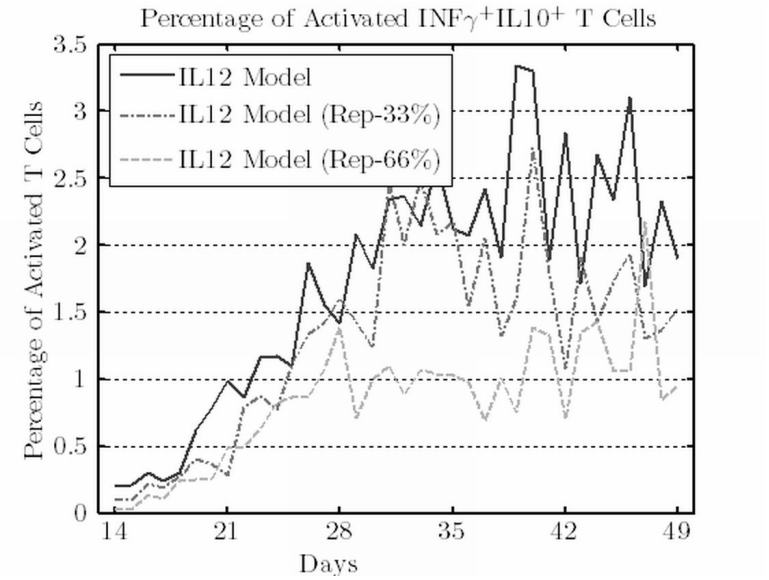

Figure 8.11: Percentage of INFγ^+IL10$^+$ T Cells. Data describe IL12 model, IL12 model with reproduction ability of INFγ^+IL10$^+$ T Cells reduced by 33%, and IL12 model with reproduction ability of INFγ^+IL10$^+$ T Cells reduced by 66%.

8.3 Natural Killer T Cells

8.3.1 Activation

As described in Section 1.3.1, NKT cells can be activated by various means. However, in the context of leishmania, internalization of CD1d peptides is believed to be the main source of activation. To assess this fact, we compared two possible mechanisms of NKT cells activation:

- internalization of CD1d peptides (CD1d model)
- detection of *stress* in Kupffer cells (Stress model)

Note that we disregarded the possibility of an IL12-mediated activation as the experiments of Amprey et al. 2004 indicate this possibility as very unlikely.

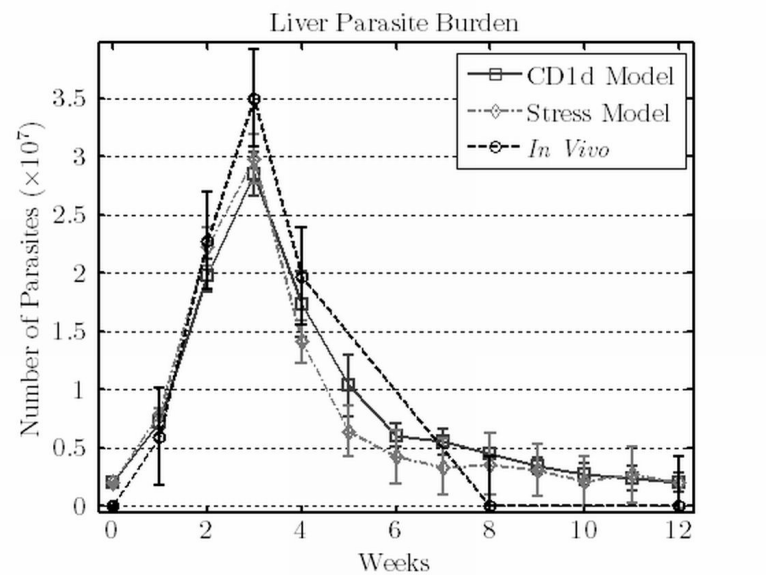

Figure 8.12: Parasite Burden. *In silico* data describe CD1d and Stress models. *In vivo* data are adapted from Murray et al. 2006.

While both mechanisms lead to comparable results for the overall model (see Figure 8.12 for the parasites burden, Figure 8.13 for the number of NKT cells, and Section B.6 for additional data), internalization of CD1d peptides produces better results when considering the percentages of activated NKT cells (see Figure 8.14). This confirm CD1d peptides internalization as the most likely factor for NKT cells activation.

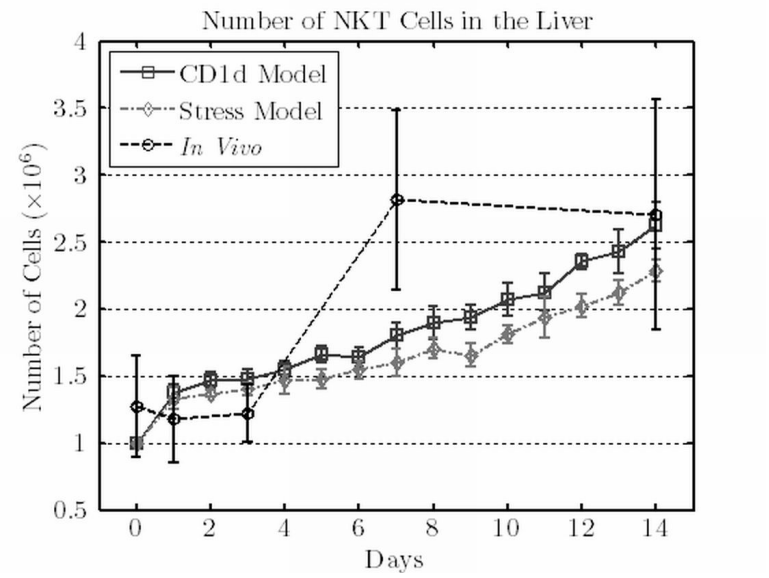

Figure 8.13: Number of NKT cells. *In silico* data describe CD1d and Stress models. *In vivo* data are taken from Stanley et al. 2008.

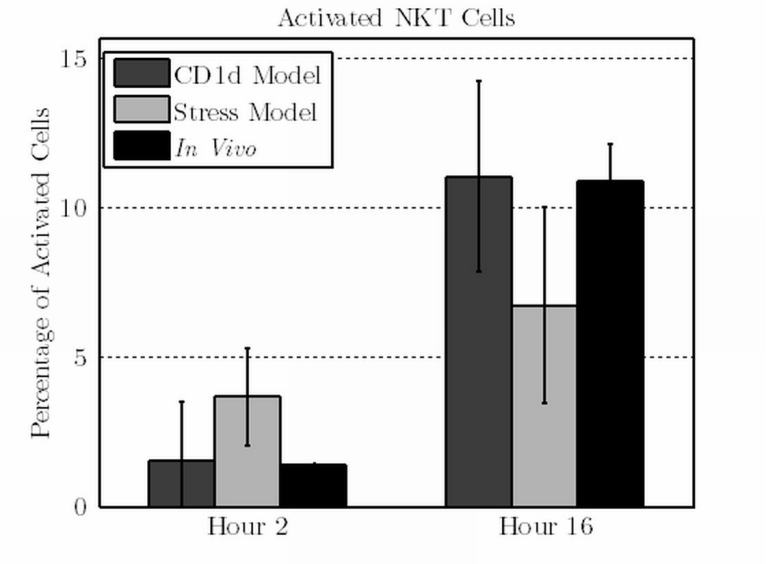

Figure 8.14: Percentage of activated NKT cells. *In silico* data describe CD1d and Stress models. *In vivo* data are taken from Amprey et al. 2004 and Beattie at al. 2010 (EJI).

8.3.2 External Activation

Stanley et al. 2008 reports that activation of NKT cells by α-galactosylceramide at day 7 and 14 after infection leads, one week later, to an increased parasite burden, thus excluding α-galactosylceramide as a therapeutic option.

However, as reported in Section 2.3, some authors suggest that different populations of NKT cells exist. Therefore, it is possible that α-galactosylceramide and *leishmania donovani* induce the activation of different subsets of NKT cells. Moreover, NKT cells activated by α-galactosylceramide are reported to produce high level of IL4, while NKT cells activated during leishmaniasis are characterized by low level of IL4[1].

Therefore, we tested the consequences of an increased CD1d-independent activation of NKT cells at day 7 (NKT↑ (Day 7) model) and 14 (NKT↑ (Day 14) model).

In the NKT↑ (Day 7) model NKT cells were activated from hour 168 to hour 216, and in NKT↑ (Day 14) model from hour 336 to hour 384 (Figures 8.15 and 8.16 indicate the effect of these activations on the number of NKT cells)

Compatibly with Stanley et al. 2008, our model indicates that an additional activation of NKT cells leads to a higher parasite burden (see Figures 8.17 and 8.18 for parasite burden, and Section B.7 for additional data). Differently form Stanley et al. 2008, however, in our model, the increase in parasite burden takes more time to display. This is probably due to the fact that α-galactosylceramide has a systemic effect, thus leading to an inflow of activated NKT cells, instead of an inflow of homeostatic cells as in our model. Finally, note that this activation, while increasing the number of parasites, does not impair disease resolution.

8.3.3 Role in Late Infection

As described in Section 8.3.1, NKT cells play a major role in controlling the infection during the early stages of visceral leishmaniasis. However, their role in the later stages is less clear. Amprey et al. 2004 reports that the percentage of NKT cells with respect to $CD4^+$ and $CD8^+$ T cells is quite low in the later stage of infection. However, no data are available on the percentage of activated cells, and it is even possible that no NKT cell is activated. Nevertheless, Section 8.3.2 suggests not only that they may unessential, but even detrimental.

Preventing NKT from activating 4 weeks after infection (NKT↓ (Day 28) model) has a perceivable effect on the parasite burden (see Figures 8.19). Moreover, the number of parasites after week 8 is generally lower when no

[1]Note that, the data of Stanley et al. 2008 indicate that NKT cells activated by α-galactosylceramide produced low levels of IL4 during their experiments.

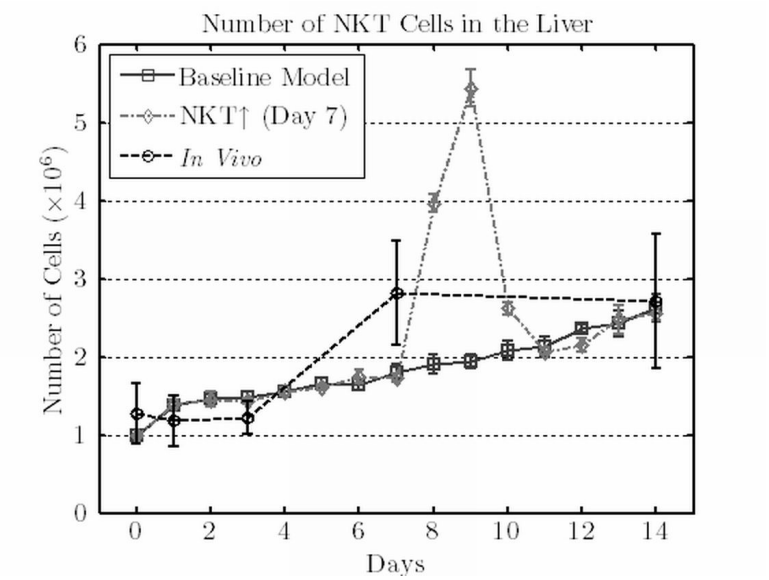

Figure 8.15: Number of NKT cells. *In silico* data describe baseline and (NKT↑ (Day 7) models. *In vivo* data are taken from Stanley et al. 2008.

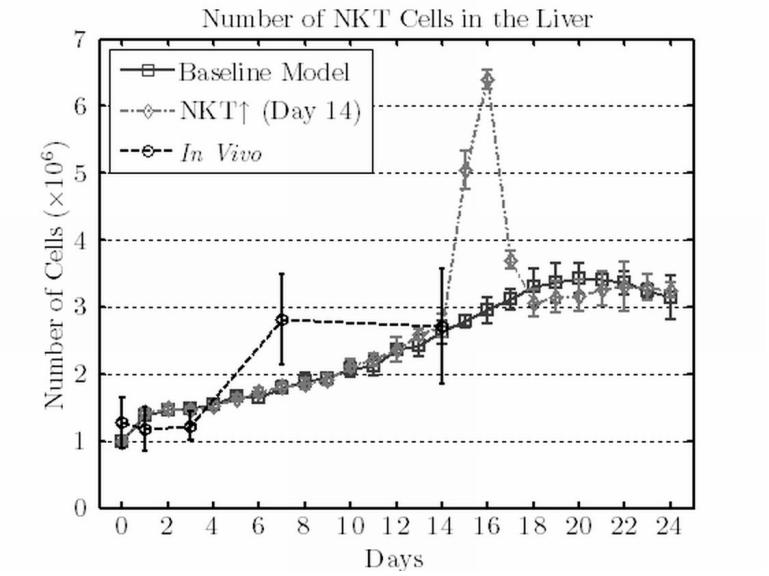

Figure 8.16: Number of NKT cells. *In silico* data describe baseline and (NKT↑ (Day 14) models. *In vivo* data were taken from Stanley et al. 2008.

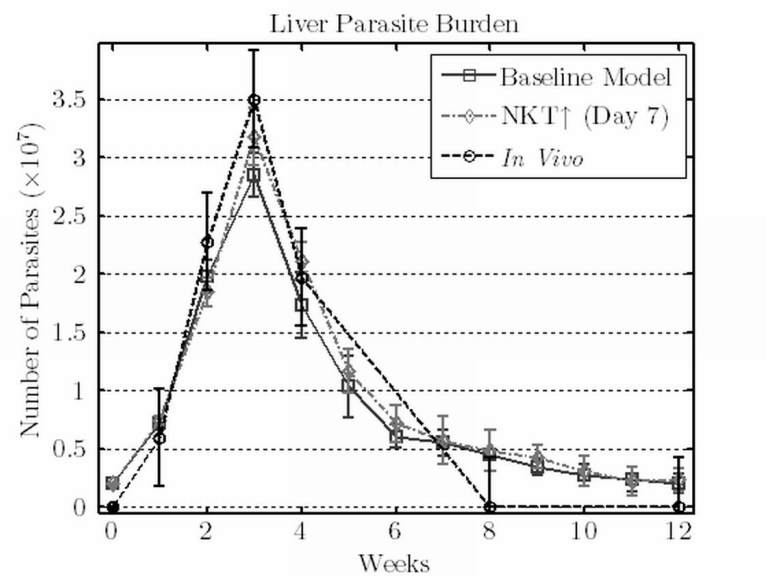

Figure 8.17: Parasite Burden. *In silico* data describe baseline and (NKT↑ (Day 7) models. *In vivo* data are adapted from Murray et al. 2006.

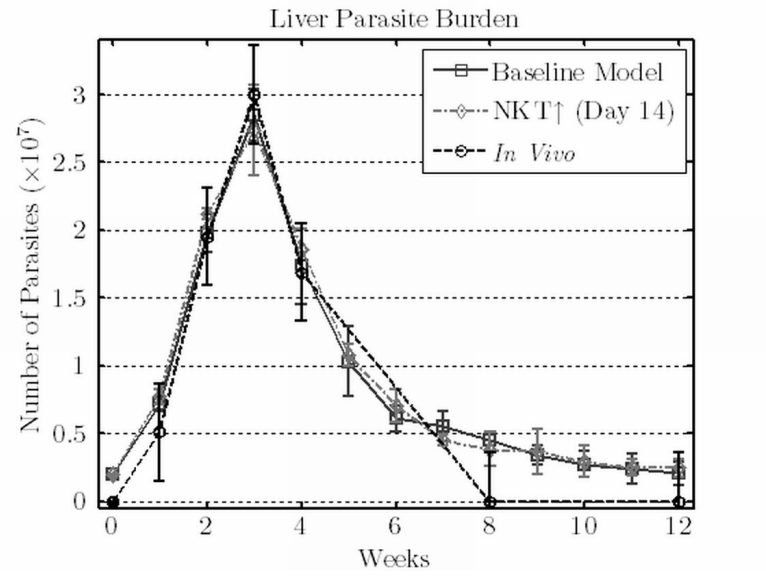

Figure 8.18: Parasite Burden. *In silico* data describe baseline and (NKT↑ (Day 14) models. *In vivo* data are adapted from Murray et al. 2006.

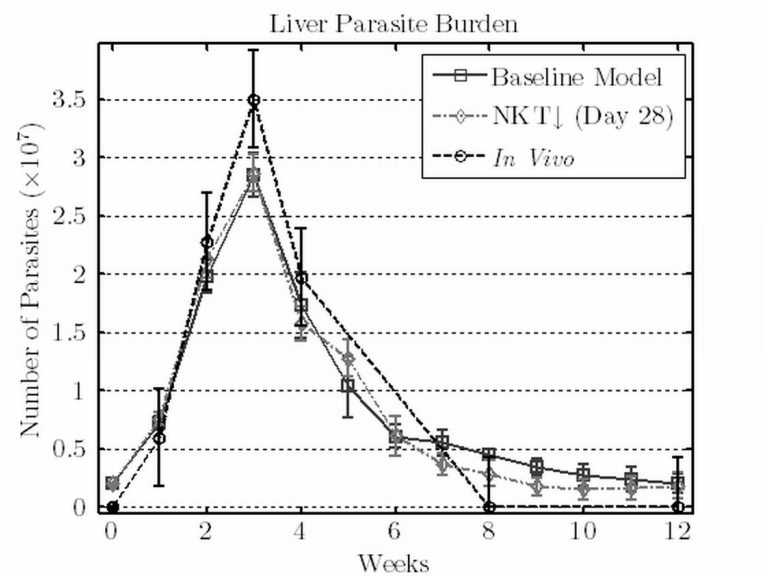

Figure 8.19: Parasite Burden. *In silico* data describe baseline and NKT↓ (Day 28) models. *In vivo* data are adapted from Murray et al. 2006.

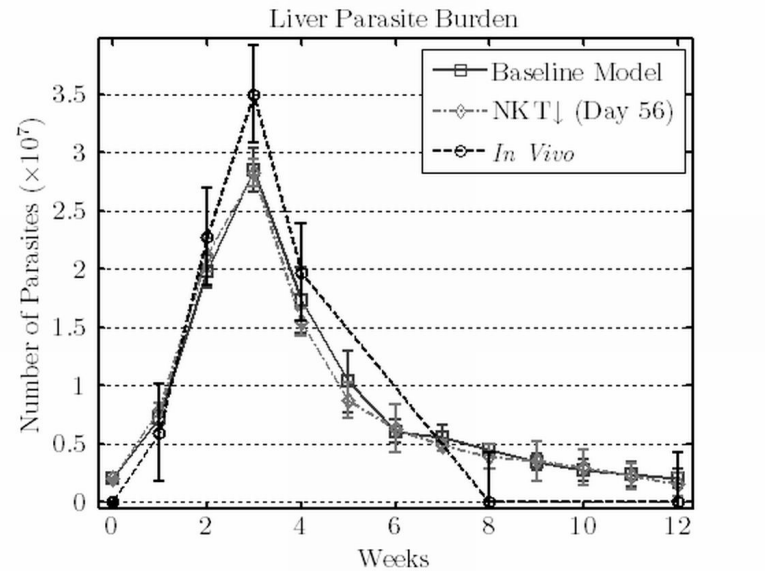

Figure 8.20: Parasite Burden. *In silico* data describe baseline and NKT↓ (Day 56) models. *In vivo* data are adapted from Murray et al. 2006.

NKT cells are activated. This result suggests that, if any, the role of NKT cells during the later stages of infection is mainly immunoregulatory.

Note that, an additional possibility exists: in later stages of infection NKT cells activate, but their deactivation activity is limited by a reduced number of SIRPα proteins, or a by a reduced effect of SIRPα ligation.

As discussed in Section 8.3.2, an additional activation of NKT cells leads to a larger parasite burden even two weeks after infection, this fact indicates that the deactivation activity of NKT cells is still present at that time, and suggests that it may continue afterward. Since no data are available on a possible decreased deactivation activity of NKT cells during later stages of infection, this hypothesis was not tested.

Preventing NKT from activating 8 weeks after infection (NKT$\downarrow$ (Day 56) model) has a limited effect on the parasite burden (see Figures 8.20), suggesting that their role is probably quite limited at such a later stage of infection.

8.4 Natural Killer Cells in Leishmaniasis

The role of NK cells during the immune response to visceral leishmaniasis is currently not fully understood. Beige mice, which are known to have defective NK cells, are unable to mount a healing response to *leishmania donovani* (Kirkpatrick & Farrell 1982*b*). However, these mice have a complex biology and other dysfunctions may contribute to prevent an adequate response. Therefore, in the context of C57BL/6 mice, no clear evidence is available on the impact of NK cells to the course of visceral leishmaniasis. To determine the role of NK cells, we tested the effect of their removal (NK^- model).

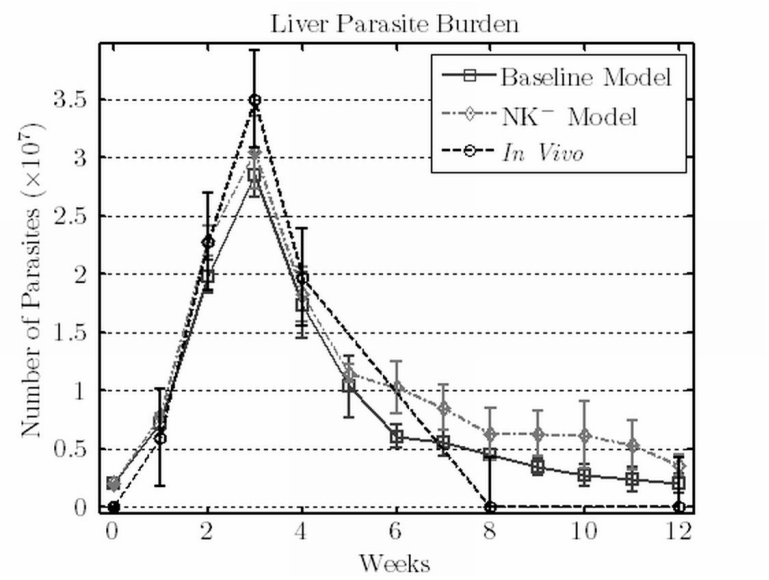

Figure 8.21: Parasite Burden. *In silico* data describe baseline and NK^- model. *In vivo* data are adapted from Murray et al. 2006.

Our model suggests that, while positively contributing to the immune response to leishmaniasis, NK cells do not have a fundamental role in controlling the infection (see Figure 8.21 and Section B.8 for additional data).

Note however, that removing both NKT and NK cells from our model prevents an effective adaptive immune response, as there is no other early source of INFγ able to drive T cells towards a type I response (see Section B.9). This situation is unlikely in vivo, because some T cells are believed get to the place of infection with a type I phenotype. However, this result suggests that a possible cause of the inability of beige mice to mount an adequate immune response to leishmaniasis is the presence of somewhat defective NKT cells.

8.5 Therapeutic Options in Leishmaniasis

An important goal of immunological modeling is the development of effective therapies, mainly by the identification of key mechanisms that should be targeted by biological experiments. This section describes three possible therapeutic options:

- Blocking the activity of IL10
- Increasing INFγ concentration
- Increasing INFγ concentration while blocking the activity of IL10

8.5.1 IL10 Blocking

As a first possible therapeutic option, we tested the effect of removing IL10 from the model, thus reproducing the effect of an anti-IL10 drug.

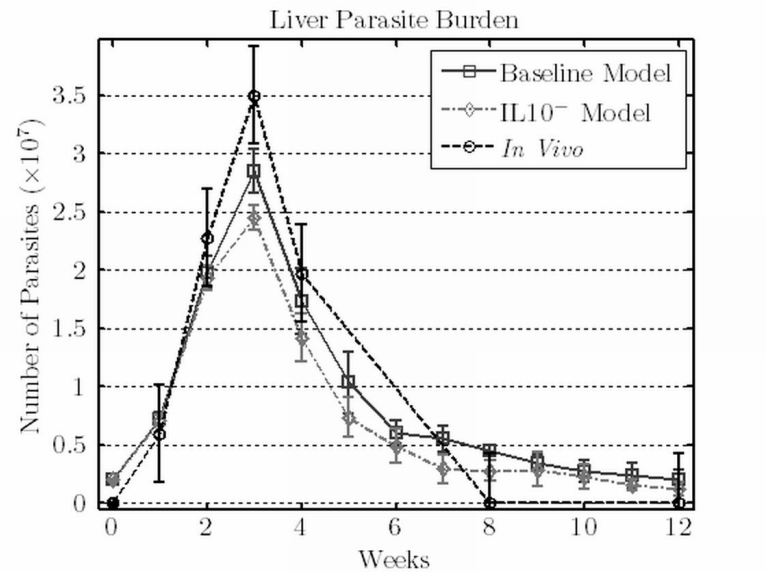

Figure 8.22: Parasite Burden. *In silico* data describe baseline and IL10$^-$ models. *In vivo* data are adapted from Murray et al. 2006.

Our model suggests that removing completely IL10 from the model (IL10$^-$ model) leads to slightly lower parasite burden and facilitates disease resolution (See Figure 8.22 and Section B.10 for additional data).

8.5.2 INFγ Injection

INFγ is fundamental for the immune response to *leishmania donovani*. However, albeit its role is mainly pro-inflammatory, its supposed ability to stim-

ulate the production of IL10 by T_H1 cells indicates a possible indirect anti-inflammatory role. Therefore, the effect of increasing INFγ concentration is not easily predictable.

To better understand the effect of a temporary increase in INFγ concentration, we performed four different experiments. Specifically, INFγ concentration was increased for 10 hours at different times:

- 12 days after infection (INF$\gamma\uparrow$ (Day 12) model)
- 24 days after infection (INF$\gamma\uparrow$ (Day 24) model)
- 36 days after infection (INF$\gamma\uparrow$ (Day 36) model)
- 48 days after infection (INF$\gamma\uparrow$ (Day 48) model)

12 Days After Infection

In a first experiment, we increased INFγ concentration from hour 290 to hour 300 (Figure 8.23 indicates the effect on INFγ concentration). These experimental conditions lead to a reduced parasite burden. However, they do not facilitate disease resolution (see Figure 8.24 for parasite burden and Section B.11 for additional data).

24 Days After Infection

In a second experiment, we increased INFγ concentration from hour 580 to hour 590 (Figure 8.25 indicates the effect on INFγ concentration). These experimental conditions slightly reduce the parasite burden, but do not significantly facilitate disease resolution (see Figure 8.26 for parasite burden and Section B.12 for additional data). Moreover, INFγ concentration is increased beyond the maximum level reached in the baseline model. Therefore, this slight improvement of the immune response induces an increased stress to the organism, which can be dangerous. This observation suggests that this is unlikely to be a good therapeutic option.

36 Days After Infection

In a third experiment, we increased INFγ concentration from 870 hour to 880 hour (Figure 8.27 indicates the effect on INFγ concentration). These experimental conditions lead to limited improvements over the baseline model (see Figure 8.28 for parasite burden and Section B.13 for additional data).

48 Days After Infection

In a fourth experiment, we increased INFγ concentration from hour 1160 to hour 1170 (Figure 8.29 indicates the effect on INFγ concentration). These

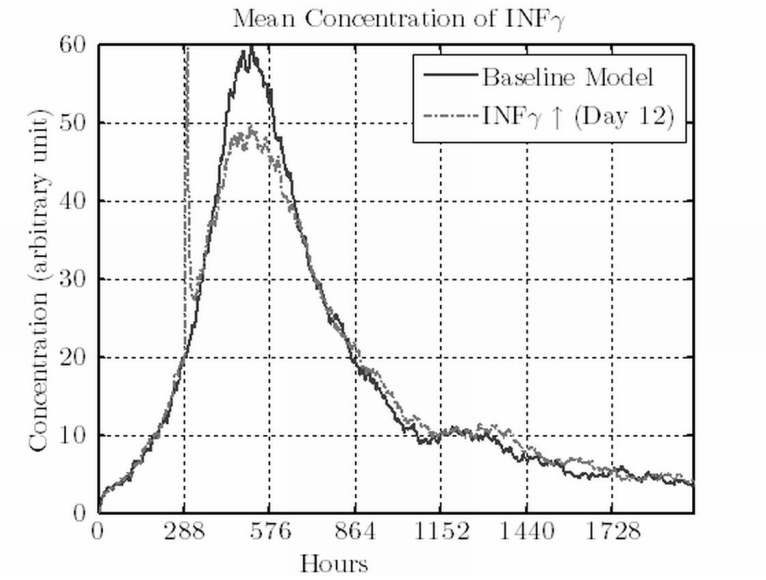

Figure 8.23: INFγ concentration. Data describe baseline and INF$\gamma \uparrow$ (Day 12) models.

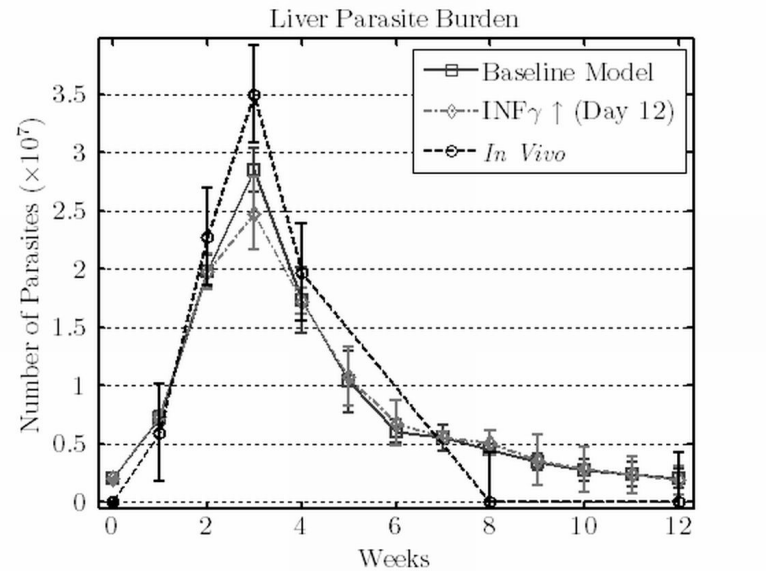

Figure 8.24: Parasite Burden. *In silico* data describe baseline and INF$\gamma \uparrow$ (Day 12) models. *In vivo* data are adapted from Murray et al. 2006.

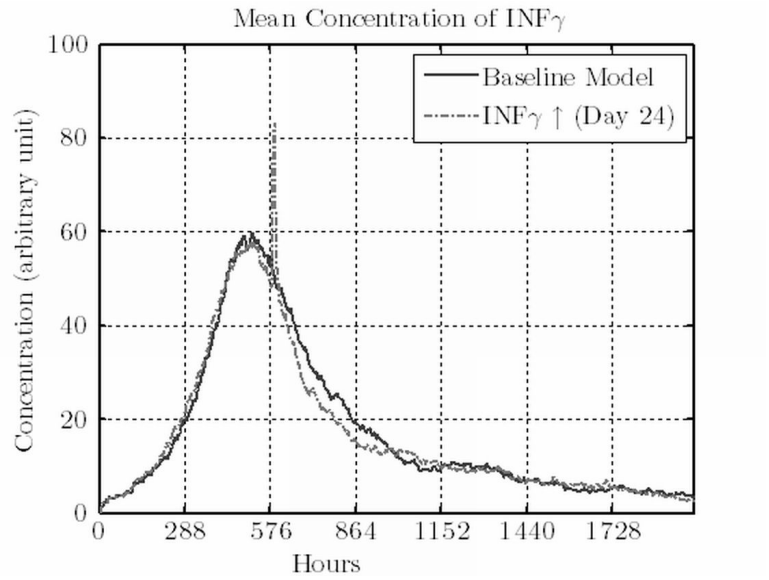

Figure 8.25: INFγ concentration. Data describe baseline and INF$\gamma \uparrow$ (Day 24) models.

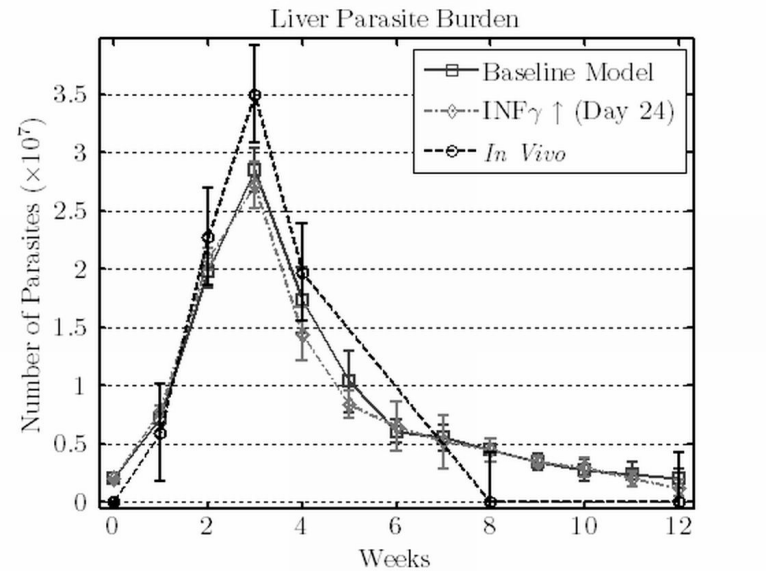

Figure 8.26: Parasite Burden. *In silico* data describe baseline and INF$\gamma \uparrow$ (Day 24) models. *In vivo* data were taken from Murray et al. 2006.

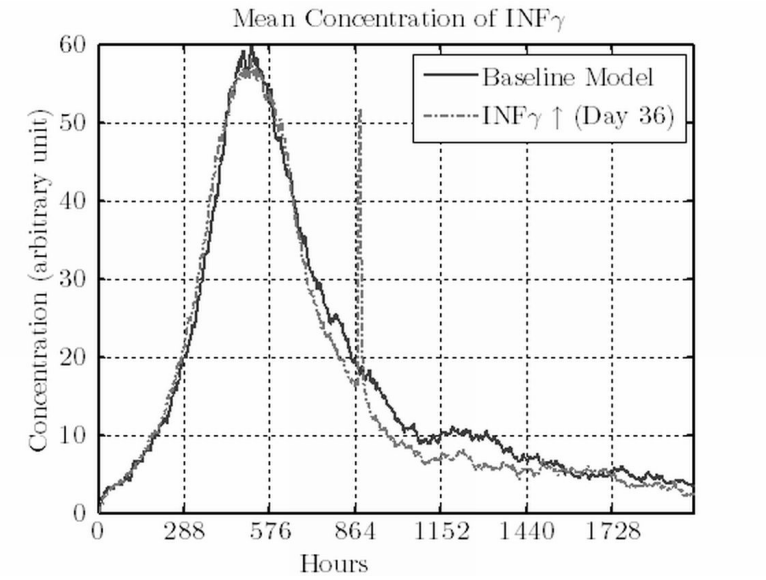

Figure 8.27: INFγ concentration. Data describe baseline and INF$\gamma \uparrow$ (Day 36) models.

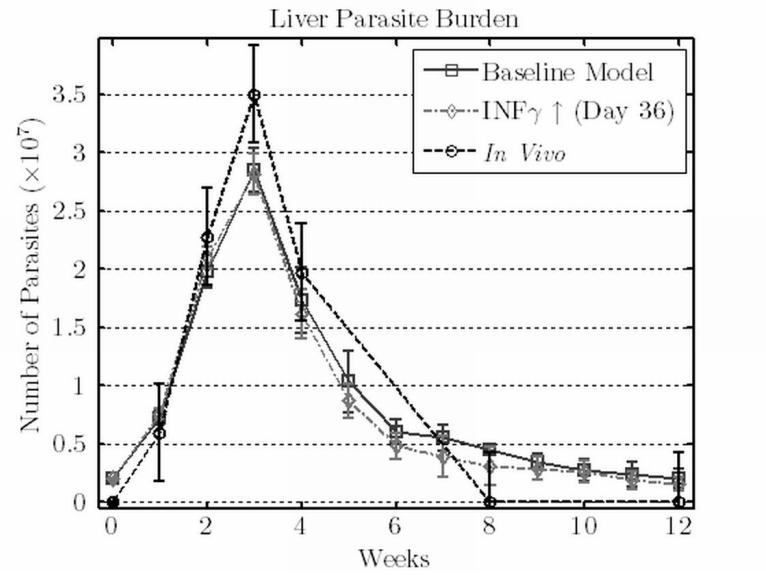

Figure 8.28: Parasite Burden. *In silico* data describe baseline and INF$\gamma \uparrow$ (Day 36) models. *In vivo* data were taken from Murray et al. 2006.

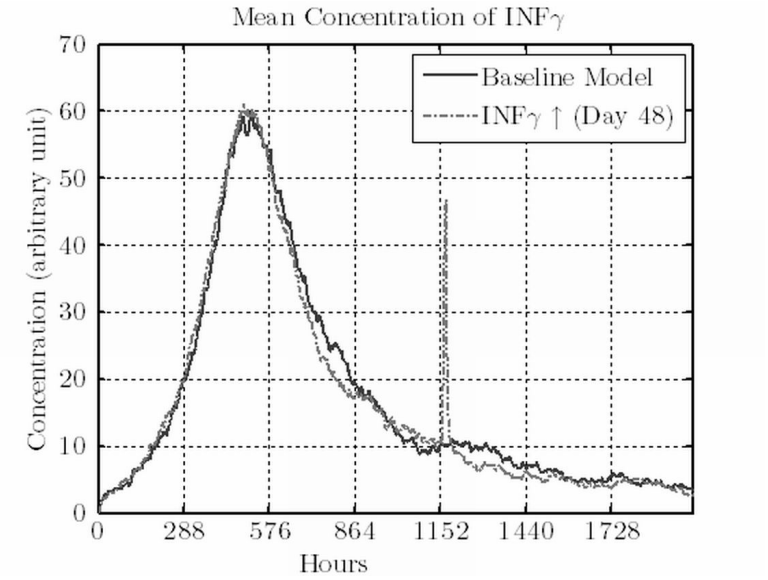

Figure 8.29: INFγ concentration. Data describe baseline and INF$\gamma \uparrow$ (Day 48) models.

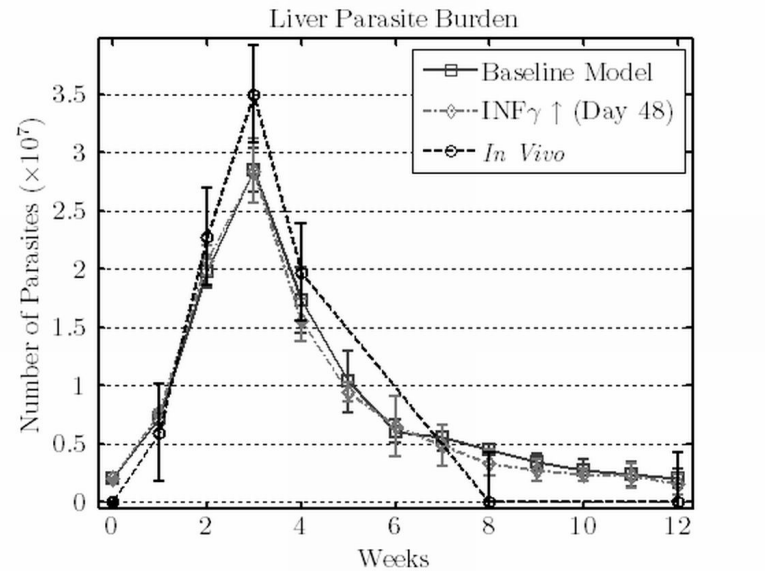

Figure 8.30: Parasite Burden. *In silico* data describe baseline and INF$\gamma \uparrow$ (Day 48) models. *In vivo* data were taken from Murray et al. 2006.

experimental conditions slightly facilitate disease resolution (see Figure 8.30 for parasite burden and Section B.14 for additional data).

8.5.3 IL10 Blocking and INFγ Injection

Finally, we tested the effect of increasing INFγ concentration in absence of IL10. Specifically, INFγ concentration was increased for 10 hours in absence of IL10 at following times:

- 12 days after infection (IL10$^-$INF$\gamma\uparrow$ (Day 12) model)
- 24 days after infection (IL10$^-$INF$\gamma\uparrow$ (Day 24) model)
- 36 days after infection (IL10$^-$INF$\gamma\uparrow$ (Day 36) model)
- 48 days after infection (IL10$^-$INF$\gamma\uparrow$ (Day 48) model)

12 Days After Infection

Increasing INFγ concentration from hour 290 to hour 300 (Figure 8.31 indicates the effect on INFγ concentration), while blocking IL10, leads to a strongly decreased parasite burden, but appears to have only a limited effect on disease resolution (see Figure 8.32 for parasite burden and Section B.15 for additional data). While the parasite burden is lowered (as a consequence of the reduced deactivation of macrophages), these results are similar to those presented in Section 8.5.2.

24 Days After Infection

Increasing INFγ concentration from hour 580 to hour 590 (Figure 8.33 indicates the effect on INFγ concentration), while blocking IL10, leads to a decreased parasite burden and facilitates disease resolution. (see Figure 8.34 for parasite burden and Section B.16 for additional data). Similarity to Section 8.5.2, INFγ concentration is increased with respect to baseline model, albeit to a lesser extent.

36 Days After Infection

Increasing INFγ concentration from hour 870 to hour 880 (Figure 8.35 indicates the effect on INFγ concentration), while blocking IL10, leads to a lower parasite burden and facilitates disease resolution (See Figure 8.36 for parasite burden and Section B.17 for additional data). The improvements over the results of Section 8.5.2 are evident. These experimental conditions seem to be overall quite effective.

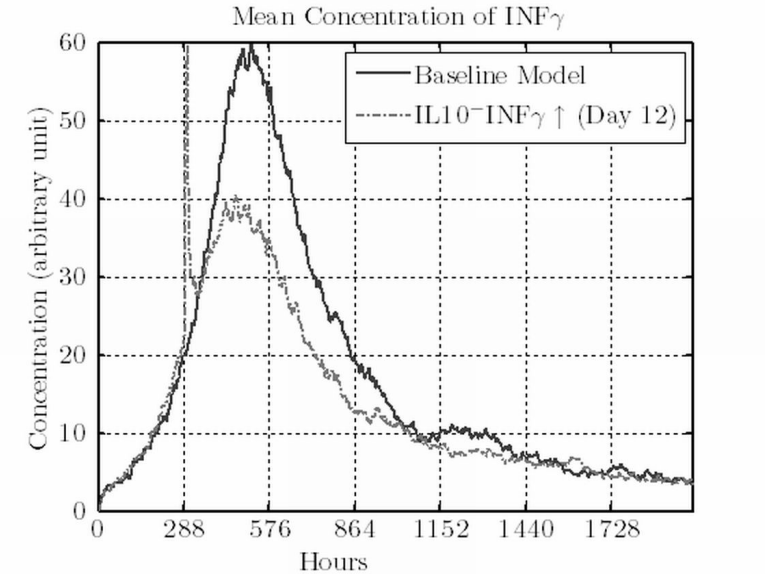

Figure 8.31: INFγ concentration. Data describe baseline and IL10^{-}INFγ $\uparrow$ (Day 12) models.

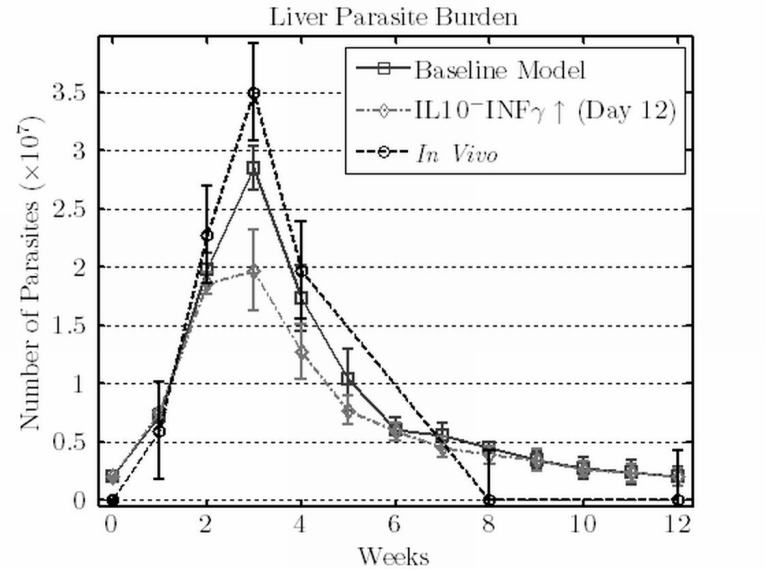

Figure 8.32: Parasite Burden. *In silico* data describe baseline and IL10^{-}INFγ $\uparrow$ (Day 12) models. *In vivo* data are adapted from Murray et al. 2006.

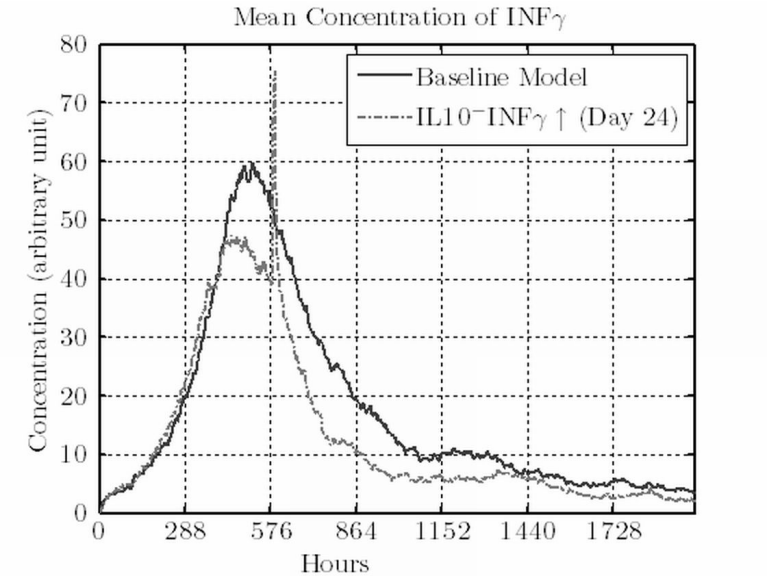

Figure 8.33: INFγ concentration. Data describe baseline and IL10^{-}INFγ $\uparrow$ (Day 24) models.

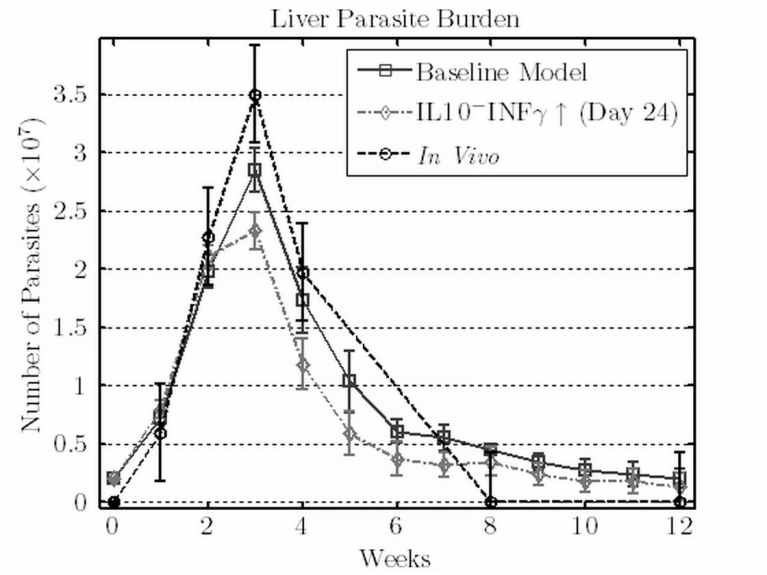

Figure 8.34: Parasite Burden. *In silico* data describe baseline and IL10^{-}INFγ $\uparrow$ (Day 24) models. *In vivo* data were taken from Murray et al. 2006.

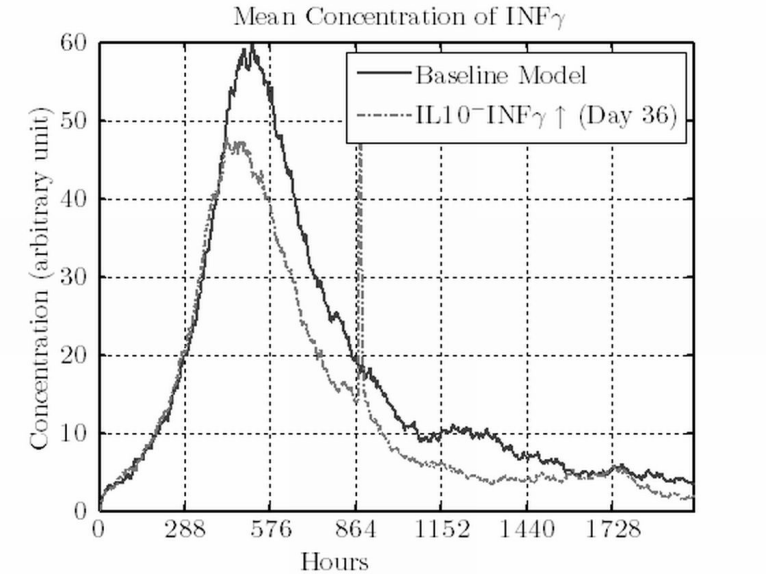

Figure 8.35: INFγ concentration. Data describe baseline and IL10^{-}INFγ $\uparrow$ (Day 36) models.

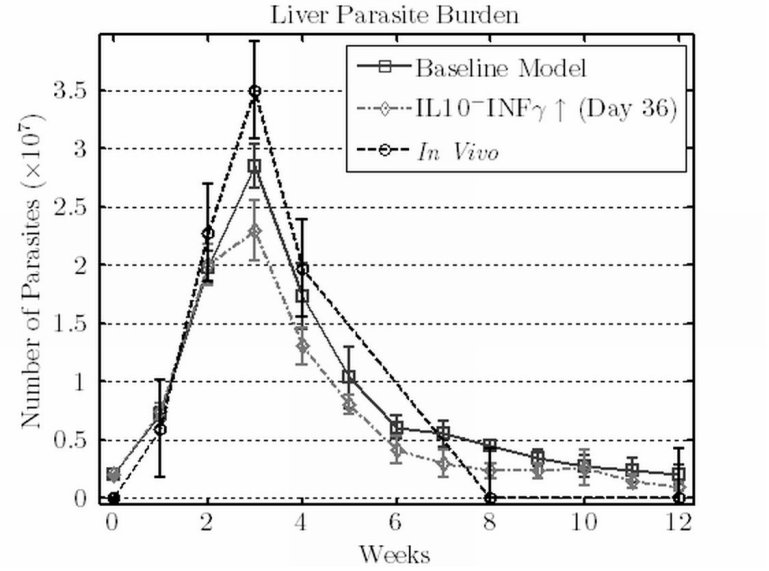

Figure 8.36: Parasite Burden. *In silico* data describe baseline and IL10^{-}INFγ $\uparrow$ (Day 36) models. *In vivo* data were taken from Murray et al. 2006.

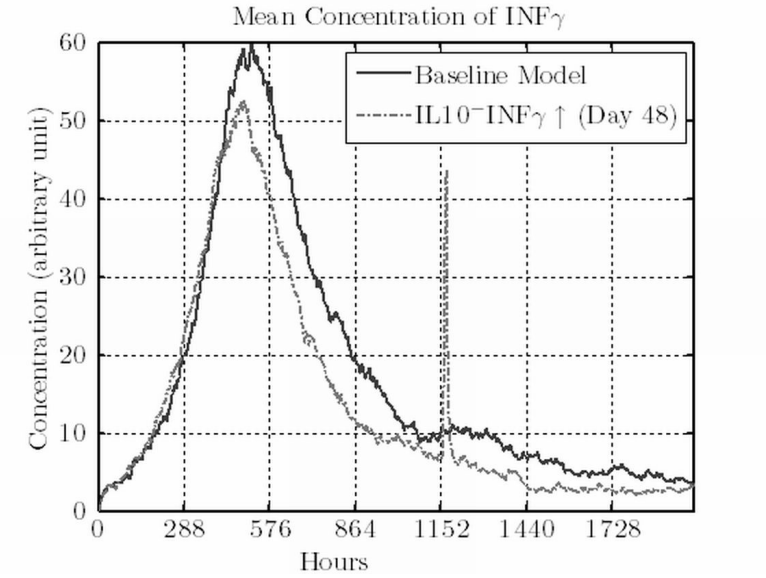

Figure 8.37: INFγ concentration. Data describe baseline and IL10^{-}INFγ $\uparrow$ (Day 48) models.

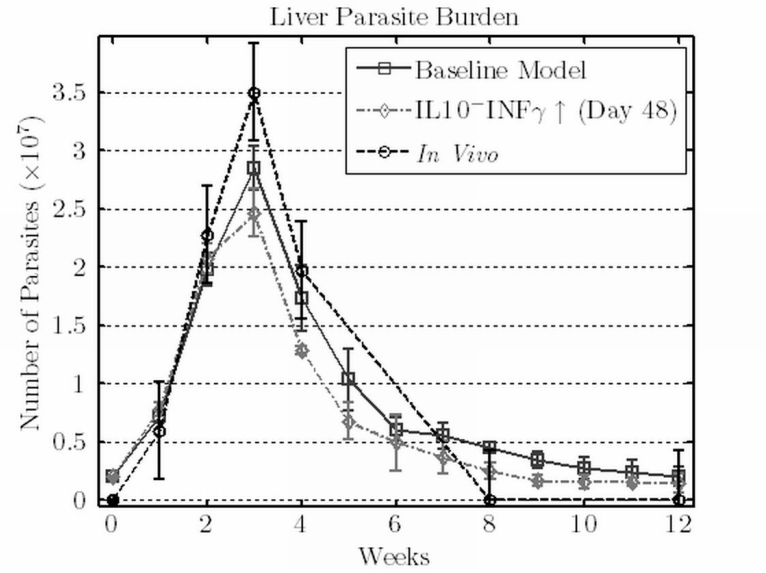

Figure 8.38: Parasite Burden. *In silico* data describe baseline and IL10^{-}INFγ $\uparrow$ (Day 48) models. *In vivo* data were taken from Murray et al. 2006.

48 Days After Infection

Increasing INFγ concentration from hour 1160 to hour 1170 (Figure 8.37 indicates the effect on INFγ concentration), while blocking IL10, decreases the parasite burden and facilitates disease resolution (See Figure 8.38 for parasite burden and Section B.18 for additional data). Again, these experimental conditions seem to be overall quite effective.

8.5.4 Conclusions

From the above experiments stem the following key points:

- increasing INFγ negatively affect the parasite burden, with an effect dependent on the time of subministration. However, disease resolution is only limitedly affected.
- removing IL10 slightly reduce the parasite burden and facilitate disease resolution.

The above effects seem to be rather independent, and can be combined to obtain a lower parasite burden while facilitating disease resolution.

Our experiments indicate that increasing the quantity of INFγ during the later stages of infection, while blocking IL10, seems to be the most effective therapeutic option. However, given the systemic nature of visceral leishmaniasis, these therapeutic indications require additional analyzes to account for the effects on the spleen and bone marrow.

8.6 Concluding Remarks

The results presented in this chapter should not be considered *definitive*. They need to be verified by biological experiments. Moreover, these experiments will likely provide new data that will be used to design a better model.

Additionally, the understating of the *granuloma process* obtained by our model, can be used to build new models focusing on different aspects of granulomas. Probably, the more natural evolution of the model is the introduction of space (as discussed in Section 4.1.2).

Finally, the information on the roles of the cells, can be used to build a *distilled* model with only the essential cells. This new model will probably be unable to simulate realistically the biological process, but should be able to study the basic mechanisms behind granuloma formation and maintenance, and provide a better understanding of the *causes* that led the immune system to develop such an articulate immune response.

Chapter 9

Sensityivity Analysis of the Model

This chapter illustrates the results of sensitivity analysis (SA) on our model. Section 9.1 presents the reasons for our choice of partial rank correlated coefficients (PRCC), while Section 9.2 illustrates the results of PRCC on the parasite burden.

9.1 Why PRCC?

While many importance measure exist (see Section 4.3 and references within), the characteristics of the model to be analyzed provide important information to support the decision of the SA technique to be used.

A first characteristic to be considered is the number of parameters to be analyzed. Analyzing all the parameters allows a more extensive validation of the model, but requires a large number experiments. We decided to analyze all the parameters to evaluate possible hidden relations.

A second characteristic to be considered is the time required to perform a single simulation. Simulating 50 granulomas with Snoopy under normal conditions takes about one minute on the hardware we have been using. However, if the number of entities increase, the simulations take far more time (up to half an hour in our experiments). Moreover, since Snoopy does not allow the simulations to be scripted, human intervention was required to start the simulations and save the results. Therefore, only a limited number of experiments could be performed.

Finally, the nonlinearity and stochasticity of the model was taken into account.

The chosen importance measure was PRCC. PRCC allows the analysis of large number of parameters with relatively small number of experiments, and deals pretty well with nonlinearities. Moreover, Marino et al. 2008 reports that using averages of experimental results, instead of experimental results

directly, allows PRCC to produce good results even for stochastic models.

To analyzed the 57 parameters of our model, we used the average of 3 experiments performed on 400 parameter sets (leading to 1200 simulations). 50 granulomas were simulated for each experiment. Since the number of parasites is the most influential output value, SA was performed on that.

9.2 Parameter Sets

SA was under baseline model experimental conditions. To allow only for a limited deviation from the studied behavior, most parameters were varied from 50% to 150% of the value presented in Section 6.3. Tables 9.1 to 9.6 describe the ranges of variation for the parameters. Additionally, a dummy parameter that has no effect on the outcome of the model, was introduced varying from 1 to 10.

The PRCC of the dummy parameter is an indication of the stochastic effects. Only parameters with a PRCC significantly larger than the PRCC of the dummy parameters should be considered as influential. The parameter sets were generated using Latin Hypercube sampling with equally spaced intervals for each parameter, and are not listed.

Parameter name	min	max
CytDiff	0.1250	0.3750
CellDiff	0.025	0.075
IL2Effectiveness	0.05	0.15
IL4Effectiveness	0.5	1.5
IL10Effectiveness	0.5	1.5
IL12Effectiveness	0.5	1.5
INFgEffectiveness	0.5	1.5

Table 9.1: Range of variation for environment-related parameters

Parameter name	min	max
LDKill	0.000005	0.000015
LDRep	0.0045	0.0135
LDDA	0.025	0.075

Table 9.2: Range of variation for Leishmania-related parameters

9.3 PRCC of Parasite Burden

This section describes the results of PRCC for the parameters of the model. Only the parameters with p-values less than 0.01 for at least 10 consecutive hours are presented.

Parameter name	min	max
CytAct	0.0024	0.0073
MKill	0.0125	0.0375
MacArr	0.2	0.6
MacCyt	1	3
MHCILife	1	6
MHCIILife	20	200
CD1dLife	5	40
MacActivationDecay	0.0005	0.0015
MHCIProd	0.0185	0.0555
MHCIIProd	0.0075	0.0225
CD1dProd	0.0120	0.0360
MonoLeave	0.025	0.075
KCIncomeRate	0.00005	0.00015
ActivationFight	0.01	0.03
KCCC	75	125

Table 9.3: Range of variation for phagocytes-related parameters

Parameter name	min	max
NKTDA	0.025	0.075
NKTArr	0.15	0.45
NKTCD1dAct	0.0650	0.1950
NKTDeact	0.15	0.45
NKTLife	300	500
NKTIL4Prod	0.01	0.03
NKTINFgProd	1	3
NKTChem	0.005	0.015

Table 9.4: Range of variation for NKT cells-related parameters

Parameter name	min	max
NKMacAct	0.001	0.003
NKDeact	0.05	0.15
NKArr	0.04	0.12
NKLife	300	500
NKEvol	250	750
IL12NKAct	0.00025	0.00075
IL12NKDeac	0.05	0.15
NKCytProd	1	3

Table 9.5: Range of variation for NK cells-related parameters

Parameter name	min	max
Th1IL10Diff	0.0001	0.0004
TCellDiff	0.002	0.006
TRep	0.002	0.006
SpleenTCellArr	0.025	0.075
LiverTCellArr	0.025	0.075
TCellAct	0.0034	0.0104
TDeact	0.15	0.45
TChem	0.005	0.015
ToZeroProd	0.0005	0.0015
FromZeroProd	0.0005	0.0015
Th1Evol	60	180
TCellKeepProd	0.02	0.06
TCellCytProd	1	3
TimeTStart	70	120
TimeTStop	100	150
Th1IL10RepMod	0	1

Table 9.6: Range of variation for T cells-related parameters

Since the parasite burden affects either directly or indirectly all the entities of the model, using this value to calculate the PRCC should provide a good indication of the importance of the parameters analyzed. Both the PRCC and p-values were calculated with MATALB adapting the functions described by Marino et al. 2008.

9.3.1 Environment

The diffusion of cytokines is a very important parameter for the parasite burden (see Figure 9.1). The PRCC of CytDiff is much larger than the PRCC of the dummy parameter, indicating the strong influence of this parameter on the number of parasites. Moreover, the p-values, lower than 0.01 for most of the simulation, indicate the validity of the result. Increasing the diffusion of cytokines leads to a smaller amount of INFγ, and thus to a limited activation of Kupffer Cells, which results in a large parasite burden. This is clearly captured by the large positive PRCC values. The early negative values are not statistically significant, and are likely due to the small amount of cytokines in the early stages of granuloma formation.

The diffusion of cells appears to be less important than the diffusion of cytokines for the parasite burden (see Figure 9.2). The PRCC of CellDiff is significantly larger than the PRCC of the dummy parameter for most of the simulation, indicating that the result is not due to stochastic effects. The oscillations in the early stages are a consequence of the stochasticity of the model, as confirmed by the comparison with the value of the PRCC of the

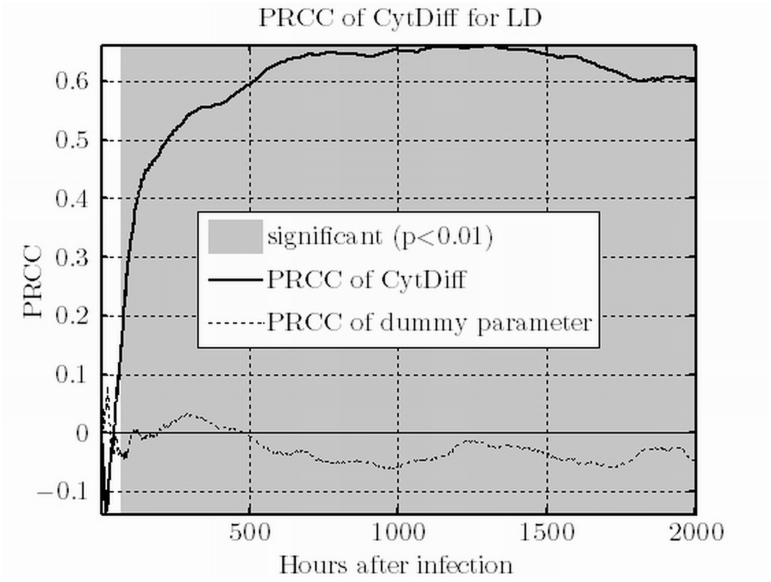

Figure 9.1: PRCC of CytDiff and dummy parameter.

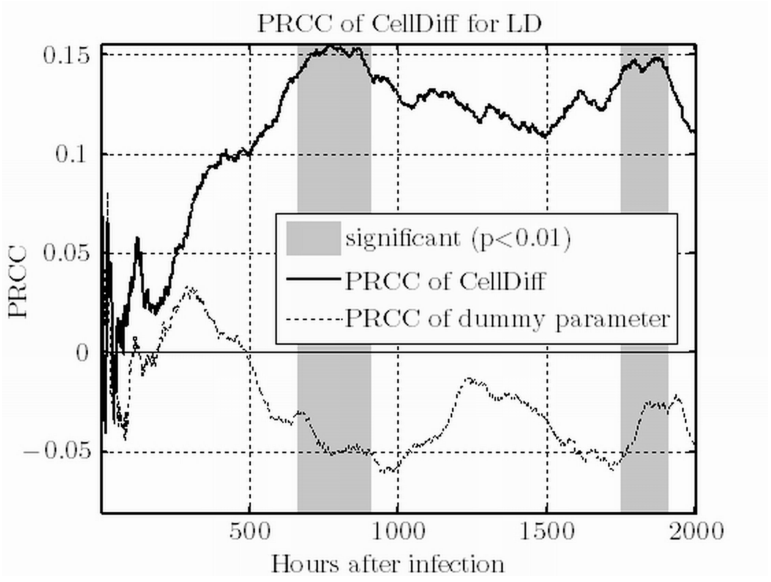

Figure 9.2: PRCC of CellDiff and dummy parameter.

dummy parameter.

Increasing the diffusion, thus diminishing the number of cells, increases the parasite burden, as the inflammatory response is weaker. The statistically significant zones appear to be less clear. The first zone (between 500 and 100 hours) is probably explained by the fact that, as the parasite burden decreases, the number of peptides displayed by Kupffer cells decreases. This results in a lower probability of activation of the cells, and thus to a higher parasite burden. The second zone (after 1500 hours), is probably due to the lower number of leukocytes and parasites in the later stage of infection, leading again to a lower probability of activation. The reproduction of cells due to the cytokines in the environment probably explains the large non-significant zone between the two significant zones.

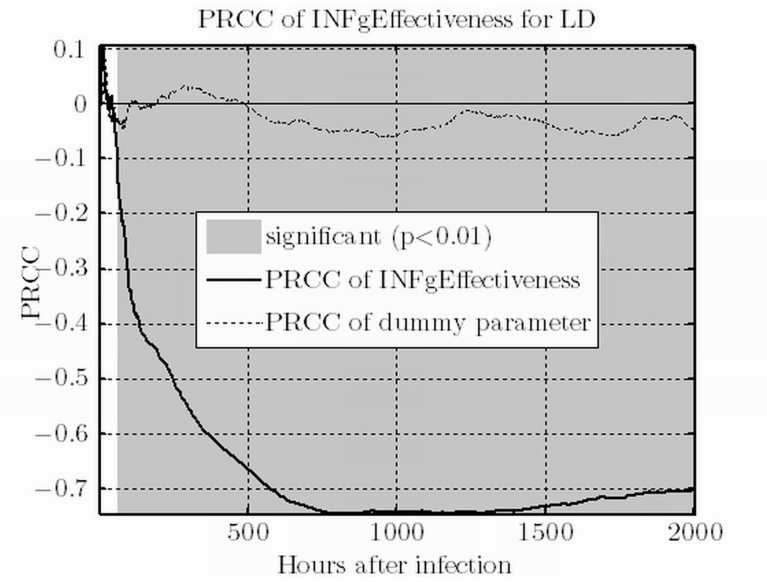

Figure 9.3: PRCC of INFgEffectiveness and dummy parameter.

The effectiveness of INFγ is very important for the parasite burden (see Figure 9.3). The PRCC of INFgEffectiveness is much larger than the PRCC of the dummy parameter, and the parameter is statistically significant for most of the simulation. These results clearly indicate the strong influence of this parameter on the number of parasites. As expected from the inflammatory role of INFγ, increasing INFgEffectiveness results in a diminished number of parasites. The early positive values are not statistically significant, and are due to the stochasticity of the model, as confirmed by the comparison with the values of the PRCC of the dummy parameter.

Note that the role INFγ results to be mainly inflammatory, even in a model with an INFγ-induced production of IL10 by T_H1 cells.

The effectiveness of IL10 clearly affects the parasite burden during the

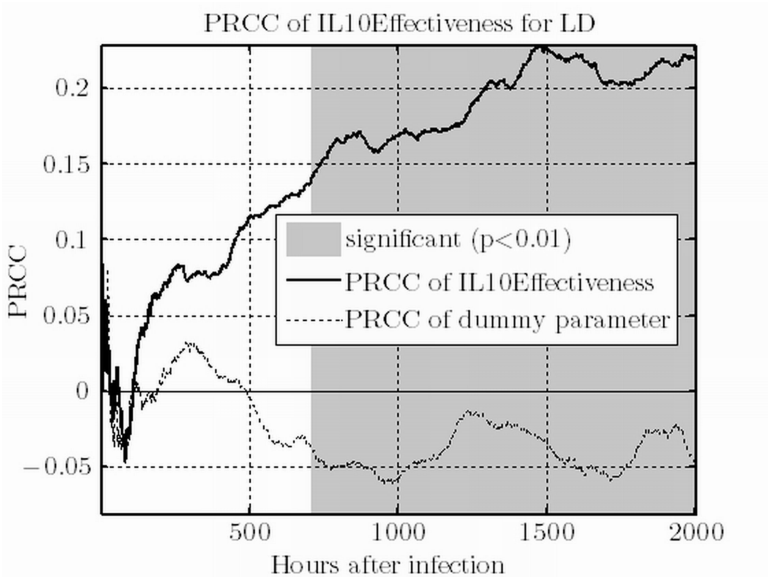

Figure 9.4: PRCC of IL10EFFECTIVENESS and dummy parameter.

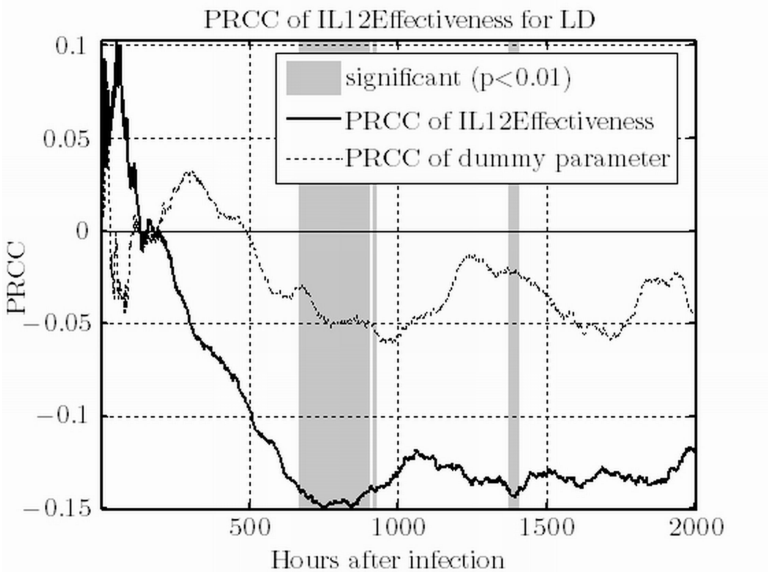

Figure 9.5: PRCC of IL12EFFECTIVENESS and dummy parameter.

later stages of infection (see Figure 9.4). The PRCC of IL10EFFECTIVENESS is significantly larger than the PRCC of the dummy parameter, and the p-values are lower than 0.01 about 600 hours after infection. These results clearly indicate the strong influence of this parameter on the number of parasites. As expected from the anti-inflammatory role of IL10, increasing IL10EFFECTIVENESS results in an increased number of parasites. The statistical non-significant role of the parameter in the initial stages of infection is a consequence of the limited number of IL10-producing cells at the beginning of the disease.

The effectiveness of IL12 has a limited effect on the parasite burden. While the PRCC of IL12EFFECTIVENESS appears to be larger than the PRCC of the dummy parameter, the parameter is statistically significant only around the peak of the infection. The effectiveness of IL12 influences both the activation of NK cells and the cytokine production of some T_H1 cells. The negative value of the PRCC confirms its inflammatory role.

9.3.2 *Leishmania Donovani*

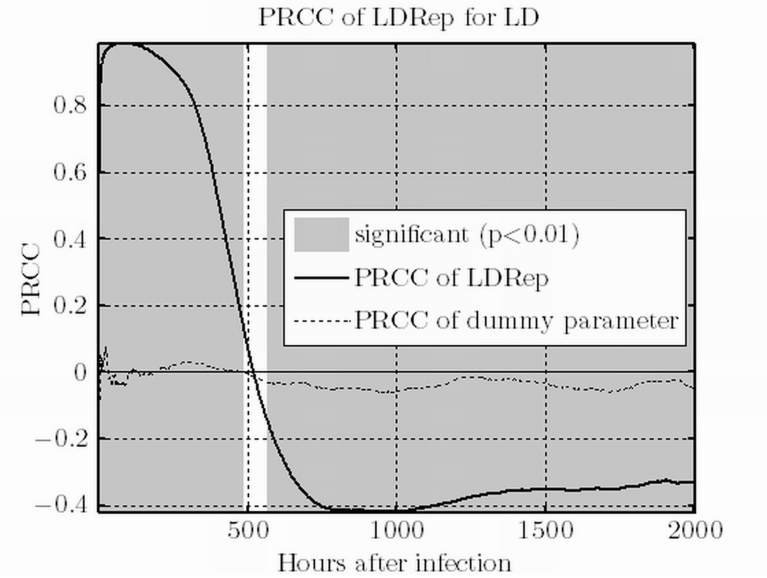

Figure 9.6: PRCC of LDREP and dummy parameter.

The reproduction rate of the parasite is a very important parameter for the parasite burden (see Figure 9.6). The PRCC of LDREP is much larger than the PRCC of the dummy parameter, and the p-values are lower than 0.01 for most of the simulation, thus indicating the strong influence of this parameter on the number of parasites.

Interestingly, the role of LDREP appears to be double. Up to about hour 500, and therefore before the parasite burden reached a maximum,

an increased reproduction rate leads to a larger parasite burden. However, subsequently, a higher reproduction rate leads to a lower parasite burden. This apparently strange result, is a consequence of the stronger immune response triggered by a slightly higher parasite burden, and is partly due to the limited variation of the parameter.

9.3.3 Macrophages

The arrival rate of Kupffer cells has a limited effect on the parasite burden (see Figure 9.7). Specifically, MacArr appears to be statistically significant only in the early stages of the disease, since it affects only the initial size of the granuloma, and thus the killing ability of the granuloma, which increases with the number of Kupffer cells. The p-values higher than 0.01 and the values of PRCC comparable with the values of PRCC of the dummy parameter indicates the negligible effect of his parameter on the parasite number during the later stages of infection.

The killing ability of macrophages clearly affects the parasite burden in the first 500 hours after infection (see Figure 9.8). However, the p-values higher than 0.01 and the PRCC value comparable with those of the dummy parameter, suggest a negligible role of MKill after hour 500. A possible explanation of this quite unexpected result is the role of the level of classical activation, which controls the killing ability of Kupffer cells to a larger extent.

The sensitivity of phagocytes to cytokine-induced (de)activation is a very important parameter for the parasite burden (see Figure 9.9). Besides a small zone at the beginning of the disease, the PRCC of CytAct is much larger than the PRCC of the dummy parameter, indicating the strong influence of this parameter on the number of parasites. Moreover, the p-values, lower than 0.01 for most of the simulation, indicate the validity of the result. As expected from the high INFγ concentration with respect of IL10, increasing the sensitivity of phagocytes to cytokines leads to a larger classical activation, and thus to a lower parasite burden.

The speed of reciprocal down-regulation by (de)activations of phagocytes seems to be important only in the later stage of the disease (see Figure 9.10). The PRCC of ActivationFight is significantly different from the PRCC of the dummy parameter only 600 hours after infection, and this result is supported by the by p-values, which are less than 0.01 in the same zone. The decrease in the parasite burden is due to the increased deactivation of phagocytes in the later stage of the disease. A larger ActivationFight indicates that the deactivation takes more time to down-regulate the classical activation, and thus that the killing activity of the Kupffer cells is increased.

The productions of MHC class I and II peptides by phagocytes is quite important for the parasite burdens (see Figures 9.11 and 9.12). MHCIProd and MHCIIProd, have qualitatively similar PRCC and p-values. In both cases, besides an initial zone, the p-values of the parameter is less the 0.01

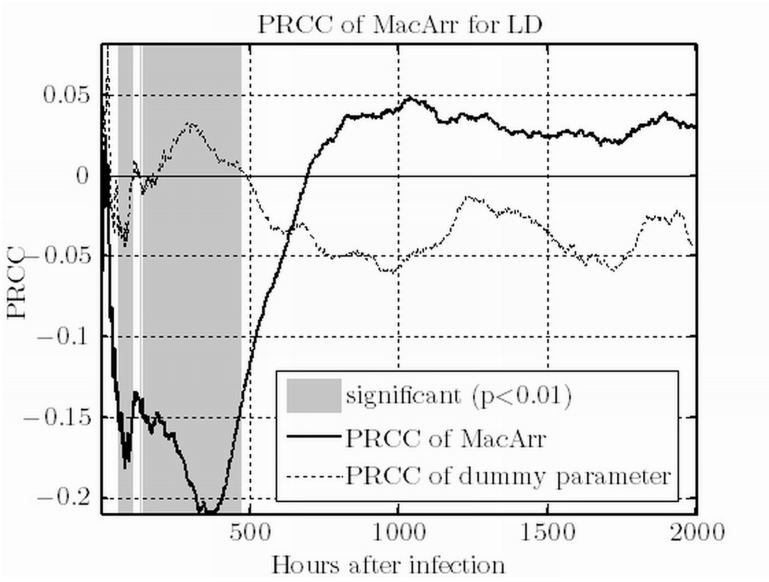

Figure 9.7: PRCC of MacArr and dummy parameter.

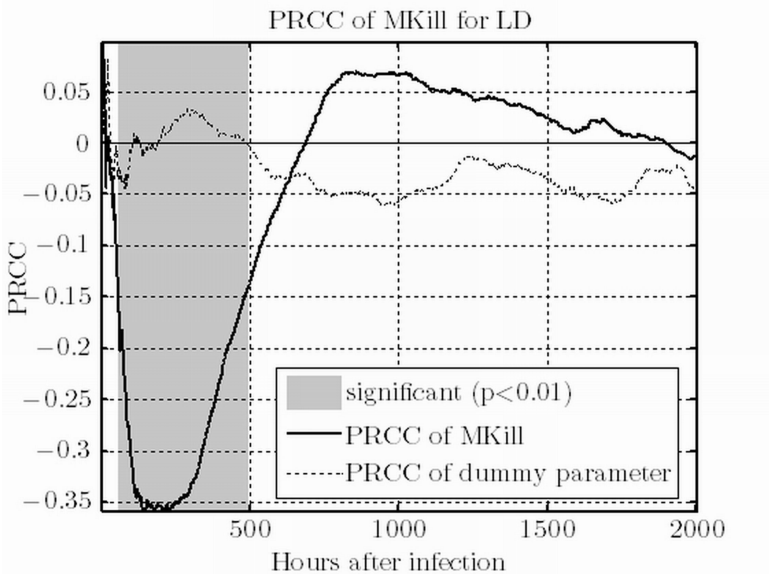

Figure 9.8: PRCC of MKill and dummy parameter.

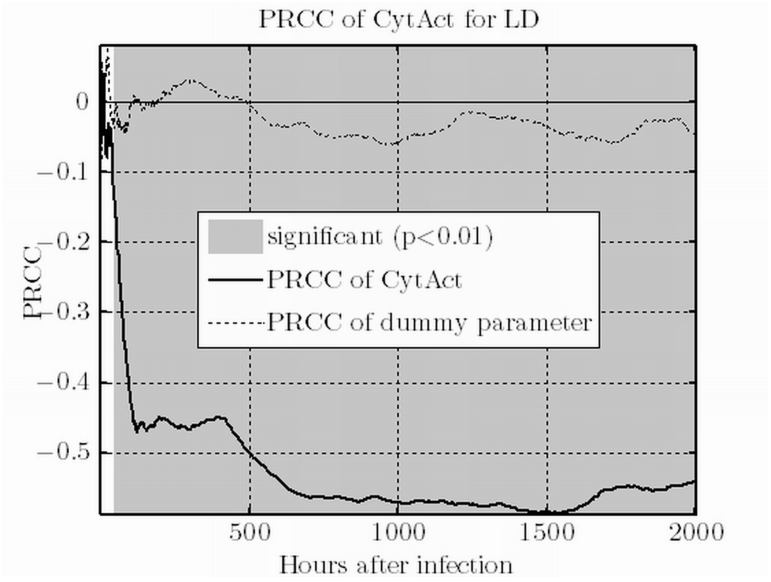

Figure 9.9: PRCC of CytAct and dummy parameter.

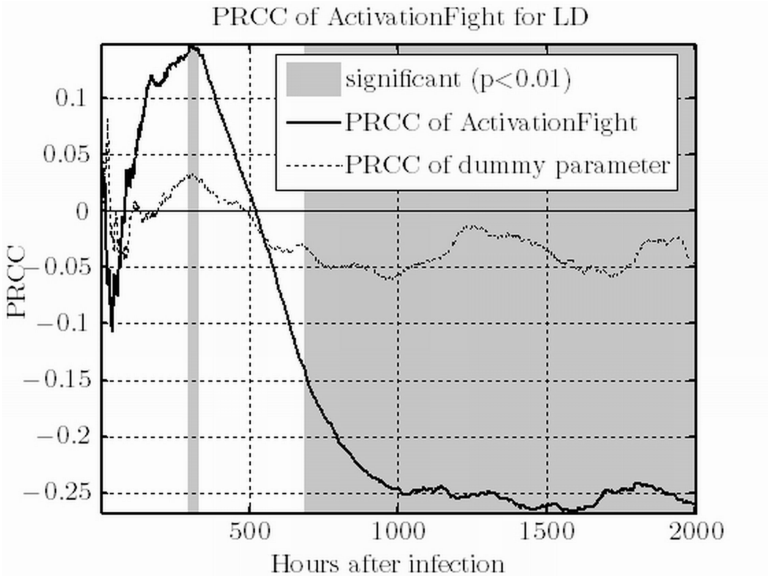

Figure 9.10: PRCC of ActivationFight and dummy parameter.

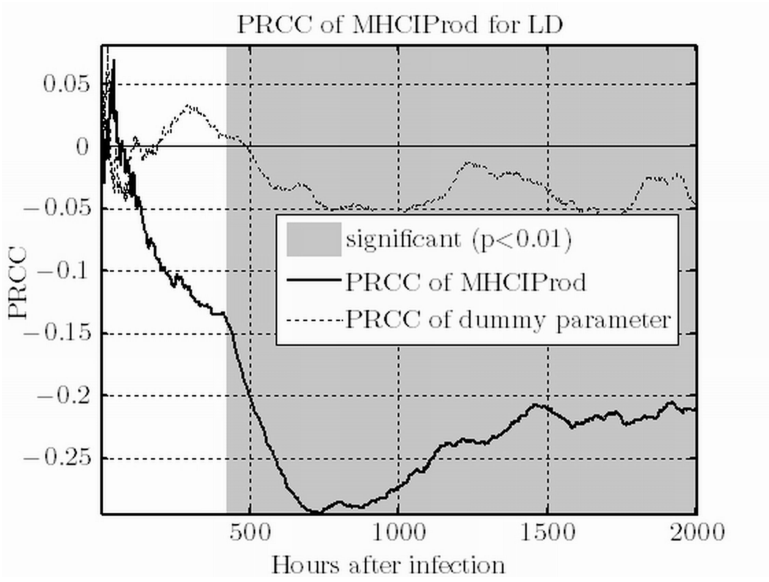

Figure 9.11: PRCC of MHCIPROD and dummy parameter.

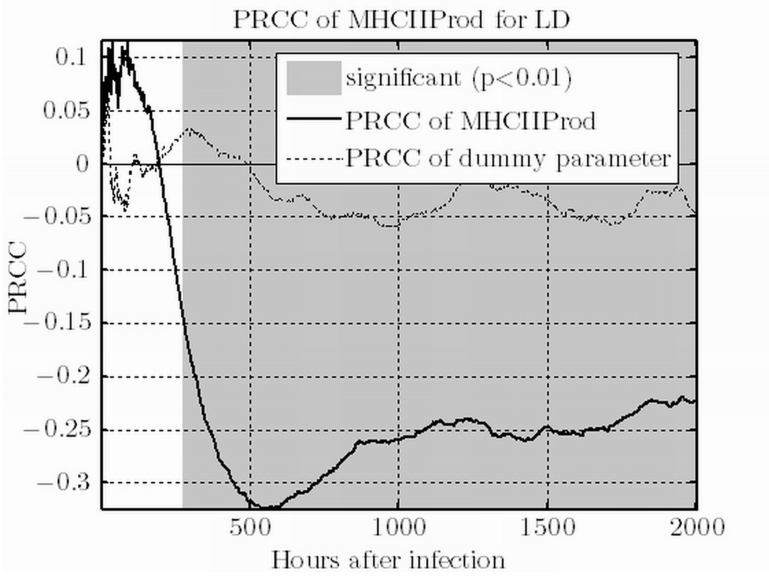

Figure 9.12: PRCC of MHCIIPROD and dummy parameter.

for the whole disease. The initial statistical non-significant zone is connected with the number of peptides produced by the Kupffer cells before the adaptive immune response. The PRCC confirms that a larger peptide production leads to a lower parasite burden. Moreover, the PRCC indicates that the importance of MHC class I and II peptides, and thus the role of $CD4^+$ and $CD8^+$ T cells are comparable.

The effect of MHCILife is connected with MHCIProd, and the results are similar (see Figures 9.13). Note that both MHCIILife and CD1dLife do not appear to be statistically significant, suggesting that the actual half-life of a MHC - peptide complex is not very relevant if it is long enough.

The production of CD1d peptides by phagocytes is again quite important for the parasite burden (see Figure 9.14). However, CD1dProd has a distinctly different behavior with respect to MHCIProd and MHCIIProd. In the first statistically significant zone, the negative PRCC — significantly smaller than the PRCC of the dummy parameter — is an indication of the infection control activity of NKT cells in the early stages of infection. In the second statistically significant zone, the positive PRCC — larger than the PRCC of the dummy parameter — is an indication of the anti-inflammatory activity of NKT cells in the later stages of infections (see also Section 8.3.3).

9.3.4 Natural Killer T Cells

The production of INFγ by NKT cells is very important for the parasite burden (see Figure 9.15). The PRCC and p-values of iNKTINFgProd are strongly connected with those of INFgEffectiveness (see Figure 9.3), and will not be further commented.

The deactivation activity of NKT cells is very important for the parasite burden (see Figure 9.16). iNKTDA is statistically significant for most of the disease and the large PRCC clearly indicates how increasing the NKT cells-induced deactivation of Kupffer cells leads to a larger parasite burden.

The time between the activation and the deactivation of NKT cells is rather important for the parasite burden (see Figure 9.17). The role of iNKTDeact is inverse with respect to CD1dProd: a large iNKTDeact indicates a fast deactivation, and thus less NKT cells. The PRCC and p-values of iNKTDeact clearly indicate the aforementioned connection with CD1dProd (see Figure 9.17), and are indications of the correct behavior of the model.

9.3.5 T Cells

The cytokine production of T cells is very important for the parasite burden (see Figure 9.18). Since the T cells response is biased towards a type I immune response, the PRCC and p-values of TCellCytProd are strongly

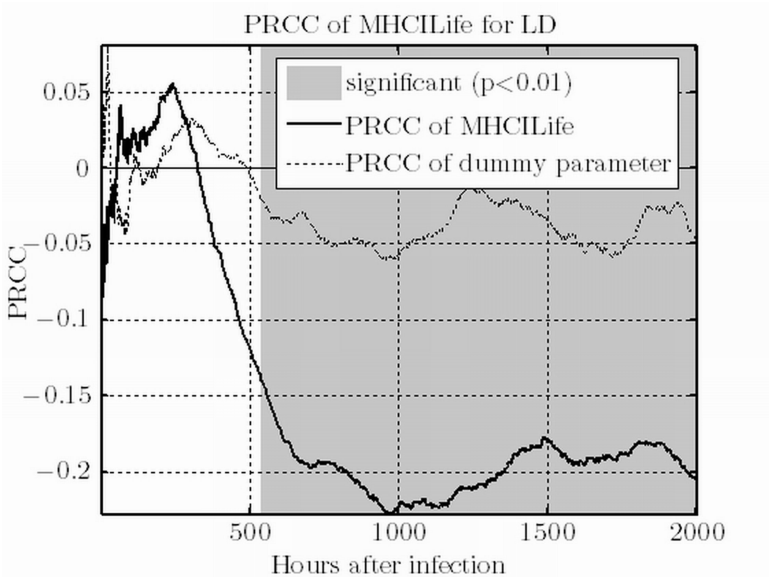

Figure 9.13: PRCC of MHCILife and dummy parameter.

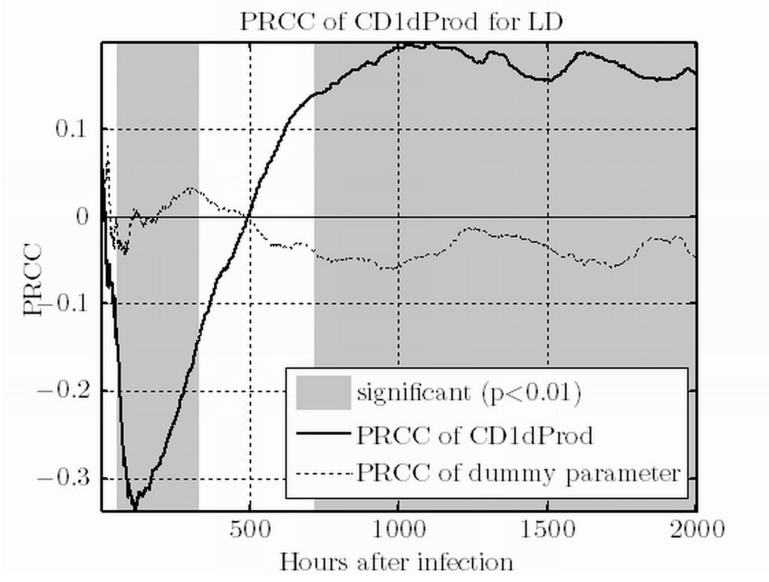

Figure 9.14: PRCC of CD1dProd and dummy parameter.

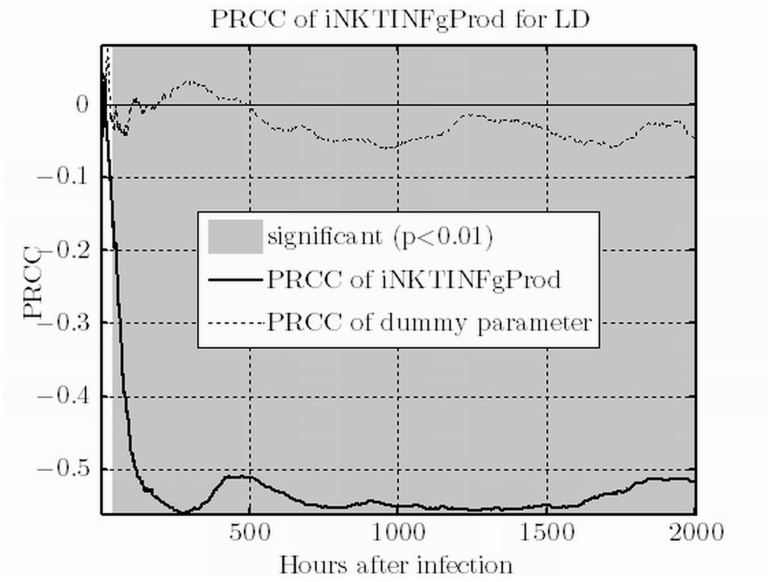

Figure 9.15: PRCC of iNKTINFgProd and dummy parameter.

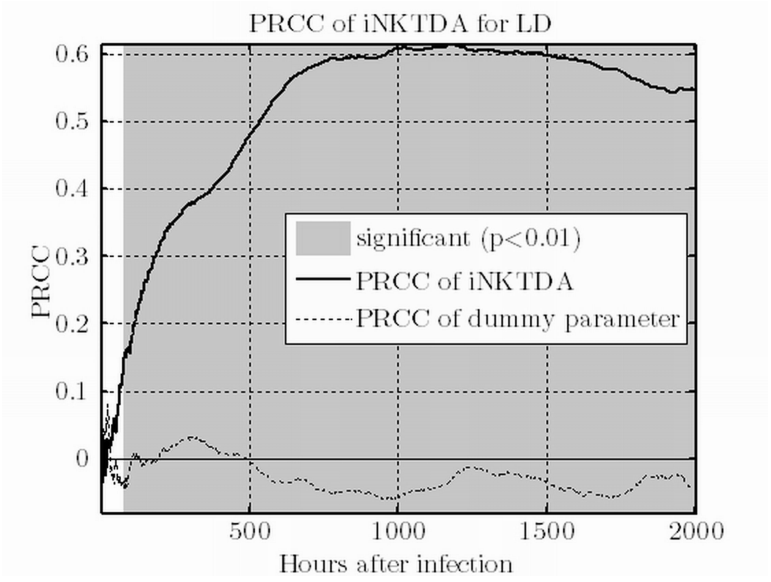

Figure 9.16: PRCC of iNKTDA and dummy parameter.

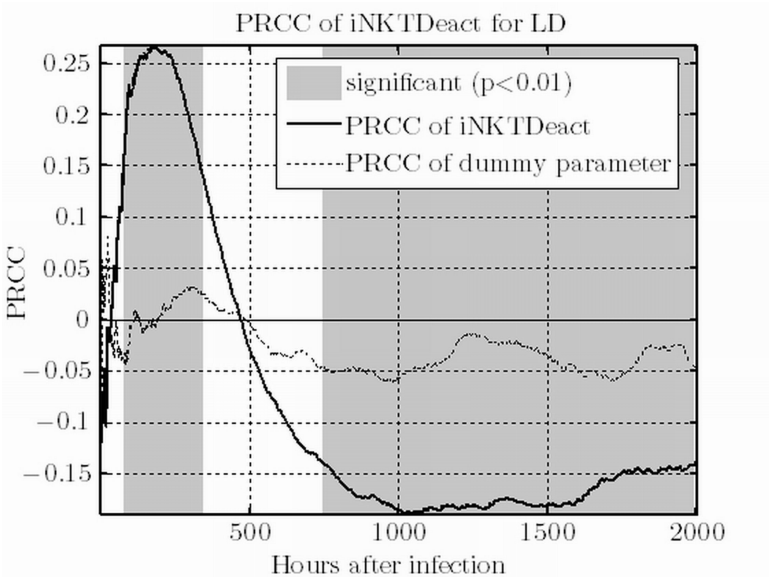

Figure 9.17: PRCC of iNKTDeact and dummy parameter.

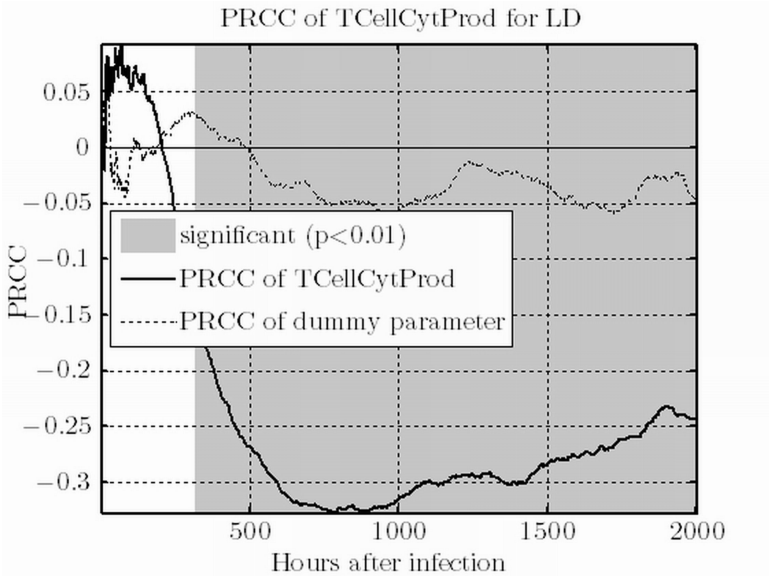

Figure 9.18: PRCC of TCellCytProd and dummy parameter.

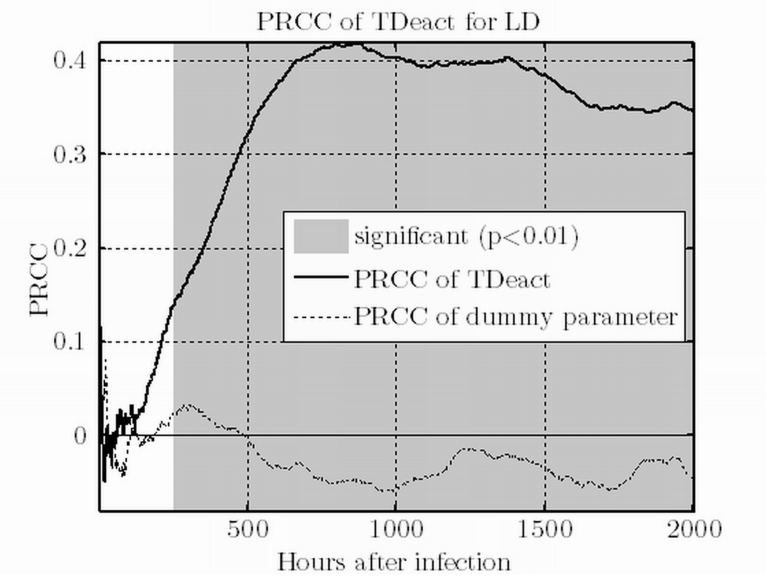

Figure 9.19: PRCC of TDeact and dummy parameter.

connected with those of INFgEffectiveness (see Figure 9.3). The initial statistically non-significant zone is due to the delayed T cells response.

The deactivation of T cells is very important for the parasite burden (see Figure 9.18). Similarly to iNKTDeact (see Section 9.3.4), a large TDeact indicates a fast deactivation. As indicated by the large positive PRCC, a faster deactivation leads to an increased parasite burden, and the p-values less than 0.01 for most of the model, indicate the validity of this result. It is worth noticing that, contrary to iNKTDeact, the effect of TDeact is more uniform. This result indicates that the effect of T cells is mainly pro-inflammatory (as expected given the high percentage of INFγ^+ T cells).

The activation rate of T cells is not so important for the parasite burden (see Figure 9.20). The PRCC of TCellAct is not significantly larger than the PRCC of the dummy parameters and the statistically significant zones are rather small. This result indicates that, in our model, the production of MHC peptides is more important than the probability of interacting with those peptides.

9.3.6 Number of Significant Parameters

Figure 9.21 indicates the number of statistically significant parameters over time. While the rapid increase around hour 100 is clearly due to the arrival of T cells, the subsequent increases result from the structure of the model and the interactions of the entities modeled. Additionally, the stabilization of the number of statistically significant parameters 1000 hours after infection,

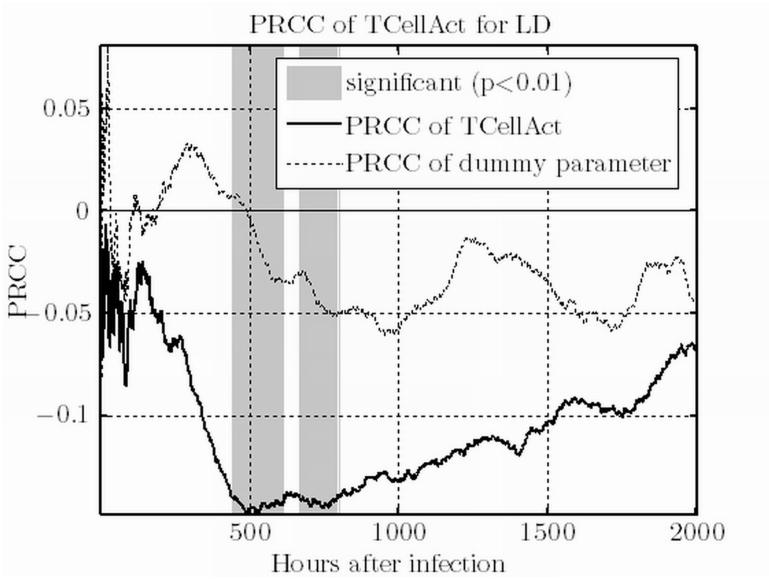

Figure 9.20: PRCC of TCellAct and dummy parameter.

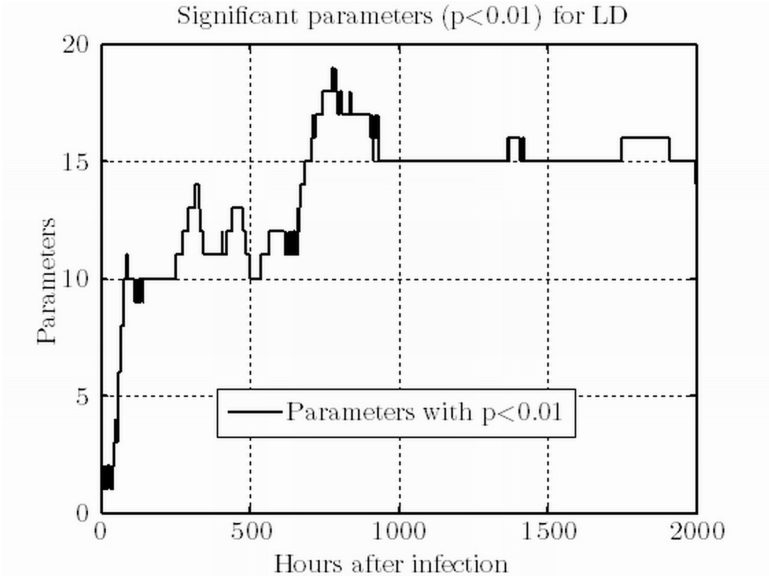

Figure 9.21: Number of statistically significant parameters

indicates that after a while all the interactions have come (and stay) into play.

While Figure 9.21 hardly measures of the complexity of the model, it is an indication of its complex nature.

Chapter 10

Summary and Conclusions

As described in the Introduction, this thesis had a number of goals. The aim of this chapter is to discuss to which extent these goals were met, and to point out the implications or our results for immunology and immunological modeling.

10.1 Insight Into Granuloma Formation

A better understanding of the dynamics of granulomas was the primary goal of this thesis. As discussed in Section 8.1, our model allowed a characterization of the different aspects of granulomas that would have been impossible *in vivo*. This characterization allowed us to understand how the course of leishmaniasis emerges from a rather heterogeneous population of granulomas, and allowed us to draw important conclusions on the granuloma as an *immunological process*.

The results presented in Section 8.1 imply that the immune system is able to deal with leishmaniasis quite efficiently in most of the cases. Therefore, if we wish to improve the immune response, we need to develop therapies that focus on a smaller collection of granulomas rather than on the whole population. Additionally, we can think of designing biological experiments that will try to force the immune system into developing a less heterogeneous population of granulomas, to better study the effect of specific populations of granulomas.

Moreover, the above results indicate the importance of stochasticity for the evolution of visceral leishmaniasis, suggesting that other granulomatous infections may have a similar heterogeneity and discouraging the use of deterministic population dynamics models to represent these diseases.

Section 8.3 provided us with important insight on the double-edged nature of NKT cells and on their activation mechanisms. While the results on the activation of NKT cells are probably quite specific, the results on their behavior are likely to be more general.

This remarkable *self-control* of NKT cells is quite interesting, as it is obtained by a homogeneous population, and indicates how NKT cells may acquire an immunoregulatory function over time. This result suggests that the immune response in the liver may be improved by preventing the activation of NKT cells at the later stages of an infection, and therefore indicates possible future lines of research.

Moreover, the fact that both NKT and T cells seem to display both inflammatory and immunoregulatory functions over time, may suggest phylogenetic connections between the two populations.

From a modeling point of view, the importance of the double-edged nature of NKT in leishmaniasis suggests that immunological modelers should deal very carefully with these cells, taking into account the appropriate functions.

Section 8.4 provided us with interesting information on the supporting role of NK cells. Quite interestingly, these cells seem to possess a mainly inflammatory role and our results suggest the boosting of NK cells immune response as a possible therapeutic option for certain diseases. However, these considerations heavily depend on our model of NK cells evolution, and additional modeling efforts are needed to account for other possibilities such as the existence of different populations of NK cells (e.g., an INFγ^+IL10$^-$ population and an INFγ^+IL10$^+$ population).

10.2 Therapeutic Options

The comparison of different therapeutic options for leishmaniasis was a second goal of this thesis. As discussed in Section 8.5 none of the tested simple therapeutic options seem to be very effective by itself. However, the efficacy of the combined effect of just two of them suggested interesting possibilities to improve the immune response. The implication for immunological research are obvious, but the systemic nature of visceral leishmaniasis, call for a careful validation of our conclusions.

These results also indicate that some diseases may be better dealt with by using a sequence of drugs, and suggest that computational immunological models should be built to account for experiments with multiple drugs. Note that these results clearly point out the importance of *in silico* experiments, as the design and realization of these experiments *in vivo* would have been quite expensive and time-consuming.

10.3 Testing of Biological Hypotheses

The comparison of the different biological hypotheses was the third goal of this thesis. Section 8.2 compared different mechanism of phenotypic changes in T_H1 cells, and therefore different biological hypotheses. Albeit not very

strong, our results clearly indicate possible directions for biological research that should clarify the possible role of INFγ and IL12 in the production of IL10 by T_H1. Since many other possibilities exist, additional research efforts are needed to study the phenomenon, ideally in a more controlled environment (for example *in vitro*). However, the rather marginal role that INFγ^+IL10$^+$ T_H1 cells seem to play suggests that it may not be worth an extensive study in the context of visceral leishmaniasis.

Section 8.3.1 indicated that a simple stress-mediated activation is insufficient to model the response of NKT cells. Besides confirming the importance of CD1d-mediated activation, this result suggests that immunological modelers should avoid a simple stress-mediated activation mechanism for NKT cells. Additional research efforts are needed to evaluate if a *delayed* stress-mediated activation may provide a good alternative.

The above results indicate that using a complex model is an effective way of comparing contrasting hypotheses. Even if the results may not be too *sharp*, they clearly indicate possible research lines to restrict the number of plausible hypotheses.

10.4 Modeling Process

Chapter 5 was devoted to achieve our fourth goal: a clear description of the modeling steps. While listing the assumptions and simplifications used may seem a very simple way of dealing with this goal, it allowed us to describe how we moved from the biological process to the numerical model, while keeping track of the information used (and not used).

Note that, a more *structured* representation (perhaps by the use of ontologies) would have better indicated the connection between the assumptions, but would have introduced a somewhat subjective classification.

We believe that a more consistent use of a precise description of assumptions could be very useful in understanding the results of numerical models. The assumptions and simplifications characterize the experimental setup of a numerical model, and similarly to the "Materials and Methods" section of biological articles, allow for the reproducibility of the results. While it is well-possible that more efficient way of presenting the assumptions and simplifications used exist, Chapter 5 can be easily checked by biological experts and permit fast communications.

A methodology to build complex *assumptions trees* is certainly an interesting future research line and automatic code generation from UML diagrams provides a somewhat similar concept. An even more ambitious goals would be the building of an *hypothesis repository*, that would allow modelers (and to a lesser extent biologists) to better comprehend the consequences of *in silico* (and *in vitro*) experiments.

Additional indications of the modeling steps have been presented in

Chapters 7 and 9. The comparison to *in vivo* data presented in Chapter 7 is essential, since it allows to assess the *extrinsic* validity of the model. However, the sensitivity analysis presented in Chapter 9 is a great added value, as it allows to assess the *intrinsic* validity of the model.

It should be noted that sensitivity analysis was not used only as a *final verification*, but as a tools to gain important insights during the whole development of the model. These insights allowed us to improve the model and to better represent the biological reality.

We believe that the above considerations in conjunction with the discussion presented in Section 4.1, provide a good indication of our *modeling process*.

10.5 Conclusions

Sections 10.1 to 10.4 indicate how, albeit to different extents, all the goals set in the Introduction, were achieved. The relevance of our model, and results, to immunology and immunological modeling were clearly discussed and many possible research lines are indicated. While the complexity of the model did not allow us to present an extensive description of its building and results, we believe that the key points were clearly indicated.

Part III

Bibliography and Index

Bibliography

Afrin, F., Rajesh, R., Anam, K., Gopinath, M., Pal, S. & Ali, N. (2002), 'Characterization of Leishmania donovani Antigens Encapsulated in Liposomes That Induce Protective Immunity in BALB/c Mice', *Infect. Immun.* **70**(12), 6697–6706.

Akopyants, N. S., Kimblin, N., Secundino, N., Patrick, R., Peters, N., Lawyer, P., Dobson, D. E., Beverley, S. M. & Sacks, D. L. (2009), 'Demonstration of Genetic Exchange During Cyclical Development of Leishmania in the Sand Fly Vector', *Science* **324**(5924), 265–268.

Albergante, L., Timmis, J., Andrews, P. S., Beattie, L. & Kaye, P. M. (2010), A Petri Net Model of Granulomatous Inflammation, *in* E. Hart, C. McEwan, J. Timmis & A. Hone, eds, 'ICARIS', Vol. 6209 of *Lecture Notes in Computer Science*, Springer, pp. 1–3.

Alberts, B., Johnson, A., Lewis, J., Raff, M., Roberts, K. & Walter, P. (2008), *Molecular Biology of the Cell, Fifth Edition*, Garland.

Amprey, J. L., Im, J. S., Turco, S. J., Murray, H. W., Illarionov, P. A., Besra, G. S., Porcelli, S. A. & Späth, G. F. (2004), 'A Subset of Liver NK T Cells Is Activated during Leishmania donovani Infection by CD1d-bound Lipophosphoglycan', *The Journal of Experimental Medicine* **200**(7), 895–904.

Ananko, E., Podkolodny, N., Stepanenko, I., Ignatieva, E., Podkolodnaya, O. & Kolchanov, N. (2002), 'GeneNet: a database on structure and functional organisation of gene networks', *Nucleid Acids Research* **30**(1), 398–401.

Beattie, L. (2010), Private communication.

Beattie, L., Peltan, A., Maroof, A., Kirby, A., Brown, N., Coles, M., Smith, D. F. & Kaye, P. M. (2010), 'Dynamic Imaging of Experimental *Leishmania donovani*-Induced Hepatic Granulomas Detects Kupffer Cell-Restricted Antigen Presentation to Antigen-Specific $CD8^+$ T Cells', *PLoS Pathog* **6**(3), e1000805.

Beattie, L., Svensson, M., Bune, A., Brown, N., Maroof, A., Zubairi, S., Smith, K. R. & Kaye, P. M. (2010), '*Leishmania donovani*-induced expression of signal regulatory protein alpha on Kupffer cells enhances hepatic invariant NKT-cell activation', *European Journal of Immunology* **40**(1), 117–123.

Bendelac, A., Savage, P. B. & Teyton, L. (2007), 'The biology of NKT cells', *Annual Review of Immunology* **25**, 297–336.

Benlagha, K., Weiss, A., Beavis, A., Teyton, L. & Bendelac, A. (2000), 'In Vivo Identification of Glycolipid AntigenŰSpecific T Cells Using Fluorescent Cd1d Tetramers', *The Journal of Experimental Medicine* **191**(11), 1895–1904.

Bhattacharyya, S., Ghosh, S., Jhonson, P. L., Bhattacharya, S. K. & Majumdar, S. (2001), 'Immunomodulatory Role of Interleukin-10 in Visceral Leishmaniasis: Defective Activation of Protein Kinase C-Mediated Signal Transduction Events', *Infection and Immunity* **69**(3), 1499–1507.

Biron, C., Nguyen, K., Pien, G., Cousens, L. & Salazar-Mather, T. (1999), 'Natural killer cells in antiviral defense: Function and regulation by innate cytokines', *Annual Review of Immunology* **17**, 189–220.

Bluestone, J. A., Mackay, C. R., O'Shea, J. J. & Stockinger, B. (2009), 'The functional plasticity of T cell subsets', *Nature Review Immunology* **9**(6), 811–816.

Boehm, T. (2009), 'One problem, two solutions', *Nat Immunol* **10**(8), 811–813.

Bordon, Y. (2010), 'Innate immunity: An unexpected guest at the regulatory table', *Nat Rev Immunol* **10**(1), 9.

Bradley, D. J. & Kirkley, J. (1977), 'Regulation of Leishmania populations within the host. I. the variable course of Leishmania donovani infections in mice', *Clin. Exp. Immunol.* **30**, 119–129.

Carnaud, C., Lee, D., Donnars, O., Park, S.-H., Beavis, A., Koezuka, Y. & Bendelac, A. (1999), 'Cutting Edge: Cross-Talk Between Cells of the Innate Immune System: NKT Cells Rapidly Activate NK Cells', *J Immunol* **163**(9), 4647–4650.

Choi, B.-S. & Kropf, P. (2009), 'Evaluation of T cell responses in healing and nonhealing leishmaniasis reveals differences in T helper cell polarization ex vivo and in vitro', *Parasite Immunology* **31**(4), 199–209.

Coles, M. C. & Raulet, D. H. (2000), 'NK1.1$^+$ T Cells in the Liver Arise in the Thymus and Are Selected by Interactions with Class I Molecules on CD4$^+$CD8$^+$ Cells', *J Immunol* **164**(5), 2412–2418.

Cooper, A. M. (2009), 'Cell-Mediated Immune Responses in Tuberculosis', *Annual Review of Immunology* **27**, 393–422.

COPE: Horst Ibelgaufts' Cytokines & Cells Online Pathfinder Encyclopaedia (2010), `http://www.copewithcytokines.org`.

De Steenwinkel, J. E., De Knegt, G. J., Ten Kate, M. T., Van Belkum, A., Verbrugh, H. A., Hernandez-Pando, R., Van Soolingen, D. & Bakker-Woudenberg, I. A. (2009), 'Immunological parameters to define infection progression and therapy response in a well-defined tuberculosis model in mice', *Int J Immunopathol Pharmacol* **22**, 723–734.

Desjeux, P. (2004), 'Leishmaniasis: current situation and new perspectives', *Comparative Immunology, Microbiology and Infectious Diseases* **27**(5), 305–318. Advances on some vector-borne diseases.

Eberl, G. & MacDonald, H. R. (2000), 'Selective induction of NK cell proliferation and cytotoxicity by activated NKT cells', *European Journal of Immunology* **30**(4), 985–992.

Fallahi-Sichani, M., Schaller, M. A., Kirschner, D. E., Kunkel, S. L. & Linderman, J. J. (2010), 'Identification of key processes that control tumor necrosis factor availability in a tuberculosis granuloma', *PLoS computational biology* **6**(5).

Feuerer, M., Hill, J. A., Mathis, D. & Benoist, C. (2009), 'Foxp3$^+$ regulatory T cells: differentiation, specification, subphenotypes', *Nature Immunology* **10**(7), 689–695.

Flugge, A. J., Timmis, J., Andrews, P. S., Moore, J. & Kaye, P. M. (2009), Modelling and simulation of granuloma formation in visceral leishmaniasis, *in* 'IEEE Congress on Evolutionary Computation', IEEE, pp. 3052–3059.

Fujii, S.-i., Liu, K., Smith, C., Bonito, A. J. & Steinman, R. M. (2004), 'The Linkage of Innate to Adaptive Immunity via Maturing Dendritic Cells In Vivo Requires CD40 Ligation in Addition to Antigen Presentation and CD80/86 Costimulation', *J. Exp. Med.* **199**(12), 1607–1618.

Gammack, D., Doering, C. & Kirschner, D. (2004), 'Macrophage response to Mycobacterium tuberculosis infection', *Mathematical Biology* (48), 218–242.

Gammack, D., Segovia-Juarez, J. L., Ganguli, S., Marino, S. & Kirschner, D. (2005), 'Understanding the Immune Response in Tuberculosis Using Different Mathematical Models and Biological Scales', *SIAM Journal of Multiscale Modeling and Simulation* **3**(2), 312–345.

Ganguli, S., Gammack, D. & Kirschner, D. E. (2005), 'A Metapopulation Model of Granuloma Formation in the Lung During Infection with Mycobacterium Tuberculosis', *Mathematical Biosciences and Engineering* **2**(3), 535–560.

Gardner, M. (1970), 'The fantastic combinations of John Conway's new solitaire game "life"', *Scientific American* **223**, 120–123.

Ghosh, S., Bhattacharyya, S., Sirkar, M., Sa, G. S., Das, T., Majumdar, D., Roy, S. & Majumdar, S. (2002), 'Leishmania donovani Suppresses Activated Protein 1 and NF-κB Activation in Host Macrophages via Ceramide Generation: Involvement of Extracellular Signal-Regulated Kinase', *Clinical Immunology* **70**(12), 6828–6838.

Ghosh, S., Bhattacharyya, S., Sirkar, M., Sa, G. S., Das, T., Majumdar, D., Roy, S. & Majumdar, S. (2005), 'Leishmania lipophosphoglycan activates the transcription factor activating protein 1 in J774A.1 macrophages through the extracellular signal-related kinase (ERK) and p38 mitogen-activated protein kinase', *Molecular & Biochemical Parasitology* **139**(1), 117–127.

Gillespie, D. T. (1977), 'Exact stochastic simulation of coupled chemical reactions', *The Journal of Physical Chemistry* **81**(25), 2340–2361.

Godfrey, D. I., Stankovic, S. & Baxter, A. G. (2010), 'Raising the NKT cell family', *Nat Immunol* **11**(3), 197–206.

Gorak, P. M. A., Engwerda, C. R. & Kaye, P. M. (1998), 'Dendritic cells, but not macrophages, produce IL-12 immediately following Leishmania donovani infection', *European Journal of Immunology* **98**(2), 689–695.

Greter, M., Hofmann, J. & Becher, B. (2009), 'Neo-Lymphoid Aggregates in the Adult Liver Can Initiate Potent Cell-Mediated Immunity', *PLoS Biol* **7**(5), e1000109.

Gudmundsdottir, H., Wells, A. D. & Turka, L. A. (1999), 'Dynamics and Requirements of T Cell Clonal Expansion In Vivo at the Single-Cell Level: Effector Function Is Linked to Proliferative Capacity', *J Immunol* **162**(9), 5212–5223.

Gutierrez, Y., Maksem, J. A. & Reiner, N. E. (1984), 'Pathologic changes in murine leishmaniasis (Leishmania donovani) with special reference to the dynamics of granuloma formation in the liver', *Am. J. Pathol.* **114**, 222–230.

Havil, J. (2003), *Gamma : Exploring Euler's Constant*, Princeton University Press.

Heiner, M., Gilbert, D. & Donaldson, R. (2008*a*), Petri Nets for Systems and Synthetic Biology, pp. 215–264.

Heiner, M., Gilbert, D. & Donaldson, R. (2008*b*), Petri Nets for Systems and Synthetic Biology, *in* M. Bernardo, P. Degano & G. Zavattaro, eds, 'SFM', Vol. 5016 of *Lecture Notes in Computer Science*, Springer, pp. 215–264.

Heiner, M., Koch, I. & Will, J. (2004), 'Model validation of biological pathways using Petri nets–demonstrated for apoptosis', *Biosystems* **75**(1-3), 15–28. Computational Systems Biology.

Heiner, M., Richter, R., Schwarick, M. & Rohr, C. (2008), 'Snoopy - A Tool to Design and Execute Graph-Based Formalisms', *Petri Net Newsletter* **74**, 8–22.

Helminga, L. & Gordon, S. (2008), 'The molecular basis of macrophage fusion', *Immunobiology* **212**(9-10), 785–793.

Henrickson, S. E., Mempel, T. R., Mazo, I. B., Liu, B., Artyomov, M. N., Zheng, H., Peixoto, A., Flynn, M. P., Senman, B., Junt, T., Wong, H. C., Chakraborty, A. K. & von Andrian, U. H. (2008), 'T cell sensing of antigen dose governs interactive behavior with dendritic cells and sets a threshold for T cell activation', *Nat Immunol* **9**(3), 282–291.

Holtzman, M. J., Green, J. M., Jayaraman, S. & Arch, R. H. (2000), 'Regulation of T cell apoptosis', *Apoptosis* **5**(5), 459–471.

Huang, Q., Liu, D., Majewski, P., Schulte, L. C., Korn, J. M., Young, R. A., Lander, E. S. & Hacohen, N. (2001), 'The Plasticity of Dendritic Cell Responses to Pathogens and Their Components', *Science* **294**(5543), 870–875.

Iman, R. L. & Conover, W. J. (1979), 'The Use of the Rank Transform in Regression', *Technometrics* **21**(4), 499–509.

Iman, R. L. & Conover, W. J. (1982), 'A distribution-free approach to inducing rank correlation among input variables', *Communications in Statistics - Simulation and Computation* **11**(3), 311–334.

Jamieson, A. M., Isnard, P., Dorfman, J. R., Coles, M. C. & Raulet, D. H. (2004), 'Turnover and Proliferation of NK Cells in Steady State and Lymphopenic Conditions', *J Immunol* **172**(2), 864–870.

Kawano, T., Cui, J., Koezuka, Y., Toura, I., Kaneko, Y., Motoki, K., Ueno, H., Nakagawa, R., Sato, H., Kondo, E., Koseki, H. & Taniguchi, M. (1997), 'CD1d-Restricted and TCR-Mediated Activation of Vα14 NKT Cells by Glycosylceramides', *Science* **278**(5343), 1626–1629.

Kirkpatrick, C. E. & Farrell, J. P. (1982*a*), 'Leishmaniasis in beige mice.', *Infect. Immun.* **38**(3), 1208–1216.

Kirkpatrick, C. E. & Farrell, J. P. (1982*b*), 'Leishmaniasis in beige mice', *Infect. Immun.* **38**, 1208–1216.

Klügl, F. (2008), A validation methodology for agent-based simulations, *in* 'SAC '08: Proceedings of the 2008 ACM symposium on Applied computing', ACM, New York, NY, USA, pp. 39–43.

Korn, T., Bettelli, E., Oukka, M. & Kuchroo, V. K. (2009), 'IL-17 and Th17 Cells', *Annual Review of Immunology* **27**, 485–517.

Lay, G., Poquet, Y., Salek-Peyron, P., Puissegur, M.-P., Botanch, C., Bon, H., Levillain, F., Duteyrat, J.-L., Emile, J.-F. & Altare, F. (2007), 'Langhans giant cells from *M. tuberculosis*-induced human granulomas cannot mediate mycobacterial uptake, journal = The Journal of Pathology', **211**(1), 76–85.

Lazarski, C. A., Chaves, F. A., Jenks, S. A., Wu, S., Richards, K. A., Weaver, J. & Sant, A. J. (2005), 'The Kinetic Stability of MHC Class II:Peptide Complexes Is a Key Parameter that Dictates Immunodominance', *Immunity* **23**(1), 29–40.

Leavy, O. (2006), 'Variable neutrophils', *Nat Rev Immunol* **6**(11), 794–794.

Leavy, O. (2009), 'The T_H1 two step', *Nature Reviews Immunology* **9**(6), 387.

Linderman, J. J., Riggs, T., Pande, M., Miller, M., Marino, S. & Kirschner, D. E. (2010), 'Characterizing the Dynamics of $CD4^+$ T Cell Priming within a Lymph Node', *J Immunol* **184**(6), 2873–2885.

Litman, G. W. & Cannon, J. P. (2009), 'Immunology: Immunity's ancient arms', *Nature* **459**(7248), 784–786.

Lotka, A. J. (1925), *Elements of Physical Biology*, Baltimore: Williams and Wilkins.

Luke, S., Cioffi-Revilla, C., Panait, L., Sullivan, K. & Balan, G. (2005), 'MASON: A Multiagent Simulation Environment', *Simulation* **81**(7), 517–527.

Mantovani, A., Sica, A., Sozzani, S., Allavena, P., Vecchi, A. & Locati, M. (2004), 'The chemokine system in diverse forms of macrophage activation and polarization', *Trends in Immunology* **25**(12), 677–686.

Marino, S., Hogue, I. B., Ray, C. J. & Kirschner, D. E. (2008), 'A methodology for performing global uncertainty and sensitivity analysis in systems biology', *Journal of Theoretical Biology* **254**(1), 178–196.

Marino, S. & Kirschner, D. E. (2004), 'The human immune response to Mycobacterium tuberculosis in lung and lymph node', *Journal of Theoretical Biology* **227**(4), 463–486.

Maroof, A., Beattie, L., Zubairi, S., Svensson, M., Stager, S. & Kaye, P. M. (2008), 'Posttranscriptional Regulation of Il10 Gene Expression Allows Natural Killer Cells to Express Immunoregulatory Function', *Immunity* **29**(2), 295–305.

Marsan, M. A. (1990), 'Stochastic Petri Nets: An Elementary Introduction.', *Lecture Notes in Computer Science; Advances in Petri Nets 1989* **424**, 1–29. NewsletterInfo: 36.

Marsan, M. A., Balbo, G., Conte, G., Donatelli, S., Franceschinis, G., Computing, P., Wiley, J., Almeida, V., Almeida, J. & Analysis, C. M. P. (1995), *Modelling with Generalized Stochastic Petri Nets*, John Wiley & Sons.

Matozaki, T., Murata, Y., Okazawa, H. & Ohnishi, H. (2009), 'Functions and molecular mechanisms of the CD47-SIRPα signalling pathway', *Trends in Cell Biology* **19**(2), 72–80.

Matsuda, J. L., Mallevaey, T., Scott-Browne, J. & Gapin, L. (2008), 'CD1d-restricted iNKT cells, the "Swiss-Army knife" of the immune system', *Current Opinion in Immunology* **20**(3), 358–368.

Matsuda, J. L., Naidenko, O. V., Gapin, L., Nakayama, T., Taniguchi, M., Wang, C.-R., Koezuka, Y. & Kronenberg, M. (2000), 'Tracking the Response of Natural Killer T Cells to a Glycolipid Antigen Using Cd1d Tetramers', *J. Exp. Med.* **192**(5), 741–754.

McFarlane, E., Perez, C., Charmoy, M., Allenbach, C., Carter, K. C., Alexander, J. & Tacchini-Cottier, F. (2008), 'Neutrophils Contribute to Development of a Protective Immune Response during Onset of Infection with Leishmania donovani', *Infection and Immunity* **76**(2), 532–541.

McIlroy, D., Tanguy-Royer, S., Le Meur, N., Guisle, I., Royer, P.-J., Leger, J., Meflah, K. & Gregoire, M. (2005), 'Profiling dendritic cell maturation with dedicated microarrays', *J Leukoc Biol* **78**(3), 794–803.

McKay, M. D., Beckman, R. J. & Conover, W. J. (1979), 'A comparison of three methods for selecting values of input variables in the analysis of output from a computer code', *Technometrics* **21**, 239–245.

Mehrotra, P. T., Donnelly, R. P., Wong, S., Kanegane, H., Geremew, A., Mostowski, H. S., Furuke, K., Siegel, J. P. & Bloom, E. T. (1998), 'Production of IL-10 by Human Natural Killer Cells Stimulated with IL-2 and/or IL-12', *J Immunol* **160**(6), 2637–2644.

Melby, P. C., Tryon, V. V., Chandrasekar, B. & Freeman, G. L. (1998), 'Cloning of Syrian Hamster (Mesocricetus auratus) Cytokine cDNAs and Analysis of Cytokine mRNA Expression in Experimental Visceral Leishmaniasis', *Infect. Immun.* **66**(5), 2135–2142.

Miralles, G. D., Stoeckle, M. Y., McDermott, D. F., Finkelman, F. D. & Murray, H. W. (1994), 'Th1 and Th2 cell-associated cytokines in experimental visceral leishmaniasis', *Infect. Immun.* **62**(3), 1058–1063.

M'Kendrick, A. G. (1925), 'Applications of Mathematics to Medical Problems', *Proceedings of the Edinburgh Mathematical Society* **44**(-1), 98–130.

Mood, A. M., Graybill, F. A. & Boes, D. C. (1974), *Introduction to the Theory of Statistics*, 3 edn, McGraw-Hill Companies.

Mosser, D. M. & Edwards, J. P. (2008), 'Exploring the full spectrum of macrophage activation', *Nature Reviews Immunology* **8**(12), 958–969.

Murphy & Kenneth (2007), *Immunobiology 7 (Janeway's Immunobiology)*, Garland Science.

Murray, H. W., Tsai, C. W., Liu, J. & Ma, X. (2006), 'Responses to Leishmania donovani in Mice Deficient in Interleukin-12 (IL-12), IL-12/IL-23, or IL-18', *Infect. Immun.* **74**(7), 4370–4374.

Murray, J. D. (2002), *Mathematical biology: I. An introduction*, Interdisciplinary Applied Mathematics, Springer New York.

Murray, J. D. (2003), *Mathematical Biology II: Spatial Models and Biomedical Applications*, Interdisciplinary Applied Mathematics, Springer New York.

Nakagawa, R., Nagafune, I., Tazunoki, Y., Ehara, H., Tomura, H., Iijima, R., Motoki, K., Kamishohara, M. & Seki, S. (2001), 'Mechanisms of the Antimetastatic Effect in the Liver and of the Hepatocyte Injury Induced by α-Galactosylceramide in Mice', *J Immunol* **166**(11), 6578–6584.

Nandana, D. & Reiner, N. E. (2005), 'Leishmania donovani engages in regulatory interference by targeting macrophage protein tyrosine phosphatase SHP-1', *Clinical Immunology* **114**(3), 266–277.

Nathan, C. (2006), 'Neutrophils and immunity: challenges and opportunities', *Nat Rev Immunol* **6**(3), 173–182.

Naylor, K., Li, G., Vallejo, A. N., Lee, W.-W., Koetz, K., Bryl, E., Witkowski, J., Fulbright, J., Weyand, C. M. & Goronzy, J. J. (2005), 'The Influence of Age on T Cell Generation and TCR Diversity', *J Immunol* **174**(11), 7446–7452.

Paget, C., Bialecki, E., Fontaine, J., Vendeville, C., Mallevaey, T., Faveeuw, C. & Trottein, F. (2009), 'Role of Invariant NK T Lymphocytes in Immune Responses to CpG Oligodeoxynucleotides', *J Immunol* **182**(4), 1846–1853.

Parekh, V. V., Singh, A. K., Wilson, M. T., Olivares-Villagomez, D., Bezbradica, J. S., Inazawa, H., Ehara, H., Sakai, T., Serizawa, I., Wu, L., Wang, C.-R., Joyce, S. & Van Kaer, L. (2004), 'Quantitative and Qualitative Differences in the In Vivo Response of NKT Cells to Distinct α- and β-Anomeric Glycolipids', *J Immunol* **173**(6), 3693–3706.

Peters, N. C., Egen, J. G., Secundino, N., Debrabant, A., Kimblin, N., Kamhawi, S., Lawyer, P., Fay, M. P., Germain, R. N. & Sacks, D. (2008), 'In Vivo Imaging Reveals an Essential Role for Neutrophils in Leishmaniasis Transmitted by Sand Flies', *Science* **321**(5891), 970–974.

Peters, N. & Sacks, D. (2006), 'Immune privilege in sites of chronic infection: Leishmania and regulatory T cells', *Immunological Reviews* **213**(1), 159–179.

Pollard, J. W. (2009), 'Trophic macrophages in development and disease', *Nature Reviews Immunology* **9**(4), 259–270.

Ray, J. C. J., Flynn, J. L. & Kirschner, D. E. (2009), 'A Synergy between Individual TNF-Dependent Functions Determines Granuloma Performance for Controlling Mycobacterium tuberculosis Infection', *Journal of Immunology* **182**, 3706–3717.

Read, M., Timmis, J., Andrews, P. & Kumar, V. (2009), Using UML to Model EAE and Its Regulatory Network, *in* P. Andrews, J. Timmis, N. Owens, U. Aickelin, E. Hart, A. Hone & A. Tyrrell, eds, 'Artificial Immune Systems', Vol. 5666 of *Lecture Notes in Computer Science*, Springer Berlin / Heidelberg, pp. 4–6.

Reiner, N., Ng, W. & McMaster, W. (1987), 'Parasite-accessory cell interactions in murine leishmaniasis. II. Leishmania donovani suppresses macrophage expression of class I and class II major histocompatibility complex gene products', *The Journal of Immunology* **138**(6), 1926–1932.

Rutz, S., Janke, M., Kassner, N., Hohnstein, T., Krueger, M. & Scheffold, A. (2008), 'Notch regulates IL-10 production by T helper 1 cells', *Proceedings of the National Academy of Sciences of the United Sttes of America (PNAS)* **105**(9), 3497–3502.

Saltelli, A., K., C. & E.M., S., eds (2000), *Sensitivity Analysis*, Wiley.

Saltelli, A., Tarantola, S. & Chan, K. P.-S. (1999), 'A quantitative model-independent method for global sensitivity analysis of model output', *Technometrics* **41**(1), 39–56.

Schleicher, U., Liese, J., Knippertz, I., Kurzmann, C., Hesse, A., Heit, A., Fischer, J. A., Weiss, S., Kalinke, U., Kunz, S. & Bogdan, C. (2007), 'NK cell activation in visceral leishmaniasis requires TLR9, myeloid DCs, and IL-12, but is independent of plasmacytoid DCs', *J. Exp. Med.* **204**(4), 893–906.

Schulz, E. G., Mariani, L., Radbruch, A. & Hï£¡fer, T. (2009), 'Sequential Polarization and Imprinting of Type 1 T Helper Lymphocytes by Interferon-γ and Interleukin-12', *Immunity* **30**(5), 673–683.

Smith-Garvin, J. E., Koretzky, G. A. & Jordan, M. S. (2009), 'T Cell Activation', *Annual Review of Immunology* **27**(1), 591–619.

Stanley, A. C., Zhou, Y., Amante, F. H., Randall, L. M., Haque, A., Pellicci, D. G., Hill, G. R., Smyth, M. J., Godfrey, D. I., & Engwerda, C. R. (2008), 'Activation of Invariant NKT Cells Exacerbates Experimental Visceral Leishmaniasis', *PLoS Pathogens* **4**(2).

Sullivan, B. A., Nagarajan, N. A., Wingender, G., Wang, J., Scott, I., Tsuji, M., Franck, R. W., Porcelli, S. A., Zajonc, D. M. & Kronenberg, M. (2010), 'Mechanisms for Glycolipid Antigen-Driven Cytokine Polarization by Valpha14i NKT Cells', *J Immunol* **184**(1), 141–153.

Svensson, M., Zubairi, S., Maroof, A., Kazi, F., Taniguchi, M. & Kaye, P. M. (2005), 'Invariant NKT Cells Are Essential for the Regulation of Hepatic CXCL10 Gene Expression during Leishmania donovani Infection', *Infect. Immun.* **73**(11), 7541–7547.

The sharing principle (2009), *Nature* **459**(7248), 752.

Trinchieri, G. (2007), 'Interleukin-10 production by effector T cells: Th1 cells show self control', *The Journal of Experimental Medicine* **204**(2), 239–243.

van Zandbergen, G., Klinger, M., Mueller, A., Dannenberg, S., Gebert, A., Solbach, W. & Laskay, T. (2004), 'Cutting Edge: Neutrophil Granulocyte Serves as a Vector for Leishmania Entry into Macrophages', *The Journal of Immunology* **20**(11), 6521–6525.

Vincenzo Capasso, D. B. (2005), *An Introduction to Continuous-Time Stochastic Processes*, Birkhauser.
URL: *http://hdl.handle.net/2434/24667*

Volterra, V. (1927), 'Fluctuations in the Abundance of a Species considered Mathematically', *Nature* **119**, 12–13.

Wigginton, J. E. & Kirschner, D. (2001), 'A Model to Predict Cell-Mediated Immune Regulatory Mechanisms During Human Infection with Mycobacterium tuberculosis', *J Immunol* **166**(3), 1951–1967.

Will, J. & Heiner, M. (2002), 'Petri Nets in biology, chemistry, and medicine - bibliography', *Computer Science Reports 04/2002* .

Wolfram, S. (1994), *Cellular Automata and Complexity*, Addison-Wesley.

Yang, X. O., Nurieva, R., Martinez, G. J., Kang, H. S., Chung, Y., Pappu, B. P., Shah, B., Chang, S. H., Schluns, K. S., Watowich, S. S., Feng, X.-H., Jetten, A. M. & Dong, C. (2008), 'Molecular Antagonism and Plasticity of Regulatory and Inflammatory T Cell Programs', *Immunity* **29**(1), 44–56.

Yang, Z. & Bjorkman, P. J. (2008), 'Structure of UL18, a peptide-binding viral MHC mimic, bound to a host inhibitory receptor', *Proceedings of the National Academy of Sciences* **105**(29), 10095–10100.

Yokoyama, W., Kim, S. & French, A. (2004*a*), 'The dynamic life of natural killer cells', *Annual Review of Immunology* **22**, 405–429.

Yokoyama, W. M., Kim, S. & French, A. R. (2004*b*), 'The Dynamic Life of Natural Killer Cells', *Annual Review of Immunology* **22**(1), 405–429.

Zhu, J. & Paul, W. E. (2008), 'CD4 T cells: fates, functions, and faults', *Blood* **112**(5), 1557–1569.

Index

Part IV

Appendices

Appendix A

Mathematical Proofs

This chapter presents the mathematical proof of some results of Chapter 4.

Note that throughout this Chapter, $\log(x)$ is to be interpreted as the natural logarithm of x.

A.1 Distribution of the Minimum of Independent Negative Exponentially Distributed Variables

Theorem 1. *Let $X_1, \ldots, X_n$ be n exponentially distributed independent random variables with parameters $\lambda_1, \ldots, \lambda_n$, then*

$$X_{min} = min\,(X_1, \ldots, X_n)$$

is exponentially distributed with parameter

$$\lambda_{min} = \lambda_1 + \cdots + \lambda_n$$

Proof. Let $X_1, \ldots, X_n$ be n independent random variables, with cumulative distribution functions $F_{X_1}, \ldots, F_{X_n}$, the cumulative distribution function of

$$X_{\min} = \min\,(X_1, \ldots X_n)$$

is

$$F_{X_{\min}}(x) = 1 - \prod_{i=1}^{n} (1 - F_{X_i}(x))$$

(see Mood et al. 1974).

Therefore, if the X_i are exponentially distributed with parameters λ_i, the cumulative distribution function of their minimum is

$$\begin{aligned} F_{X_{\min}}(x) &= 1 - \prod_{i=1}^{n} \left(1 - F_{X_i}(x)\right) \\ &= 1 - \prod_{i=1}^{n} \left(1 - 1 + e^{\lambda_i x}\right) \\ &= 1 - \prod_{i=1}^{n} \left(e^{\lambda_i x}\right) \\ &= 1 - e^{\left(\sum_{i=1}^{n} \lambda_i\right) \cdot x} \end{aligned}$$

which is the cumulative distribution function of an exponentially distributed random variables with parameter

$$\lambda_{\min} = \sum_{i=1}^{n} \lambda_i$$

□

A.2 Memoryless Property of Exponentially Distributed Random Variables

Theorem 2. *Let X be an exponentially distributed random variable with parameter λ, then*

$$P[X > x + k | X > x] = P[X > k]$$

$\forall x, k > 0$

Proof. By definition, we have

$$\begin{aligned} P[X > x + k | X > x] &= \frac{P[X > x + k]}{P[X > x]} \\ &= \frac{e^{-\lambda(x+k)}}{e^{-\lambda x}} \\ &= e^{-\lambda k} \\ &= P[X > k] \end{aligned}$$

□

A.3 Half-life

Theorem 3. *Consider the Petri nets system of Figure A.1, if the parameter of transition t is:*

$$\lambda = \frac{n_p}{t_{1/2}} \cdot \log(2)$$

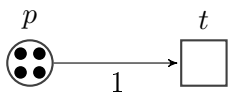

Figure A.1: A Petri net system modeling a decay process

where n_p indicates the number of tokens of place p, then the number of tokens of place p decreases with half-life $t_{1/2}$.

Proof. The theorem will be proven for a generic number of tokens n, with $n \geq 2$ and even. Let n_p the initial number of tokens, and let τ_i be the expected sojourn time in the marking with $n - i$ tokens in p. Given the linearity of the expectation, we need to prove that, after $t_{1/2}$ time units, the number of tokens in p is $n_p/2$

$$\sum_{i=1}^{n/2} \tau_i \leq t_{1/2} < \sum_{i=1}^{n/2+1} \tau_i \tag{A.1}$$

Using the properties of negatively exponential distribution, Inequality A.1 can be rewritten as

$$\sum_{i=1}^{n/2} \frac{t_{1/2}}{(n-i+1)\cdot\log(2)} \leq t_{1/2} < \sum_{i=1}^{n/2+1} \frac{t_{1/2}}{(n-i+1)\cdot\log(2)}$$

which is equivalent to

$$\frac{t_{1/2}}{\log(2)} \cdot \sum_{i=1}^{n/2} \frac{1}{n-i+1} \leq t_{1/2} < \frac{t_{1/2}}{\log(2)} \cdot \sum_{i=1}^{n/2+1} \frac{1}{n-i+1} \tag{A.2}$$

Since $t_{1/2} > 0$, we can multiply the terms of Inequality A.2 by

$$\frac{\log(2)}{t_{1/2}}$$

obtaining

$$\sum_{i=1}^{n/2} \frac{1}{n-i+1} \leq \log(2) < \sum_{i=1}^{n/2+1} \frac{1}{n-i+1}$$

which is equivalent to

$$\sum_{i=1}^{n} \frac{1}{i} - \sum_{i=1}^{n/2} \frac{1}{i} \leq \log(2) < \sum_{i=1}^{n} \frac{1}{i} - \sum_{i=1}^{n/2} \frac{1}{i} + \frac{2}{n} \tag{A.3}$$

Let

$$H_n = \sum_{i=1}^{n} \frac{1}{i}$$

be the nth harmonic number. Inequality A.3 can be rewritten as

$$H_n - H_{n/2} \leq \log(2) < H_n - H_{n/2} + \frac{2}{n} \tag{A.4}$$

which implies

$$H_n \leq \log(2) + H_{n/2} < H_n + \frac{2}{n}$$

It is possible to demonstrate that (Havil 2003):

$$\frac{1}{2(n+1)} < H_n - \log(n) - \gamma < \frac{1}{2n} \tag{A.5}$$

which implies

$$\frac{1}{n+2} < H_{n/2} - \log(n) + \log(2) - \gamma < \frac{1}{n} \tag{A.6}$$

Inequality A.5 implies that

$$H_n < \frac{1}{2n} + \log(n) + \gamma \tag{A.7}$$

and

$$\frac{1}{2(n+1)} + \log(n) + \gamma + \frac{2}{n} < H_n + \frac{2}{n} \tag{A.8}$$

where γ is the Euler-Mascheroni constant.

Additionally, Inequality A.6 implies that

$$\frac{1}{n+2} + \log(n) + \gamma < \log(2) + H_{n/2} < \frac{1}{n} + \log(n) + \gamma \tag{A.9}$$

The inequality

$$\frac{1}{2n} + \log(n) + \gamma \leq \frac{1}{n+2} + \log(n) + \gamma \tag{A.10}$$

can be simplified to

$$\frac{1}{2n} \leq \frac{1}{n+2}$$

which is true $\forall n \geq 2$. Moreover, the inequality

$$\frac{1}{n} + \log(n) + \gamma \leq \frac{1}{2(n+1)} + \log(n) + \gamma + \frac{2}{n} \tag{A.11}$$

can be simplified to

$$\frac{1}{n} \leq \frac{5n+4}{2n(n+1)}$$

which leads to

$$2n + 2 \leq 5n + 4$$

which is true $\forall n > 1$

Therefore,

$$\begin{aligned}
H_n &< \frac{1}{2n} + \log(n) + \gamma && \text{by Inequality A.7} \\
&\leq \frac{1}{n+2} + \log(n) + \gamma && \text{by Inequality A.10} \\
&\leq \log(2) + H_{n/2} && \text{by Inequality A.9} \\
&\leq \frac{1}{n} + \log(n) + \gamma && \text{by Inequality A.9} \\
&\leq \frac{1}{2(n+1)} + \log(n) + \gamma + \frac{2}{n} && \text{by Inequality A.11} \\
&< H_n + \frac{2}{n} && \text{by Inequality A.8}
\end{aligned}$$

which demonstrate Inequality A.4. □

Appendix B

Additional Model Results

This chapter describes additional results of the models presented in Chapters 7 and 8. Due to their *accessory* role, the data are only limitedly commented.

B.1 Removal of Natural Killer T Cells

The NK cells response of the NKT^- model seems unaffected (see Figure B.1). The low percentage of $CD4^+INF\gamma^+IL10^-$ T cells at day 38 (see Figure B.2) is likely due to the reduced parasite burden (see Figure 7.10), while the low percentage of $CD4^+INF\gamma^+IL10^+$ T cells indicates a stronger inflammatory response (see Figure B.3).

B.2 Removal of T Cells

The removal of T cells leads to stronger NKT and NK cells responses (see Figures B.4, B.5, and B.6) due to the increased parasite burden (see Figure 7.11). However, NKT and NK cells are not able to control infection, as expected.

B.3 Removal of INFγ

Similarly to the removal of T cells (Sections 7.2.2 and B.2), the removal of INFγ leads to an increased parasite burden, and thus to stronger NKT and NK cells responses (see Figures B.7, B.8, and B.9). Moreover, no T_H1 cells are present in the model (see Figures B.10 and B.11). Note that the small percentage of T_H1 cells indicates antigen non-specific T cells used for the calculation, but not modeled.

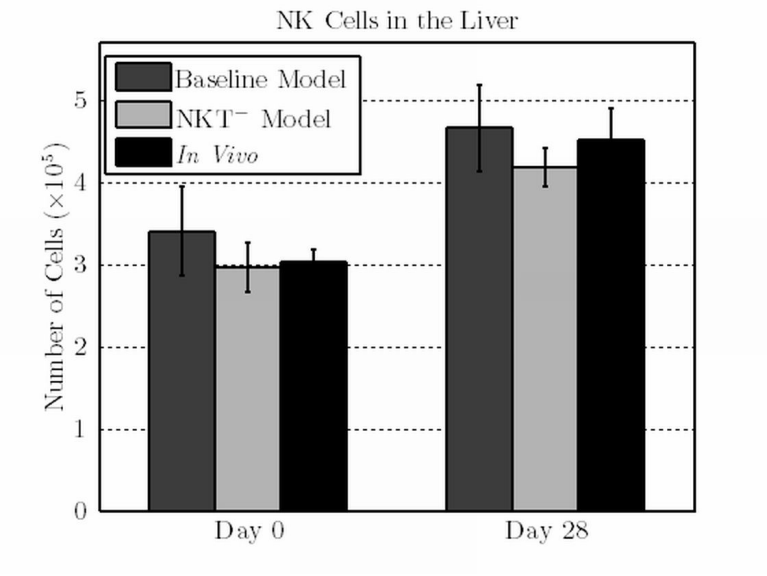

Figure B.1: Number of NK Cells. *In silico* data describe the results of baseline and NKT$^-$ models. *In vivo* data are taken from Maroof et al. 2008

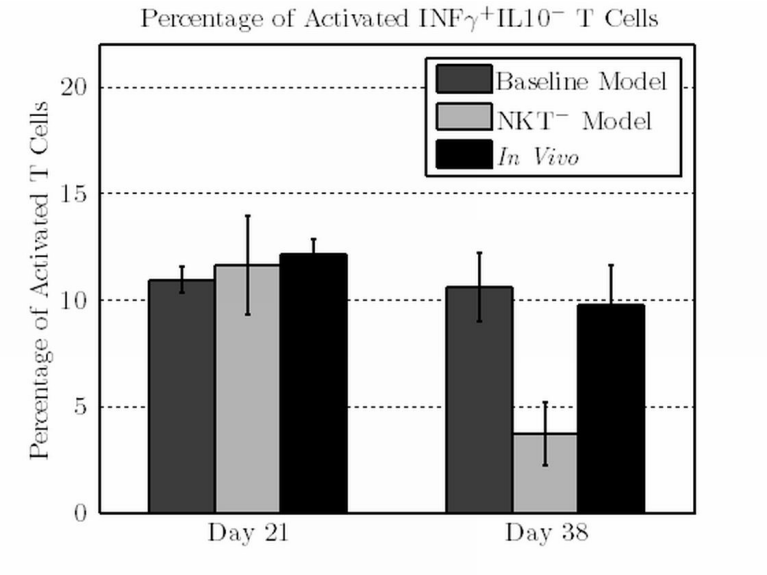

Figure B.2: Percentage of activated T_H1 cells. *In silico* data describe the results of baseline and NKT$^-$ models. *In vivo* data are taken from unpublished data

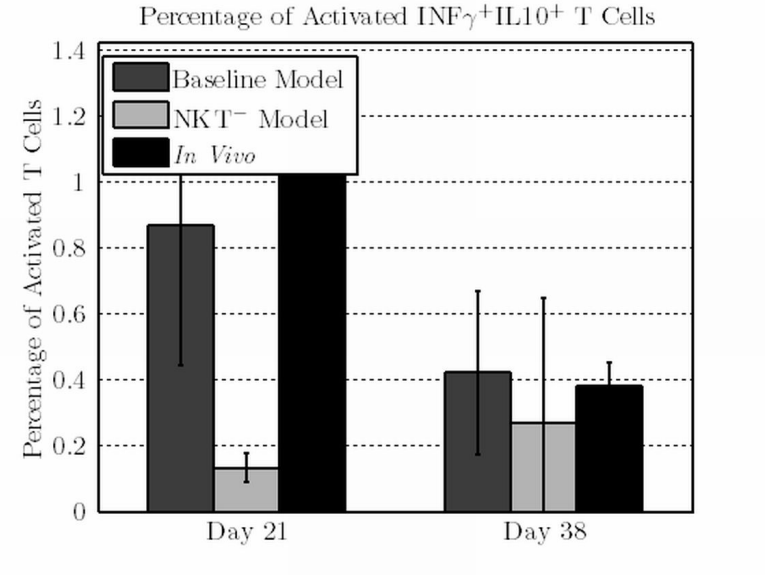

Figure B.3: Percentage of activated T_H1 cells. *In silico* data describe the results of baseline and NKT^- models. *In vivo* data are taken from unpublished data

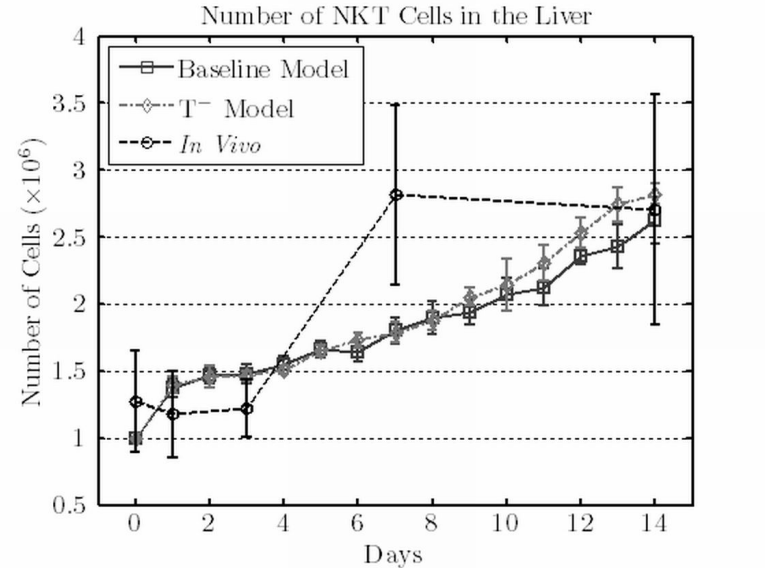

Figure B.4: Number of NKT cells. *In silico* data describe the results of baseline and T^- models. *In vivo* data are taken from Stanley et al. 2008

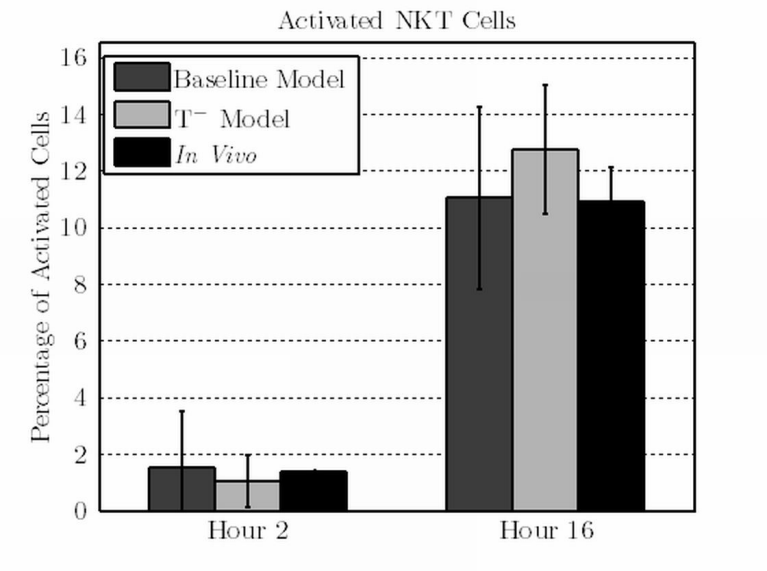

Figure B.5: Percentage of activated NKT Cells. *In silico* data describe the results of baseline and T^- models. *In vivo* data are taken from Amprey et al. 2004 and Beattie at al. 2010 (EJI)

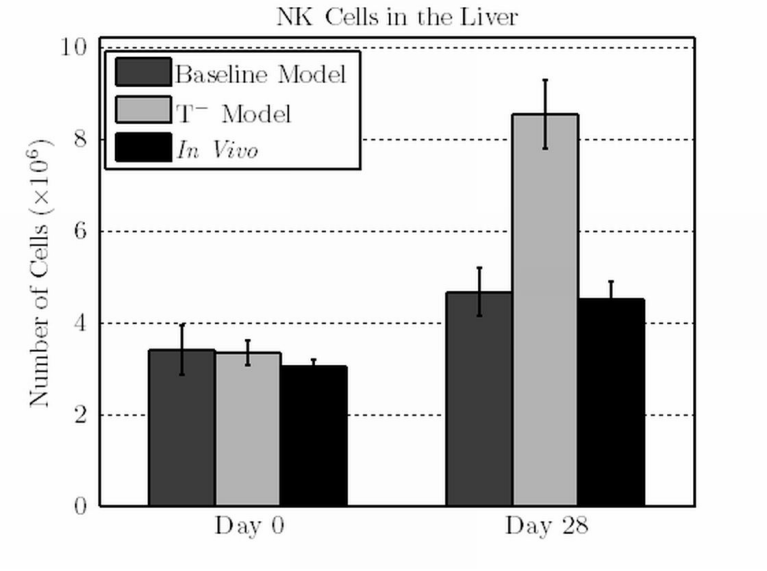

Figure B.6: Number of NK Cells. *In silico* data describe the results of baseline and T^- models. *In vivo* data are taken from Maroof et al. 2008

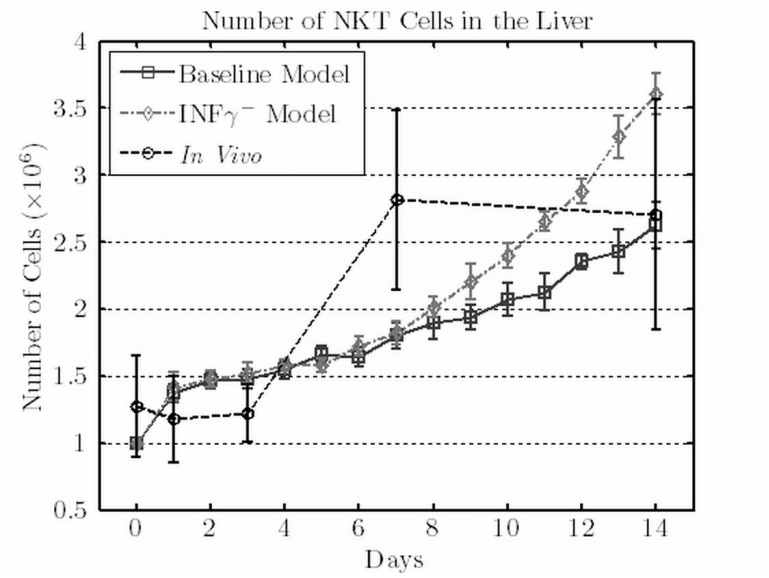

Figure B.7: Number of NKT cells. *In silico* data describe the results of baseline and INFγ^- models. *In vivo* data are taken from Stanley et al. 2008

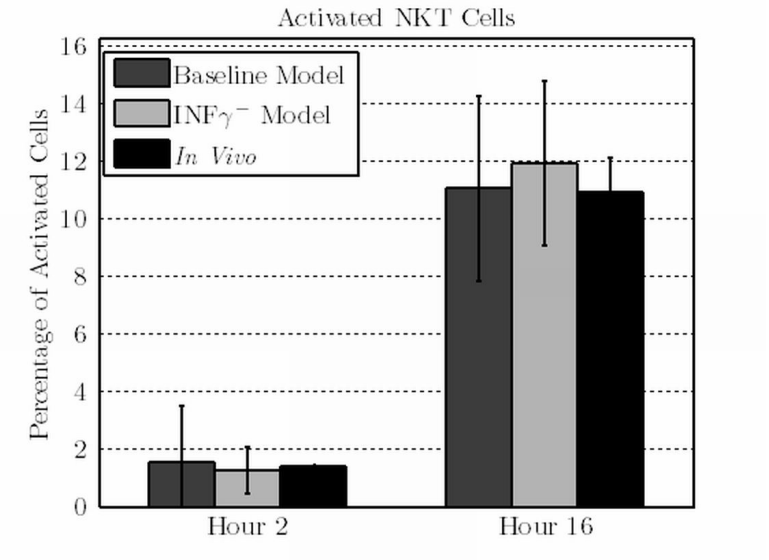

Figure B.8: Percentage of activated NKT Cells. *In silico* data describe the results of baseline and INFγ^- models. *In vivo* data are taken from Amprey et al. 2004 and Beattie at al. 2010 (EJI)

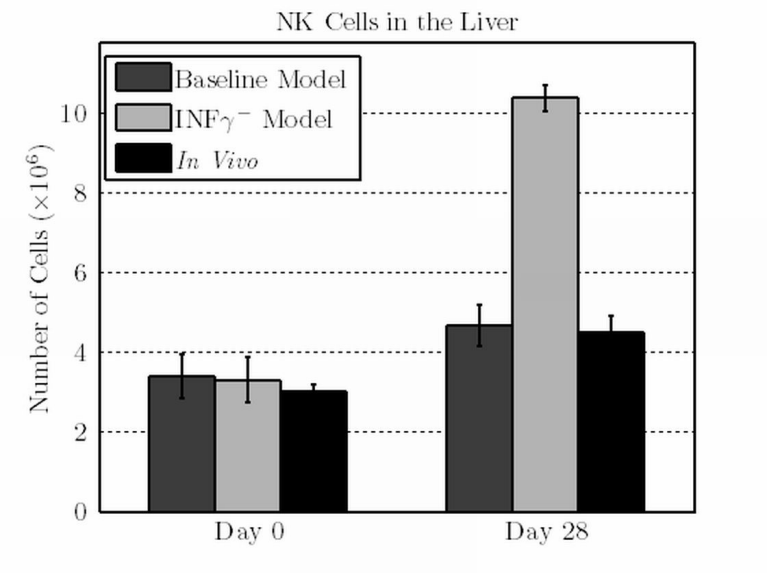

Figure B.9: Number of NK Cells. *In silico* data describe the results of baseline and INFγ^- models. *In vivo* data are taken from Maroof et al. 2008

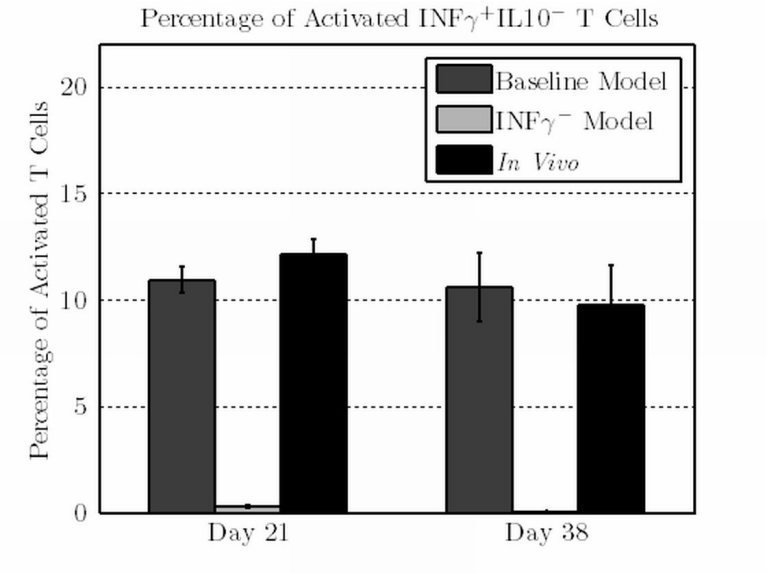

Figure B.10: Percentage of activated T_H1 cells. *In silico* data describe the results of baseline and INFγ^- models. *In vivo* data are taken from unpublished data

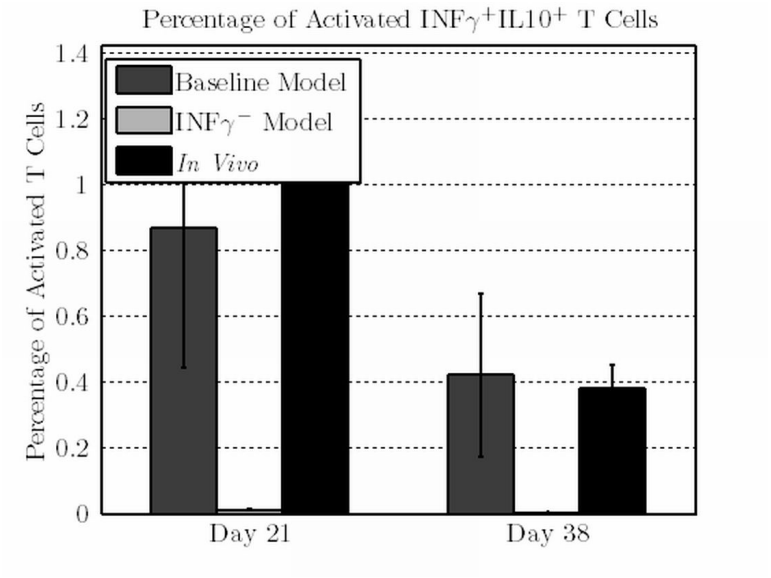

Figure B.11: Percentage of activated T_H1 cells. *In silico* data describe the results of baseline and INFγ^- models. *In vivo* data are taken from unpublished data

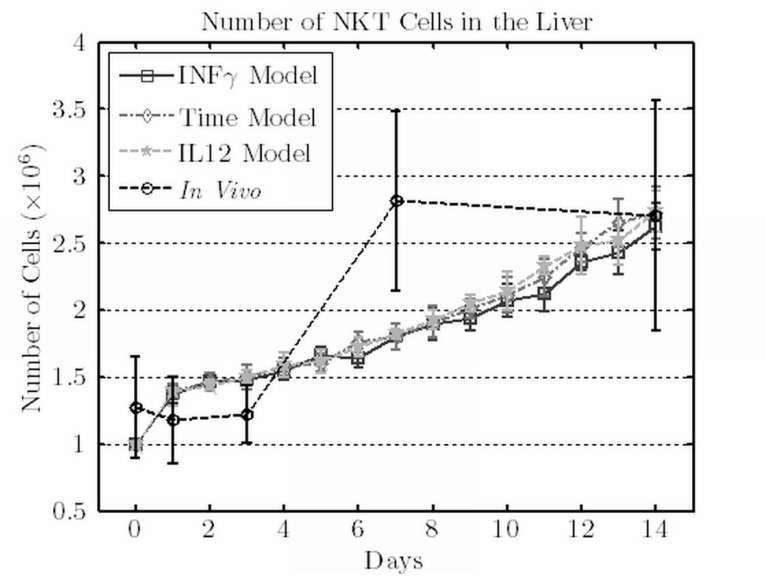

Figure B.12: Number of NKT cells. *In silico* data describe the results of INFγ, Time and IL12 models. *In vivo* data are taken from Stanley et al. 2008

B.4 INFγ-, Time-, and IL12-Dependent Models

The NKT and NK cells immune responses are very similar in the three models of T_H1 phenotypic change (see Figures B.12, B.13, and B.14).

B.5 Analysis of IL12-Dependent Model

The NK an NKT cells immune responses are unaffected by the reduced reproduction ability of INFγ^+IL10$^+$ T cells (see Figures B.15, B.16, and B.17). Moreover, the percentage of INFγ^+IL10$^-$ T cells is only slightly affected (see Figure B.18)

B.6 Activation of Natural Killer T Cells

The two models of activation of NKT cells only marginally affect the NK and T cells responses (see Figures B.19, B.20, and B.21)

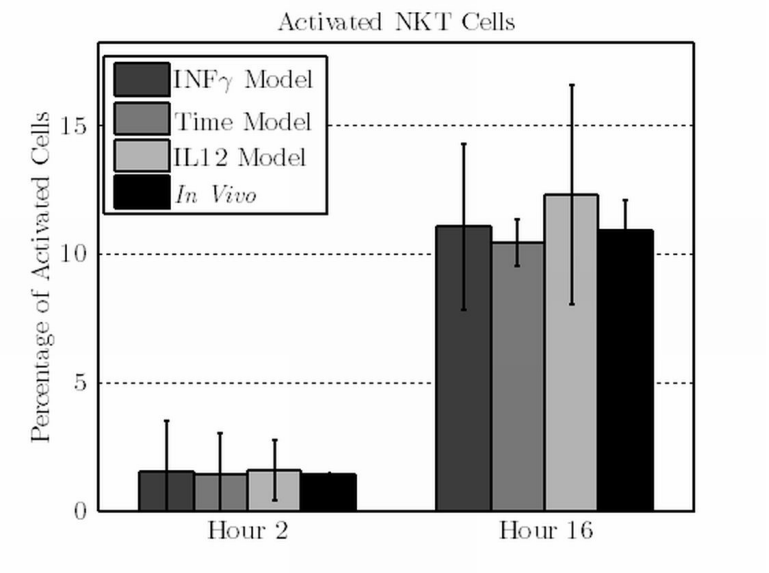

Figure B.13: Percentage of activated NKT Cells. *In silico* data describe the results of INFγ, Time and IL12 models. *In vivo* data are taken from Amprey et al. 2004 and Beattie at al. 2010 (EJI)

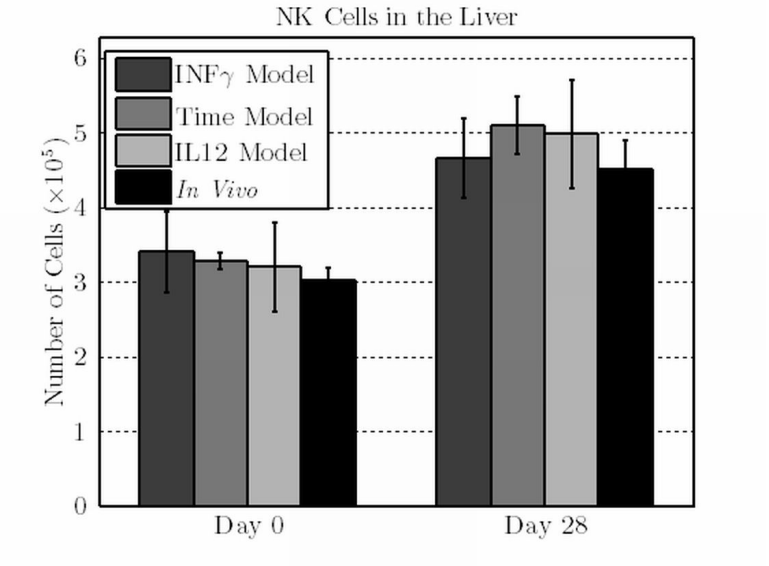

Figure B.14: Number of NK Cells. *In silico* data describe the results of INFγ, Time and IL12 models. *In vivo* data are taken from Maroof et al. 2008

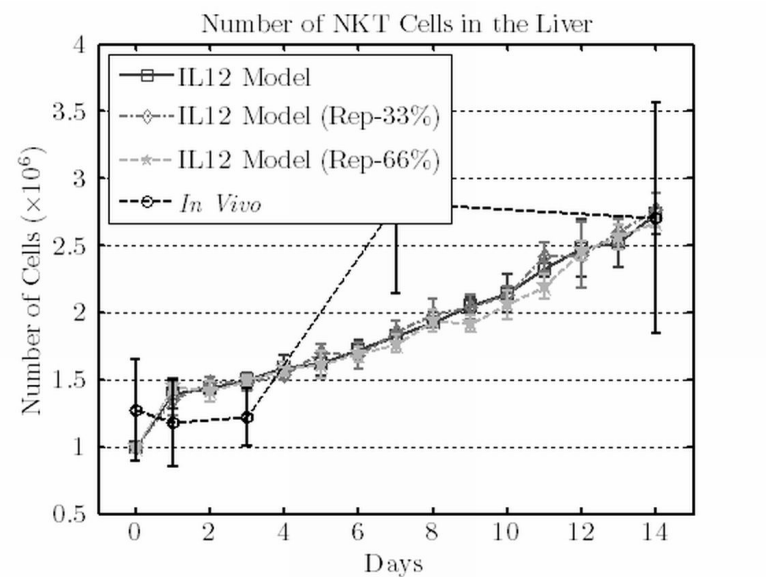

Figure B.15: Number of NKT cells. *In silico* data describe IL12 model, IL12 model with reproduction ability of INFγ^+IL10$^+$ T Cells reduced by 33%, and IL12 model with reproduction ability of INFγ^+IL10$^+$ T Cells reduced by 66%. *In vivo* data are taken from Stanley et al. 2008

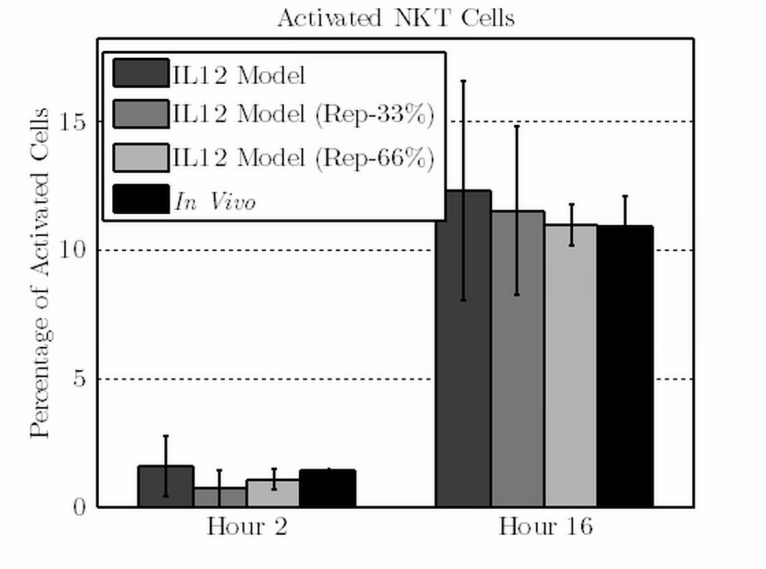

Figure B.16: Percentage of activated NKT Cells. *In silico* data describe IL12 model, IL12 model with reproduction ability of INFγ^+IL10$^+$ T Cells reduced by 33%, and IL12 model with reproduction ability of INFγ^+IL10$^+$ T Cells reduced by 66%. *In vivo* data are taken from Amprey et al. 2004 and Beattie at al. 2010 (EJI)

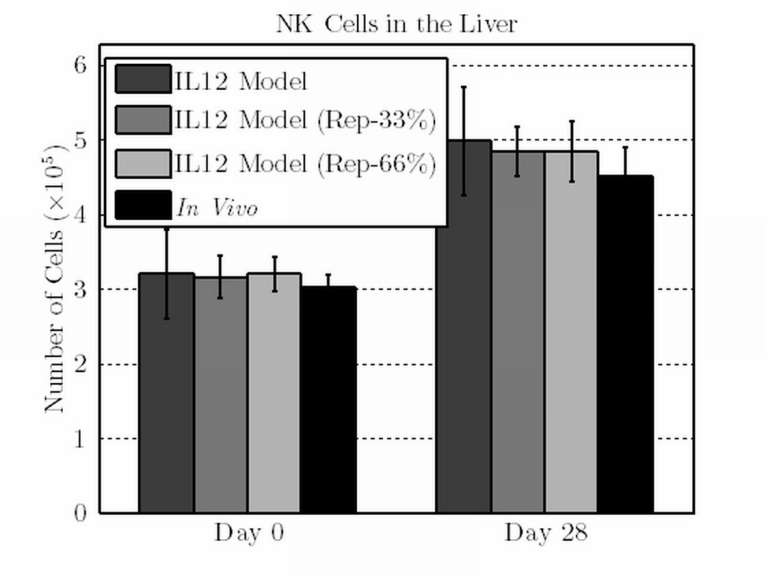

Figure B.17: Number of NK Cells. *In silico* data describe IL12 model, IL12 model with reproduction ability of INFγ^+IL10$^+$ T Cells reduced by 33%, and IL12 model with reproduction ability of INFγ^+IL10$^+$ T Cells reduced by 66%. *In vivo* data are taken from Maroof et al. 2008

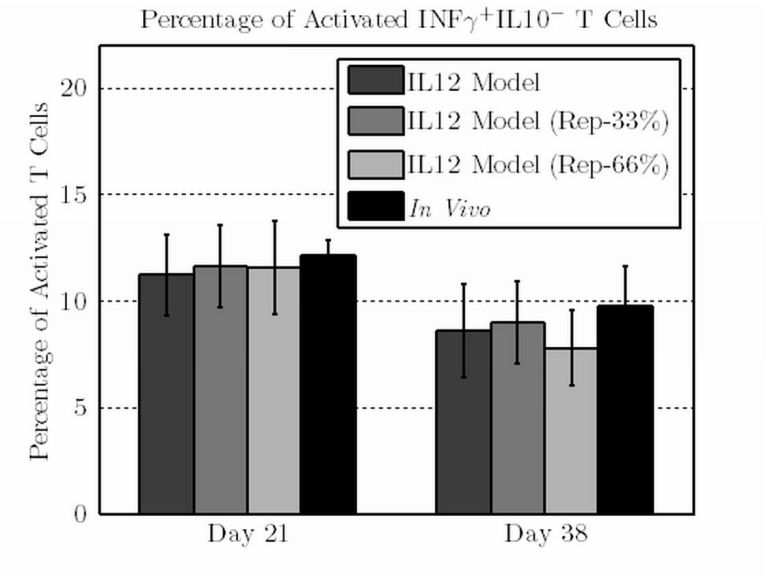

Figure B.18: Percentage of activated T_H1 cells. *In silico* data describe IL12 model, IL12 model with reproduction ability of INFγ^+IL10$^+$ T Cells reduced by 33%, and IL12 model with reproduction ability of INFγ^+IL10$^+$ T Cells reduced by 66%. *In vivo* data are taken from unpublished data

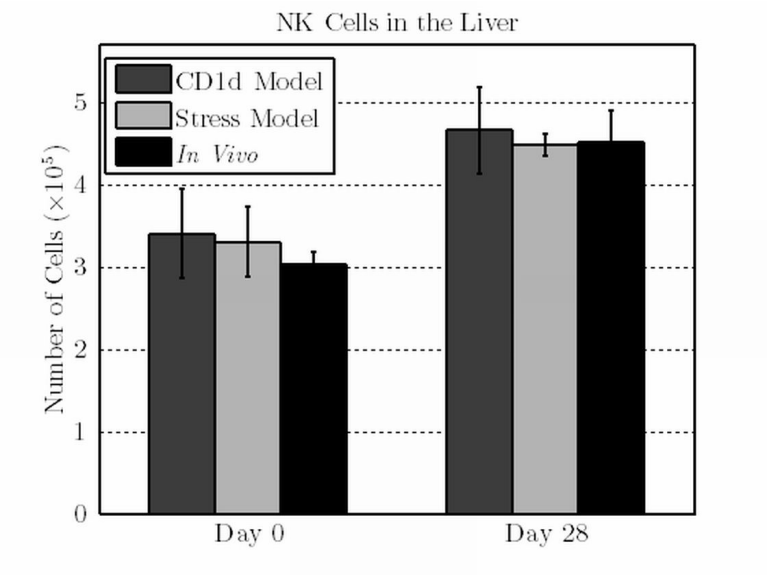

Figure B.19: Number of NK Cells. *In silico* data describe CD1d and stress models. *In vivo* data are taken from Maroof et al. 2008

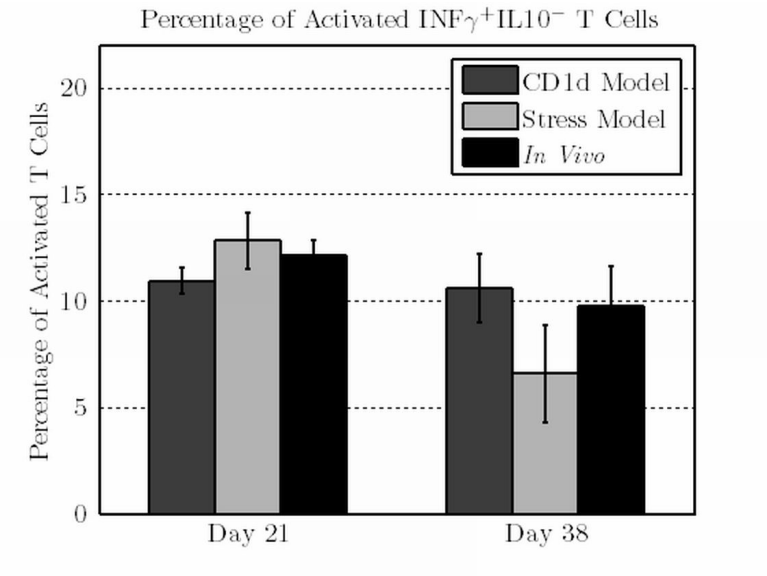

Figure B.20: Percentage of activated T_H1 cells. *In silico* data describe CD1d and stress models. *In vivo* data are taken from unpublished data

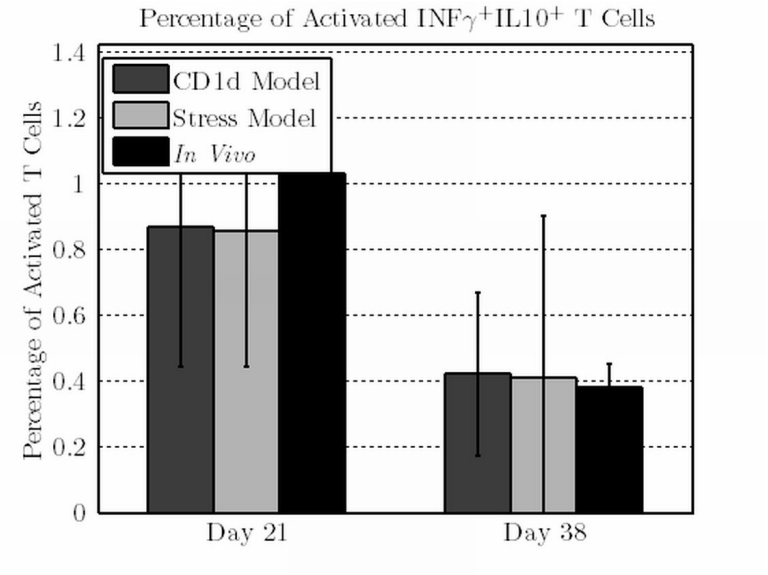

Figure B.21: Percentage of activated T_H1 cells. *In silico* data describe CD1d and stress models. *In vivo* data are taken from unpublished data

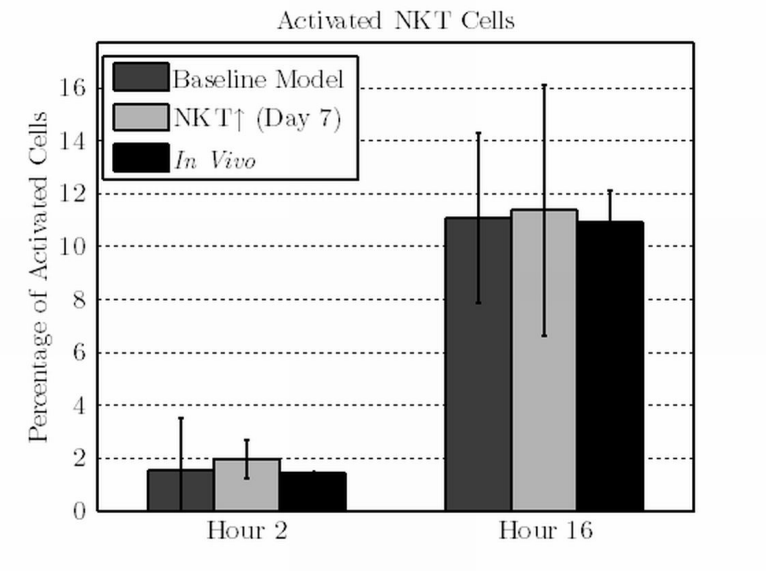

Figure B.22: Percentage of activated NKT Cells. *In silico* data describe baseline and (NKT↑ (Day 7) models. *In vivo* data are taken from Amprey et al. 2004 and Beattie at al. 2010 (EJI)

B.7 Direct Activation of Natural Killer Cells

As expected, the direct activation of NKT cells does not affect the percentage of activated NKT cells in the first hours after infection (see Figures B.22 and B.22), and the NK cells response (see Figures B.27 and B.27).

The percentages of activated T_H1 cells are indirectly affected (see Figures B.24, B.25, B.28, and B.29) as the parasite burden is changed (see Figures 8.15 and 8.16).

B.8 Role of Natural Killer Cells

The removal of NK cells slightly affects the NKT cells response (see Figures B.30, and B.31) and the T cells response (see Figures B.33, and B.33), as a result of the increased parasite burden (see Figure 8.21). As expected, no NK cell is present in the model (see Figure B.32).

B.9 Removal of Natural Killer and Natural Killer T Cells

Removing both NK and NKT cells (NK^-NKT^- Model) leads to a very high parasite burden (see Figure B.35) and to the absence of T_H1 cells (see Figure B.38 and B.39). Similarly to Section B.3, the small percentage of T_H1

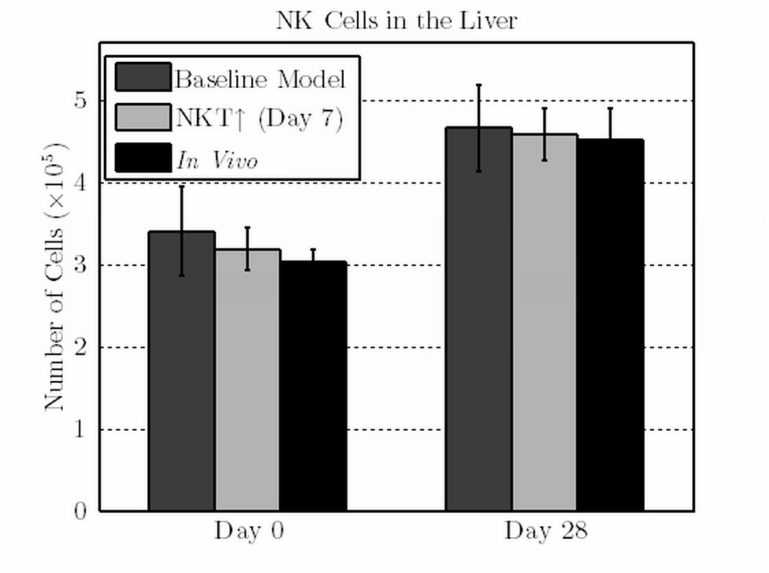

Figure B.23: Number of NK Cells. *In silico* data describe baseline and (NKT↑ (Day 7) models. *In vivo* data are taken from Maroof et al. 2008

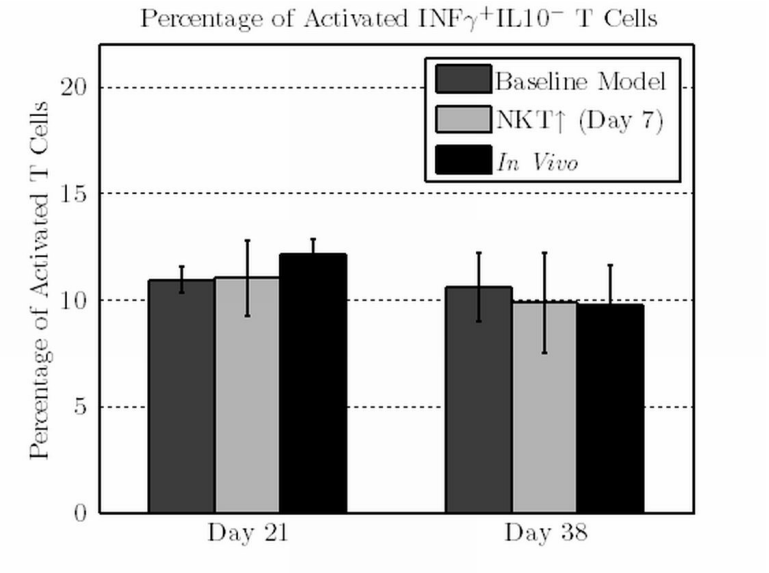

Figure B.24: Percentage of activated T_H1 cells. *In silico* data describe baseline and (NKT↑ (Day 7) models. *In vivo* data are taken from unpublished data

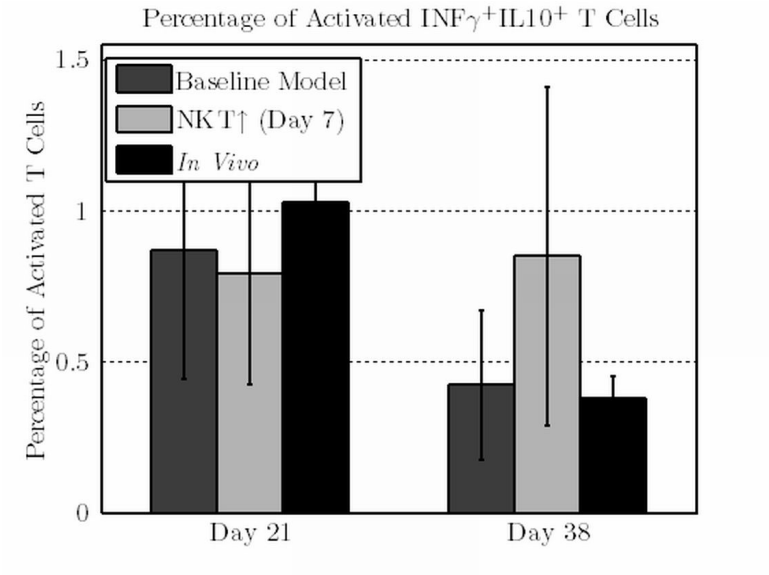

Figure B.25: Percentage of activated T_H1 cells. *In silico* data describe baseline and (NKT↑ (Day 7) models. *In vivo* data are taken from unpublished data

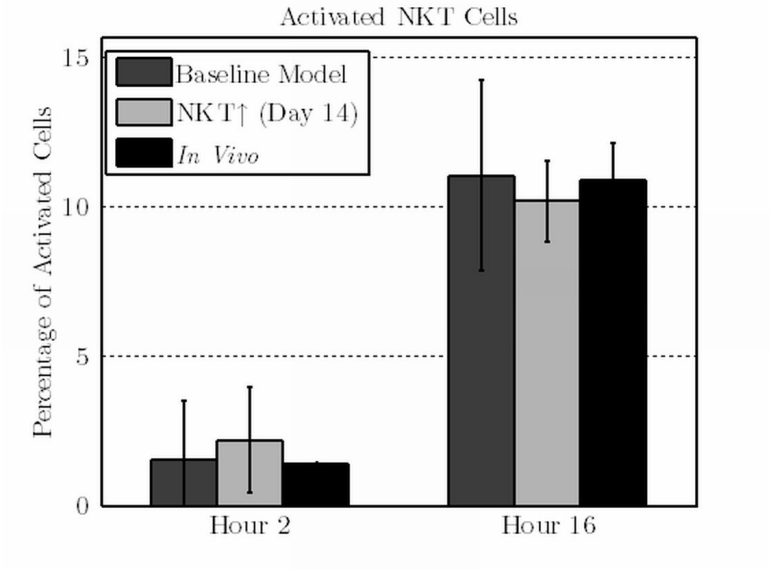

Figure B.26: Percentage of activated NKT Cells. *In silico* data describe baseline and (NKT↑ (Day 14) models. *In vivo* data are taken from Amprey et al. 2004 and Beattie at al. 2010 (EJI)

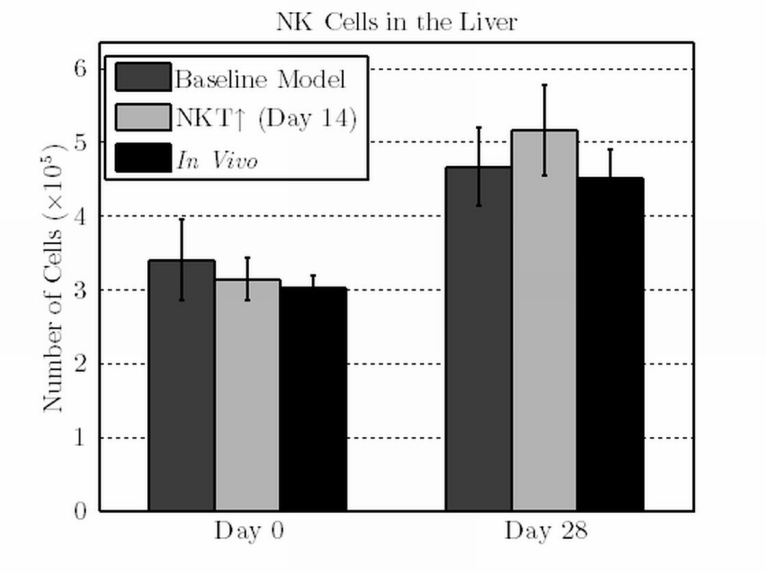

Figure B.27: Number of NK Cells. *In silico* data describe baseline and (NKT↑ (Day 14) models. *In vivo* data are taken from Maroof et al. 2008

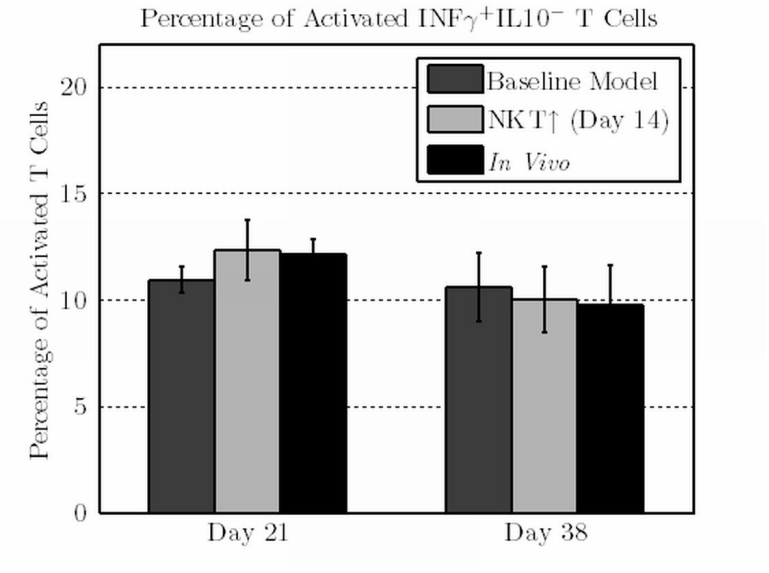

Figure B.28: Percentage of activated T_H1 cells. *In silico* data describe baseline and (NKT↑ (Day 14) models. *In vivo* data are taken from unpublished data

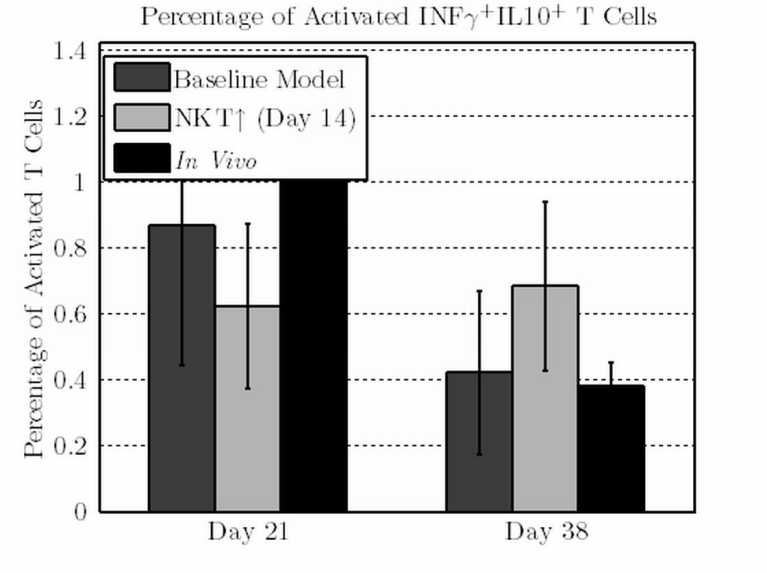

Figure B.29: Percentage of activated T_H1 cells. *In silico* data describe baseline and (NKT↑ (Day 14) models. *In vivo* data are taken from unpublished data

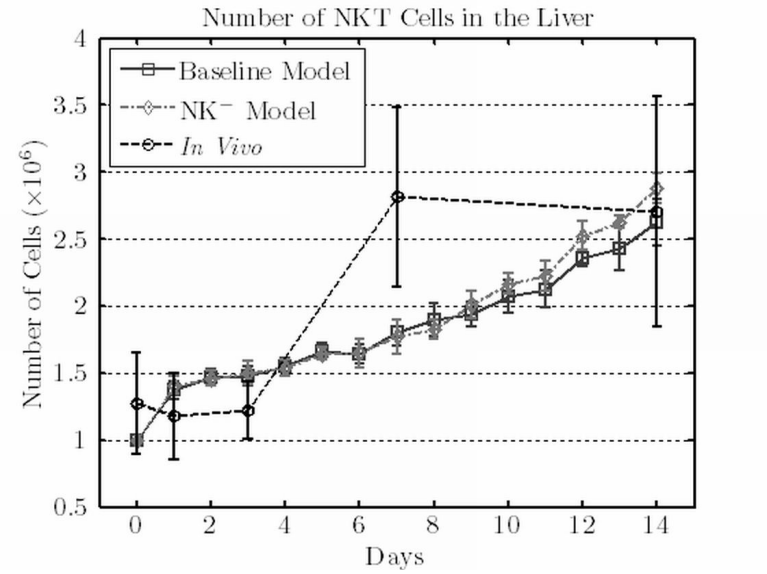

Figure B.30: Number of NKT cells. *In silico* data were obtained from the baseline and NK^- models. *In vivo* data are taken from Stanley et al. 2008

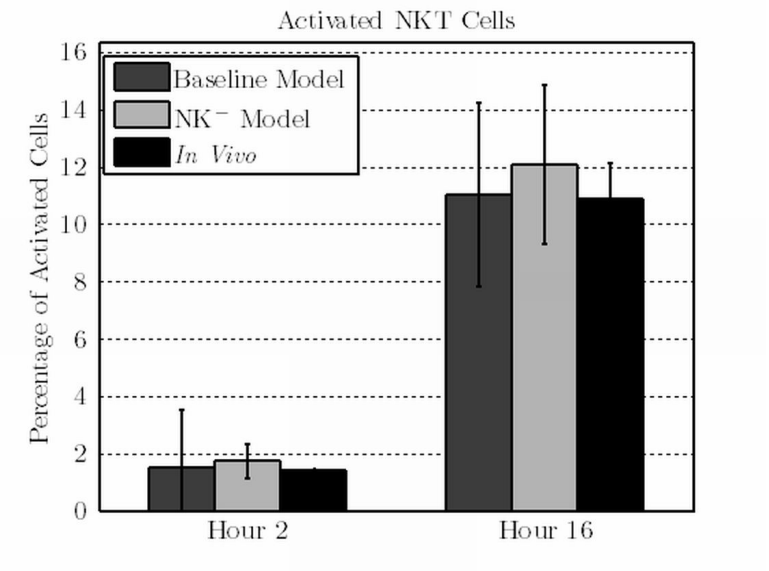

Figure B.31: Percentage of activated NKT Cells. *In silico* data were obtained from the baseline and NK$^-$ models. *In vivo* data are taken from Amprey et al. 2004 and Beattie at al. 2010 (EJI)

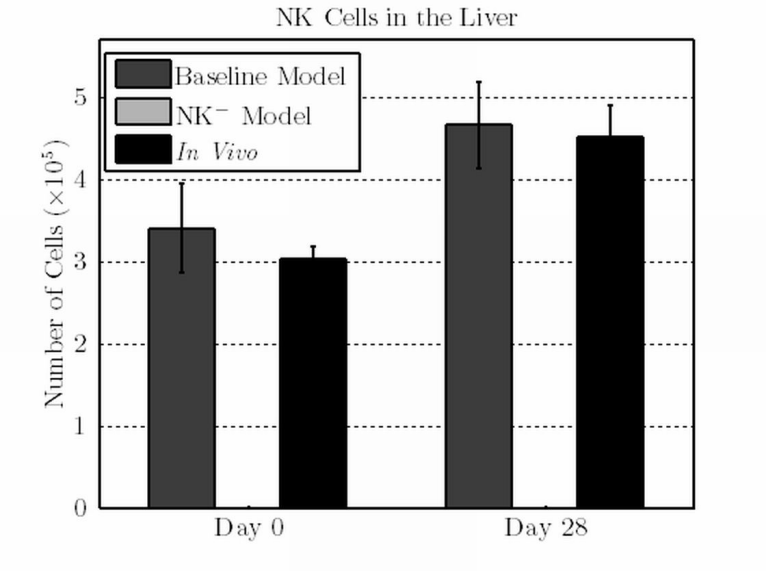

Figure B.32: Number of NK Cells. *In silico* data were obtained from the baseline and NK$^-$ models. *In vivo* data are taken from Maroof et al. 2008

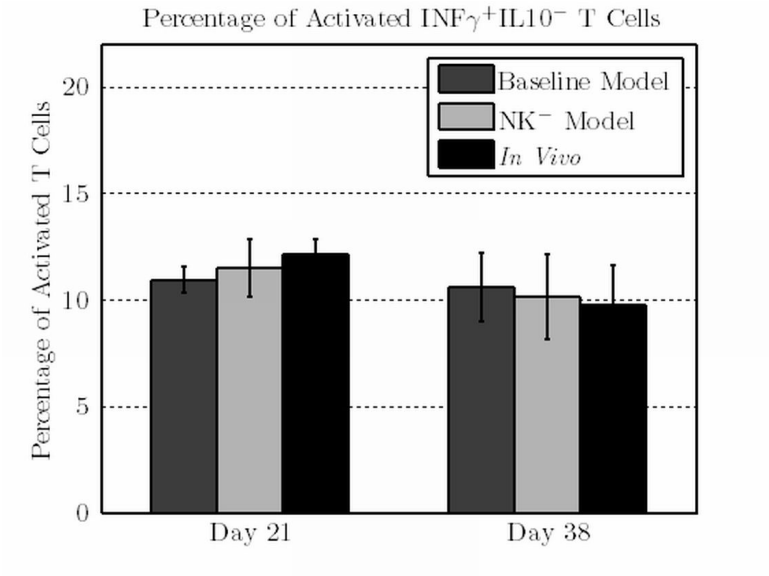

Figure B.33: Percentage of activated T_H1 cells. *In silico* data were obtained from the baseline and NK^- models. *In vivo* data are taken from unpublished data

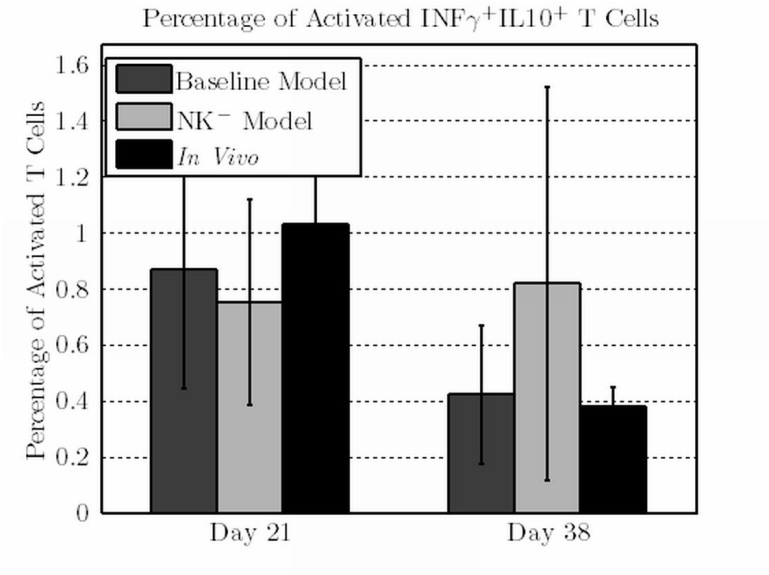

Figure B.34: Percentage of activated T_H1 cells. *In silico* data were obtained from the baseline and NK^- models. *In vivo* data are taken from unpublished data

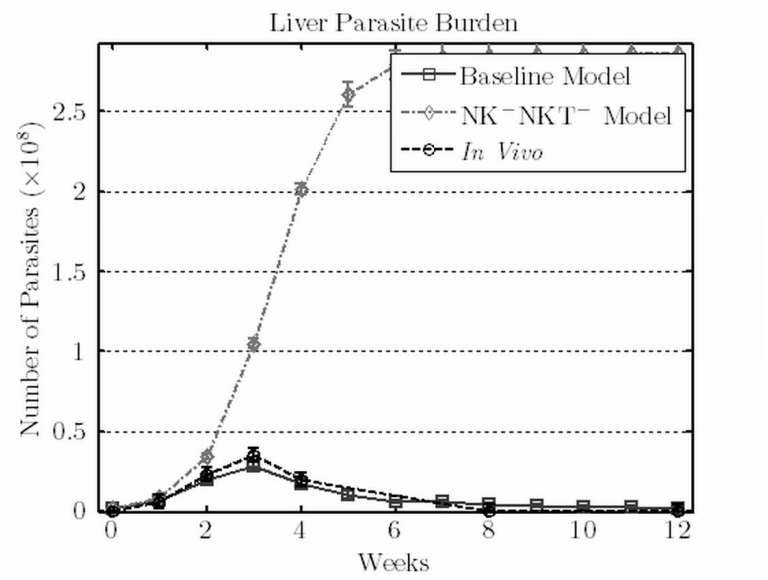

Figure B.35: Parasite Burden. *In silico* data describe baseline and $NK^{-}NKT^{-}$ models. *In vivo* data are adapted from Murray et al. 2006

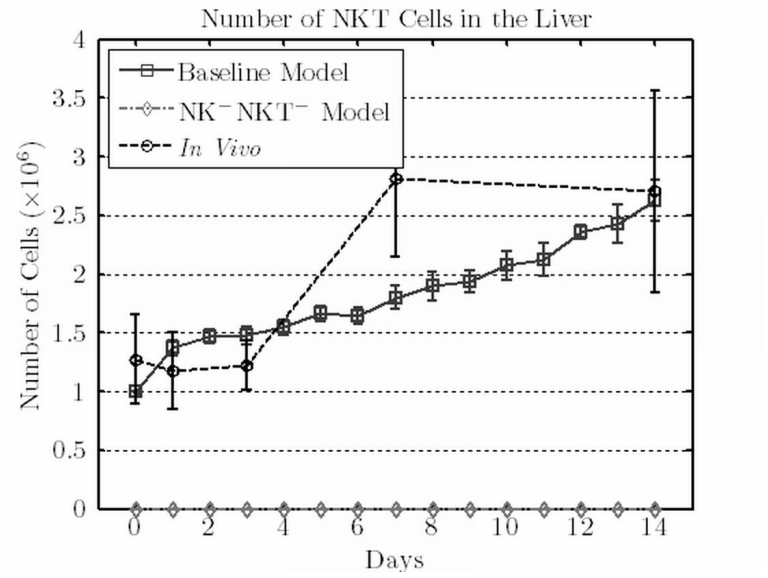

Figure B.36: Number of NKT cells. *In silico* data describe baseline and $NK^{-}NKT^{-}$ models. *In vivo* data are taken from Stanley et al. 2008

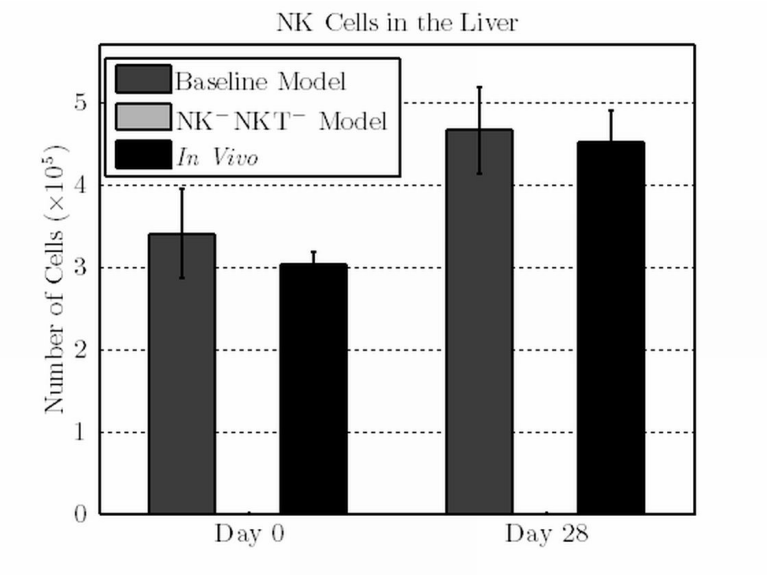

Figure B.37: Number of NK Cells. *In silico* data describe baseline and $NK^{-}NKT^{-}$ models. *In vivo* data are taken from Maroof et al. 2008

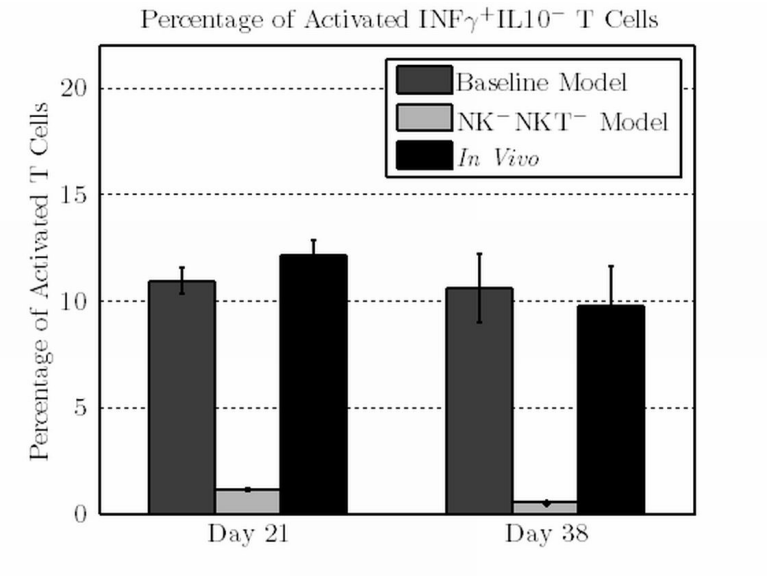

Figure B.38: Percentage of activated T_H1 cells. *In silico* data describe baseline and $NK^{-}NKT^{-}$ models. *In vivo* data are taken from unpublished data

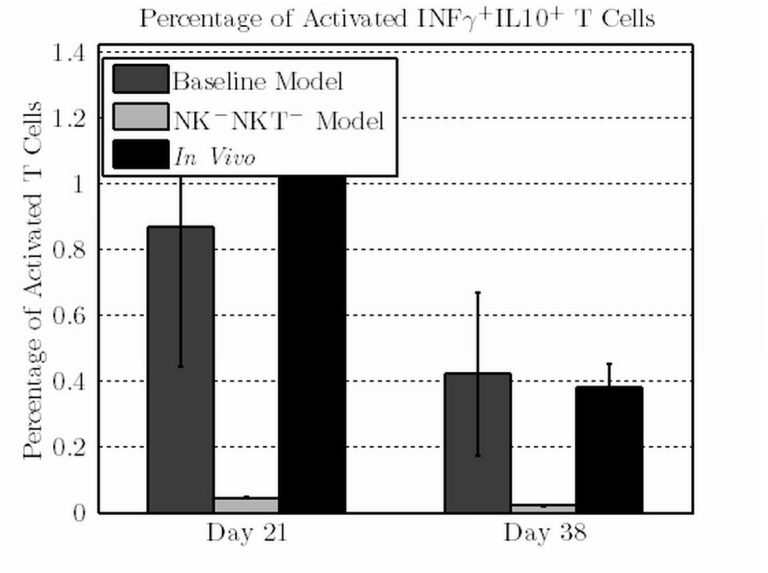

Figure B.39: Percentage of activated T_H1 cells. *In silico* data describe baseline and NK^-NKT^- models. *In vivo* data are taken from unpublished data

cells indicates antigen non-specific T cells used for the calculation, but not modeled. As expected, no NK and NKT cells are present (see Figures B.36 and B.37).

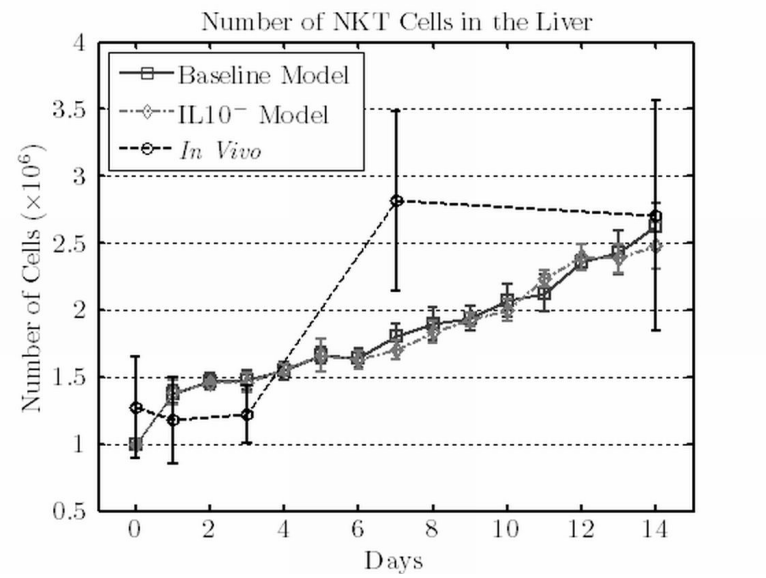

Figure B.40: Number of NKT cells. *In silico* data describe baseline and IL10$^-$ models. *In vivo* data are taken from Stanley et al. 2008

B.10 Removal of IL10

Removing IL10 only marginally affect the NKT cells response (see Figures B.40 and B.41), the NK cells response (see Figure B.42), and the T cells response (see Figures B.43 and B.44).

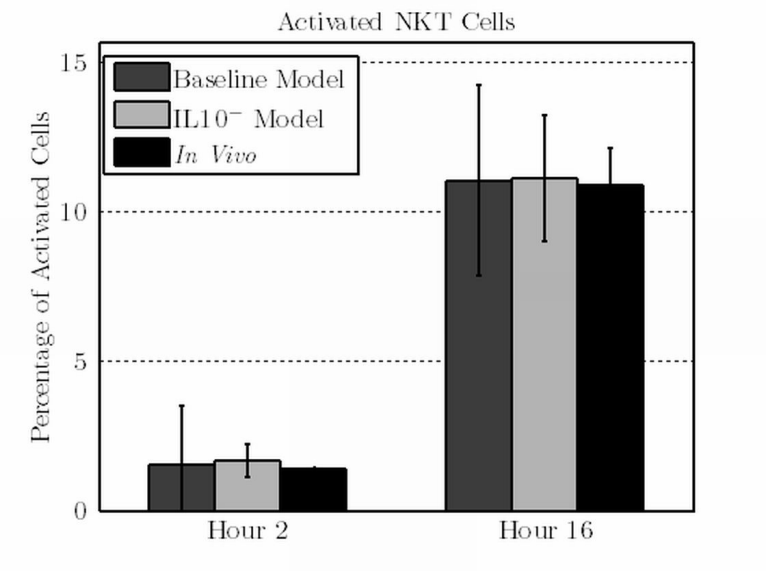

Figure B.41: Percentage of activated NKT Cells. *In silico* data describe baseline and IL10$^-$ models. *In vivo* data are taken from Amprey et al. 2004 and Beattie at al. 2010 (EJI)

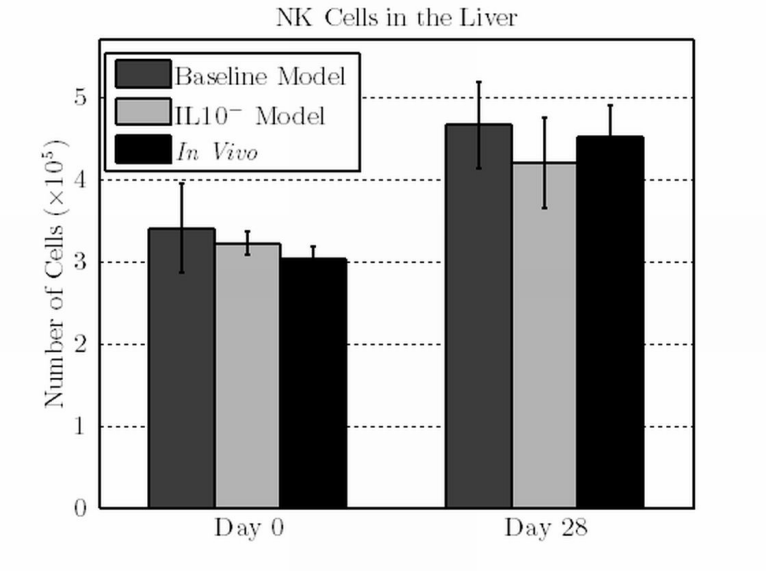

Figure B.42: Number of NK Cells. *In silico* data describe baseline and IL10$^-$ models. *In vivo* data are taken from Maroof et al. 2008

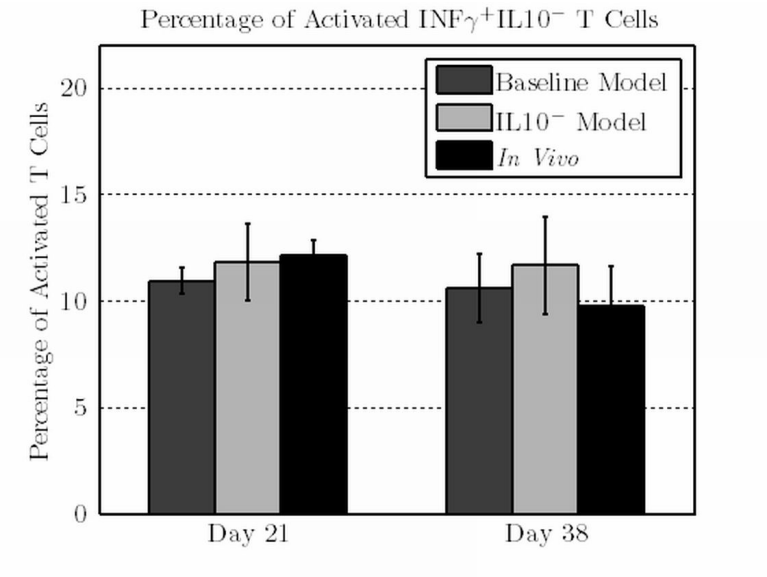

Figure B.43: Percentage of activated T_H1 cells. *In silico* data describe baseline and $IL10^-$ models. *In vivo* data are taken from unpublished data

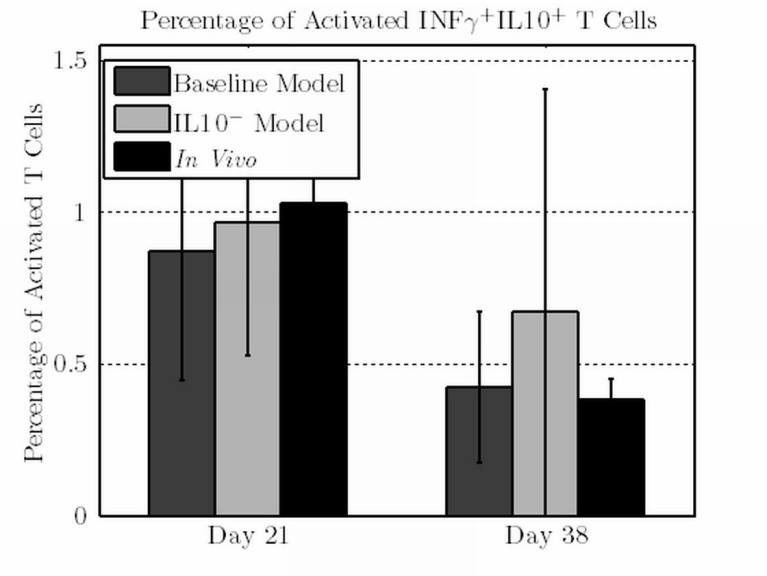

Figure B.44: Percentage of activated T_H1 cells. *In silico* data describe baseline and $IL10^-$ models. *In vivo* data are taken from unpublished data

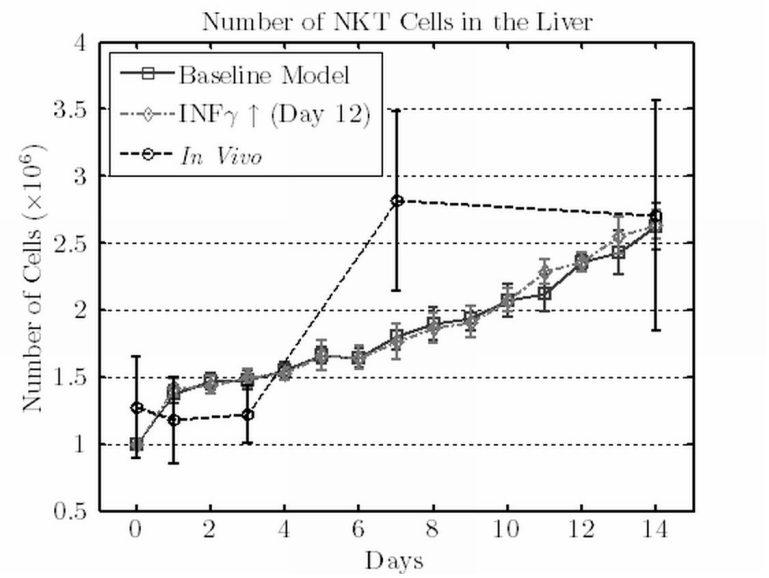

Figure B.45: Number of NKT cells. *In silico* data describe baseline and INFγ ↑ (Day 12) models. *In vivo* data are taken from Stanley et al. 2008

B.11 INFγ Injection 12 Days After Infection

The increase of INFγ concentration 12 days after infection, has no effect on the NKT cells response (see Figures B.45 and B.46) and the NK cells response (see Figure B.47). The effect on the T cell populations is, however, less marginal (see Figures B.48 and B.49), probably as a consequence of the different parasite burden (see Figure 8.24).

B.12 INFγ Injection 24 Days After Infection

The increase of INFγ concentration 24 days after infection, has no effect on the NKT cells response (see Figures B.50 and B.51) and the NK cells response (see Figure B.52). Moreover, the effect on T cell populations is marginal (see Figures B.53 and B.54).

B.13 INFγ Injection 36 Days After Infection

The increase of INFγ concentration 36 days after infection, has no effect on the NKT cells response (see Figures B.55 and B.56) and the NK cells response (see Figure B.57). The effect on $INF\gamma^{+}IL10^{-}$ T cells is marginal (see Figure B.58). However, the percentage of $INF\gamma^{+}IL10^{+}$ T cells is strongly increased 38 days after infection (see Figure B.59).

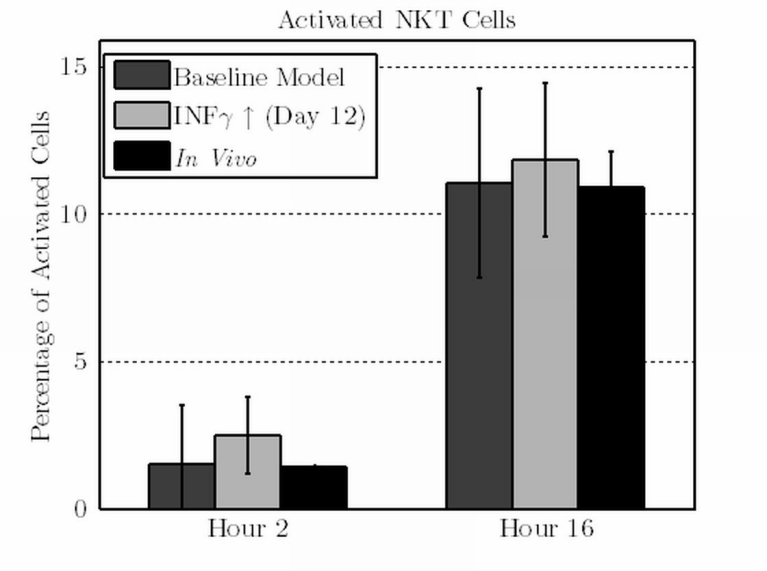

Figure B.46: Percentage of activated NKT Cells. *In silico* data describe baseline and INF$\gamma\uparrow$ (Day 12) models. *In vivo* data are taken from Amprey et al. 2004 and Beattie at al. 2010 (EJI)

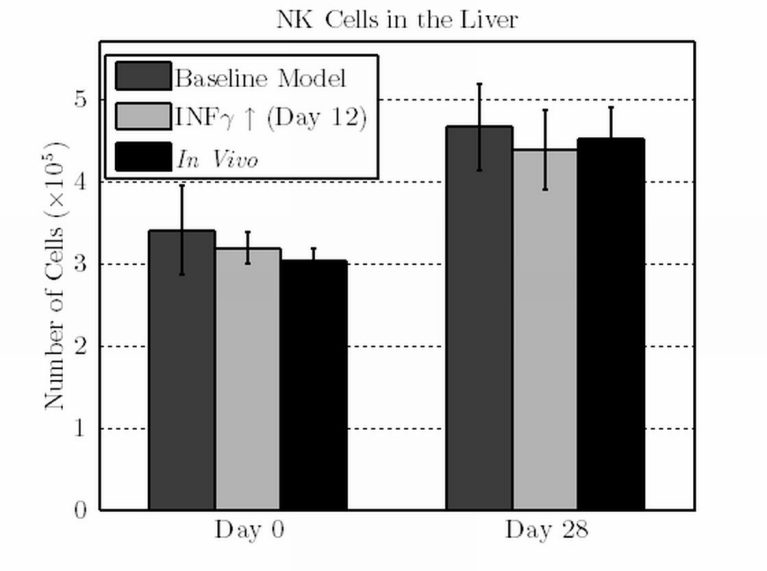

Figure B.47: Number of NK Cells. *In silico* data describe baseline and INF$\gamma\uparrow$ (Day 12) models. *In vivo* data are taken from Maroof et al. 2008

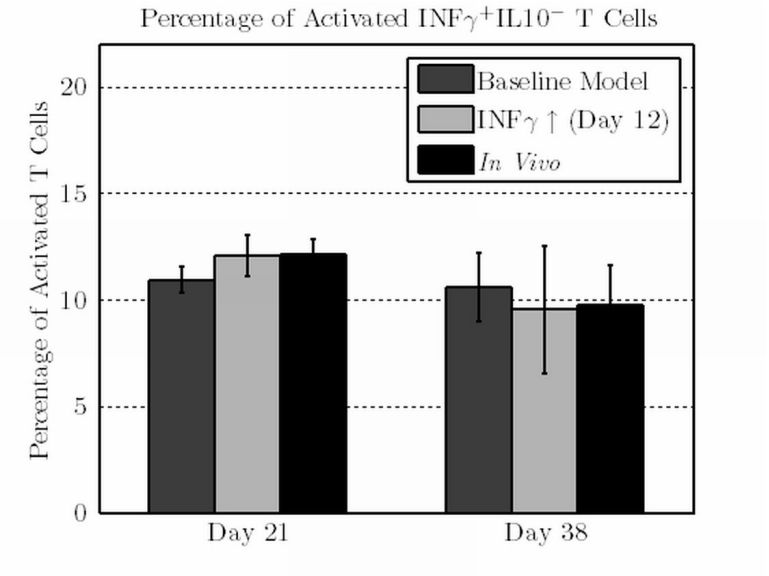

Figure B.48: Percentage of activated T_H1 cells. *In silico* data describe baseline and INF$\gamma \uparrow$ (Day 12) models. *In vivo* data are taken from unpublished data

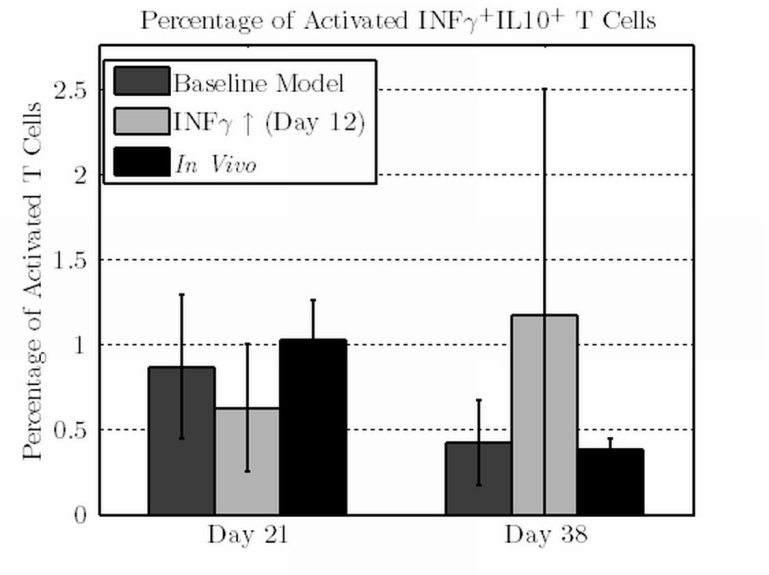

Figure B.49: Percentage of activated T_H1 cells. *In silico* data describe baseline and INF$\gamma \uparrow$ (Day 12) models. *In vivo* data are taken from unpublished data

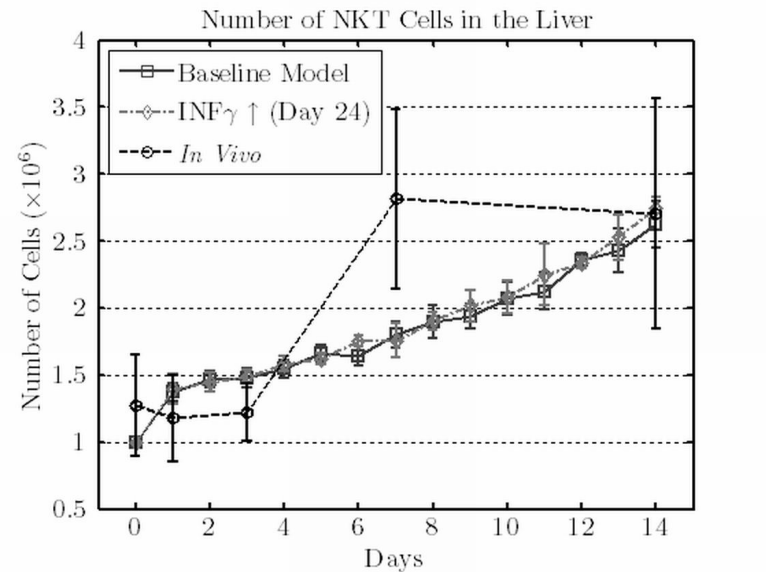

Figure B.50: Number of NKT cells. *In silico* data describe baseline and INF$\gamma\uparrow$ (Day 24) models. *In vivo* data are taken from Stanley et al. 2008

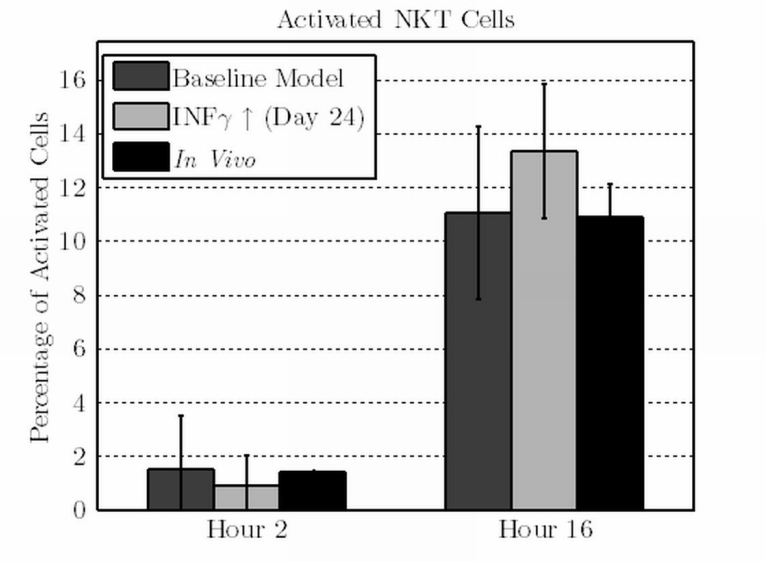

Figure B.51: Percentage of activated NKT Cells. *In silico* data describe baseline and INF$\gamma\uparrow$ (Day 24) models. *In vivo* data are taken from Amprey et al. 2004 and Beattie at al. 2010 (EJI)

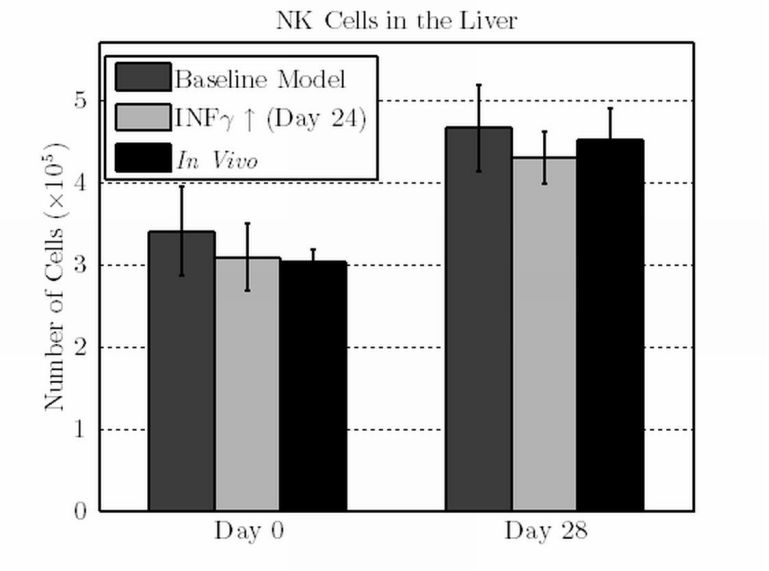

Figure B.52: Number of NK Cells. *In silico* data describe baseline and INFγ ↑ (Day 24) models. *In vivo* data are taken from Maroof et al. 2008

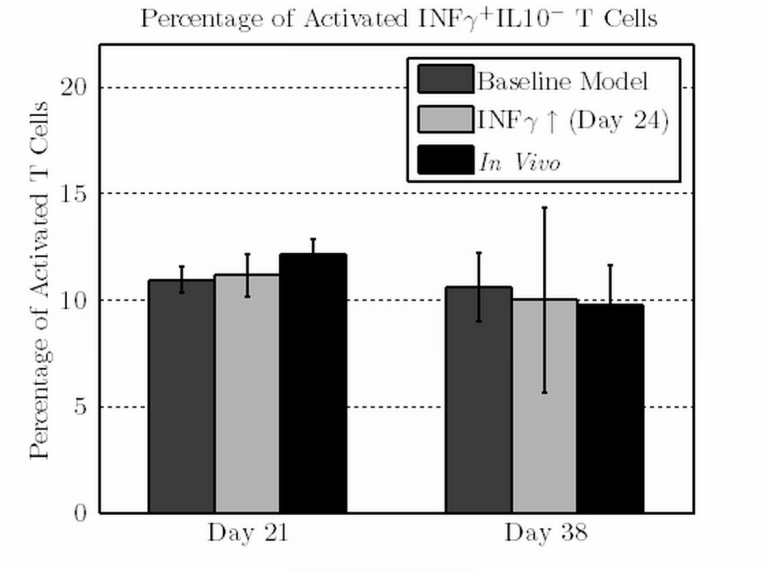

Figure B.53: Percentage of activated T_H1 cells. *In silico* data describe baseline and INFγ ↑ (Day 24) models. *In vivo* data are taken from unpublished data

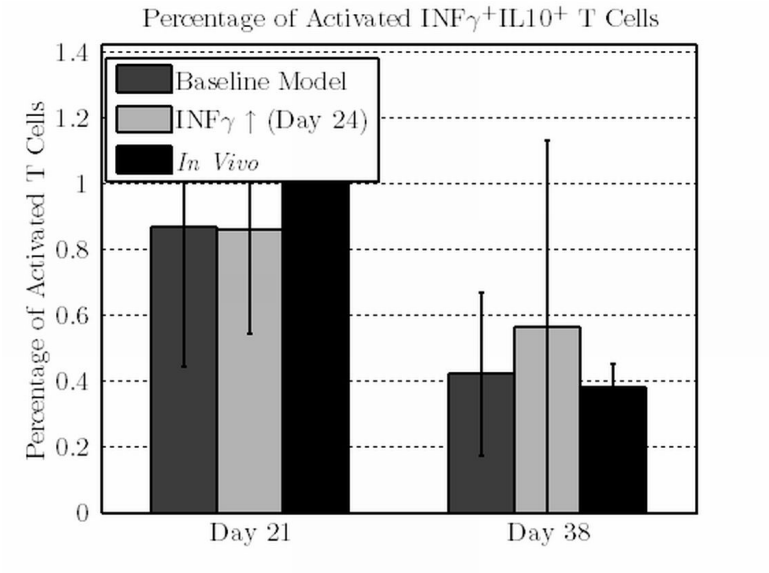

Figure B.54: Percentage of activated T_H1 cells. *In silico* data describe baseline and INF$\gamma \uparrow$ (Day 24) models. *In vivo* data are taken from unpublished data

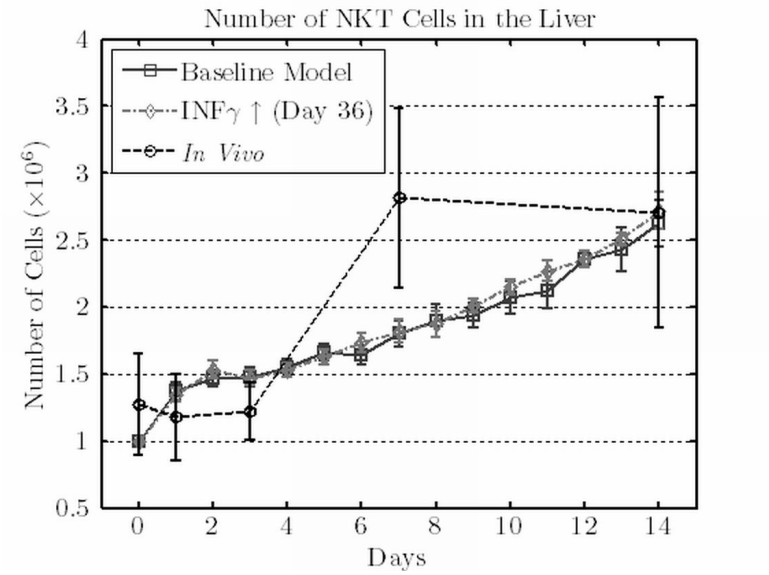

Figure B.55: Number of NKT cells. *In silico* data describe baseline and INF$\gamma \uparrow$ (Day 36) models. *In vivo* data are taken from Stanley et al. 2008

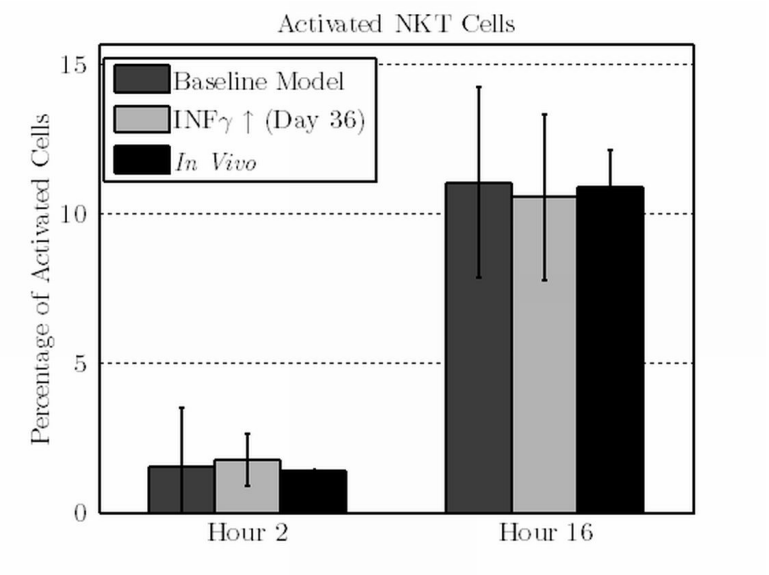

Figure B.56: Percentage of activated NKT Cells. *In silico* data describe baseline and INFγ ↑ (Day 36) models. *In vivo* data are taken from Amprey et al. 2004 and Beattie at al. 2010 (EJI)

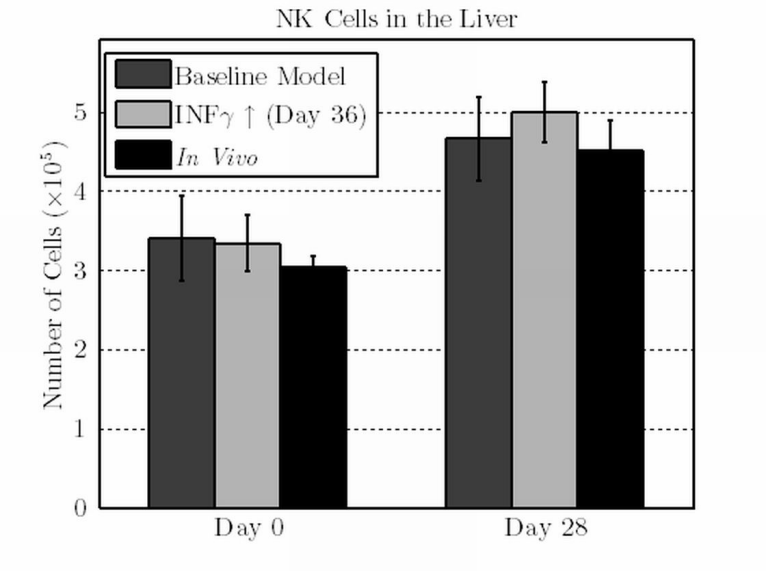

Figure B.57: Number of NK Cells. *In silico* data describe baseline and INFγ ↑ (Day 36) models. *In vivo* data are taken from Maroof et al. 2008

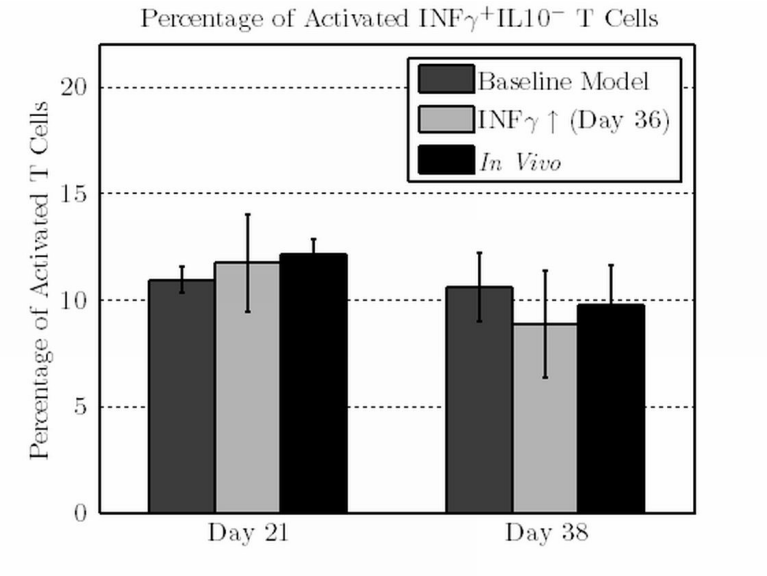

Figure B.58: Percentage of activated T_H1 cells. *In silico* data describe baseline and INF$\gamma \uparrow$ (Day 36) models. *In vivo* data are taken from unpublished data

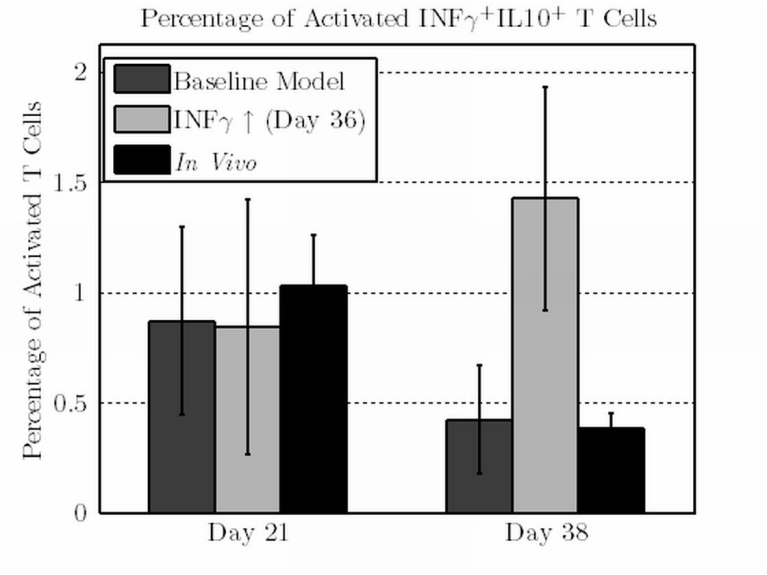

Figure B.59: Percentage of activated T_H1 cells. *In silico* data describe baseline and INF$\gamma \uparrow$ (Day 36) models. *In vivo* data are taken from unpublished data

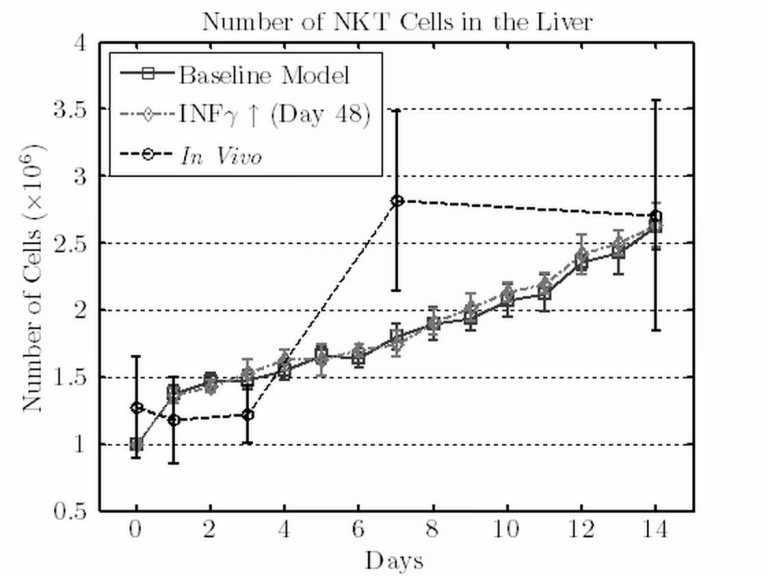

Figure B.60: Number of NKT cells. *In silico* data describe baseline and INFγ ↑ (Day 48) models. *In vivo* data are taken from Stanley et al. 2008

B.14 INFγ Injection 48 Days After Infection

The increase of INFγ concentration 48 days after infection, has no effect on the NKT cells response (see Figures B.60 and B.61), the NK cells response (see Figure B.62), and $INF\gamma^{+}IL10^{-}$ T cells percentage (see Figure B.63). The, anomalous percentage of $INF\gamma^{+}IL10^{+}$ T cells (see Figure B.64) seems to be due to stochastic effects, as the trends of the percentage look comparable (see Figure B.65).

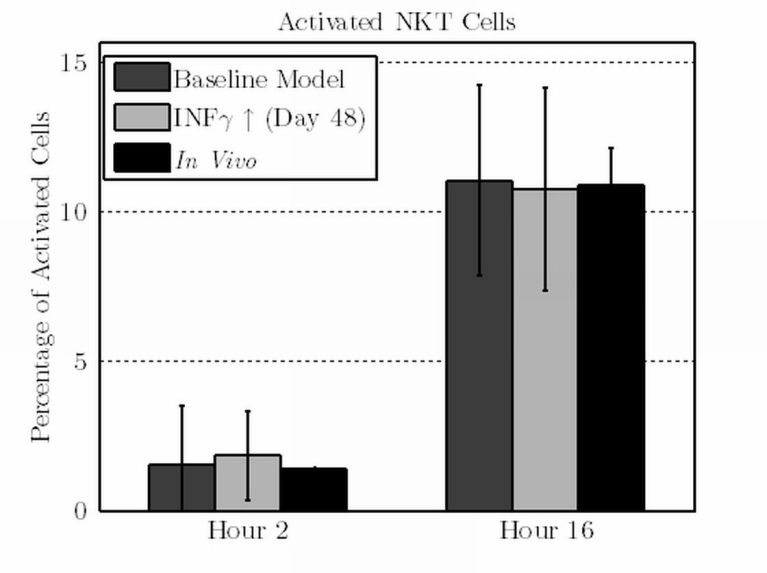

Figure B.61: Percentage of activated NKT Cells. *In silico* data describe baseline and INF$\gamma\uparrow$ (Day 48) models. *In vivo* data are taken from Amprey et al. 2004 and Beattie at al. 2010 (EJI)

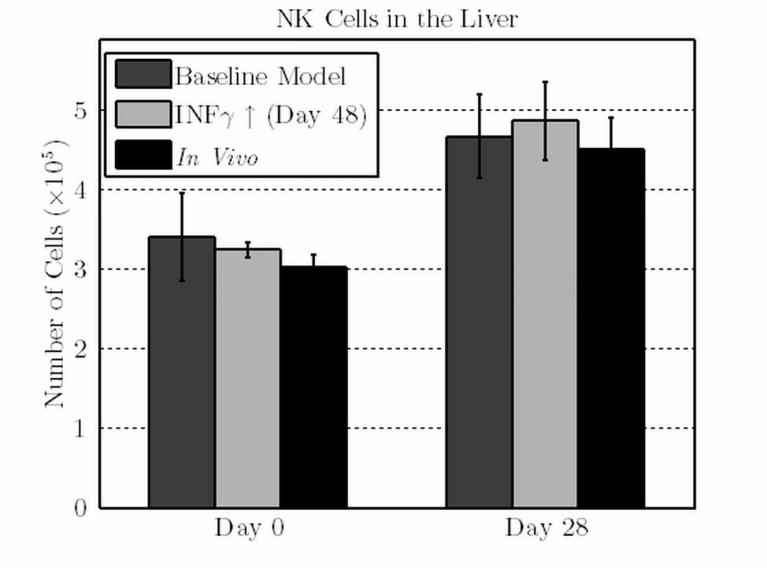

Figure B.62: Number of NK Cells. *In silico* data describe baseline and INF$\gamma\uparrow$ (Day 48) models. *In vivo* data are taken from Maroof et al. 2008

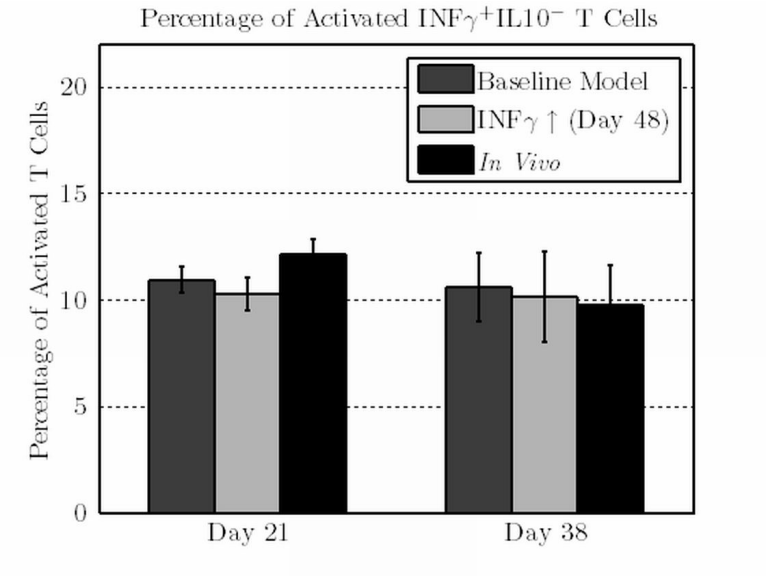

Figure B.63: Percentage of activated T_H1 cells. *In silico* data describe baseline and INF$\gamma \uparrow$ (Day 48) models. *In vivo* data are taken from unpublished data

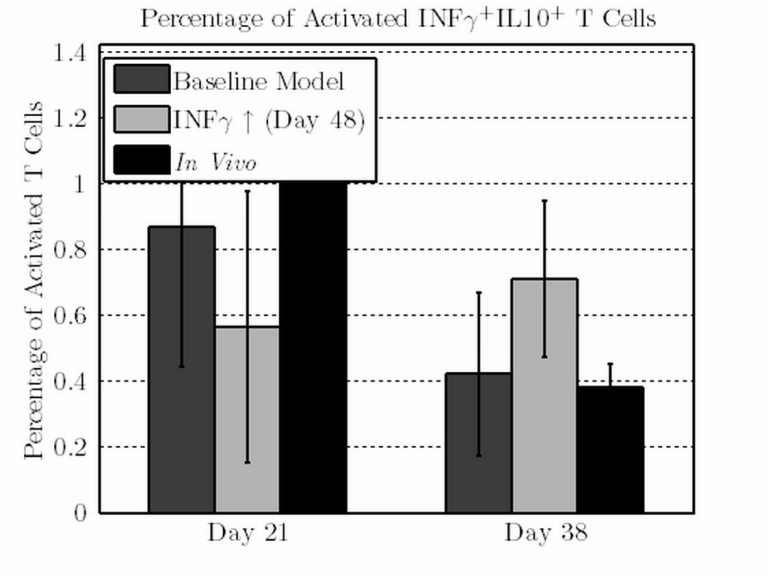

Figure B.64: Percentage of activated T_H1 cells. *In silico* data describe baseline and INF$\gamma \uparrow$ (Day 48) models. *In vivo* data are taken from unpublished data

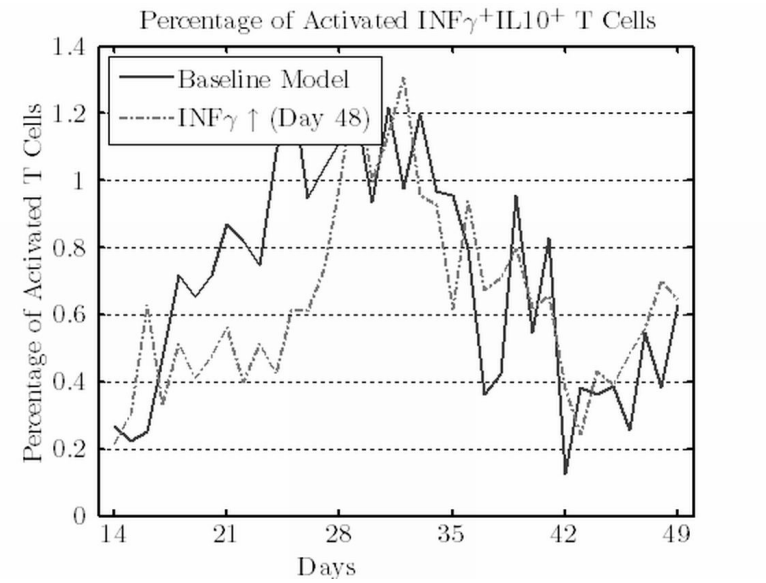

Figure B.65: Percentage of INFγ^+IL10$^+$ T Cells. Data describe baseline and INF$\gamma\uparrow$ (Day 48) models

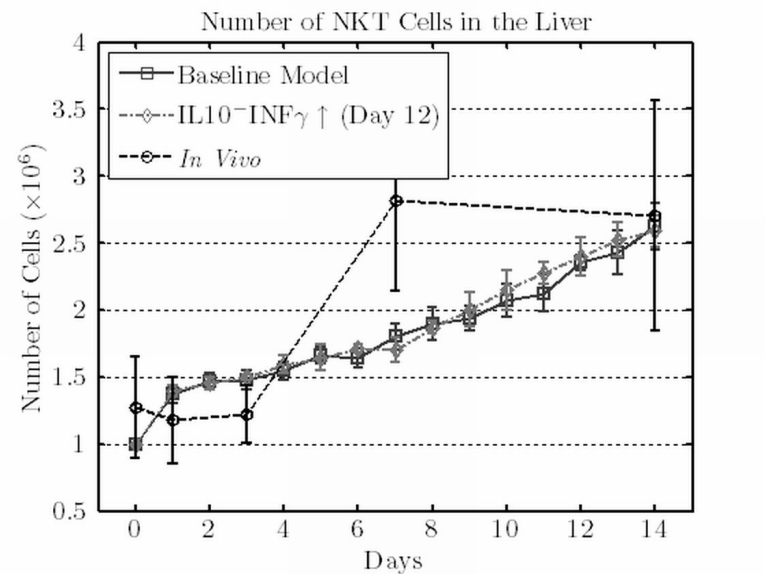

Figure B.66: Number of NKT cells. *In silico* data describe baseline and IL10⁻INFγ ↑ (Day 12) models. *In vivo* data are taken from Stanley et al. 2008

B.15 IL10 Removal and INFγ Injection 12 Days After Infection

The increase of INFγ concentration 12 days after infection with the removal of IL10, has no effect on the NKT cells response (see Figures B.66 and B.67) and the NK cells response (see Figure B.68). The effect on T cells in only marginal (see Figures B.69 and B.70).

B.16 IL10 Removal and INFγ Injection 24 Days After Infection

The increase of INFγ concentration 24 days after infection with the removal of IL10, has no effect on the NKT cells response (see Figures B.71 and B.72) and the NK cells response (see Figure B.73). However, the effect on T cells in clearly detectable (see Figures B.74 and B.75).

B.17 IL10 Removal and INFγ Injection 36 Days After Infection

The increase of INFγ concentration 36 days after infection with the removal of IL10, has no effect on the NKT cells response (see Figures B.76 and B.77)

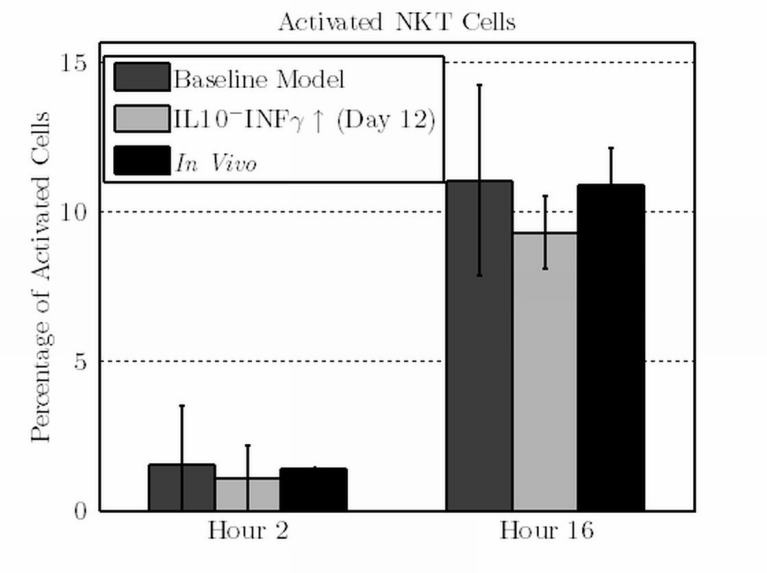

Figure B.67: Percentage of activated NKT Cells. *In silico* data describe baseline and IL10^{-}INFγ $\uparrow$ (Day 12) models. *In vivo* data are taken from Amprey et al. 2004 and Beattie at al. 2010 (EJI)

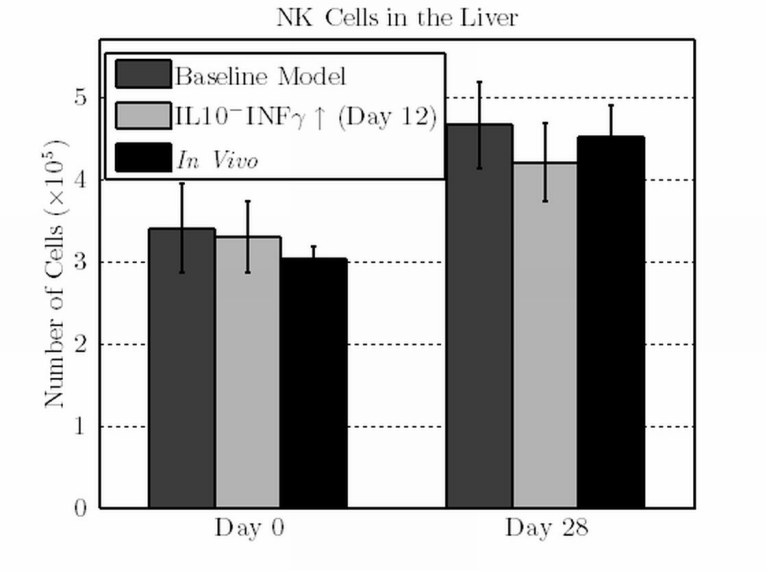

Figure B.68: Number of NK Cells. *In silico* data describe baseline and IL10^{-}INFγ $\uparrow$ (Day 12) models. *In vivo* data are taken from Maroof et al. 2008

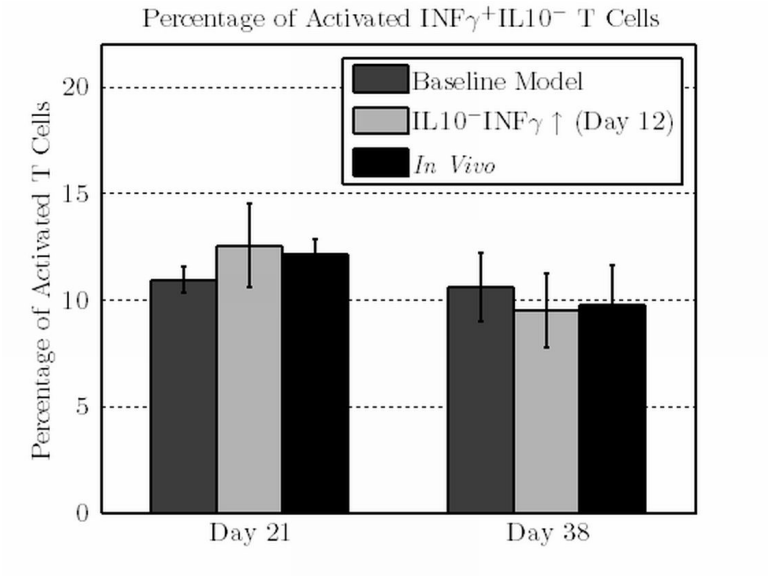

Figure B.69: Percentage of activated T_H1 cells. *In silico* data describe baseline and IL10$^-$INF$\gamma\uparrow$ (Day 12) models. *In vivo* data are taken from unpublished data

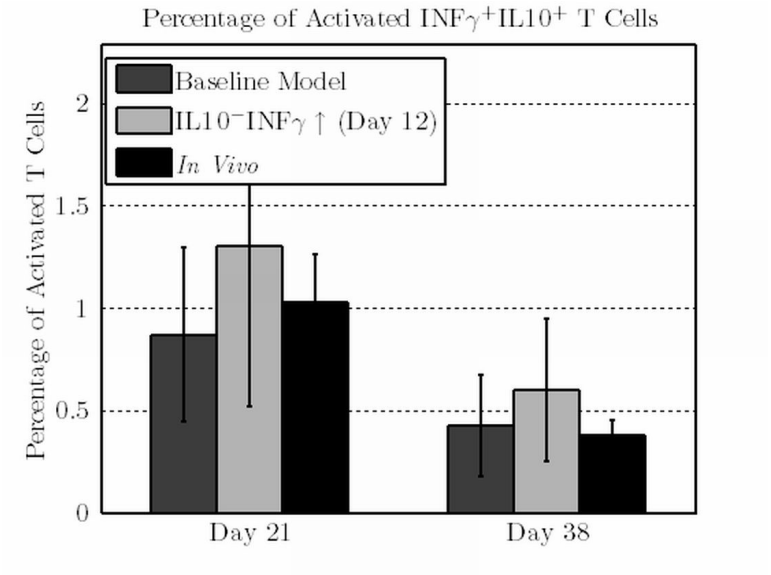

Figure B.70: Percentage of activated T_H1 cells. *In silico* data describe baseline and IL10$^-$INF$\gamma\uparrow$ (Day 12) models. *In vivo* data are taken from unpublished data

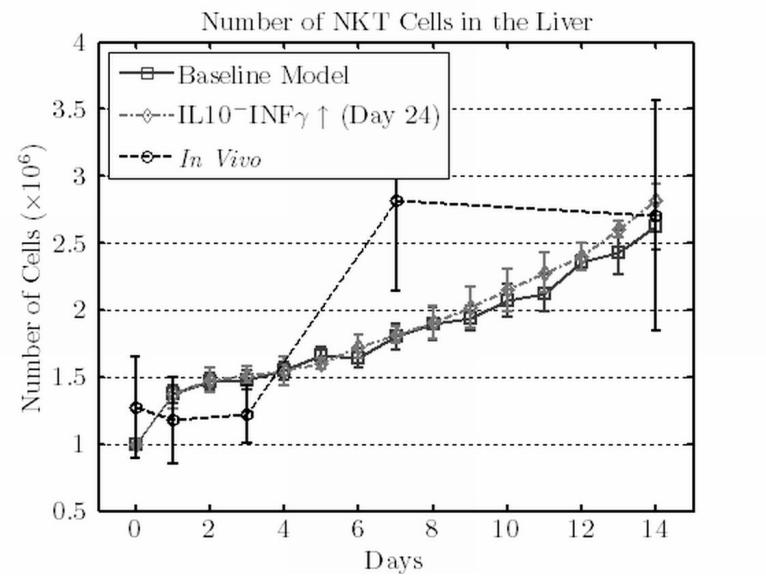

Figure B.71: Number of NKT cells. *In silico* data describe baseline and IL10^{-}INF$\gamma \uparrow$ (Day 24) models. *In vivo* data are taken from Stanley et al. 2008

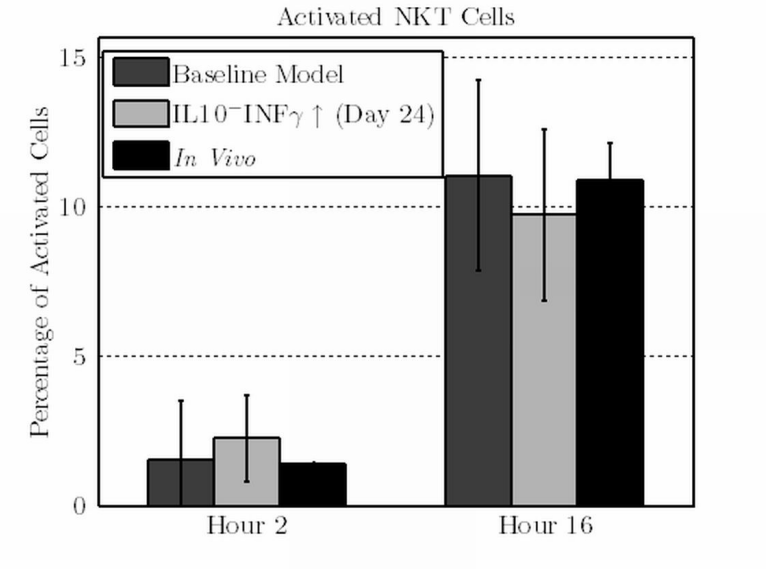

Figure B.72: Percentage of activated NKT Cells. *In silico* data describe baseline and IL10^{-}INF$\gamma \uparrow$ (Day 24) models. *In vivo* data are taken from Amprey et al. 2004 and Beattie at al. 2010 (EJI)

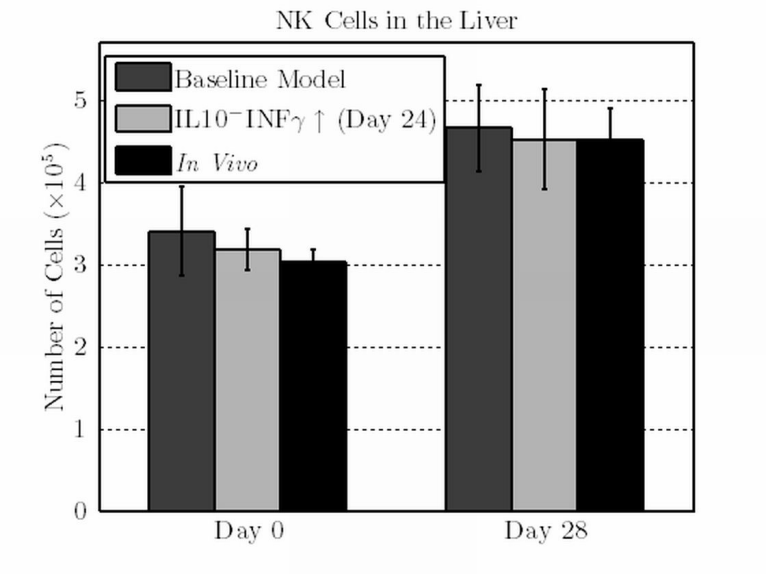

Figure B.73: Number of NK Cells. *In silico* data describe baseline and IL10$^-$INF$\gamma \uparrow$ (Day 24) models. *In vivo* data are taken from Maroof et al. 2008

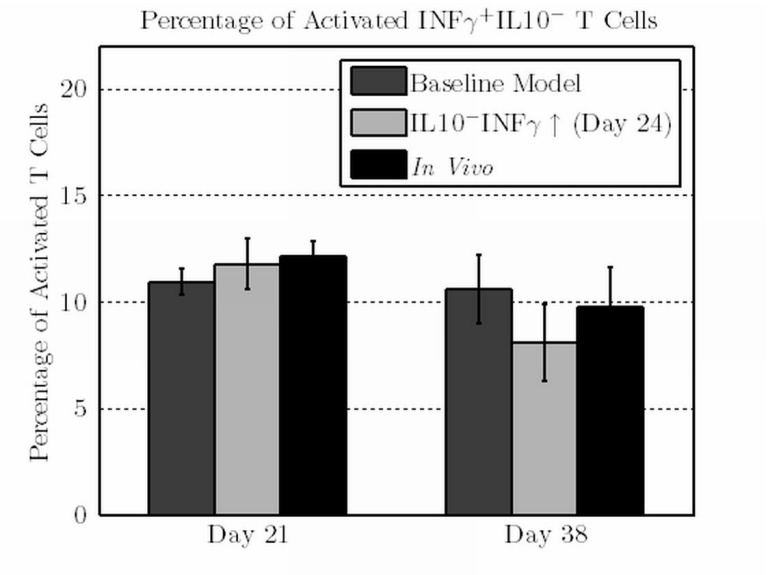

Figure B.74: Percentage of activated T_H1 cells. *In silico* data describe baseline and IL10$^-$INF$\gamma \uparrow$ (Day 24) models. *In vivo* data are taken from unpublished data

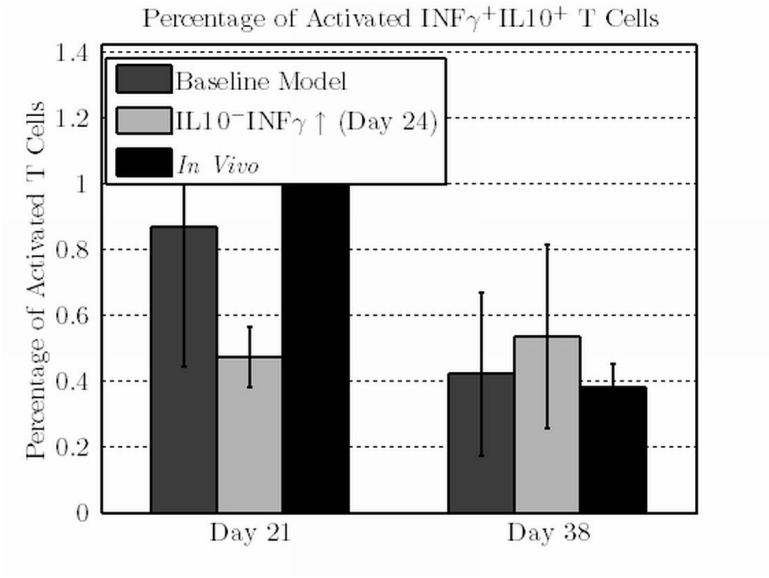

Figure B.75: Percentage of activated T_H1 cells. *In silico* data describe baseline and IL10$^-$INF$\gamma\uparrow$ (Day 24) models. *In vivo* data are taken from unpublished data

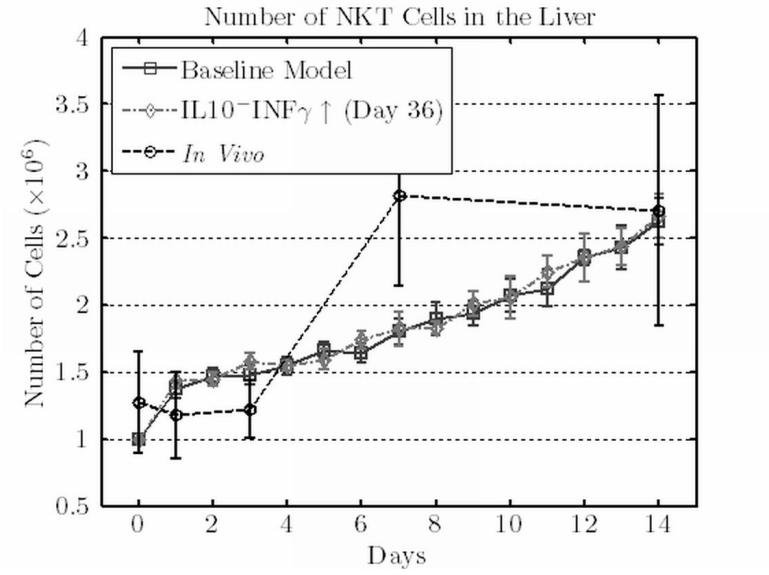

Figure B.76: Number of NKT cells. *In silico* data describe baseline and IL10$^-$INF$\gamma\uparrow$ (Day 36) models. *In vivo* data are taken from Stanley et al. 2008

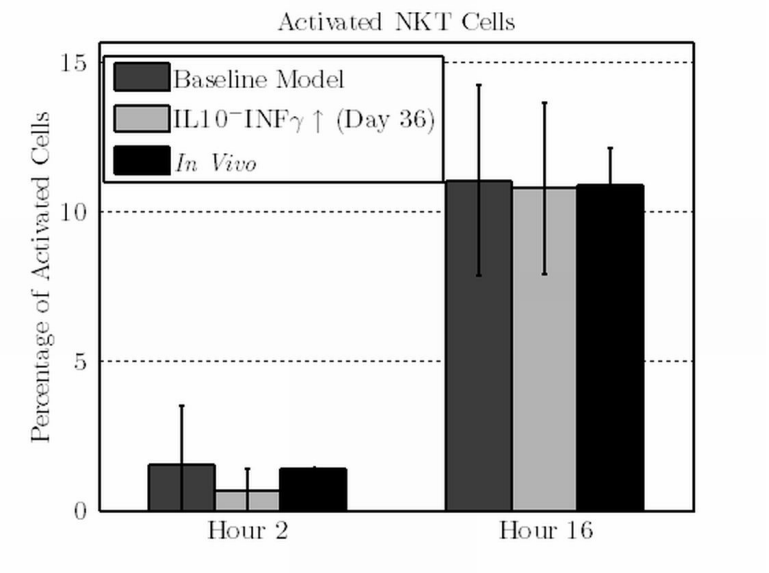

Figure B.77: Percentage of activated NKT Cells. *In silico* data describe baseline and IL10^{-}INFγ $\uparrow$ (Day 36) models. *In vivo* data are taken from Amprey et al. 2004 and Beattie at al. 2010 (EJI)

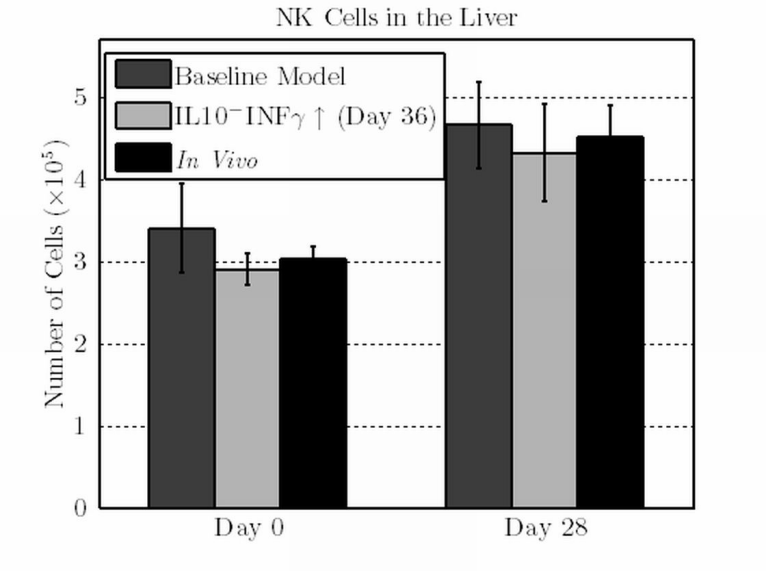

Figure B.78: Number of NK Cells. *In silico* data describe baseline and IL10^{-}INFγ $\uparrow$ (Day 36) models. *In vivo* data are taken from Maroof et al. 2008

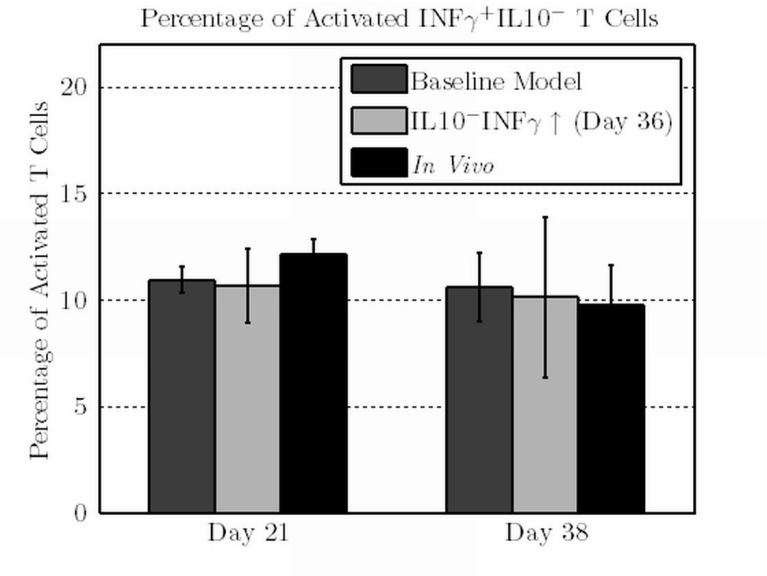

Figure B.79: Percentage of activated T_H1 cells. *In silico* data describe baseline and IL10$^-$INF$\gamma\uparrow$ (Day 36) models. *In vivo* data are taken from unpublished data

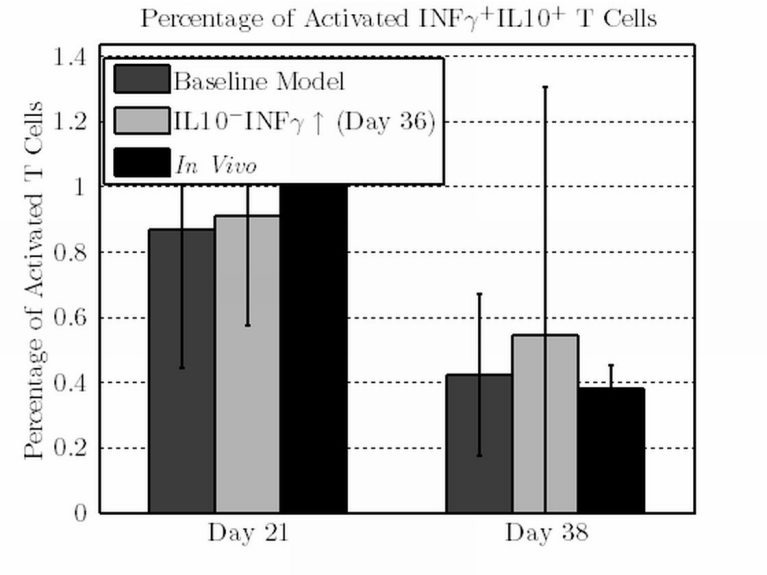

Figure B.80: Percentage of activated T_H1 cells. *In silico* data describe baseline and IL10$^-$INF$\gamma\uparrow$ (Day 36) models. *In vivo* data are taken from unpublished data

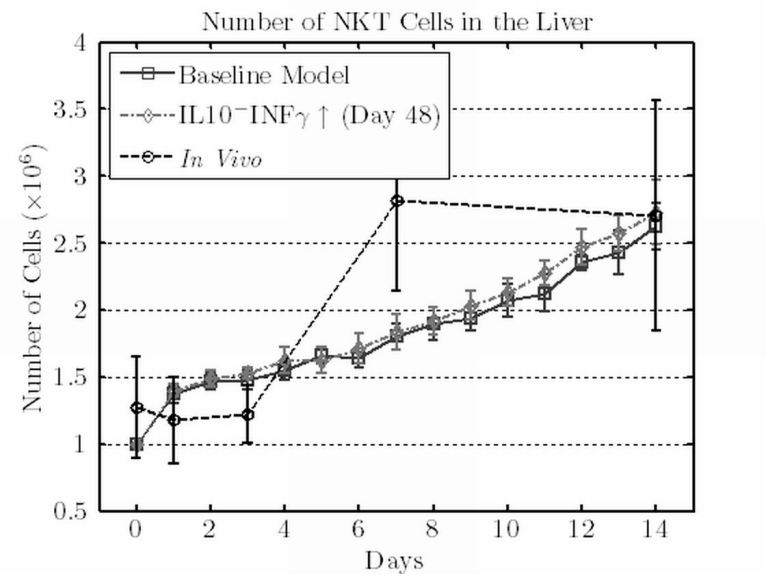

Figure B.81: Number of NKT cells. *In silico* data describe baseline and IL10$^-$INFγ $\uparrow$ (Day 48) models. *In vivo* data are taken from Stanley et al. 2008

and the NK cells response (see Figure B.78). However, the effect on T cells in clearly detectable (see Figures B.79 and B.80). Specifically, the large standard deviation in the percentage of INFγ^+IL10$^+$ T cells is an indication of the effect of INFγ (see Figure B.80).

B.18 IL10 Removal and INFγ Injection 48 Days After Infection

The increase of INFγ concentration 48 days after infection with the removal of IL10, has no effect on the NKT cells response (see Figures B.81 and B.82) and the NK cells response (see Figure B.83). However, the effect on T cells in clearly detectable (see Figures B.84 and B.85).

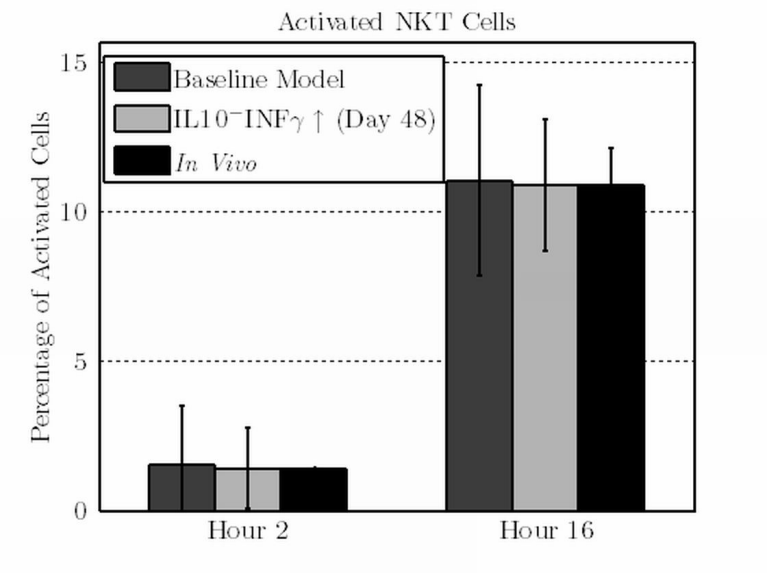

Figure B.82: Percentage of activated NKT Cells. *In silico* data describe baseline and IL10^{-}INFγ $\uparrow$ (Day 48) models. *In vivo* data are taken from Amprey et al. 2004 and Beattie at al. 2010 (EJI)

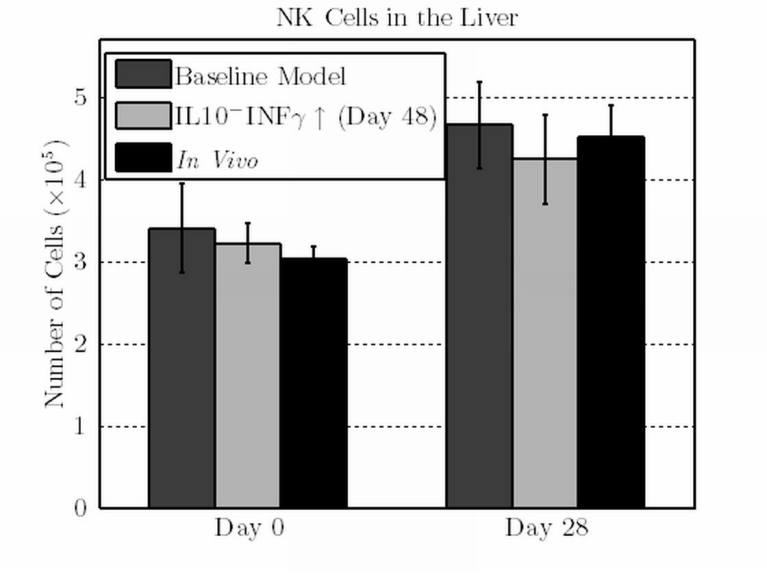

Figure B.83: Number of NK Cells. *In silico* data describe baseline and IL10^{-}INFγ $\uparrow$ (Day 48) models. *In vivo* data are taken from Maroof et al. 2008

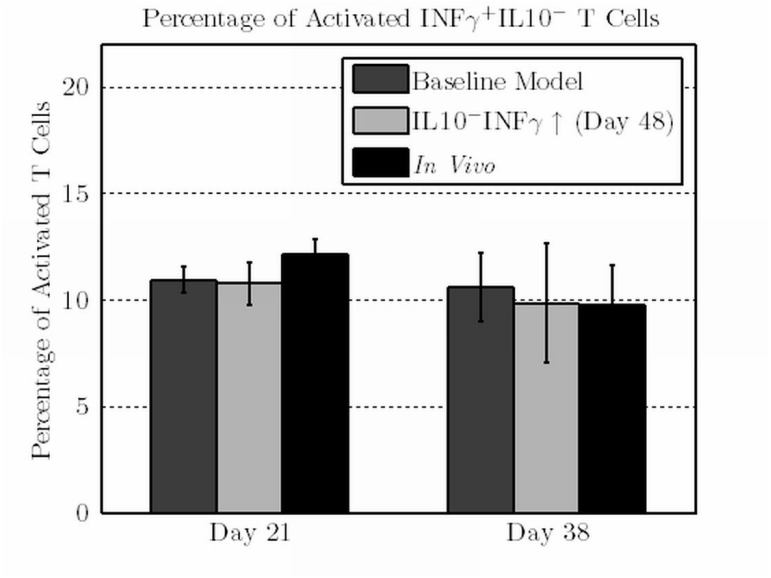

Figure B.84: Percentage of activated T_H1 cells. *In silico* data describe baseline and IL10$^-$INF$\gamma\uparrow$ (Day 48) models. *In vivo* data are taken from unpublished data

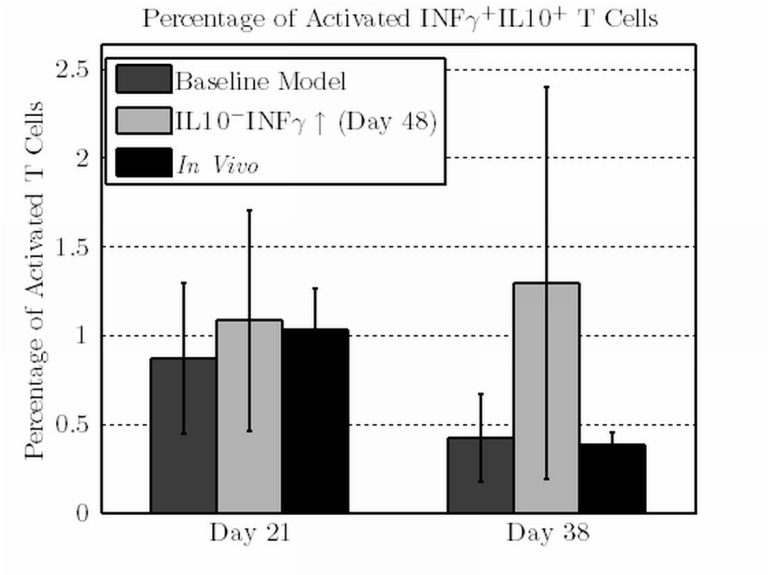

Figure B.85: Percentage of activated T_H1 cells. *In silico* data describe baseline and IL10$^-$INF$\gamma\uparrow$ (Day 48) models. *In vivo* data are taken from unpublished data